

2016

# Peptidomimetic Polymers: Advances in Monomer Design and Polymerization Methods

Brandon Andrew Chan

*Louisiana State University and Agricultural and Mechanical College*

Follow this and additional works at: [https://digitalcommons.lsu.edu/gradschool\\_dissertations](https://digitalcommons.lsu.edu/gradschool_dissertations)



Part of the [Chemistry Commons](#)

---

## Recommended Citation

Chan, Brandon Andrew, "Peptidomimetic Polymers: Advances in Monomer Design and Polymerization Methods" (2016). *LSU Doctoral Dissertations*. 3676.

[https://digitalcommons.lsu.edu/gradschool\\_dissertations/3676](https://digitalcommons.lsu.edu/gradschool_dissertations/3676)

This Dissertation is brought to you for free and open access by the Graduate School at LSU Digital Commons. It has been accepted for inclusion in LSU Doctoral Dissertations by an authorized graduate school editor of LSU Digital Commons. For more information, please contact [gradetd@lsu.edu](mailto:gradetd@lsu.edu).

PEPTIDOMIMETIC POLYMERS: ADVANCES IN MONOMER  
DESIGN AND POLYMERIZATION METHODS

A Dissertation

Submitted to the Graduate Faculty of the  
Louisiana State University and  
Agricultural and Mechanical College  
in partial fulfillment of the  
requirements for the degree of  
Doctor of Philosophy

in

The Department of Chemistry

by  
Brandon Andrew Chan  
B.S., University of Michigan – Ann Arbor, 2009  
August 2016

Victrix causa diis placuit, sed victa Catoni

-Lucan, *Pharsalia*

## ACKNOWLEDGEMENTS

First and foremost I would like to thank my advisor Prof. Donghui Zhang for her guidance, mentorship, and the plethora of opportunities to be at the cusp of cutting edge research throughout my time in graduate school. I also want to thank her for her encouragement and enthusiasm for each of the works contained in this document. Without it, I may have easily lost interest early in my graduate school career. I also want to thank her for supporting my plans to attend law school to become a patent attorney. On a related note, I want to acknowledge Prof. John Pojman who put me in contact with the right people to answer my questions about pursuing patent law. I also want to thank Profs. Paul Russo and David Spivak for their support and encouragement for both completion of my degree and for support of my law school plans.

I want to also thank those in the LSU Department of Chemistry who have lent much support to the collection of data and assistance with experiments I never thought I would have ended up running. Specifically I want to acknowledge Connie David and Dr. Jeonhoon Lee for their assistance in ESI MS and MALDI TOF MS respectively, Dr. Rafael Cueto for teaching me everything I ever wanted to learn about polymer characterization and help with instrumentation, Drs. Thomas Weldeghiorghis and Fengli Zhang for their assistance in running NMR experiments, Dr. Frank Fronczek for his assistance in X-ray crystallography, and Prof. Evgueni Nesterov for the generous use of the UV-vis spectrometer. I final want to thank all Zhang group members for their help, support, encouragement, and listening to my rants.

I would also like to thank my wife, Katie, for her patience, love, and support as we both go through the graduate school process together.

## TABLE OF CONTENTS

ACKNOWLEDGEMENTS.....	iii
LIST OF TABLES.....	vii
LIST OF FIGURES.....	ix
LIST OF SCHEMES.....	xvii
LIST OF ABBREVIATIONS AND ACRONYMS.....	xx
ABSTRACT.....	xxiii
CHAPTER I. INTRODUCTION TO PEPTIDOMIMETIC POLYMERS.....	1
1.1 Overview of peptidomimetic polymers.....	1
1.2 Polypeptides.....	2
1.2.1 Solid phase synthesis of polypeptides.....	3
1.2.2 Polypeptide synthesis via the ring-opening polymerization of <i>N</i> -carboxyanhydride monomers.....	4
1.2.3 Post-polymerization modification of polypeptides.....	23
1.3 Polypeptoids.....	29
1.3.1 Solid phase synthesis of polypeptoids.....	31
1.3.2 Ring-opening polymerization of <i>N</i> -alkyl substituted glycine based NCA monomers to synthesize polypeptoids.....	32
1.4 Ring-opening polymerization of <i>N</i> -thiocarboxyanhydrosulfides.....	43
CHAPTER II. MULTIVALENT BINDING INTERACTIONS OF MANNOSE FUNCTIONALIZED GLYCOPOLYPEPTIDES WITH CONCAVALIN	
A.....	46
2.1 Objectives.....	46
2.2 Multivalent binding, glycopolymers, and glycopolypeptides.....	46
2.2.1 Multivalent carbohydrate-lectin interactions.....	47
2.2.2 Glycopolymers.....	49
2.2.3 Glycopolypeptides.....	56
2.3 Results and discussion.....	65
2.3.1 Synthesis and characterization of glycopolypeptides.....	65
2.3.2 Circular dichroism of glycopolypeptides.....	69
2.3.3 Binding studies of PPLG and PPDLG mannose with ConA .....	71
2.3.3.1 Binding kinetic study.....	72
2.3.3.2 Binding stoichiometry from quantitative precipitation assay.....	75
2.3.4 Varying binding epitope density.....	78
2.4 Dynamic light scattering of glycopolypeptides.....	82
2.5 Conclusions.....	84
2.6 Experimental.....	87
2.6.1 Instrumentation and general considerations.....	87
2.6.2 Synthesis of $\gamma$ -propargyl-L-glutamate <i>N</i> -carboxyanhydride.....	88
2.6.3 General procedure for the polymerization of $\gamma$ -propargyl-L-glutamate <i>N</i> -carboxyanhydride.....	89
2.6.4 Glycosylation of poly( $\gamma$ -propargyl-L-glutamate) via CuAAC.....	90

2.6.5 Circular dichroism.....	91
2.6.6 Turbidity assay.....	91
2.6.7 Quantitative precipitation assay.....	91
2.7 Supplemental data for Chapter II.....	92
CHAPTER III. 1,1,3,3-TETRAMETHYLGUANIDINE PROMOTED RING- OPENING POLYMERIZATION OF <i>N</i> -BUTYL <i>N</i> -CARBOXYANHYDRIDE USING ALCOHOL INITIATORS.....	94
3.1 Objectives.....	94
3.2 Introduction to organocatalysis in polymerization.....	94
3.3 Results and discussion.....	97
3.3.1 Initial results.....	97
3.3.2 Competition with TMG initiation.....	100
3.3.3 Demonstration of a living polymerization.....	105
3.3.4 Kinetic study of the polymerization.....	106
3.3.5 Expanding the breadth of alcohol initiators and their dependence on sterics and electronics.....	109
3.3.6 Elucidation of an initiating pathway.....	110
3.3.7 Macroinitiation of Bu-NCA with poly(ethylene glycol) monomethyl ether.....	123
3.4 Conclusions.....	124
3.5 Experimental.....	126
3.5.1 Instrumentation and general considerations.....	126
3.5.2 Synthesis of <i>N</i> -butyl <i>N</i> -carboxyanhydride.....	128
3.5.3 General polymerization procedure.....	129
3.5.4 General kinetics procedure.....	131
3.6 Supplemental data for Chapter III.....	131
CHAPTER IV. <i>N</i> -THIOCARBOXYANHYDROSULFIDES AS POTENTIAL ALTERNATIVES TO <i>N</i> -CARBOXYANHYDRIDE MONOMERS IN THE SYNTHESIS OF PEPTIDOMIMETIC POLYMERS.....	138
4.1 Objectives.....	138
4.2 Background of <i>N</i> -thiocarboxyanhydrosulfides.....	139
4.3 Results and discussion.....	143
4.3.1 Synthesis and ROP of R-NTAs.....	143
4.3.2 Amino acid based NTA monomers.....	158
4.3.2.1 ROP of amino acid based NTA monomers in solution state.....	160
4.3.2.2 Solid state ROP of amino acid based NTAs.....	168
4.4 Conclusions.....	173
4.5 Experimental.....	175
4.5.1 Instrumentation and general considerations.....	175
4.5.2 <i>N</i> -methyl <i>N</i> -thiocarboxyanhydrosulfide synthesis.....	176
4.5.3 <i>N</i> -butyl <i>N</i> -thiocarboxyanhydrosulfide synthesis.....	177
4.5.4 General polymerization procedure of Me-NTA.....	178
4.5.5 General polymerization procedure of Bu-NTA.....	179
4.5.6 DL-methionine <i>N</i> -thiocarboxyanhydrosulfide synthesis.....	181
4.5.7 General polymerization procedure of DL-methionine NTA.....	182
4.5.8 Methylation of poly(DL-methionine).....	183
4.5.9 Synthesis of $\gamma$ -benzyl-L-glutamate <i>N</i> -thiocarboxyanhydrosulfide (BLG NTA).....	183

4.5.10 Solid state polymerization of BLG NTA.....	184
4.6 Supplemental data for Chapter IV.....	185
CHAPTER V. CONCLUSIONS AND FUTURE WORK.....	189
REFERENCES.....	193
APPENDIX – COPYRIGHT PERMISSIONS.....	224
VITA.....	238

## LIST OF TABLES

Table 2.1. Molecular weight characterization data for a series of PPLG obtained from the ROP of PLG NCA using benzylamine initiator.....	67
Table 2.2. Molecular weight characterization data for a series of PPDLG obtained from the ROP of PDLG NCA.....	68
Table 2.3. Initial binding rate constants ( $k_i$ ) for a series of PPLG and PPDLG mannose.....	74
Table 2.4. Binding stoichiometry data for a series of helical and random coil glycopolypeptides.....	80
Table 3.1. TMG-mediated polymerization of Bu-NCAs to afford poly( <i>N</i> -butyl glycine)s in the presence or absence of benzyl alcohol in different solvents.....	102
Table 3.2. Molecular weight analysis of PNBGs obtained by ROP of Bu-NCAs using TMG initiators at varying $[M]_0:[TMG]_0$ ratio.....	103
Table 3.3. ROP of Bu-NCA in the presence of equimolar BnOH and TMG.....	105
Table 3.4. Chain extension of PNBG polymers prepared by TMG-mediated polymerization of Bu-NCA using BnOH initiators.....	106
Table 3.5. The observed polymerization rate constant ( $k_{obs}$ ) for BnOH-initiated polymerization of Bu-NCA with varying BnOH loadings and constant initial monomer and TMG concentrations.....	108
Table 3.6. The observed polymerization rate constant ( $k_{obs}$ ) for a series of BnOH-initiated polymerization of Bu-NCA with varying TMG loadings and constant initial monomer and BnOH concentrations.....	108
Table 3.7. ROP of Bu-NCA in the presence of TMG and different alcohols.....	111
Table 3.8. Change of imine and hydroxyl proton chemical shifts upon formation of hydrogen bonding complexes between TMG and various alcohols/phenol/acids and the pKa of the alcohols/phenol/acid.....	112
Table 3.9. Polymerization of Bu-NCA by sodium phenoxide.....	122
Table 3.10. TMG-promoted polymerization of Bu-NCA using a hydroxyl-terminated PEG ( $M_n = 550 \text{ g}\cdot\text{mol}^{-1}$ , PDI=1.04) macroinitiator.....	125
Table 4.1. Molecular weight data for TMG initiated ROP of Me-NTA.....	147
Table 4.2. Chain extension of polysarcosine prepared by TMG-mediated polymerization of Me-NTA.....	149



Table 4.3. Molecular weight characterization data for benzylamine initiated ROP of Me-NTA.....	152
Table 4.4. Molecular weight characterization data for the ROP of Bu-NTA using benzylamine and TMG initiators.....	157
Table 4.5. Molecular weight characterization data for a series of PNBGs obtained via benzyl alkoxide initiator.....	158
Table 4.6. Molecular weight characterization data for benzylamine/TBD initiated ROP of BLG NTA.....	163
Table 4.7. Molecular weight data of PBLG polymerized at varying $[M]_0$ .....	166
Table 4.8. Molecular weight characterization data for the ROP of DL-methionine NTA initiated by BnNH <sub>2</sub> or TMG.....	169
Table 4.9. Molecular weight characterization data for the solid state ROP of BLG-NTA using hexylamine initiator.....	171
Table 4.10. Molecular weight characterization from the solid state ROP of BLG NTA using TMG initiator.....	173
Table 4.11. Molecular weight characterization data for a series of poly(Z-lysine)s obtained from the solid state ROP of Z-lysine NTA.....	174
Table C1. Molecular weight characterization data for HMDS initiated ROP of Me-NTA.....	185
Table C2. Molecular weight characterization for a series of polymerizations of Me-NTA initiated by various organobases and organocatalysts.....	186

## LIST OF FIGURES

Figure 1.1. Generic structures of polypeptides and polypeptoids, the two types of peptidomimetic polymers covered in this work.....	1
Figure 1.2. Generic scheme detailing the stepwise process of peptide synthesis using solid resin anchors.....	5
Figure 1.3. Proposed reaction pathway of AAMMA in the ROP of amino acid based NCA monomers via initiation by TETA. Reprinted from Reference 120 with permission from the American Chemical Society. Copyright 2015 American Chemical Society.....	23
Figure 1.4. Scheme showing the solid phase synthesis of oligopeptoids using the submonomer method.....	32
Figure 1.5. Generic structure of R-NCA and the many alkyl side chain variations that have been synthesized.....	34
Figure 1.6. MALDI TOF MS spectrum of the synthesis of a tetrablock copolypeptoid through stepwise monomer addition. Reproduced from Reference 155 with permission of John Wiley & Sons.....	36
Figure 2.1. (A) Binding of ConA to a glycopolymer with maximum binding epitope density. Mannose binding epitopes are represented by the semicircles. (B) Binding of ConA to a glycopolymer with lower binding epitope density and spacing in between each of the binding species. Though example A binds more ConA, the example in B displays more effective binding with respect to a per mannose residue basis (mannose/ConA) due to usage of all of the available mannose receptors versus that of A where a number of mannosides are rendered inaccessible due to sterics.....	55
Figure 2.2. Diagrams outlining the various synthetic strategies to access glycopolypeptides in the ROP of NCAs.....	58
Figure 2.3. <sup>1</sup> H NMR spectrum of PPLG ([M] <sub>0</sub> :[I] <sub>0</sub> =100:1) (blue) collected in CDCl <sub>3</sub> and subsequent PPLG mannose (red) and PPLG mannose-galactose (green) collected in D <sub>2</sub> O.....	70
Figure 2.4. (A) CD spectra for a series of PPLG mannose glycopolypeptides. Samples were prepared at 1.0 mg/mL in HEPES buffered saline. Each curve is the average of three runs. (B) Plot of percent helicity versus DP <sub>n</sub> . Percent helicity values were calculated using the formula ( $([\theta_{222}] + 3000) / 39000$ ).....	71
Figure 2.5. CD spectra for a series of PPDLG mannose glycopolypeptides. Samples were prepared at 1.0 mg/mL in HEPES buffered saline. Each curve is the average of three runs.....	71
Figure 2.6. Glycoclustering due to ConA and the glycopolypeptide forming highly ordered species and a diagram of ConA indicating the distance between binding sites.....	72

Figure 2.7. Plot of $k_i$ versus $DP_n$ obtained from turbidity assay experiments for helical (black) and random coil (red) glycopolypeptides. The $k_i$ for L 174 is not plotted. Some error bars are smaller than the plot markers.....	73
Figure 2.8. Plot of binding stoichiometry versus $DP_n$ obtained from quantitative precipitation assay experiments for helical (black) and random coil (red) glycopolypeptides. Some error bars are smaller than the plot markers.....	79
Figure 2.9. Plot of mannose/ConA versus $DP_n$ obtained from quantitative precipitation assay experiments for helical (black) and random coil (red) glycopolypeptides. Some error bars are smaller than the plot markers.....	80
Figure 2.10. Turbidity curves obtained from the analysis of a series of PPLG mannose/galactose at varying epitope densities ( $DP_n=105$ ) in the presence of ConA (mannose:ConA=50:1) at 420 nm. The shown curves are the averages of three independent runs.....	82
Figure 2.11. DLS results of three separate runs of PPLG mannose ( $DP_n=13$ ) taken in HEPES buffered saline at a concentration of 1 mg/mL. Correlograms for each respective run are shown in the inset.....	83
Figure 2.12. DLS results of three separate runs of PPDLG mannose ( $DP_n=103$ ) taken in HEPES buffered saline at a concentration of 1 mg/mL. Correlograms for each respective run are shown in the inset.....	84
Figure 2.13. DLS results of three separate runs for PPLG mannose ( $DP_n=23$ ) bearing no cationic charge on the side chains (A) and 9% cationic charge (B) as determined by $^1H$ NMR. Samples were prepared at concentrations of 1 mg/mL in HEPES buffered saline. Correlograms for each respective run are shown in the insets.....	86
Figure 2.14. $^1H$ NMR spectrum of PLG-NCA collected in $CDCl_3$ .....	89
Figure 2.15. $^{13}C\{^1H\}$ NMR spectrum of PLG NCA collected in $CDCl_3$ .....	90
Figure A1. Plots of absorption at 420 nm versus time obtained from turbidity assay experiments with helical glycopolypeptides. The shown curves are the averages of three runs.....	92
Figure A2. Plots of absorption at 420 nm versus time obtained from turbidity assay experiments with random coil glycopolypeptides. The shown curves are the averages of three runs.....	92
Figure A3. Sigmoidal plots obtained from quantitative precipitation assay experiments with helical glycopolypeptides. The shown curves are the averages of two independent experiments. An inset of an exemplary curve plotted in the linear scale is included for reference. Some error bars are smaller than the plot markers.....	93

Figure A4. Sigmoidal plots obtained from quantitative precipitation assay experiments with random coil glycopolypeptides. The shown curves are the averages of two independent experiments. An inset of an exemplary curve plotted in the linear scale is included for reference. Some error bars are smaller than the plot markers.....93

Figure 3.1.  $^1\text{H}$  NMR spectrum of PNBG obtained via ROP of Bu-NCA with benzyl alcohol initiator and TMG promotor ( $[\text{M}]_0:[\text{BnOH}]_0=25:1$ ). Polymerization was performed at  $[\text{M}]_0=1.0$  M,  $50$  °C, in THF for 24 h.  $[\text{TMG}]_0$  was held at  $0.6$  mM. The spectrum was collected in  $\text{CD}_2\text{Cl}_2$ ..... 99

Figure 3.2. MALDI-TOF MS spectra of a low molecular weight PNBG obtained by BnOH-initiated polymerization of Bu-NCA in the presence of TMG under the standard conditions ( $[\text{M}]_0=1.0$  M,  $[\text{TMG}]_0=0.6$  mM,  $[\text{M}]_0:[\text{BnOH}]_0=25:1$ , THF,  $50$  °C) and the PNBG polymer structures corresponding to the respective mass ions. CHCA was used as the matrix.....102

Figure 3.3. SEC-DRI chromatograms of PNBG polymers obtained by ROP of Bu-NCAs in the presence of benzyl alcohol and TMG with increasing  $[\text{M}]_0:[\text{BnOH}]_0$  ratio and a constant initial monomer and TMG concentration ( $[\text{M}]_0=1.0$  M and  $[\text{TMG}]_0=0.6$  mM) in  $50$  °C THF.....102

Figure 3.4. SEC-DRI chromatograms of PNBG polymers obtained from the ROP of Bu-NCA using TMG as initiators ( $[\text{M}]_0=1.0$  M,  $50$  °C, THF)..... 104

Figure 3.5.  $^1\text{H}$  NMR spectrum of PNBGs obtained via ROP of Bu-NCA with TMG initiator ( $[\text{M}]_0:[\text{TMG}]_0=25:1$ ). Polymerization was performed at  $[\text{M}]_0=1.0$  M,  $50$  °C, in THF for at least 24 h. The spectrum was collected in  $\text{CDCl}_3$ .....104

Figure 3.6. MALDI-TOF MS spectra of PNBGs obtained from ROP of Bu-NCA using TMG initiator alone ( $[\text{M}]_0:[\text{TMG}]_0=25:1$ ,  $[\text{M}]_0=1.0$  M,  $50$  °C, THF). CHCA matrix was used in sample preparation.....105

Figure 3.7. (A) Plots of polymer molecular weight ( $M_n$ ) and molecular weight distribution (PDI) versus conversion for the TMG-mediated polymerization of Bu-NCA using BnOH initiators ( $[\text{M}]_0:[\text{BnOH}]_0:[\text{TMG}]_0=50:1:0.03$ ,  $[\text{M}]_0=1.0$  M, THF,  $50$  °C)  $R^2=0.98$ . (B) SEC-MALS-DRI chromatograms from the chain extension experiment (first reaction:  $[\text{M}]_0:[\text{BnOH}]_0:[\text{TMG}]_0=50:1:0.03$ ,  $[\text{M}]_0=1.0$  M, THF,  $50$  °C; chain extension reaction:  $[\text{M}]_0:[\text{BnOH}]_0=100:1$ ).....106

Figure 3.8. (A) Plots of  $\ln([\text{M}]_0:[\text{M}])$  versus reaction time for the TMG-promoted polymerization of Bu-NCA using BnOH initiators at various initial BnOH loading ( $[\text{M}]_0:[\text{BnOH}]_0=25:1-100:1$ ,  $[\text{M}]_0=0.15$  M,  $[\text{TMG}]_0=90$   $\mu\text{M}$ , THF- $d_8$ ,  $50$  °C); (B) plots of  $\ln([\text{M}]_0:[\text{M}])$  versus reaction time for the TMG-promoted polymerization of Bu-NCA using BnOH initiators at various initial TMG loading; (C) plots of  $k_{\text{obs}}$  versus  $[\text{BnOH}]_0$  for the TMG-promoted polymerization of Bu-NCA using BnOH initiators; (D) plots of  $\ln([\text{M}]_0:[\text{M}])$  versus reaction time for the  $\text{BnNH}_2$ -initiated polymerization of Bu-NCA with (red) or without TMG present (black) ( $[\text{M}]_0:[\text{BnNH}_2]_0=50:1$ ,  $[\text{M}]_0=0.15$  M,  $[\text{TMG}]_0=90$  or  $0$   $\mu\text{M}$ , THF- $d_8$ ,  $50$  °C)..... 107

Figure 3.9. ESI-MS spectrum of the reaction product from the 1:1 (molar ratio) reaction of Bu-NCA and TMG in 50 °C THF. The spectrum was obtained in positive ionization mode.....	117
Figure 3.10. <sup>1</sup> H NMR spectrum of the reaction product from the 1:1 (molar ratio) reaction of Bu-NCA and TMG in 50 °C THF. The spectrum was collected in CDCl <sub>3</sub> solvent.....	117
Figure 3.11. ESI-MS spectrum of the reaction product from the 1:1:1 (molar ratio) reaction of Bu-NCA, TMG and BnOH in 50 °C THF. The spectrum was obtained in positive ionization mode.....	118
Figure 3.12. <sup>1</sup> H NMR spectrum of the reaction product from the 1:1:1 (molar ratio) reaction of Bu-NCA, TMG and BnOH in 50 °C THF. The spectrum was collected in CDCl <sub>3</sub> solvent.....	118
Figure 3.13. Overlaid <sup>1</sup> H NMR spectra of benzyl alcohol (red), TMG (green), and an equimolar mixture of benzyl alcohol and TMG (blue) in THF-d <sub>8</sub> . The spectra were collected at 0.5 M concentration for the respective compounds.....	120
Figure 3.14. Overlaid <sup>1</sup> H NMR spectra of the 1:1 mixture of benzyl alcohol and TMG at 27 °C (blue) and 50 °C (red) in THF-d <sub>8</sub> . The spectra were collected at 0.5 M concentration.....	121
Figure 3.15. Reaction scheme of TMG-promoted ROP of Bu-NCA using a PEG-OH ( $M_n = 550 \text{ g}\cdot\text{mol}^{-1}$ ) macroinitiator and SEC chromatograms of the PEG-OH precursor and the PEG- <i>b</i> -PNBG hetero-block copolymers obtained from the reaction ([M] <sub>0</sub> : [PEG-OH] <sub>0</sub> = 25:1-100:1).....	122
Figure 3.16. Representative MALDI-TOF MS spectra of the PEG- <i>b</i> -PNBG block copolymers obtained from the TMG-promoted ROP of Bu-NCAs using PEG ( $M_n = 550 \text{ g}\cdot\text{mol}^{-1}$ , PDI=1.04) macroinitiator ([M] <sub>0</sub> : [PEG-OH] <sub>0</sub> = 25:1, [M] <sub>0</sub> = 1.0 M, [TMG] <sub>0</sub> = 0.6 mM).....	124
Figure 3.17. <sup>1</sup> H NMR spectrum of the PEG- <i>b</i> -PNBG block copolymers obtained from the TMG-promoted ROP of Bu-NCAs using PEG ( $M_n = 550 \text{ g}\cdot\text{mol}^{-1}$ , PDI=1.04) macroinitiator ([M] <sub>0</sub> : [PEG-OH] <sub>0</sub> = 25:1, [M] <sub>0</sub> = 1.0 M, [TMG] <sub>0</sub> = 0.6 mM).....	125
Figure 3.18. <sup>1</sup> H NMR spectrum of Bu-NCA collected in CDCl <sub>3</sub> .....	130
Figure 3.19. <sup>13</sup> C{ <sup>1</sup> H} NMR spectrum of Bu-NCA collected in CDCl <sub>3</sub> .....	130
Figure B1. MALDI-TOF MS spectra of the PNBG polymers obtained via TMG-promoted ROP of Bu-NCA with methanol initiators ([M] <sub>0</sub> : [MeOH] <sub>0</sub> = 25:1, [M] <sub>0</sub> = 1.0 M, [TMG] <sub>0</sub> = 0.6 mM).....	131
Figure B2. MALDI-TOF MS spectra of the PNBG polymers obtained by TMG-promoted ROP of Bu-NCAs using ethanol initiators ([M] <sub>0</sub> : [EtOH] <sub>0</sub> = 25:1, [M] <sub>0</sub> = 1.0 M, [TMG] <sub>0</sub> = 0.6 mM).....	132

Figure B3. MALDI-TOF MS spectra of the PNBG polymers obtained by TMG-promoted ROP of Bu-NCAs using <i>n</i> -propanol initiators ( $[M]_0:[n\text{-PrOH}]_0 = 25:1$ , $[M]_0 = 1.0$ M, $[TMG]_0 = 0.6$ mM).....	132
Figure B4. MALDI-TOF MS spectra of the PNBG polymers obtained by TMG-promoted ROP of Bu-NCAs using 2-methoxyethanol initiators ( $[M]_0:[2\text{-MeOEtOH}]_0 = 25:1$ , $[M]_0 = 1.0$ M, $[TMG]_0 = 0.6$ mM).....	133
Figure B5. Overlaid $^1\text{H}$ NMR spectra of TMG (red), TMG (green), and the 1:1 mixture of benzoic acid and TMG (blue). Spectra were collected in THF- $d_8$ at 0.5 M concentrations for the respective compounds. THF- $d_8$ is denoted by the asterisks (*).....	133
Figure B6. Overlaid $^1\text{H}$ NMR spectra of methanol (red), TMG (green), and the 1:1 mixture of both compounds (blue) in THF- $d_8$ . Spectra were collected at 0.5 M concentrations for the respective compounds. THF- $d_8$ is denoted by the asterisks (*).....	134
Figure B7. Overlaid $^1\text{H}$ NMR spectra of ethanol (red), TMG (green), and the 1:1 mixture of both compounds (blue) in THF- $d_8$ . Spectra were collected at 0.5 M concentrations for the respective compounds. THF- $d_8$ is denoted by the asterisks (*).....	134
Figure B8. Overlaid $^1\text{H}$ NMR spectra of 2-methoxyethanol (red), TMG (green), and the 1:1 mixture of both compounds (blue) in THF- $d_8$ . Spectra were collected at 0.5 M concentrations for the respective compounds. THF- $d_8$ is denoted by the asterisks (*).....	135
Figure B9. Overlaid $^1\text{H}$ NMR spectra of <i>n</i> -propanol (red), TMG (green), and the 1:1 mixture of both compounds (blue) in THF- $d_8$ . Spectra were collected at 0.5 M concentrations for the respective compounds. THF- $d_8$ is denoted by the asterisks (*).....	135
Figure B10. Overlaid $^1\text{H}$ NMR spectra of 2,2,2-trifluoroethanol (red), TMG (green), and the 1:1 mixture of both compounds (blue) in THF- $d_8$ . Spectra were collected at 0.5 M concentrations for the respective compounds. THF- $d_8$ is denoted by the asterisks (*).....	136
Figure B11. Overlaid $^1\text{H}$ NMR spectra of isopropyl alcohol (red), TMG (green), and the 1:1 mixture of both compounds (blue) in THF- $d_8$ . Spectra were collected at 0.5 M concentrations for the respective compounds. THF- $d_8$ is denoted by the asterisks (*).....	136
Figure B12. Overlaid $^1\text{H}$ NMR spectra of <i>tert</i> -butyl alcohol (red), TMG (green), and the 1:1 mixture of both compounds (blue) in THF- $d_8$ . Spectra were collected at 0.5 M concentrations for the respective compounds. THF- $d_8$ is denoted by the asterisks (*).....	137

Figure B13. Overlaid $^1\text{H}$ NMR spectra of phenol (red), TMG (green), and the 1:1 mixture of both compounds (blue) in THF- $d_8$ . Spectra were collected at 0.5 M concentrations for the respective compounds. THF- $d_8$ is denoted by the asterisks (*).	137
Figure 4.1. Generic chemical structures of NCA and NTA monomers.	140
Figure 4.2. Chemical structures of the various initiators investigated in the ROP of Me-NTA.	145
Figure 4.3. SEC-DRI-MALS traces from the ROP of Me-NTA ( $[\text{M}]_0=1.0$ M) in the presence of TMG initiator with increasing $[\text{M}]_0:[\text{TMG}]_0$ ratios in $\text{CH}_2\text{Cl}_2$ at ambient temperature.	147
Figure 4.4. MALDI TOF MS spectrum of TMG initiated ROP of Me-NTA ( $[\text{M}]_0:[\text{TMG}]_0 = 25:1$ , $[\text{M}]_0 = 1.0$ M).	148
Figure 4.5. $^1\text{H}$ NMR spectrum of polysarcosine obtained from the ROP of Me-NTA with TMG initiator ( $[\text{M}]_0:[\text{TMG}]_0=25:1$ , $[\text{M}]_0=1.0$ M in $\text{CH}_2\text{Cl}_2$ ). The spectrum was collected in $\text{D}_2\text{O}$ .	148
Figure 4.6. FTIR spectra of a low molecular weight polysarcosine synthesized via the ROP of Me-NTA using TMG initiator ( $[\text{M}]_0:[\text{TMG}]_0=25:1$ ) and TMG.	149
Figure 4.7. (A) SEC-MALS-DRI chromatograms from the chain extension experiment (first reaction: $[\text{M}]_0:[\text{TMG}]_0=100:1$ , $[\text{M}]_0=1.0$ M, DCM, 22 °C; chain extension reaction: $[\text{M}]_0:[\text{TMG}]_0=200:1$ ) (B) Plots of $M_n$ and PDI versus conversion for the ROP of Me-NTA using TMG initiator ( $[\text{M}]_0:[\text{TMG}]_0=100:1$ , $[\text{M}]_0=1.0$ M, 22°C in DCM).	151
Figure 4.8. SEC-DRI-MALS traces from the ROP of Me-NTA ( $[\text{M}]_0=1.0$ M) in the presence of benzylamine initiator with increasing $[\text{M}]_0:[\text{BnNH}_2]_0$ ratios in $\text{CH}_2\text{Cl}_2$ at ambient temperature for 18 h.	153
Figure 4.9. MALDI TOF MS spectrum of benzylamine initiated ROP of Me-NTA ( $[\text{M}]_0:[\text{BnNH}_2]_0 = 25:1$ , $[\text{M}]_0 = 1.0$ M).	153
Figure 4.10. $^1\text{H}$ NMR spectrum of polysarcosine obtained from the ROP of Me-NTA with benzylamine initiator ( $[\text{M}]_0:[\text{BnNH}_2]_0=25:1$ , $[\text{M}]_0=1.0$ M in $\text{CH}_2\text{Cl}_2$ ). The spectrum was collected in $\text{D}_2\text{O}$ .	154
Figure 4.11. $^1\text{H}$ NMR spectra taken in $\text{CDCl}_3$ of Me-NTA at $t_0$ , 2 weeks, and 4 weeks exposed to the ambient air. “ $t_0$ ” refers to the time at which the synthesis and purification of the particular batch of monomer used in the study was complete.	156
Figure 4.12. SEC-MALS-DRI traces from the ROP of Bu-NTA with $\text{BnONa}$ initiator ( $[\text{M}]_0=1.0$ M) in 50 °C THF.	159

Figure 4.13. $^1\text{H}$ NMR spectrum of PNBG obtained from the ROP of Bu-NTA with benzyl alkoxide ( $[\text{M}]_0:[\text{BnONa}]_0=50:1$ , $[\text{M}]_0=0.5$ M in THF, $50^\circ\text{C}$ ). The spectrum was collected in $\text{CDCl}_3$ .....	159
Figure 4.14. Crystal structure of BLG NTA as obtained via X-ray crystallography.....	163
Figure 4.15. Plot of conversion percent versus reaction time in the solution state ROP of BLG-NTA at various $[\text{M}]_0$ . All polymerizations were carried out at $[\text{M}]_0:[\text{I}]_0=80:1$ at $50^\circ\text{C}$ in dioxane using hexylamine initiator unless otherwise noted. Conversions were analyzed $^1\text{H}$ NMR.....	165
Figure 4.16. SEC-DRI-MALS traces of the ROP of BLG-NTA at varying monomer concentrations after 48 h ( $[\text{M}]_0:[\text{I}]_0=80:1$ at $50^\circ\text{C}$ in dioxane). Monomer conversion percentages at 48 h are shown in Table 4.7.....	165
Figure 4.17. $^1\text{H}$ NMR spectrum of benzylamine initiated poly(DL-methionine) ( $[\text{M}]_0:[\text{BnNH}_2]_0=25:1$ , $[\text{M}]_0=0.5$ M). The spectrum was collected in deuterated trifluoroacetic acid.....	170
Figure 4.18. $^1\text{H}$ NMR spectrum of poly(S,S-dimethyl-DL-methionine) obtained from the methylation of poly(DL-methionine) ( $[\text{M}]_0:[\text{I}]_0=25:1$ , $[\text{M}]_0=0.5$ M) with iodomethane followed by dialysis and lyophilization. The spectrum was collected in $\text{D}_2\text{O}$ .....	172
Figure 4.19. (A) SEC-DRI-MALS traces from the solid state polymerization of BLG-NTA using hexylamine initiator. (B) SEC-DRI-MALS traces from the solid state polymerization of BLG-NTA using TMG initiator.....	173
Figure 4.20. Plots of molecular weight ( $M_n$ ) and PDI versus conversion for the solid-state polymerization ( $[\text{M}]_0:[\text{I}]_0=80:1$ , $[\text{M}]_0=0.5$ M, hexanes, $50^\circ\text{C}$ , $R^2=0.99$ ) of BLG NTA using hexylamine initiator.....	174
Figure 4.21. $^1\text{H}$ NMR spectrum of Me-NTA in $\text{CDCl}_3$ .....	178
Figure 4.22. $^{13}\text{C}\{^1\text{H}\}$ NMR spectrum of Me-NTA in $\text{CDCl}_3$ .....	179
Figure 4.23. $^1\text{H}$ NMR spectrum of Bu-NTA collected in $\text{CDCl}_3$ .....	180
Figure 4.24. $^{13}\text{C}\{^1\text{H}\}$ NMR spectrum of Bu-NTA obtained in $\text{CDCl}_3$ .....	180
Figure 4.25. $^1\text{H}$ NMR spectrum of DL-methionine NTA collected in $\text{CDCl}_3$ .....	181
Figure 4.26. $^{13}\text{C}\{^1\text{H}\}$ NMR spectrum of DL-methionine NTA collected in $\text{CDCl}_3$ ...	182
Figure 4.27. $^1\text{H}$ NMR spectrum of BLG-NTA collected in $\text{CDCl}_3$ .....	184



Figure 4.28. $^{13}\text{C}\{^1\text{H}\}$ NMR spectrum of BLG NTA collected in $\text{CDCl}_3$ .....	185
Figure C1. $^1\text{H}$ NMR spectrum of polysarcosine obtained from the ROP of Me-NTA with NHC initiator ( $[\text{M}]_0:[\text{NHC}]_0=25:1$ , $[\text{M}]_0=1.0$ M in $\text{CH}_2\text{Cl}_2$ ). The spectrum was collected in $\text{D}_2\text{O}$ .....	187
Figure C2. SEC-DRI-MALS chromatograms for a series of poly(Z-lysine)s obtained from the solid state ROP of Z-Lys NTA using hexylamine initiator ( $[\text{M}]_0=0.2$ M, $80^\circ\text{C}$ , 48 h in heptane).....	188

## LIST OF SCHEMES

Scheme 1.1. Generic synthesis of an $\alpha$ -amino acid based NCA via the Fuchs-Farthing method of phosgenation (A) or halogenating agents (B) and the resulting impurities from each method.....	7
Scheme 1.2. Generic primary amine initiated ROP of an $\alpha$ -amino acid based NCA.....	9
Scheme 1.3. (A) Formation of urea species via nucleophilic attack on C2 (B) formation of isocyanate via deprotonation of $-\text{NH}$ and subsequent rearrangement to hydantoic acid.....	12
Scheme 1.4. Generic scheme of the formation of a terminal pyroglutamate species via backbiting.....	12
Scheme 1.5. Termination of a growing polypeptide chain via reaction with DMF and subsequent reinitiation by released dimethylamine.....	13
Scheme 1.6. Hydrolysis of NCAs.....	14
Scheme 1.7. Activated monomer mechanistic pathway for the ROP of a generic amino acid based NCA.....	15
Scheme 1.8. Proposed ROP mechanism of NCAs via transition metal catalysts.....	17
Scheme 1.9. Proposed mechanisms for the organosilane amine mediated ROP of NCAs. Reproduced from Reference 104 with permission of The Royal Society of Chemistry.....	20
Scheme 1.10. ROP of NCA monomers using PhS-TMS initiator.....	20
Scheme 1.11. "NAM"-like reaction pathway in the ROP of NCA monomers using rare earth borohydrides. Reproduced from Reference 111 with permission of John Wiley & Sons.....	21
Scheme 1.12. Functionalization of L-glutamic acid via esterification under acidic conditions for post-polymerization modification.....	24
Scheme 1.13. Post-polymerization modification reactions of poly(L-glutamic acid) derivatives.....	25
Scheme 1.14. Various post-polymerization transformations of poly( $\gamma$ -4-vinylbenzene-L-glutamate).....	26
Scheme 1.15. Thioether alkylation with various alkyl halides and triflates. Reprinted from Reference 134 with permission from the American Chemical Society. Copyright 2016 American Chemical Society.....	27

Scheme 1.16. Thiol-ene coupling of poly(L-cysteine).....	28
Scheme 1.17. Thiol-ene coupling of poly( <i>O</i> -pentenyl-L-serine).....	29
Scheme 1.18. (A) Thiol-ene coupling of poly(DL-allylglycine) and of poly(DL-propargyl glycine) (B) as described by Schlaad et al.....	29
Scheme 1.19. Generic synthesis of R-NCAs.....	33
Scheme 1.20. Synthesis of <i>N</i> -methyl glycine NCA.....	34
Scheme 1.21. Generic reaction mechanism of nucleophilic ZROP.....	38
Scheme 1.22. Synthesis of cyclic polypeptoids via ZROP of R-NCAs using NHC initiator.....	39
Scheme 1.23. Proposed mechanism of DBU-mediated ZROP of R-NCAs. Reprinted from Reference 19 with permission from the American Chemical Society. Copyright 2016 American Chemical Society.....	40
Scheme 1.24. Thiol-ene photochemical reaction between poly( <i>N</i> -allyl glycine) and a functional thio-moiety.....	42
Scheme 1.25. Post-polymerization modification reactions with poly( <i>N</i> -propargyl glycine).....	43
Scheme 1.26. ROP of <i>N</i> -Me NTA with PEGylated amines.....	45
Scheme 1.27. Homopolymerization (A) and random copolymerization (B) of sarcosine and <i>N</i> -butyl NTAs using rare earth borohydride initiators.....	45
Scheme 2.1. Synthesis of sialic acid based glycopolymers via amidation.....	50
Scheme 2.2. ROMP of glycosylated norbornene.....	50
Scheme 2.3. Synthesis of galactose functionalized L-lysine NCA as reported by Deming et al.....	59
Scheme 2.4. Post-polymerization synthesis of a glycopolypeptide via the reaction between poly(lysine) and gluconolactone as described by Feng et al.....	60
Scheme 2.5. Glycopolypeptide synthesis via thiourea linkage formation as described by Li et al.....	61
Scheme 2.6. Synthesis of PLG-NCA from L-glutamic acid.....	66
Scheme 2.7. Polymerization of PLG-NCA via benzylamine initiator.....	67
Scheme 2.8. Glycosylation of PPLG via CuAAC using copper wire method.....	68
Scheme 2.9. Glycosylation of PPLG with varying mannose and galactose loadings..	81

Scheme 2.10. Synthesis of cationically charged glycopolypeptides via CuAAC.....	85
Scheme 3.1. ROP of Bu-NCA via BnOH initiator and TMG organocatalyst.....	98
Scheme 3.2. The mechanism of the primary amine-initiated ROP of Bu-NCA.....	114
Scheme 3.3. Three proposed initiation mechanisms of the TMG-promoted ROP of Bu-NCA using alcohol initiators.....	115
Scheme 3.4. Proposed propagation pathways following different initiating mechanisms shown in Scheme 3.3.....	116
Scheme 3.5. Proposed reaction pathways for the formation of the reaction products from the 1:1 (molar ratio) reaction of Bu-NCA and TMG or the 1:1:1 reaction of Bu-NCA, TMG and BnOH in 50 °C THF.....	119
Scheme 4.1. Synthesis of Me-NTA.....	143
Scheme 4.2. Generic polymerization of Me-NTA.....	144
Scheme 4.3. Polymerization of Bu-NTA.....	156
Scheme 4.4. Synthesis of BLG NTA.....	161
Scheme 4.5. Proposed dealkylation and racemization mechanisms of amino acid based NTAs.....	162
Scheme 4.6. Synthesis of DL-methionine NTA.....	166
Scheme 4.7. Polymerization of DL-methionine NTA.....	167
Scheme 4.8. Methylation of poly(DL-methionine) with iodomethane.....	170
Scheme 4.9. Solid-state polymerization of BLG NTA using hexylamine initiator...	172
Scheme 4.10. ROP of Z-lysine NTA using hexylamine initiator via solid state methods.....	175

## LIST OF ACRONYMS AND ABBREVIATIONS

AAMMA	Accelerated amine mechanism through monomer activation
AMM	Activated monomer mechanism
APTES	(3-aminopropyl)triethoxysilane
BBB	Blood brain barrier
BnSH	Benzylmercaptan
Cbz	<i>N</i> -benzyl chloroformate
CD	Circular dichroism
ConA	Concanavalin A
CuAAC	Copper mediated alkyne/azide cycloaddition
DBU	1,8-Diazabicycloundec-7-ene
DCM	Dichloromethane
DLS	Dynamic light scattering
DMF	Dimethylformamide
DMSO	Dimethylsulfoxide
DP <sub>n</sub>	Number average degree of polymerization
ESI-MS	Electrospray ionization mass spectroscopy
Fmoc	Fluorenylmethyloxycarbonyl
FTIR	Fourier transform infrared spectroscopy
GRGDS	Pentapeptide composed of glycine-arginine-glycine-aspartic acid-serine (in that specific order)
HEPES	4-(2-hydroxyethyl)-1-piperazineethanesulfonic acid
HMDS	Hexamethyldisilazane
MALDI-TOF MS	Matrix assisted light desorption ionization time of flight mass spectroscopy

$M_n$	Number average molecular weight
NCA	<i>N</i> -carboxyanhydride
NHC	<i>N</i> -heterocyclic carbene
NTA	<i>N</i> -thiocarboxyanhydrosulfide
NMR	Nuclear magnetic resonance spectroscopy
PDI	Polydispersity index
PDLG	$\gamma$ -propargyl-DL-glutamate
PEG	Poly(ethylene glycol)
PhS-TMS	Phenyl trimethyl sulfide
PLG	$\gamma$ -propargyl-L-glutamate
PMDETA	<i>N,N,N',N',N''</i> -pentamethyldiethylenetriamine
PNBG	Poly( <i>N</i> -butyl glycine)
PNMG	Poly( <i>N</i> -methyl glycine)
PPDLG	Poly( $\gamma$ -propargyl-DL-glutamate)
PPLG	Poly( $\gamma$ -propargyl-L-glutamate)
PS	Poly(styrene)
R-NCA	<i>N</i> -alkyl substituted NCA
ROMP	Ring-opening metathesis polymerization
ROP	Ring-opening polymerization
SEC-MALS-DRI	Size exclusion chromatography equipped with multiangle light scattering and differential refractive index detectors
TETA	Triethylenetetramine
TFA	Trifluoroacetic acid
THF	Tetrahydrofuran
TMG	1,1,3,3-tetramethylguanidine

TMS	Trimethylsilane
TREN	Triethylaminetriamine
UV- <i>vis</i>	Ultraviolet visible spectroscopy
XAA	<i>S</i> -ethoxythiocarbonyl mercaptoacetic acid
Z-Lys	$\epsilon$ -carbobenzyloxy-L-lysine
ZROP	Zwitterionic ring-opening polymerization

## ABSTRACT

This work is focused on the design, synthesis and characterization of polypeptide and polypeptoid polymers. The former are composed of amino acid repeat units and possess intramolecular hydrogen bonding interactions allowing for the self-assembly into well-defined secondary structures (e.g.  $\alpha$ -helix). Polypeptoids are based on *N*-alkyl substituted glycine and lack intramolecular hydrogen bonding interactions, resulting in enhanced proteolytic stability and thermal processability. Physicochemical properties of polypeptoids are strongly dependent on the side chain structures, allow for control of the solubility, crystallinity, and conformation of the polymers. Well-defined polypeptides and polypeptoids are synthesized by the ring-opening polymerization (ROP) of their corresponding *N*-carboxyanhydride monomers (NCA), enabling access to high molecular weight polymers having well-defined structures.

Chapter II is focused on the synthesis and characterization of glycopolypeptides by a combination of controlled polymerization methods and copper mediated alkyne/azide cycloaddition chemistry and investigation of the multivalent binding of the glycopolypeptides with Concanavalin A, a model lectin. The focus of the study is on understanding the effect of molecular characteristics of the glycopolypeptides such as chain length, epitope density and backbone conformation on the binding kinetics and stoichiometry.

Chapter III is focused on the development of an organo-promoted ring-opening polymerization of *N*-substituted NCAs using alcohol initiators in conjunction with 1,1,3,3-tetramethylguanidine (TMG), an organic promotor. It was found that TMG activates the alcohols through hydrogen bonding interaction. The activated alcohol moieties can initiate the NCAs polymerizations under mild conditions. It was



further revealed that the electronic and steric characteristics of the alcohols impact the initiation efficiency and thus the polymerization behavior.

Chapter IV is focused on the synthesis and polymerization of *N*-thiocarboxyanhydrosulfides (NTA), a mercapto analog of the NCA. NTAs exhibited enhanced moisture-stability but reduced polymerization activities relative to the NCA analogs. Several initiating systems have been uncovered to enable controlled polymerization of NTAs in open air, allowing for access to high molecular weight polypeptides and polypeptoids.

# CHAPTER I. INTRODUCTION TO PEPTIDOMIMETIC POLYMERS

## 1.1 Overview of peptidomimetic polymers

Peptidomimetic polymers are a class of polymers that bear structural resemblance and possess similar properties to proteins (e.g. well-defined secondary structures, biodegradability via proteolysis). They are being explored for their use in biologically and medically relevant applications such as antifouling surfaces<sup>1-12</sup>, therapeutics<sup>13-15</sup>, cell transfection<sup>16</sup>, and drug delivery.<sup>17-20</sup> Non-biological or medically related applications of peptidomimetic polymers include the inhibition of ice crystal growth<sup>21</sup> and the inhibition of gas hydrate formation.<sup>22</sup> Because of their structural resemblance to proteins, peptidomimetic polymers have been demonstrated to exhibit low levels of cytotoxicity in vivo, making them good candidates as biomaterials.<sup>23</sup> The peptidomimetic polymers covered in this work include polypeptides, also referred to as poly( $\alpha$ -amino acids), and polypeptoids, also known as poly(*N*-alkyl substituted glycines). Both polypeptides and polypeptoids possess similar properties to proteins such as the ability to self-assemble into well-defined secondary structures ( $\alpha$ -helices,  $\beta$ -sheets,  $\Sigma$ -strands, polyproline I helices)<sup>24-28</sup> and their ability to undergo proteolysis and enzymatic degradation, of which polypeptoids are more resistant to than polypeptides.<sup>29-30</sup> The generic structures of the two types of peptidomimetic polymers covered in this work are shown in Figure 1.1.

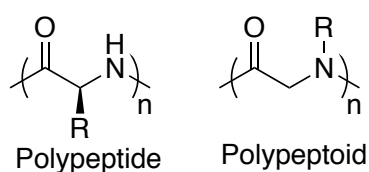


Figure 1.1. Generic structures of polypeptides and polypeptoids, the two types of peptidomimetic polymers covered in this work.

In order to be able to serve as a viable biomaterial, one set of criteria that a particular candidate polymer must exhibit is evidence of being biocompatible. One of the most commonly used polymers in various biomedical applications is poly(ethylene glycol) (PEG) as it has been reported to be relatively safe for medical applications.<sup>31</sup> However, there have been a number of issues and adverse effects that have been reported for PEG based materials such as complement activation, oxidative degradation, and the formation of reactive oxygen species.<sup>32-35</sup> Because of these reported issues, there is motivation to investigate alternative materials. Polypeptides and polypeptoids represent one avenue of alternative materials for application as biomaterials.

## **1.2 Polypeptides**

The composition of all proteins in all living organisms can be broken down into twenty amino acids. These amino acids can be sequenced in nearly infinite permutations and combinations via the peptide bond to give rise to the many proteins necessary for life. In nature, polypeptide chains of the proteins are synthesized by ribosomes during the process of translation. The polypeptides produced from translation eventually fold into the desired three dimensional structures, which are critical to their function. Poly( $\alpha$ -amino acid) polymers (a.k.a. polypeptide polymers) differing from proteins have much simplified primary sequence and are obtained by polymerization strategies. A unique characteristic of polypeptide polymers, unlike acrylic based polymers such as polystyrene and methacrylates, is the presence of hydrogen bonding interactions between the carbonyl and the amide nitrogen along the main chain backbone. These interactions contribute to the self-assembly of polypeptide polymers into well-defined secondary structures<sup>25</sup> which mimic those observed for naturally occurring proteins. These structures can consist of  $\alpha$ -helices or  $\beta$ -sheets. Polypeptides can be synthesized from a variety of naturally occurring or synthetic amino acids, allowing for tremendous molecular diversity in material design.

In addition, polypeptides are susceptible to proteolysis unlike acrylic polymers. In proteolysis, a polypeptide chain is broken down into smaller fragments<sup>36-41</sup> and eventually down to basic amino acids, providing a mechanism of material removal from the living system. The combination of these characteristics make polypeptides a suitable synthetic platform for biomedical applications.

### 1.2.1 Solid phase synthesis of polypeptides

One aspect to take into consideration in polypeptide synthesis is the sequencing of the amino acids on the chain. Exact sequences of amino acids are found in all living systems and incorrect sequences can contribute to mutations and other abnormalities. An exact sequence of amino acids may be necessary for a particular function or response such as that found in the pentapeptide GRGDS, which plays a role in integrin-mediated cell adhesion and acts as a cell binding peptide.<sup>42</sup> Changing the sequencing on this pentapeptide would most likely cause the molecule to behave differently and it may not participate in cell binding, which is observed in the exactly sequenced GRGDS. Monodisperse polypeptides with specific sequences can be synthesized using recombinant DNA techniques but these methods are time consuming and the synthetic procedures can be complicated.<sup>43-44</sup>

One method used in the synthesis of shorter yet exact peptide sequences is solid phase synthesis. Solid phase synthesis was developed by Robert Bruce Merrifield<sup>45</sup> for which he was awarded the 1984 Nobel Prize in Chemistry. The method relies on the stepwise addition of each successive amino acid starting with a solid support resin. One of the most commonly used resins is a polystyrene based resin known as “Merrifield resin” after the namesake of its creator and is used in the solid phase synthesis of peptide acids. Other resins also exist such as Rink resin, which is used when a C-terminal amide is desired in the final product but the process by which peptides are built stepwise

remains the same. The growing peptide chain is tethered onto the hydrophobic resin, preventing it from being washed away during filtration and washing steps. Solid phase peptide synthesis can be manually performed using a solid phase reactor or it can be programmed to be a fully automated process using a peptide synthesizer. Regardless of whether the process is automated or manual, the steps are the same for the addition of each additional amino acid sequence. A general scheme is shown in Figure 1.2. Starting from a labile amino acid tethered onto the resin, the exposed amine group of the amino acid is reacted with the successive amino acid. This successive amino acid has its own amine group protected to prevent additional peptide bond forming reactions from occurring. The protecting group (commonly Fmoc) is then removed exposing a labile amine allowing the addition of the next protected amino acid. This process is repeated until the desired oligopeptide is complete. The peptide is then cleaved from the solid phase resin support under acidic conditions (commonly trifluoroacetic acid). The advantage of solid phase peptide synthesis is that an exact sequence of amino acids and compositions can be obtained. However there are drawbacks. One big drawback is that the product yield and purity decrease as the chain length increases, thus making it more difficult to access longer peptide species with adequate purity. This is in part due to the increased likelihood that there would be incomplete deprotection of the amine. Deletions are also possible due to incomplete coupling. Another drawback is that excessive starting material and reagents are required to carry out the transformations, making the syntheses of oligopeptides costly.

### 1.2.2 Polypeptide synthesis via the ring-opening polymerization of *N*-carboxyanhydride monomers

Polymerizations of polypeptides would allow access to higher molecular weight polypeptides than those afforded by solid phase synthesis at large scales. However, polymerization methods sacrifice the exact sequencing of the amino acids in the peptide.

In order to obtain a well-defined system of polypeptides with adequate molecular weight control and narrow PDI, the use of a controlled or living polymerization method is

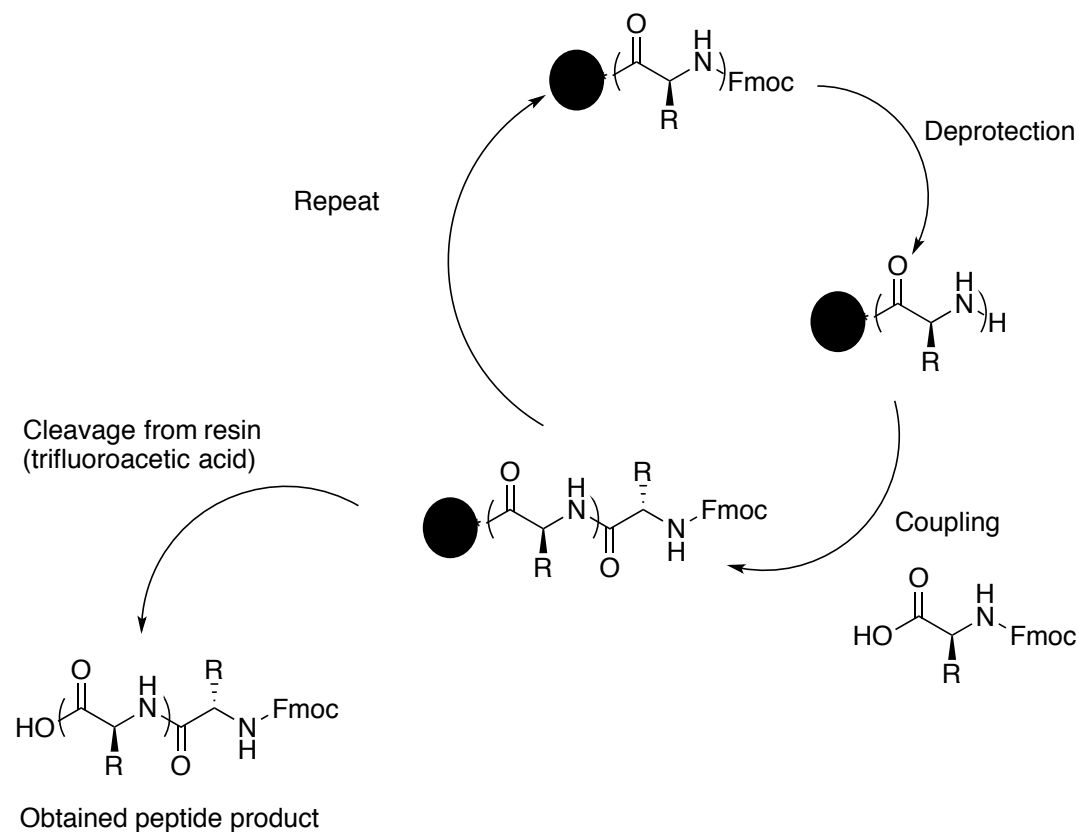


Figure 1.2. Generic scheme detailing the stepwise process of peptide synthesis using solid resin anchors.

required. Although it has been demonstrated that well-defined polypeptides can be synthesized via an alternate copolymerization of imine and carbon monoxide<sup>46</sup>, the ring-opening polymerization of heterocyclic compounds known as *N*-carboxyanhydrides is more commonly adopted among researchers.

Synthesis and purification of *N*-carboxyanhydride monomers. *N*-carboxyanhydrides (NCA) are commonly used in the polymerization of peptidomimetic polymers. NCAs were an unexpected discovery made by Herman Leuchs during the preparation of *N*-alkylcarbonyl amino acid chlorides for peptide synthesis.<sup>47-48</sup> The *N*-alkylcarbonyl amino acid chlorides were prepared via the reaction of the precursor with thionyl chloride.

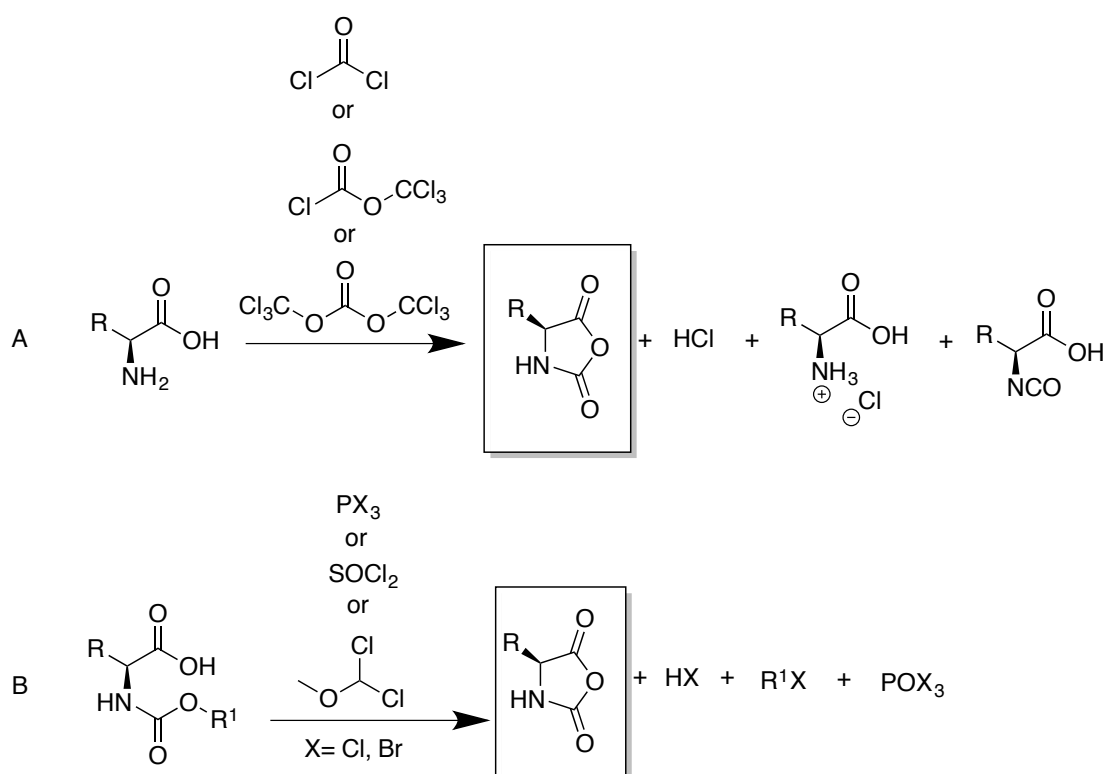
During heating and attempted vacuum distillation of the obtained product, it was observed that alkyl halide had been released and resulted in the cyclization of the amino acid derivative into the first NCA heterocycle. Polypeptides as well as polypeptoids, where the nitrogen atom along the peptide backbone is substituted with a non-proton group, are synthesized from NCAs via a ring-opening polymerization (ROP).

There are a number of ways to obtain amino acid-based NCA monomers. The route described above, the Leuchs method, uses  $\text{SOCl}_2$  as the cyclization agent. The Fuchs method of synthesis of NCA monomers involves the phosgenation of the amino acid precursor into the desired NCA via phosgene.<sup>49</sup> Farthing improved on the Fuchs method in 1950, suggesting that dry organic solvents be used in the syntheses of more hydrophilic NCAs due to their instability in aqueous media.<sup>50</sup> This method is now commonly referred to in the literature as the Fuchs-Farthing method. Phosgene was originally used to cyclize amino acids in the Fuchs-Farthing method but it is a gas making it more difficult to handle and its toxicity and use in chemical warfare has led to a number of alternatives to using phosgene directly. Alternative techniques using derivatives of phosgene such as diphosgene (liquid) and triphosgene (solid) have been developed and each of these has been used in the successful cyclization of amino acid based NCAs.<sup>51-53</sup> HCl is generated in each of these cyclization reactions whose presence can be harmful in a polymerization system and result in premature chain termination.<sup>48</sup> Additionally, chloride anions have also been shown to act as initiators in the ROP of NCAs, especially in DMF<sup>24</sup>, which would ultimately affect the resulting  $M_n$  and PDI. The presence of chloride anions could also potentially result in self-initiation.

High purity of the NCAs is essential to ensure a well-controlled polymerization behavior. There are a number of impurities that can form during the cyclization process with phosgene derivatives (i.e. diphosgene, triphosgene) or halogenating agents (e.g.

PCl<sub>3</sub>, PBr<sub>3</sub>, SOCl<sub>2</sub>) (Scheme 1.1) The formation of HCl and the effect of Cl<sup>-</sup> anions has already been noted previously. Through the Fuchs-Farthing method (Scheme 1.1, A), a number of other impurities aside from HCl are formed which include hydrochloride

Scheme 1.1. Generic synthesis of an  $\alpha$ -amino acid based NCA via the Fuchs-Farthing method of phosgenation (A) or halogenating agents (B) and the resulting impurities from each method



amino acid salts and 2-isocyanatocyl chlorides.<sup>54-55</sup> Additionally, oily residues with low volatility such as diphosgene can remain in the reaction if cyclization was incomplete or excess starting material was used. Other oily residues such as alkyl halides can form and remain present in the case of the cyclization of *N*-substituted monomer precursors (e.g. Boc, Cbz) (Scheme 1.1, B). The latter synthetic route is more relevant in the synthesis of *N*-alkyl substituted glycine based NCAs and will be discussed in subsequent sections.



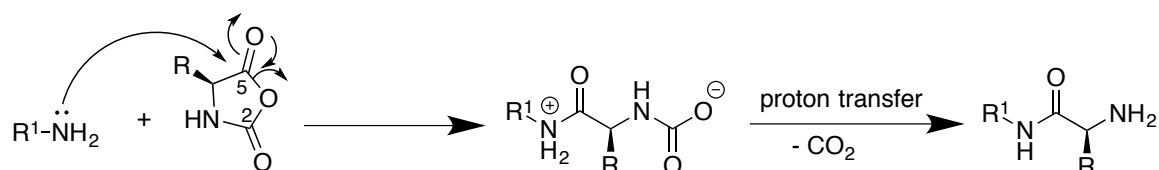
Recrystallization under anhydrous conditions is a commonly used method to purify amino acid based NCA monomers.<sup>48</sup> However, this process usually has to be repeated a number of times before NCA monomers of sufficient purity can be obtained for use in polymerizations. The addition of an organic base (i.e.  $\alpha$ -pinene)<sup>56</sup> was used in the synthesis of L-leucine NCA with diphosgene in order to remove the HCl that is formed during phosgenation but the resulting alkyl halide was difficult to remove. Another commonly used method used to purify amino acid based NCA monomers is a cold base wash, usually saturated sodium bicarbonate.<sup>53, 57-58</sup> While this can remove HCl and HCl amino acid salts, there is the inherent possibility that water, a possible initiator, can be introduced into the NCA crop, leading to premature initiation. Recently, column chromatography has been used as a possible method of NCA purification.<sup>42, 59-61</sup> Deming et al have demonstrated that column chromatography under anhydrous conditions can yield amino acid based NCA monomers that could be used to obtain high molecular weight polypeptides regardless of the hydrophilicity or hydrophobicity of the side chains and that the NCAs are tolerant and stable in silica gel.<sup>60</sup> Additionally, column chromatography is less time consuming than that of repeated recrystallizations. A number of less conventional methods have been also been used to purify NCA monomers ranging from celite filtration<sup>62</sup>, and rephosgenation to remove amino acid·HCl salts.<sup>55</sup>

Normal amine mechanism. The nucleophilic ROP of NCAs is perhaps the simplest route for polymerization. Primary amines are the most common initiators used for nucleophilic based ROP (Scheme 1.2). The reaction pathway for nucleophilic ROP or normal amine mechanism (NAM) as proposed by Waley and Watson<sup>63-64</sup> begins with an attack on the C5 position (Scheme 1.2), which results in the breaking of the weak anhydride bond forming a terminal carbamic acid. The carbamic acid subsequently undergoes a decarboxylation to form a new primary amine active chain end. This is the initiating

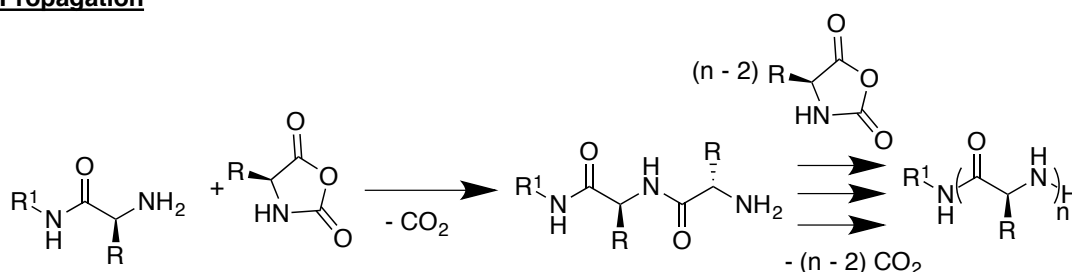
species and propagating events continue through the nucleophilic attack of subsequent NCA monomers by this primary amine chain end before a termination event suppresses the growing chain end.

Scheme 1.2. Generic primary amine initiated ROP of an  $\alpha$ -amino acid based NCA

**Initiation**



**Propagation**



One major drawback to NAM is that certain primary amines used in the reaction are basic enough to deprotonate the nitrogen atom of the NCA, leading to competition between NAM and what is known as the activated monomer mechanism (AMM).<sup>65</sup> AMM will be discussed in a subsequent section in this chapter. One method that has been used by Schlaad to avoid the effects of AMM in the ROP of amino acid based NCAs is the use of hydrochloride salts of primary amines as the initiator.<sup>66</sup> This method essentially introduces additional protons into the system and requires the assumption that in the event an NCA monomer is deprotonated, the reprotonation of the generated  $NCA^-$  species is faster than the nucleophilic attack of the  $NCA^-$  on another monomer. This assumption is supported by previous studies by Knobler<sup>67-68</sup> where the primary goal was to produce  $\alpha$ -

aminoacyl compounds from stoichiometric reactions of their respective NCAs and the hydrochloride salts of primary amines and not produce polymeric product.

One additional drawback of NAM is that the reaction is relatively slow. The rate determining step in NAM is presently inconclusive. One group of researchers argue that the rate determining step is the loss of CO<sub>2</sub> from the carbamic acid species that is formed following ring-opening. The loss of CO<sub>2</sub> drives the equilibrium towards the formation of the primary amine reactive species.<sup>69-70</sup> It was previously found that the immediate removal of CO<sub>2</sub> from the system sped up the reaction due to the instability of the carbamic acid intermediate species.<sup>71-72</sup> Molecular weight control was investigated Wooley et al and it was reported that the immediate removal of CO<sub>2</sub> by constant nitrogen flow simultaneously improved rates of polymerization and maintained the living characteristics of NAM.<sup>73</sup> Compared to a reaction with zero nitrogen flow, a threefold increase in the observed propagation rate constant  $k_p$  of the ROP of  $\gamma$ -benzyl-L-glutamate NCA using hexylamine initiator was observed in a parallel reaction using a nitrogen flow rate of 100 mL/min. Further analysis of  $M_n$  versus conversion of the hexylamine initiated ROP of  $\gamma$ -benzyl-L-glutamate NCA using a 100 mL/min flow rate of nitrogen suggested that the living character of this polymerization was maintained. Another group argues that the rate determining step is the attack on C5 by the primary amine initiator based on DFT calculations;<sup>74</sup> the nucleophilic attack at the C5 position was found to have the highest activation energy compared to other steps in NAM.

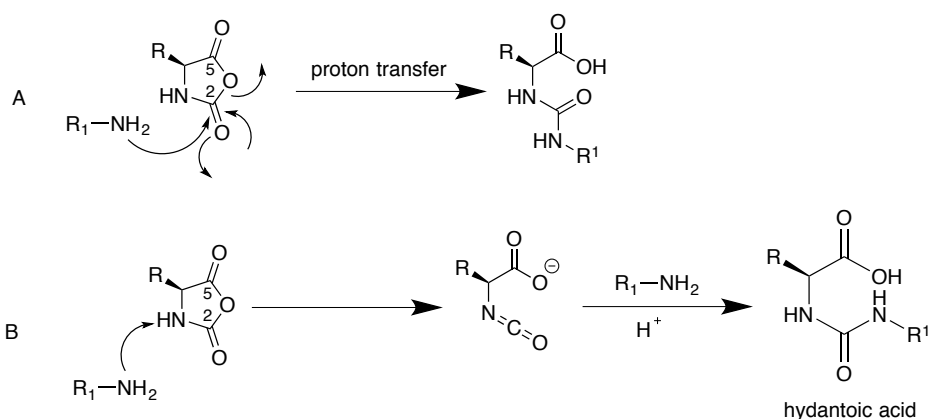
Side reactions in NCA polymerizations. Scheme 1.2 only represented the ideal scenario that would occur in NAM order to generate the desired polypeptide species. In reality there are a number of side reactions that can occur in polymerization systems. A number of them are discussed in this section.

NCA contains two electrophilic centers on C2 and C5 as indicated on the generic NCA in Scheme 1.2. In the ideal scenario, attack at the C5 carbonyl by the primary amine initiator or propagating species opens the NCA ring and forms a terminal carbamic acid. Carbon dioxide is lost through decarboxylation, which forms a new reactive primary amine terminus for subsequent propagation reactions with additional NCA monomers. However, it has been shown that there is a mode of termination for an attack on the C2 position. It is possible that the primary amine can simply attack the C2 position during the initiation step resulting in the formation of a urea species with a free carboxylate (Scheme 1.3A).<sup>48, 75</sup> The resulting ring-opened urea species does not participate in any further reactions thus rendering it a dead chain. This attack at the C2 carbonyl is not limited to the initiation step. Sela and Berger have demonstrated that the formation of a urea species can occur during propagation leading to premature termination in the case of poly(DL-phenylalanine).<sup>76-77</sup> The major factor influencing the tendency for a particular primary amine initiator to attack C2 or C5 was determined to be the nucleophilicity of the amine. Primary amine initiators with higher nucleophilicity had a much lower tendency to attack C2 thus mostly producing the desired initiating species via attack on C5.<sup>69, 78-80</sup>

Another side reaction that could occur is the formation of an isocyanate at the C2 position (Scheme 1.3B). This is usually observed following the deprotonation of the –NH proton by a strong base when the polymerization proceeds through the activated monomer mechanism (*vide infra*). It is also possible for less nucleophilic primary and secondary amine initiators to deprotonate the amido proton, leading to the formation of the isocyanate. It was also reported that the use of secondary amine initiators, especially those with branched alkyl groups, can favor rearrangement into hydantoic acids.<sup>48</sup>

During the ROP of glutamic acid based NCAs, one of the most commonly observed side reactions is an event known as backbiting, where the primary amine active chain end performs an intramolecular reaction at the  $\gamma$ -carbonyl center resulting in the

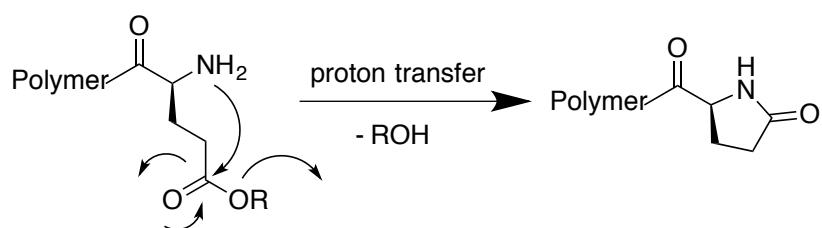
Scheme 1.3. (A) Formation of urea species via nucleophilic attack on C2 (B) formation of isocyanate via deprotonation of  $-NH$  and subsequent rearrangement to hydantoic acid



formation of a cyclic pyroglutamate through ester cleavage (Scheme 1.4). This pyroglutamate does not participate further in polymerization reactions and is thus a dead chain end, reducing the  $M_n$  and broadening the PDI. This is especially prevalent in the polymerization of  $\gamma$ -benzyl-L-glutamate NCA where backbiting products were observed by Heise et al to be the main impurities. It was suggested that the polymerization be carried out at low temperature (0 °C) to prevent the formation of backbiting impurities.<sup>81-</sup>

82

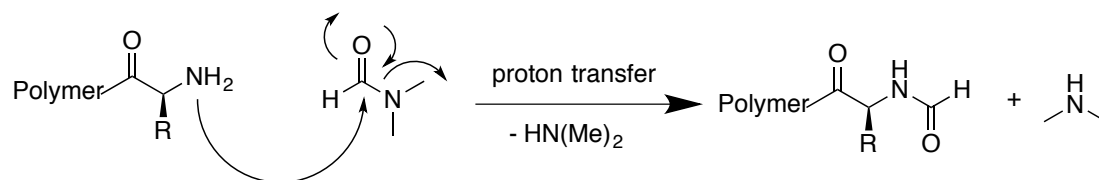
Scheme 1.4. Generic scheme of the formation of a terminal pyroglutamate species via backbiting



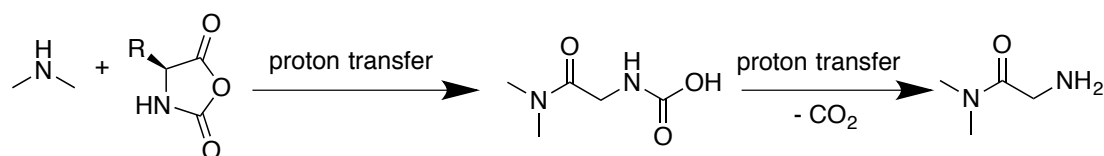
The choice of solvent can contribute to the observation of side reactions. DMF is often used in the polymerization of polypeptides due to minimal aggregation but it has been observed that DMF itself can participate in the reaction, both as an initiator and as a mode of termination.<sup>83-85</sup> Kricheldorf et al have observed that at 60 °C, the growing chain end of poly(DL-phenylalanine) can react with DMF, releasing dimethylamine. The results of this attack on DMF are twofold. First, the polypeptide is now end capped with a formamide species thus rendering it a dead chain via termination. Second, the released dimethylamine is very nucleophilic and can participate in initiation and propagation of additional NCA monomers. Both of these events (Scheme 1.5) lead to the decrease of  $M_n$  and broadening of PDI, which are undesired results of a controlled polymerization.

Scheme 1.5. Termination of a growing polypeptide chain via reaction with DMF and subsequent reinitiation by released dimethylamine

**Termination via attack on DMF**



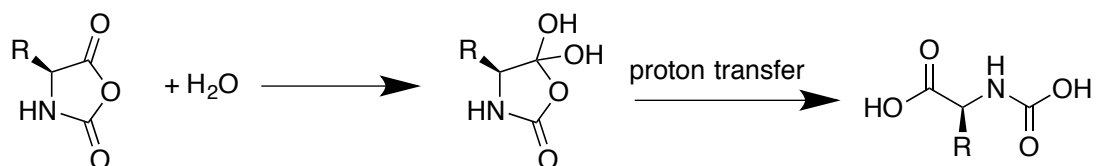
**Reinitiation by released dimethylamine**



Water is a very common impurity that can be encountered in the synthesis of NCAs and its effect on NCAs has been widely studied.<sup>86-90</sup> Water can participate in both the initiation of NCAs when  $[M]_0:[H_2O]_0 > 10$  and partake in hydrolysis at lower ratios ( $< 10^{-3}$ ) (Scheme 1.6). Other factors that could influence the behavior of water on the NCA are temperature and the structure of the NCA as more sterically hindered NCAs could

block the addition of water to the anhydride. Self-polymerization via water initiation was also observed to occur in the solid state in crystalline  $\epsilon$ -carboxybenzyl-L-lysine NCA.<sup>91</sup>

Scheme 1.6. Hydrolysis of NCAs



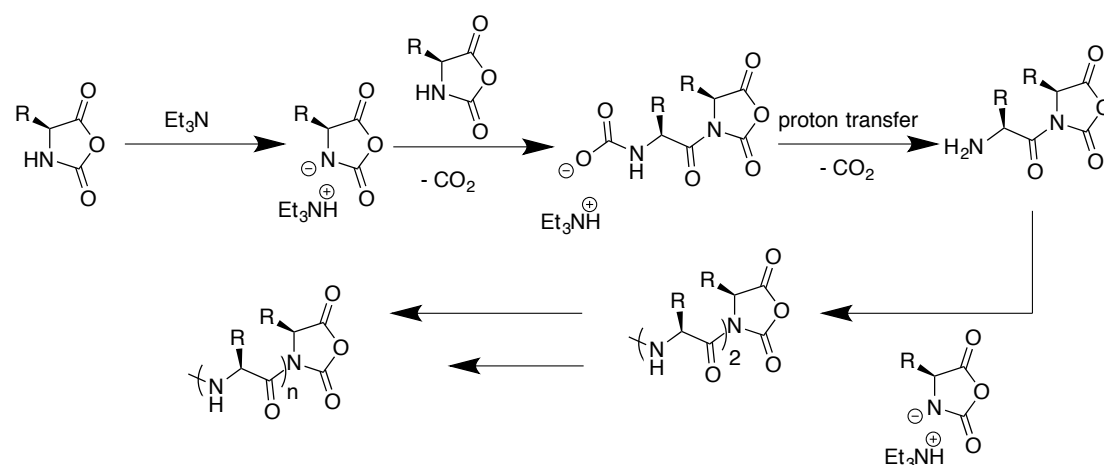
Activated monomer mechanism. A second method to initiate the polymerization of amino acid based NCAs is known as the activated monomer mechanism (AMM).<sup>92-94</sup> Unlike *N*-alkyl substituted glycine based NCAs, which will be discussed in subsequent sections, the nitrogen atom of amino acid NCAs bears a proton which can be deprotonated by a strong base, commonly triethylamine, generating negatively charged species which act as nucleophiles in the polymerization reaction (Scheme 1.7). This technique has the distinction to be able to generate higher molecular weight species than that of NAM. However, this also makes control of the polymerization difficult because initiation is much slower than that of propagation ( $k_i < k_p$ ), which yields high molecular weight polypeptides with broader than expected PDIs.<sup>48</sup> However, ROP of NCAs that proceed via AMM have higher propagation rate constants than those of NAM, allowing access to these high molecular weight polypeptides with shorter reaction times. In AMM, it is possible that the deprotonation of the amido proton can result in the formation of isocyanates, leading to premature termination (*vide supra*).

One major characteristic of AMM presented in Scheme 1.7 is that the mechanism relies upon the continual formation of “activated monomer” species via the deprotonation of additional NCA with carbamate chain ends. Much criticism has been levied against the proposed propagation mechanism.<sup>95</sup> There is a significant difference in the pKa values of

carbamates and NCAs ( $\Delta pK_a \sim 6$ ) rendering this step highly unlikely. The AMM also assumes that activated species will only react with *N*-acyl NCA chain ends versus additional NCA monomers. However, evidence for the proposed terminal cyclic initiating species obtained in AMM was presented by Peggion et al, who used  $^{14}\text{C}$  labeled amine initiators in the polymerization of  $\gamma$ -benzyl-L-glutamate NCA.<sup>96</sup> Although there is evidence for the proposed initiating species, much investigation needs to be done to elucidate the mechanism of propagation in AMM.

Transition metal catalysts. A third method for the ROP of amino acid based NCAs involves the use of transition metal catalysts. The goal of using transition metal initiators

Scheme 1.7. Activated monomer mechanistic pathway for the ROP of a generic amino acid based NCA



is to eliminate the possibility of the side reactions, such as backbiting, that can occur during polymerization of glutamate based NCAs. This ensures that higher molecular weight compounds can still be obtained and that the PDI does not unnecessarily broaden due to the presence of low molecular weight species obtained from premature termination. One of the most commonly used transition metal catalysts, Ni(bpy)COD, was developed by Deming<sup>97-98</sup> in order to overcome the drawbacks and side reactions of



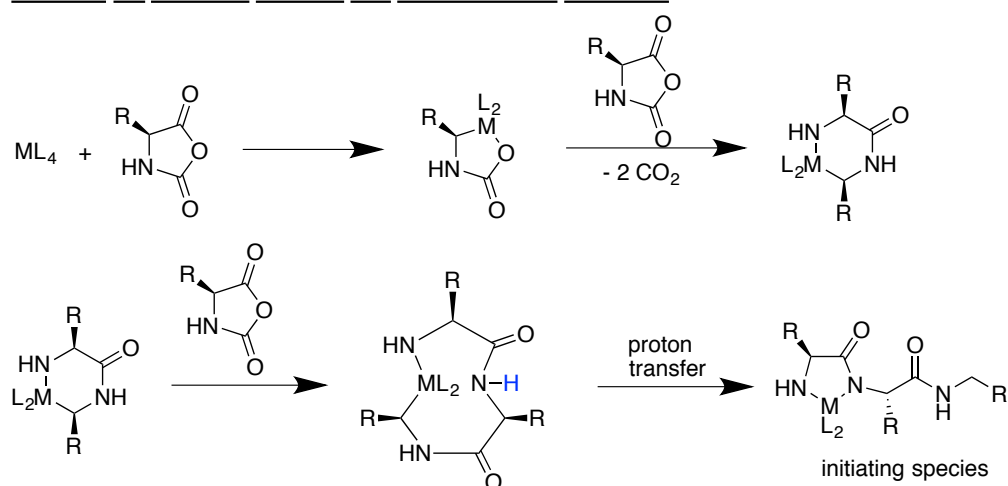
conventional nucleophilic ROP of amino acid based NCAs. Unlike the side reaction above where a nucleophilic initiator (i.e. primary amine) has the possibility of attacking the carbonyl at the C2 position resulting in the formation of an inactive urea species, the Ni(bpy)COD catalyst is regioselective and oxidatively adds across the O-C<sub>5</sub> bond exclusively, versus adding across the O-C<sub>2</sub> or N-H bonds, forming a five-membered metallacycle. Following oxidative addition, the five-membered metallacycle reacts with an additional NCA monomer to form a stable six-membered species which contracts to a five-membered amino-amidate initiating species. Propagation was proposed to occur via the free amido group on the amino-amidate attacking the C5 position of another NCA monomer once again forming a metallacycle species that can contract following proton transfer. The metal species in essence migrates along the propagating chain end.<sup>99</sup> This is summarized in Scheme 1.8. It was demonstrated that polymerizations with these initiators yielded polypeptides whose molecular weights increased linearly according to initial monomer to initiator feed ratios. The observation of narrow PDIs suggested that there was an absence of side reactions. Kinetic experiments studying the ROP of  $\gamma$ -benzyl-L-glutamate NCA by Ni(bpy)COD revealed that the polymerization proceeded in a first-order type reaction. The resulting polypeptide, poly( $\gamma$ -benzyl-L-glutamate) (PBLG), was found to retain its  $\alpha$ -helical secondary structure, a well-known and well-studied attribute.<sup>24</sup> Polymerization via organonickel catalysts has been extended to the synthesis of various block copolypeptides via the sequential addition of monomer, further demonstrating the living nature of this polymerization technique.

Additional transition metal catalysts were explored, the main requirements of an adequate transition metal catalyst being functional group tolerant towards potential functionalities on NCA monomers and their resulting polypeptides, having low valency, being able to undergo a 2-electron oxidative addition, and possessing strong electron

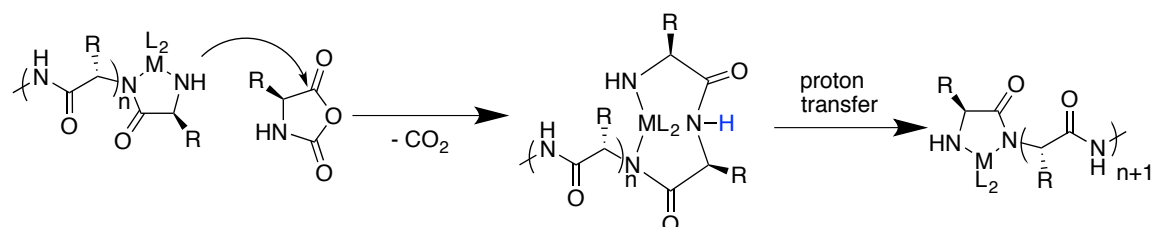
donating ligands.<sup>100</sup> Potential new catalysts based off of palladium and platinum were found to be regioselective in reacting with the N-H bonds of NCAs thus being unable to form the correct propagating species for the controlled ROP of NCAs.<sup>101</sup> Cobalt and iron catalysts (i.e.  $M(\text{PMe}_3)_4$ ,  $M=\text{Co}, \text{Fe}$ ) for the ROP of NCAs have been developed.<sup>100</sup> A much faster initiation was observed in cobalt initiators than those of nickel, allowing access to lower molecular weight polypeptides as observed in low  $[M]_0:[I]_0$  reactions. Aggregation was observed in iron catalysts, giving low yields of uncontrolled polypeptide, due to the increased Lewis acidity of iron. Aggregation can be prevented

Scheme 1.8. Proposed ROP mechanism of NCAs via transition metal catalysts

**Initiation via oxidative addition and amino-amidate formation**



**Propagation via amino-amidate**



through reaction of the iron complex with *tert*-butyl isocyanide, allowing access to well-controlled polypeptide species. Mechanistically, cobalt and iron based catalysts were

found to be similar to that of nickel. The main advantages of this initiation system are that early termination side reactions can be eliminated and the increased tolerance of the initiator to impurities. The metal species added to the reactions are removed via the addition of acidic methanol (1 mM HCl). However, no evidence (e.g. atomic absorption spectroscopy, inductively coupled plasma atomic emission spectroscopy results) for whether all of the metal species have been removed was provided. If polypeptides were to be used in biomedical applications, removal of heavy metals is important.

Organosilicon amine mediated ROP. Organosilicon amines can be used as initiators to obtain high molecular weight polypeptides through the ROP of their corresponding NCAs. PBLG<sup>102-103</sup> and PCPLG<sup>58</sup> have been shown to polymerize from their respective NCA monomers mediated by hexamethyldisilazane (HMDS). Organosilicon amine-mediated ROP of NCAs differs mechanistically from previous methods. It was initially proposed by Cheng et al that the trimethylsilane group (TMS) of HMDS is transferred to the carbonyl of the NCA and the NCA ring is opened by the resulting silyl amine. The TMS-carbamate intermediate formed in the initiation step participates in propagation via a six-membered ring transition state where the TMS group is transferred to the incoming NCA monomer, regenerating the TMS-carbamate species (Scheme 1.9a), similar to that of a group transfer polymerization. This process continues as TMS is continually transferred to incoming NCA monomers until all monomer has been consumed. Interestingly, HMDS-mediated ROP of amino acid based NCAs can be extended to their polypeptoid counterparts, specifically *N*-methyl glycine NCA.<sup>104</sup>

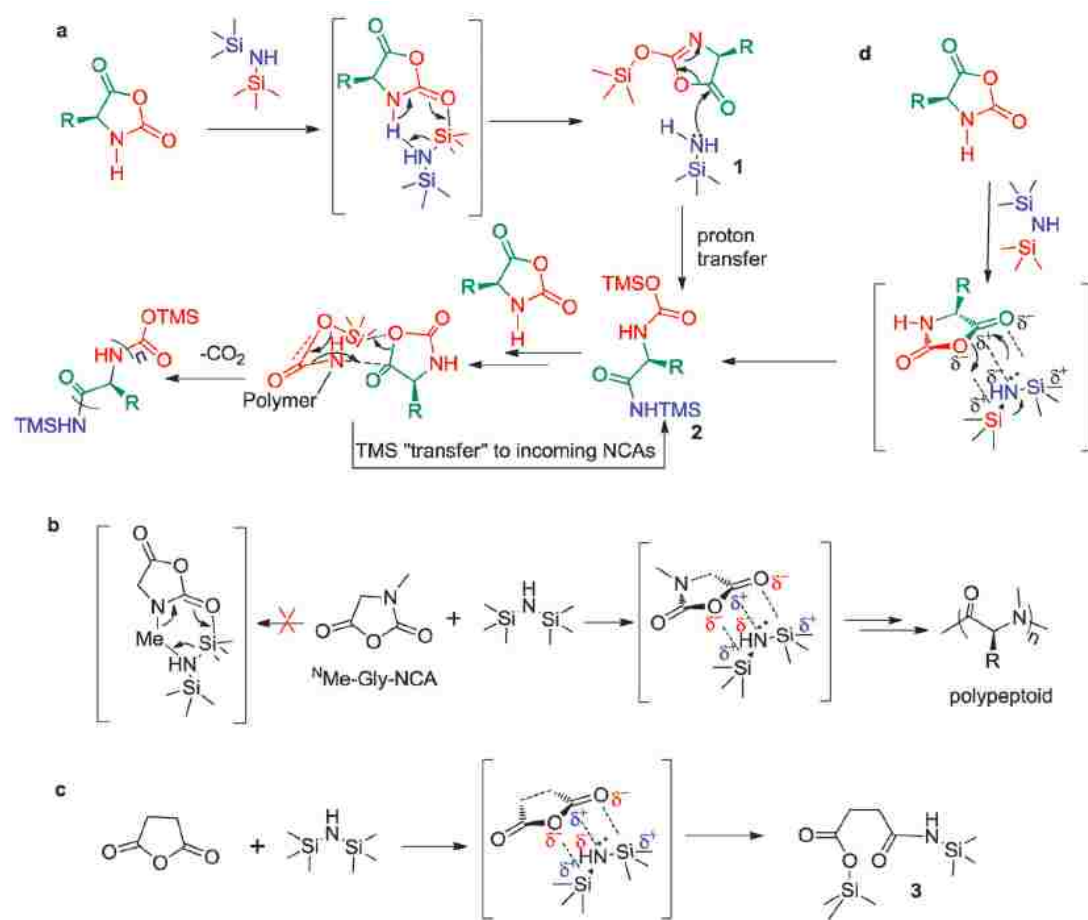
The fact that *N*-methyl glycine NCA can be polymerized via a HMDS-mediated pathway (Scheme 1.9b) led to a revision of the initially proposed mechanism.<sup>104</sup> Scheme 1.9a suggests that the NCA monomer undergoes a tautomerization in order to generate the desired intermediate product **1**, which is the propagating species. The nitrogen atom

of *N*-methyl glycine NCA does not contain a proton to undergo tautomerization. Additionally, it was demonstrated through equimolar reactions with HMDS and succinic anhydride (Scheme 1.9c) that the nitrogen atom is not necessary for HMDS to open cyclic anhydrides. A new cooperative mechanism (Scheme 1.9d) was proposed where the amide bond formation and TMS transfer occur simultaneously.

Recently, it was reported that the process can be accelerated through the use of a trimethyl sulfide species because of the combination of the increased nucleophilicity of the sulfur atom and increased reactivity of the S-Si bond (Scheme 1.10).<sup>105</sup> Through the use of a commercially available phenyl trimethyl sulfide initiator (PhS-TMS), a variety of amino acid based NCA monomers (i.e.  $\epsilon$ -carboboxy-L-lysine,  $\gamma$ -triethylene glycol-L-glutamate,  $\gamma$ -benzyl-L-glutamate,  $\gamma$ -4-vinylbenzyl-L-glutamate,  $\gamma$ -allyl-L-glutamate, *O*-diethylphospho-L-tyrosine, and  $\gamma$ -3-chloropropyl-L-glutamate) were polymerized with adequate molecular weight control and narrow polydispersities (< 1.1).

The TMS group transfer mediated ROP of amino acid based NCAs can be combined with different polymerization strategies to obtain polymers with different architectures. One such material seldom seen with respect to polypeptides is a brush copolymer composed of polypeptide “bristles.” Ring-opening metathesis polymerization (ROMP) using Grubbs’ catalyst is a commonly used method in order to obtain polymer brush backbones, usually of norbornene derivatives.<sup>106</sup> Using a norbornyl amine to synthesize a brush backbone with the intent of using the primary amine side chains in a grafting from approach to initiate ROP of amino acid based NCAs, it was found that ROMP did not proceed due to the deactivation of the Grubbs’ catalyst by the norbornyl amine.<sup>107</sup> N-TMS protection of the norbornyl amines used in this study served two purposes. One the one hand, it would allow for ROMP to proceed due to the reduced likelihood of catalyst deactivation and secondly would generate a reactive macroinitiator

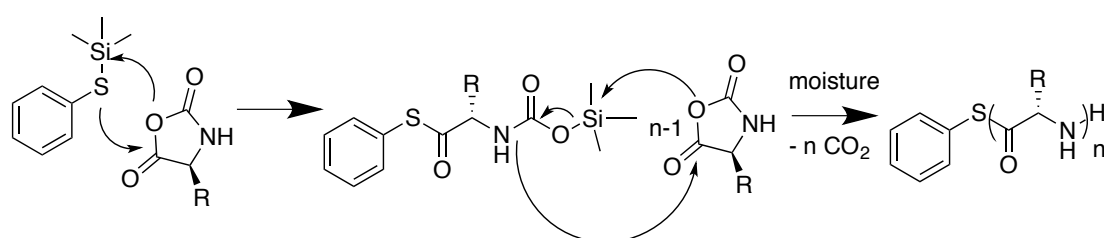
Scheme 1.9. Proposed mechanisms for the organosilane amine mediated ROP of NCAs. Reproduced from Reference 104 with permission of The Royal Society of Chemistry.



species to allow for a “grafting from” approach to synthesize the brush copolymers.<sup>108</sup>

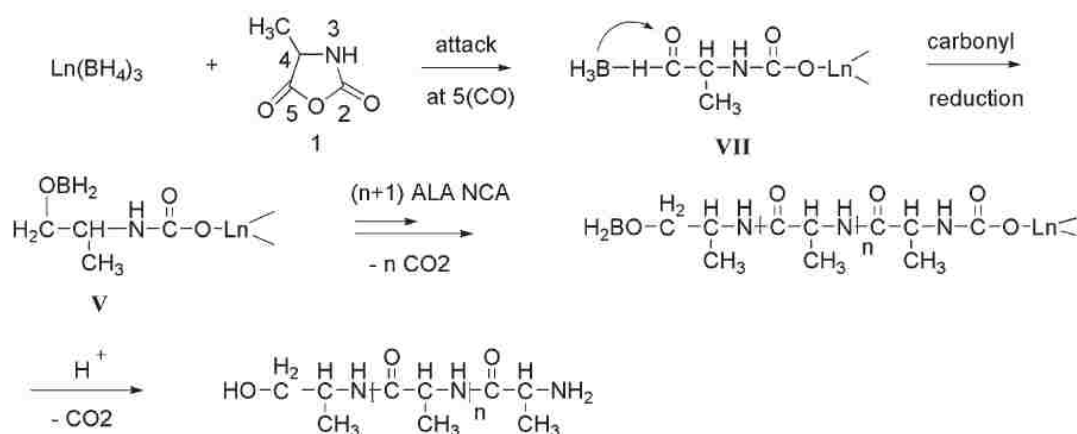
These combined methods of ROMP and TMS group transfer ROP of amino acid based NCAs were further extended to achieve other materials such as hybrid block copolymers<sup>109</sup> and supramolecular structures.<sup>110</sup>

Scheme 1.10. ROP of NCA monomers using PhS-TMS initiator



Rare earth borohydride polymerization. A method involving the use of rare earth borohydrides in the ROP of amino acid based NCA monomers was recently reported by Ling et al. Poly( $\gamma$ -benzyl-L-glutamate) and block copolypeptides with poly( $\epsilon$ -carboxybenzyl-L-lysine) with adequate molecular weight control and PDI (1.16, 1.05 in homopolypeptide and block copolypeptide respectively) were synthesized from the ROP of NCAs using coordination compounds with the structure  $M(\text{BH}_4)_3(\text{THF})_3$  where  $M = \text{Sc, Y, La, Dy}$ .<sup>111</sup> Rare earth metals are well-known catalysts in the ROP of polyesters<sup>112-118</sup> but have not been explored for their application as catalysts in the ROP of NCAs. Mechanistic studies of rare earth borohydride initiated ROP of alanine-NCA revealed the simultaneous attack of the catalyst on the C5 position and deprotonation of the nitrogen atom, giving two reactive centers from which propagation can occur via the attack of the metal-carbamic acid species on successive NCAs or via AMM. The end result is a telechelic polypeptide species. Through temperature variation (0 °C), the AMM pathway could be suppressed, allowing the NAM-like pathway to dominate (Scheme 1.11).

Scheme 1.11. “NAM”-like reaction pathway in the ROP of NCA monomers using rare earth borohydrides. Reproduced from Reference 111 with permission of John Wiley & Sons.



Accelerated amine mechanism through monomer activation. This final method for the ROP of NCAs discussed in this section is known as the accelerated amine mechanism through monomer activation (AAMMA).<sup>119</sup> The motivation for the development of this method was to obtain well-defined and well-controlled polypeptide species in short reaction times but with adequate control over the targeted molecular weight species. This essentially combines the aspects of AMM (rate of reaction) with those of NAM (control). Optimizing this polymerization strategy first entailed screening initiators that contain both primary and tertiary amines. It was found that triethylaminetriamine (TREN) initiated polymerizations of  $\gamma$ -benzyl-L-glutamate and  $\epsilon$ -carboboxy-L-lysine NCAs produced polypeptides with well-controlled molecular weights (up to  $45 \text{ kg}\cdot\text{mol}^{-1}$ ), narrow PDIs ( $< 1.19$ ) in a much shorter timeframe (2-3 h). An AMM polymerization pathway was ruled out due to the presence of only one set of narrowly distributed polymers being observed. Mark-Houwink-Sakurada plots revealed the presence of three-arm stars, which would indicate an exclusive NAM pathway.  $^{15}\text{N}$  NMR studies of TREN compared with other amines screened, namely tetramethylethylamine (TMEDA), revealed that the tertiary nitrogen of TREN was electron deficient with respect to the two tertiary nitrogen atoms of TMEDA suggesting that deprotonation of the  $-\text{NH}$  of NCAs as observed in AMM does not occur. Instead, it is proposed that the amido proton is activated by TREN via hydrogen bonding without deprotonation, leading to the observed faster propagation. This behavior is not limited to complex amines consisting of primary and tertiary amines. Recently, a system using amines consisting of primary and secondary amine components such as triethylenetetramine (TETA) produced similar results to that of TREN initiated ROP of NCAs (Figure 1.3).<sup>120</sup> TETA initiated ROP via AAMMA was also found to follow first-order kinetics and the living characteristics were confirmed through investigation of  $M_n$  with respect to conversion. High molecular weight poly( $\gamma$ -

benzyl-L-glutamate)s (up to  $46 \text{ kg}\cdot\text{mol}^{-1}$ ) with adequate PDIs ( $< 1.29$ ) were obtained from TETA initiated ROP. In summary, this discovery represents a foray into the development of metal-free initiators for the well-controlled ROP of amino acid based NCAs and it is hoped that the scope of polymerizations using this method can be expanded to give interesting polymer architectures.

### 1.2.3 Post-polymerization modification of polypeptides

Glutamic acid derivatives. In particular, polypeptides based off of glutamic acid and its derivatives have the potential for expanding side chain structural diversity, which may allow for post-polymerization modification reactions. The main reason for this variability is that the synthetic methodology used to access NCAs based off of glutamic acid

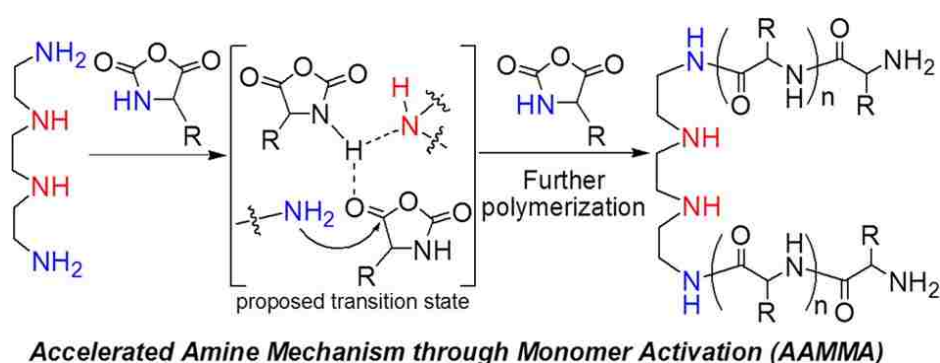


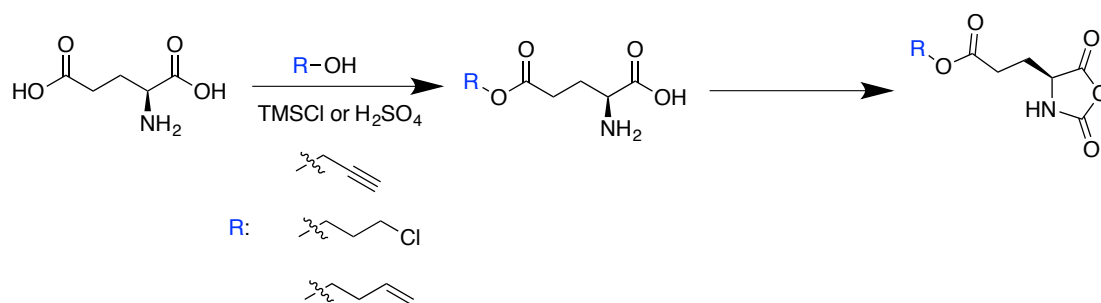
Figure 1.3. Proposed reaction pathway of AAMMA in the ROP of amino acid based NCA monomers via initiation by TETA. Reprinted from Reference 120 with permission from the American Chemical Society. Copyright 2015 American Chemical Society.

derivatives allows for a number of diverse, functional side chains to be added. This discussion will exclude those side chain functionalities that do not necessarily allow for the grafting of functional moieties such as those of  $\gamma$ -methoxy-L-glutamate<sup>121</sup>, and  $\gamma$ -cinnamyl-L-glutamate<sup>122</sup>, the latter of which only allows for photocrosslinking.



As will be explored further with *N*-alkyl substituted glycine based NCAs, the side chains of glutamic acid based NCAs can be varied in the initial synthetic steps of monomer preparation thus increasing side chain structural diversity. L-glutamic acid can

Scheme 1.12. Functionalization of L-glutamic acid via esterification under acidic conditions for post-polymerization modification.



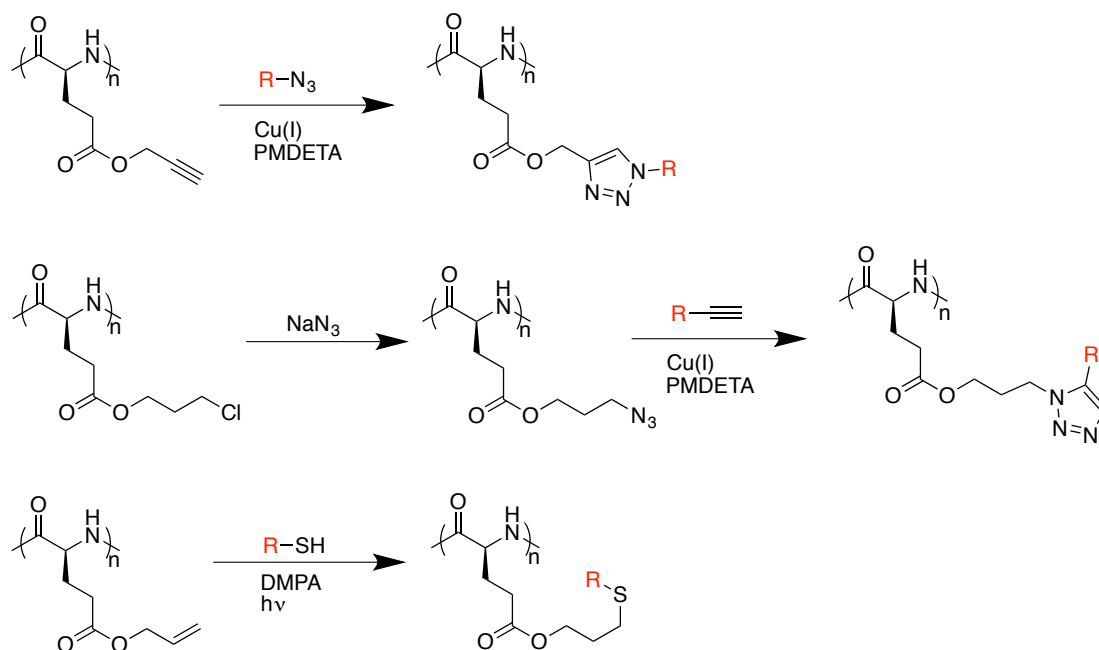
be esterified under acidic conditions (Scheme 1.12) with a primary alcohol bearing the desired functionality, in particular propargyl<sup>42, 57, 123</sup>, 3-chloro-propyl<sup>58</sup>, or allyl groups.<sup>124-125</sup> The propargyl group can participate in a copper mediated alkyne/azide cycloaddition (CuAAC) through the reaction with an azide functionalized moiety. The 3-chloro-propyl group allows for the S<sub>N</sub>2 transformation of the chloro side chains in azide functionalized side chains to allow for CuAAC via reaction with an alkyne moiety. The allyl groups on the other hand allow for thiol-ene coupling to occur. These are summarized in Scheme 1.13. The range of functional moieties to be grafted onto the side chains is nearly infinite. If an azide, alkyne, or thiol species can be synthesized, it is likely that the species can be grafted to the polypeptide side chains via post-polymerization modification barring setbacks such as sterics.

One particular subset of polypeptides, glycopolypeptides, are often synthesized via post-polymerization modification reactions.<sup>58, 123, 126-127</sup> Glycopolypeptides can serve as synthetic models to better understand carbohydrate-lectin interactions, which play a

role in a number of biological functions such as cellular signal transduction and metabolism, and protein recognition.<sup>128-129</sup> Chapter II is devoted to the study of carbohydrate-lectin interactions using glycopolypeptide scaffolds and the research and development glycopolypeptides (and glycopolymers) will be covered in much more detail in that chapter and will not be covered here.

One set of glutamic acid derived NCA precursors are not synthesized via the direct esterification of glutamic acid under acidic conditions. These precursors are synthesized using the copper chelation of glutamic acid followed by reaction of the resulting copper complex with an alkyl halide bearing the desired functionality.<sup>130</sup> One polypeptide of note is that of poly( $\gamma$ -4-vinyl-benzyl-L-glutamate).<sup>131</sup> Cheng et al have reported the versatility of the terminal vinyl group in post-polymerization modification

Scheme 1.13. Post-polymerization modification reactions of poly(L-glutamic acid) derivatives

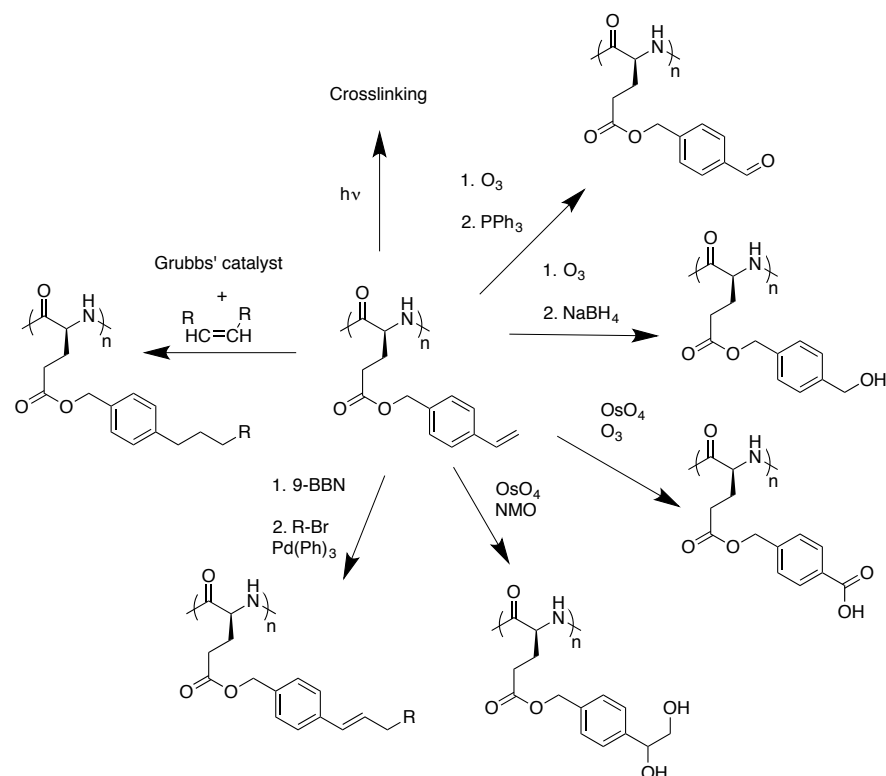


due to the number of chemical transformations that the vinyl group can undergo. New functional groups such as aldehydes, alcohols, and carboxylic acids could be formed via

ozonolysis or osmium tetroxide oxidation. The terminal alkene of poly( $\gamma$ -4-vinyl-benzene-L-glutamate) could also form new carbon-carbon bonds via metathesis using Grubb's catalyst, Suzuki coupling, and photocrosslinking. These are summarized in Scheme 1.14.

Methionine alkylation. Deming et al reported a post-polymerization reaction involving the thioether group of poly(L-methionine).<sup>132</sup> L-methionine NCA was synthesized and purified using methods previously discussed and polymerized using  $\text{Co}(\text{PMe}_3)_4$  initiator with adequate molecular weight control (up to  $58 \text{ kg}\cdot\text{mol}^{-1}$ ) as verified by end group analysis using a PEG end group ( $M_n = 2000 \text{ g}\cdot\text{mol}^{-1}$ ). The thioether group could be alkylated using various alkyl halides, or triflates, ranging from simple aliphatic groups to carbohydrates (Scheme 1.15). This wide range of functionalities demonstrates the versatility of the thioether group and shows the functional group tolerance of the

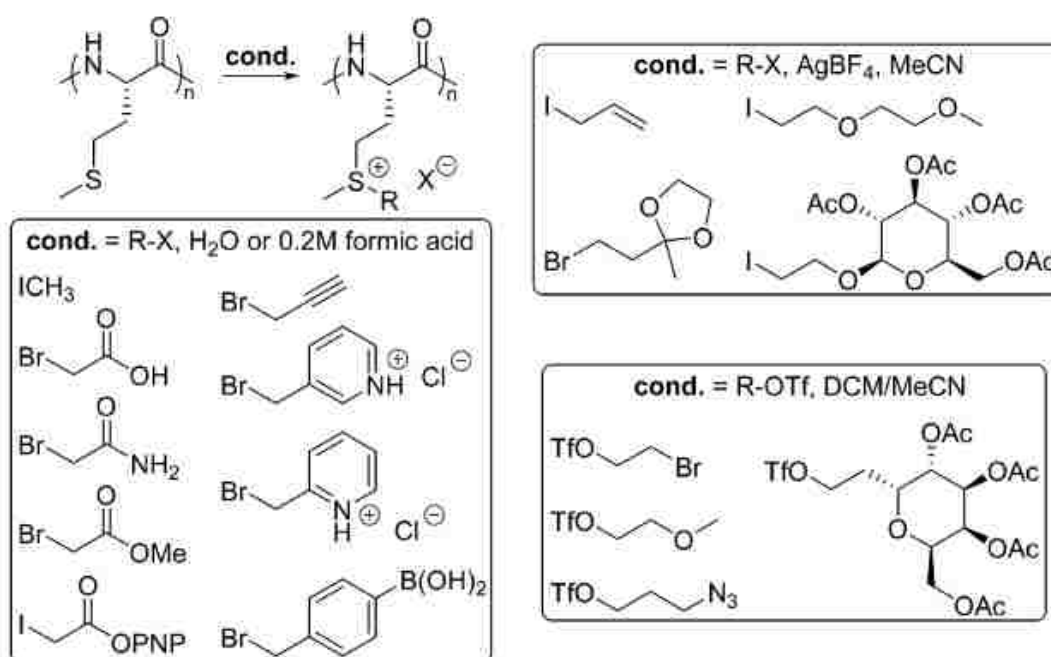
Scheme 1.14. Various post-polymerization transformations of poly( $\gamma$ -4-vinyl-benzene-L-glutamate)



thioether. The thioether alkylation was demonstrated to be reversible in the presence of a sulfur based nucleophile such as glutathione, 2-mercaptoethanol, thiourea, and 2-mercaptopyridine.<sup>133</sup> Thus, polypeptide based materials synthesized via post-polymerization thioether alkylation of poly(L-methionine) show potential future application as trigger-release materials. One drawback with poly(L-methionine) is the lack of solubility of the polypeptide in common organic solvents hence rendering characterization more difficult and requiring the end capping of the growing polypeptide chain with a large PEG species in order to allow for <sup>1</sup>H NMR end group analysis to be performed.

Thiol-ene reactions with poly(L-cysteine). One of the most versatile post-polymerization reactions is the thiol-ene coupling reaction. Patton et al reported the synthesis of *S-tert*-butylmercapto-L-cysteine NCA, which was subsequently polymerized

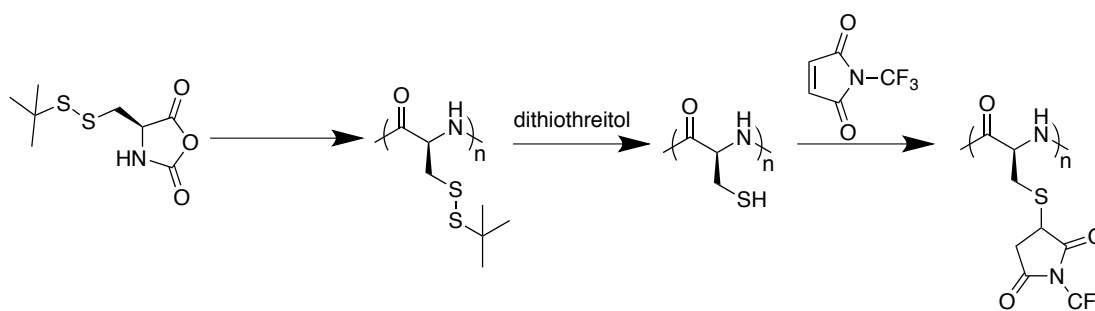
Scheme 1.15. Thioether alkylation with various alkyl halides and triflates. Reprinted from Reference 134 with permission from the American Chemical Society. Copyright 2016 American Chemical Society.



on silicon surfaces using Ni catalysts (Scheme 1.16).<sup>135</sup> The resulting polypeptide was deprotected via dithiothreitol to expose the thiol moiety on the side chains allowing for the thiol-ene coupling reaction to occur between the poly(L-cysteine) and a fluorinated maleimide.

Thiol-ene reactions with poly(L-serine). Cheng et al have reported the synthesis of an L-serine based NCA monomer bearing an *O*-pentenyl side chain, allowing for thiol-ene coupling to occur at the terminal alkene (Scheme 1.17). The advantage to serine based

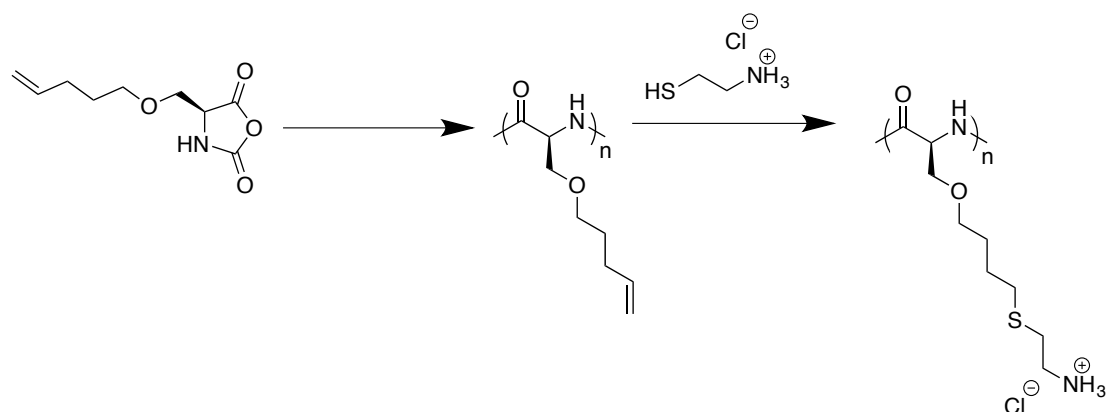
Scheme 1.16. Thiol-ene coupling of poly(L-cysteine)



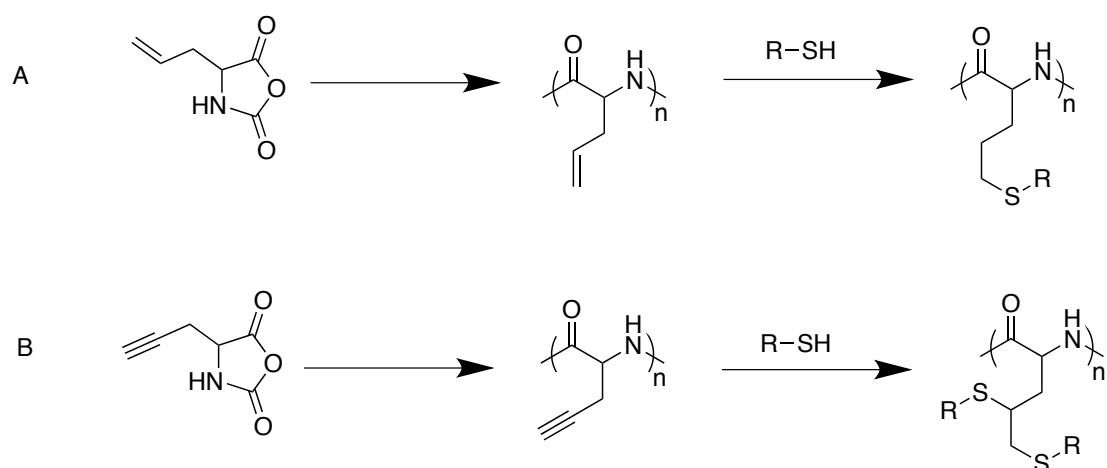
polypeptides is their water solubility, a necessary property of potential biomaterials. The resulting polypeptides maintained their  $\beta$ -sheet forming character. Applicability of the polypeptides in vivo was demonstrated via the grafting of charged cationic species via thiol-ene coupling and cellular uptake of the polypeptides was observed.

Glycine derivatives. Various glycine derivatives are commercially available such as allylglycine, and propargyl glycine, which can be subsequently cyclized into their respective NCAs.<sup>136-137</sup> The functional side chains on these species are on the  $\alpha$ -carbon versus on the nitrogen atom in polypeptoids (vide infra), thus allowing these species to be categorized under polypeptides. Similarly, the presence of unsaturated species (i.e. alkene, alkyne) on the side chains allows for thiol-ene chemistry to occur (Scheme 1.18).

Scheme 1.17. Thiol-ene coupling of poly(*O*-pentenyl-L-serine)



Scheme 1.18. (A) Thiol-ene coupling of poly(DL-allylglycine) and of poly(DL-propargyl glycine) (B) as described by Schlaad et al



### 1.3 Polypeptoids

First synthesized for drug development research, polypeptoids, or poly(*N*-alkyl glycine)s, are relatively new in the field of peptidomimetic materials. Although they bear structural resemblance to polypeptides, polypeptoids have been shown to be more resistant to proteolysis<sup>29-30, 138-140</sup> and have a number of key differences in physicochemical properties compared to those of polypeptides. The first major deviation is in the chemical structure of polypeptoids. The alkyl side chain of polypeptoids is found

on the nitrogen atom versus that of the  $\alpha$ -carbon (with respect to poly( $\alpha$ -amino acids)). By shifting the side chain to the nitrogen atom, intramolecular hydrogen bonding interactions are lost as there is no longer an  $\text{-NH}$  species to act as a hydrogen bond donor and there is the loss of main chain chirality. This has two consequences. The first is that due to the lack of strong hydrogen bonding interactions along the polypeptoid chain, there are few opportunities for the polymer to adopt a well-defined secondary structure like that of polypeptides resulting in most polypeptoids adopting random coil conformations. Chiral *N*-alkyl side chains can be installed during R-NCA synthesis to allow polyproline I helices to form, indicating the importance of side chain structure on the determination of secondary structure and polypeptoid function.<sup>27</sup> Recently, a new secondary structure observed in peptoid systems was observed which has been termed “ $\Sigma$ -strand.”<sup>28</sup> These “zigzag” like structures result from the ability of the peptoid backbone residues to adopt opposite rotations. A more positive consequence due to the loss of rigidity due to the presence of well-defined secondary structures allows for easier thermal processing of polypeptoid based materials.<sup>141</sup> Polypeptoids can also be degraded via base catalyzed hydrolysis (1.0 M NaOH), demonstrating their potential to be broken down and potentially cleared by living systems.

Side chain functionalization is important to the functionalities and properties of polypeptoids. It will be observed in subsequent sections that a variety of primary amines can be used in the synthesis of *N*-alkyl substituted glycine based NCAs. Functional groups that allow for post-polymerization modification such as allyl<sup>142</sup> or propargyl<sup>143-144</sup> groups can be installed through the initial synthesis of the monomer, thus allowing for thiol-ene and CuAAC reactions to be used to graft additional functional moieties to the side chains.

### 1.3.1 Solid phase synthesis of polypeptoids

Polypeptoids can be synthesized using a stepwise process similar to those found in solid phase peptide synthesis except that protected *N*-alkyl substituted glycine derivatives are used in place of regular amino acids. Solid phase synthesis of peptoids has been developed and refined by Zuckermann.<sup>145-146</sup> Because the synthesis of protected *N*-alkyl substituted glycines is expensive, time consuming, and low yielding, an alternative procedure known as the “submonomer method” was developed to curtail these additional synthetic steps.<sup>146</sup> The submonomer method (Figure 1.4) differs from the conventional methods discussed previously in that the first step involves an acylation of bromoacetic acid to the amine terminus of the resin. Because bromine is a good leaving group, the second step is a nucleophilic displacement of the bromine using the desired alkyl amine, creating the resulting *N*-alkyl substituted glycine. The secondary amine terminus formed in this second step becomes the reactive center of the following acylation reaction with bromoacetic acid. The processes of acylation and nucleophilic displacement are repeated until the desired peptoid sequence is complete. Similar to solid phase peptide synthesis, the final product can be cleaved from the solid resin support under acidic conditions. While the residue compositions and chain lengths can be controlled to near exactness as in solid phase peptide synthesis, solid phase stepwise synthesis of polypeptoids bears the same disadvantages namely requiring excess starting material, and has limited access to longer chain lengths due to the increased likelihood of deletions from incomplete reactions from previous steps (i.e. acylation of the secondary amine terminus or nucleophilic displacement of Br). However, due to the large variety of commercially available primary amines, there exists a great level of versatility in polymer design through side chain modification via the submonomer solid phase method.



### 1.3.2 Ring-opening polymerization of *N*-alkyl substituted glycine based NCA monomers to synthesize polypeptoids

Monomer synthesis. High molecular weight polypeptoids can be obtained from the ring-opening polymerization (ROP) of their respective *N*-alkyl substituted NCA monomers (R-NCA) at the cost of sequence specificity. *N*-substituted glycine hydrochloride salts, the precursors to *N*-alkyl substituted glycine based NCAs, are synthesized from the

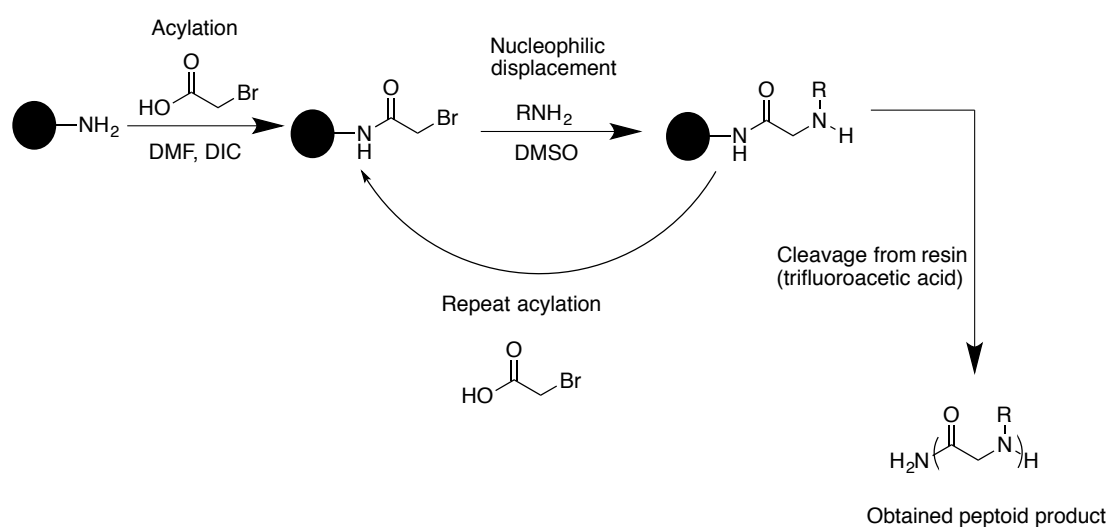
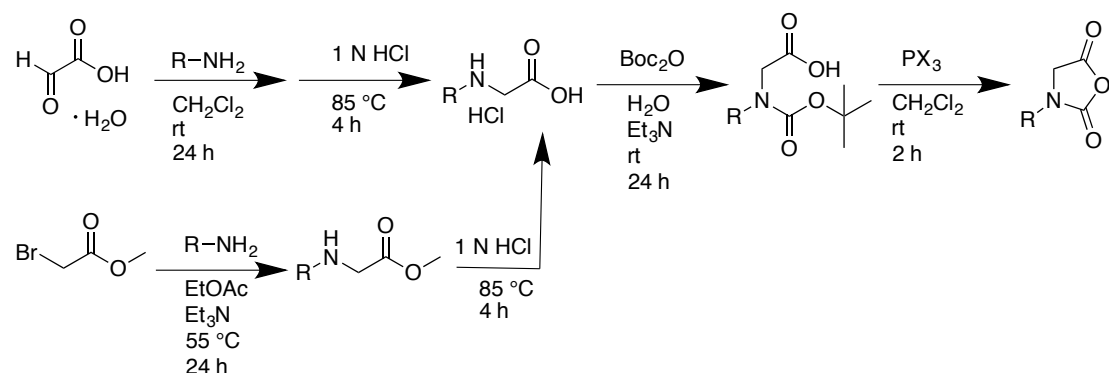


Figure 1.4. Scheme showing the solid phase synthesis of oligopeptoids using the submonomer method.

reaction between glyoxylic acid monohydrate and the primary amine bearing the desired *N*-alkyl substitution followed by acid catalyzed hydrolysis.<sup>147</sup> Alternatively, methyl bromoacetate can undergo an S<sub>N</sub>2 reaction with the primary amine followed by acid (HCl) catalyzed hydrolysis to generate the monomer precursor.<sup>27</sup> The extent of side chain structural diversity using commercially available primary amines of varying aliphatic chain length and structure is highlighted in Figure 1.5. After the synthesis of the *N*-alkyl substituted glycine hydrochloride salt, the product undergoes an *N*-Boc<sup>147</sup> or *N*-benzyl chloroformate (Cbz) protection.<sup>148</sup> In the synthesis of *N*-methyl glycine NCA, two alternative methods can be used to obtain the *N*-Boc protected monomer precursor. The first method involves the *N*-methylation of commercially available *N*-Boc glycine under

strongly basic conditions (NaH) with iodomethane.<sup>147</sup> Alternatively, commercially available sarcosine can be *N*-Boc protected under basic conditions to generate a similar compound under significantly milder conditions.<sup>149</sup> *N*-alkyl substituted glycines are cyclized into the desired R-NCA monomers using a phosphorus trihalide (chloride or bromide) or acetic anhydride.<sup>27, 49, 147-148, 150-152</sup> In the case of *N*-methyl glycine NCA, a form of phosgenation (e.g. triphosgene) can be used directly with sarcosine to obtain the corresponding NCA.<sup>153-154</sup> The synthetic steps of R-NCAs starting from glyoxylic acid monohydrate or methyl bromoacetate, and primary amine are summarized in Scheme 1.19. The synthesis of *N*-methyl NCA is summarized in Scheme 1.20. Purification of R-NCAs has been accomplished through sublimation or distillation.

Scheme 1.19. Generic synthesis of R-NCAs



Normal amine mechanism. R-NCAs can also undergo a nucleophilic ROP like their  $\alpha$ -amino acid NCA counterparts in order to produce high molecular weight polypeptoids. Primary amines are the most often used initiators for this purpose. The ROP of sarcosine-NCA or *N*-methyl glycine NCA using primary amine initiator has been known since the late 1940s.<sup>63-64</sup> The polymerization mechanism of the ROP of R-NCAs is also similar to that of amino acid based NCAs as there is an attack on the C5 position by the primary amine resulting in ring-opening followed by a decarboxylation of the resulting carbamic



synthesize block copolypeptoids via the sequential addition of monomer. A pentablock copolypeptoid (five separate, distinct blocks) was able to be synthesized through the sequential addition of additional monomer following the consumption and quantitative conversion of the previous R-NCA batch (Figure 1.6).<sup>155</sup> The living character of the ROP of sarcosine-NCA was also demonstrated through repeated enchainment experiments.

Primary amine-mediated ROP of R-NCAs via NAM was also extended to the use of solid supports bearing terminal amine groups in the form of a resin.<sup>156</sup> These primary amines displayed well-controlled molecular weights based on their monomer and initiator initial feed ratios may allow for polymerization methods to be combined with those of solid phase synthesis. However one drawback in using solid support methods is that trifluoroacetic acid salts were formed during the cleavage of the polypeptoids from the solid resins. These salts could not be removed from the precipitation methods used to obtain the synthesized polypeptoids. Additionally, the PDIs obtained through solid support methods were significantly broader (as high as 2.20) than those expected from generic NAM initiated ROP of R-NCAs.

Resins are not the only solid surfaces on which amine-mediated polymerization can occur. One major application for polypeptoids is for anti-fouling surfaces whose goals are to prevent the adhesion of proteins and bacteria.<sup>3, 5-10, 12</sup> However, each of the polypeptoids used in question were synthesized using solid phase methods and the maximum layer thickness was reported to be approximately 4 nm.<sup>5</sup> Aminopropyltrimethoxysilane bearing a terminal primary amine was immobilized onto silicon wafer surfaces so that ROP of R-NCAs (i.e. *N*-methyl glycine and *N*-butyl glycine NCAs) could take place at the amine termini.<sup>157</sup> This surface initiated method was also extended to form surface brush copolypeptoids through the sequential addition of monomer. Monolayer thicknesses of approximately 40 nm were obtained through the

surface initiated ROP of R-NCAs by primary amines as revealed by atomic force microscopy, a tenfold increase over the thicknesses previously obtained. Another example of surface initiated ROP of R-NCA monomers was reported by Lu et al using nanolithography techniques to pattern Si(111) surfaces with (3-aminopropyl)triethoxysilane (APTES) filled pores.<sup>158</sup> *N*-allyl glycine NCA was polymerized via NAM, using the terminal primary amines of APTES, producing

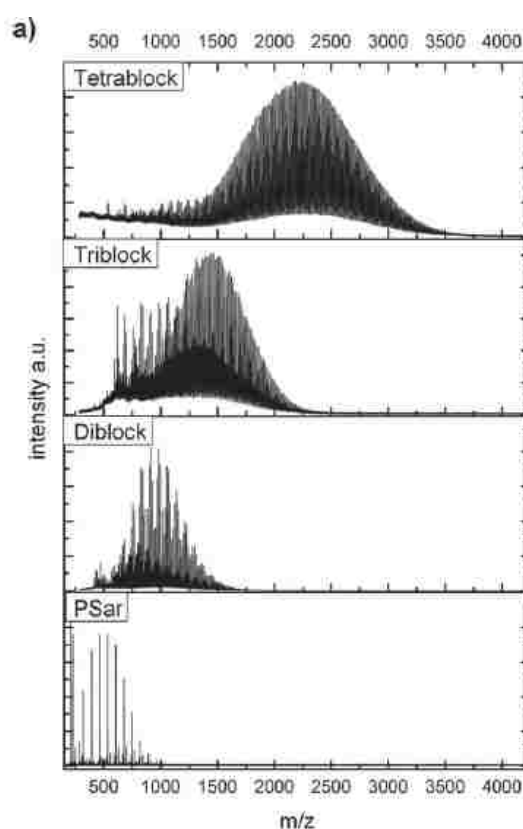


Figure 1.6. MALDI TOF MS spectrum of the synthesis of a tetrablock copolypeptoid through stepwise monomer addition. Reproduced from Reference 155 with permission of John Wiley & Sons.

patterned surfaces of polypeptoid nanorods up to heights of 35 nm. Poly(*N*-allyl glycine) has multiple applications as the polypeptoid can undergo post-polymerization modification via thiol-ene coupling (vide infra) or undergo hydrophobic collapse with heating.

Polypeptoids obtained from NAM methods have displayed a number of interesting properties such as the dependence of the side chain length (number of carbon atoms) or branching on main chain and side chain crystallization and packing.<sup>159</sup> The random copolymerization of *N*-ethyl glycine and *N*-butyl glycine NCAs has also yielded a series of thermoresponsive copolypeptoids whose cloud point temperatures could be tuned by altering the hydrophilic lipophilic balance via adjusting the feed ratios of the two R-NCAs during polymerization. Thermoresponsive bottle brush copolypeptoids were obtained from ring-opening metathesis polymerization (ROMP) of a series of random copolypeptoids polymerized using a norbornene amine based initiator in a “grafting through” technique.<sup>160-161</sup>

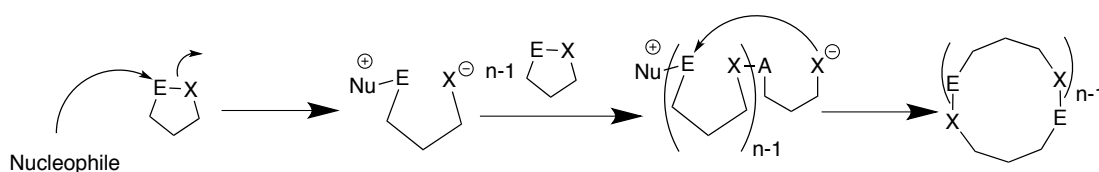
Polypeptoids obtained from NAM have also been studied in a number of applications. Xuan et al reported the synthesis of a triblock copolypeptoid via the sequential addition of monomers starting from benzylamine initiator. The ABC triblock copolypeptoids contained hydrophobic, hydrophilic, and thermoresponsive segments. Upon heating, it was observed that the triblock copolypeptoid systems formed free standing gels with narrow sol-to-gel transition windows and that the gels could be injected through a 24 gauge needle without breaking apart. Similarly using benzylamine initiator, Li et al recently reported the synthesis of core-crosslinked micelles composed of poly(*N*-ethyl glycine), poly(*N*-propargyl glycine), and poly(*N*-decyl glycine). Crosslinking was achieved via CuAAC (vide supra) using a disulfide crosslinker species which could be degraded using glutathione. The loading and gradual release of doxorubicin, a commonly used anti-cancer drug was also demonstrated.<sup>162</sup>

Zwitterionic ring-opening polymerization to afford cyclic polypeptoids. One area of interest that has always intrigued polymer chemists is the synthesis of polymers with

unique architectures (e.g. cyclic, star, dendritic). This section focuses on synthetic strategies used to obtain cyclic polypeptoids.

Recent advances in a technique known as zwitterionic ring-opening polymerization have allowed access to well-defined polymers with cyclic architectures. A generic reaction scheme for nucleophilic based ZROP is shown in Scheme 1.21. A nucleophile attacks a cyclic electrophilic species, generating a positively charged reaction center and an anionic terminus. In ZROP, the two oppositely charged termini are kept in close proximity via electrostatic interactions. During propagation, the system undergoes ring expansion in order to further increase  $DP_n$ . Guanidines, amidines, and *N*-heterocyclic carbenes (NHC) have been found to be able to stabilize the intermediate reactive species that form during ZROP. NHCs were first investigated as potential initiators in the ring-opening polymerizations of cyclic ester monomers to obtain well-defined poly(esters)<sup>163-168</sup> and poly(ethylene oxide)s,<sup>169</sup> and the scope of monomers polymerized with NHCs has been expanded to include poly(carbosiloxanes).<sup>170</sup>

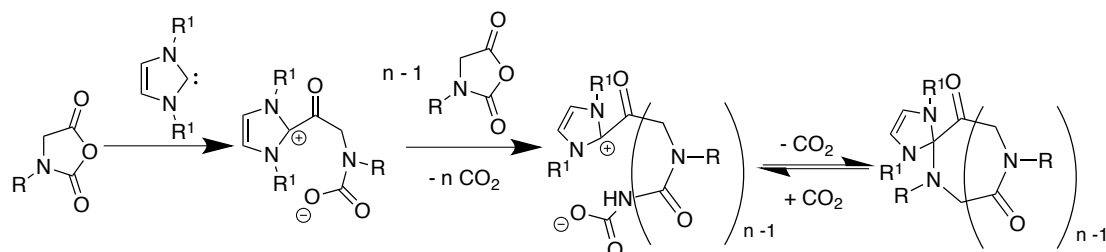
Scheme 1.21. Generic reaction mechanism of nucleophilic ZROP



Li et al reported that NHCs could also follow a ZROP type of mechanism in the ROP of R-NCAs in order to produce cyclic polypeptoid species (Scheme 1.22).<sup>147, 150</sup> Well-controlled polypeptoid species obtained from the ring-opening polymerization of *N*-butyl glycine NCA using NHC initiator were suggested to possess cyclic architectures based on the MALDI TOF MS of a low molecular weight species and from Mark- Houwink-

Sakurada plots.<sup>147</sup> This initial work represented the first foray into the synthesis of polypeptoids with unique (i.e. cyclic) architectures.

Scheme 1.22. Synthesis of cyclic polypeptoids via ZROP of R-NCAs using NHC initiator



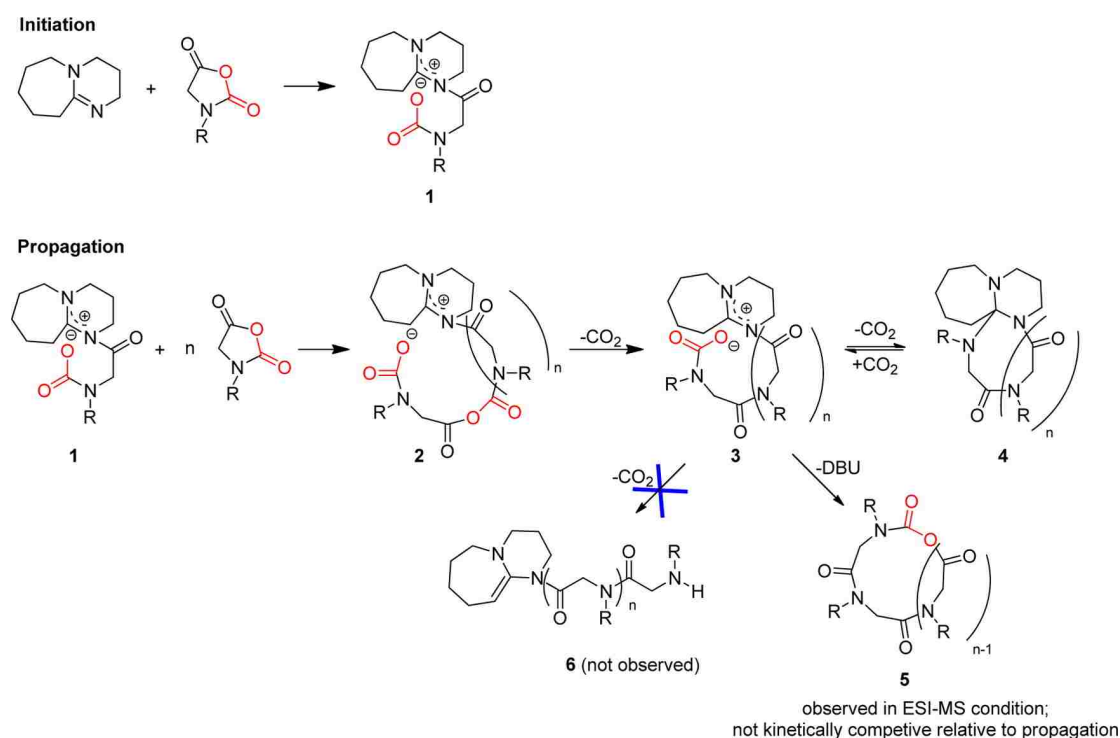
The NHC-mediated polymerization of R-NCAs was further studied in terms of polymerization kinetics, dependence on solvent and initiator, and mechanistic elucidation.<sup>150</sup> Although polymerization kinetics were revealed to follow pseudo first-order kinetics, the structure of the NHC initiator was found to play a role in determining the observed rate constants; slower rate constants were observed in more sterically hindered NHC initiators. This is not surprising as bulkier substituents on the NHC initiators would prevent access to the carbene reactive center, thus slowing down the initiation step. Polymerization solvents with low dielectric constants<sup>171</sup> such as THF ( $\epsilon=7.5$ ) and toluene ( $\epsilon=2.4$ ) gave well-defined polymers with narrow PDI values yet in contrast polymerization solvents with high  $\epsilon$  such as DMF and DMSO ( $\epsilon=36.7, 46.7$  respectively) did not, and control was poor, giving low molecular weight species regardless of the initial monomer to initiator ratios. This poor molecular weight control was suspected to be due to competition between chain propagation and backbiting by transamidation. This method has been used towards the synthesis of well-defined cyclic polypeptoids to study the effects of polymer architecture with respect to properties such



as thermoresponsive behavior (vide supra), crystalline side chain packing<sup>159</sup>, and micelle and gel formation.<sup>159, 172</sup>

One major disadvantage of NHCs is their instability to moisture. Alternative methods were sought in order to combat this drawback. Diazabicyclodecene (DBU)<sup>173</sup> and isothioureia<sup>174</sup> have been investigated as initiators in the ring-opening polymerization of cyclic ester monomers to obtain their cyclic polymeric counterparts. Well-controlled ROP of R-NCAs was observed when using DBU as the initiator in low dielectric solvents (i.e. THF, toluene) like that previously observed in NHC-mediated ROP of R-NCAs.<sup>19</sup> Mechanistic studies suggested the presence of oppositely charged chain ends during polymerization, a positively charged DBU and a negatively charged carbamate species (Scheme 1.23).

Scheme 1.23. Proposed mechanism of DBU-mediated ZROP of R-NCAs. Reprinted from Reference 19 with permission from the American Chemical Society. Copyright 2016 American Chemical Society.



Synthesis of polypeptoids with star or brush architectures. Other unique architectures that are of interest are star and brush polymers. The former was synthesized by Lahasky et al from a graft through approach, starting from a norbornene methylamine initiator in the ROP of *N*-ethyl glycine and *N*-butyl glycine NCAs.<sup>161</sup> The norbornene end group is polymerized via ROMP in order to generate the brush backbone following the polymerization of the “bristles” via NAM. Using polymeric macroinitiators bearing primary amines, Schmidt et al recently reported the synthesis of brush copolymers bearing polysarcosine side chains using poly[*N*-(6-aminoethyl)methacrylamide] macroinitiators which bore primary amine initiating species on the side chains.<sup>175</sup> Their ability as carriers of siRNA was also demonstrated. Less conventional substrates, namely amino bearing chitin<sup>176</sup> and chitosan<sup>177</sup>, were also used to generate brush copolymers bearing polysarcosine side chains. However, the poor solubility of the polymeric substrates required the addition of nicotinic or isonicotinic acid in order to maintain control of the polymerization. Star polypeptoids bearing polysarcosine arms were also reported to be polymerized from a poly(trimethylenimine) core.<sup>178</sup> Star shaped polydepsipeptides containing poly(lactide) and polysarcosine arms have been synthesized by Kimura et al for the study of these materials as potential in vivo nanocarriers.<sup>179-180</sup>

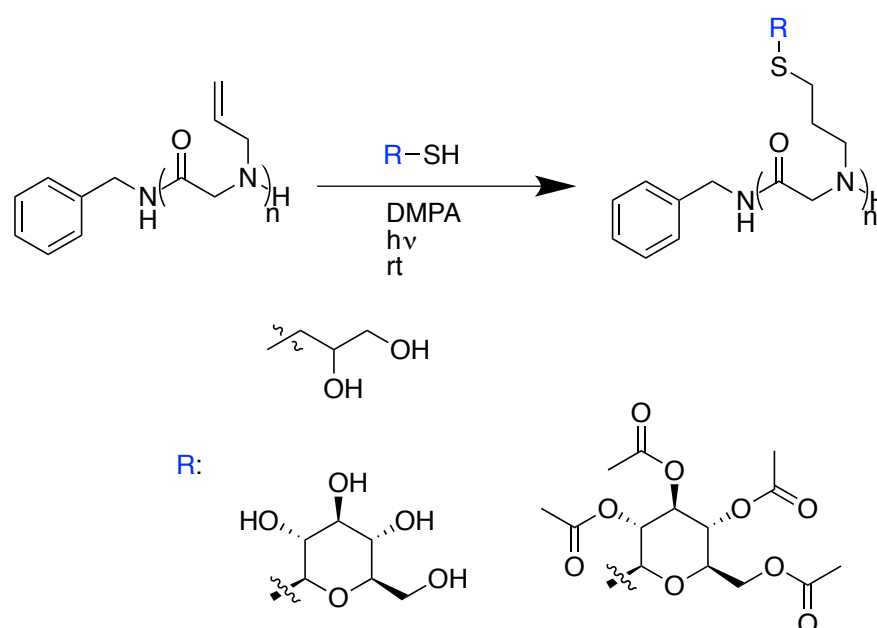
Post-polymerization modification of polypeptoids. Post-polymerization modification of the polypeptoid side chains is one method that can be used to both graft desired functionalities onto the polymer and further increase side chain structural diversity. Two polypeptoid species that allow for a variety of post-polymerization reactions to take place are poly(*N*-allyl glycine) and poly(*N*-propargyl glycine).

*N*-allyl glycine NCA was synthesized by Schlaad et al using methods described previously starting from allylamine. The resulting polypeptoid bearing allyl side chains can undergo thiol-ene photochemistry in order to install various functional moieties (e.g.

glycerol, glucose) using their respective thio-analogs (Scheme 1.24).<sup>142</sup> This demonstrates the versatility of thiol-ene chemistry and its ability to tolerate the functional groups of numerous functional moieties as well as demonstrating that the side chains of poly(*N*-allyl glycine) can be modified using such a robust reaction.

The alkyne group in poly(*N*-propargyl glycine) is more versatile than its allyl counterpart in that there are additional post-polymerization reactions that are only accessible to the propargyl species (Scheme 1.25).<sup>144</sup> In addition to thiol-ene chemistry, the propargyl group allows access to copper mediated alkyne/azide cycloaddition (CuAAC), a versatile reaction known for its chemoselectivity. However, grafting

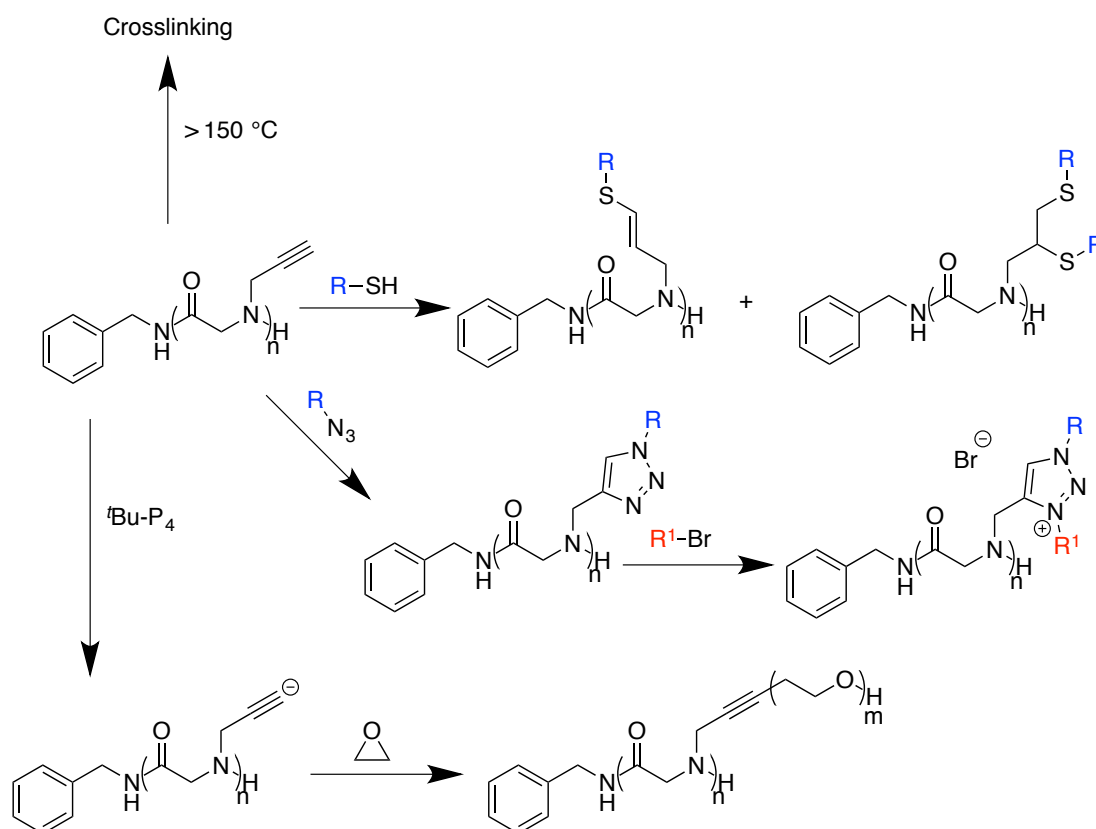
Scheme 1.24. Thiol-ene photochemical reaction between poly(*N*-allyl glycine) and a functional thio-moiety



efficiency seems to suffer in homopolymers of poly(*N*-propargyl glycine) due to the tendency for the polypeptoid to aggregate in solution, which prevent the Cu catalyst and azide species from accessing the alkyne.<sup>143</sup> Reducing the aggregation via the random copolymerization of *N*-propargyl glycine NCA with *N*-butyl glycine NCA significantly

increased the grafting density. A polypeptoid based imidazolium side chain can be obtained from the resulting triazole species obtained from successful grafting via CuAAC through the quaternization of the triazole with an alkyl bromide. The single alkyne proton can also be deprotonated under basic conditions using a phosphazene base<sup>181</sup> to yield a nucleophilic anion, which has been demonstrated to participate in the ROP of epoxides. Crosslinking of the polypeptoid network could also be obtained by heating the polymer system above 150 °C.

Scheme 1.25. Post-polymerization modification reactions with poly(*N*-propargyl glycine)



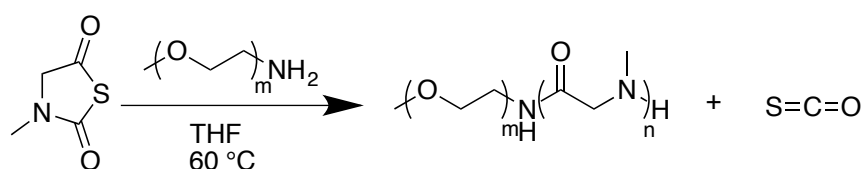
#### 1.4 Ring-opening polymerization of *N*-thiocarboxyanhydrosulfides

One of the biggest drawbacks to NCA monomer polymerization is the extreme care that must be undertaken in order to prepare, purify, and store the respective monomers. The anhydride bond is susceptible to moisture, heat, and the slightest presence

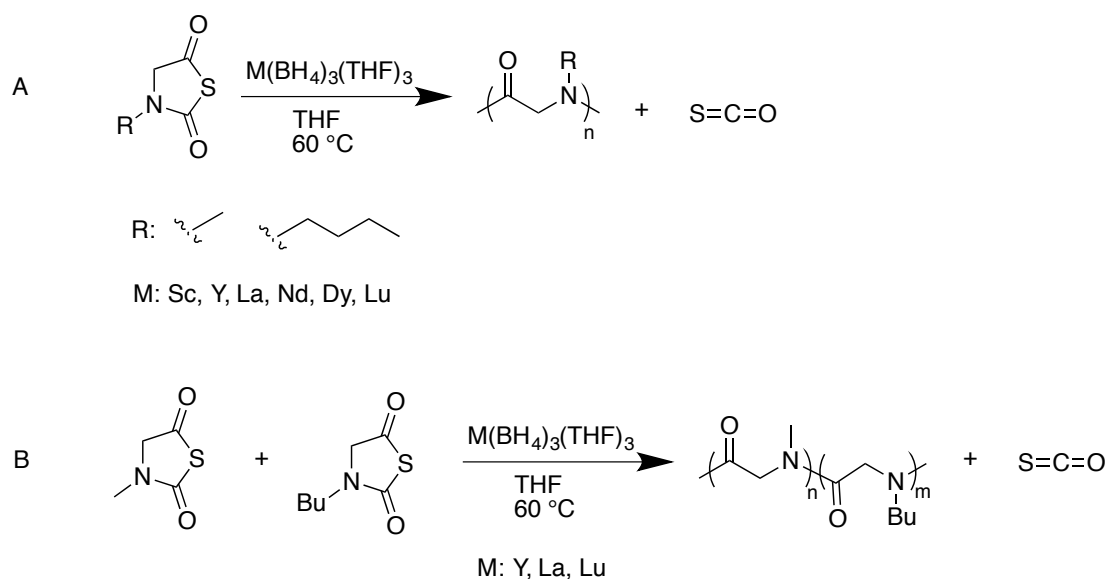
of potentially nucleophilic impurities such as chloride anions, which are generated during the synthesis, have been shown to act as potential and unwanted initiators.<sup>24</sup> These caveats with respect to the handling of NCAs limit their availability only to those who possess the necessary equipment and synthetic capability to handle them (e.g. glovebox, Schlenk techniques). A structurally similar alternative to NCA monomers substitutes a sulfur anhydride. These are collectively known as *N*-thiocarboxyanhydrosulfides (NTA). Amino acid derived NTAs have been reported to be stable for months at a time under ambient conditions and the monomers do not have to be synthesized under strict moisture free conditions like those of NCAs; synthesis of NTAs can be carried out in open air.<sup>182</sup> It is possible then that NTAs could be the gateway to obtaining well-controlled peptidomimetic materials in polymerizations for those lacking the capability to carry out the synthesis and polymerization of conventional NCA monomers. NTAs were originally synthesized for use in small peptide synthesis<sup>183-188</sup> and have been applied in the modification of textiles with peptides.<sup>189</sup> Recently there have been a number of research efforts to show that NTAs could be feasible alternatives to NCAs. This was disputed by Kricheldorf, who demonstrated that a series polysarcosines, poly(DL-phenylalanine)s, and poly(DL-leucine)s synthesized from their corresponding NTAs using a primary amine initiator did not exhibit good control over the obtained molecular weights.<sup>190</sup> Much more recently, Ling and coworkers have demonstrated that *N*-methyl glycine NTA could be polymerized using a PEG-functionalized primary amine and heat (60 °C) in order to obtain polypeptoids that exhibited good molecular weight control relative to the initial monomer and initiator feed ratios (Scheme 1.26).<sup>182</sup> Additionally, it was demonstrated that rare earth borohydride initiators (Scheme 1.27) could also be used in the ROP of *N*-methyl glycine NTA to obtain well-controlled species of polysarcosine in addition to block copolypeptoids from the ROP of *N*-butyl glycine NTA using the polysarcosine as a

macroinitiator in addition to benzylamine.<sup>191-192</sup> These polysarcosine and PNBG copolypeptoids have been shown to exhibit lower critical solution temperature behavior and the cloud points of these polymers can be tuned based on the feed ratios of sarcosine and *N*-butyl glycine NTA monomers during the polymerization.<sup>192</sup> These recent developments show that R-NTA monomers exhibit some promise as potential alternatives to R-NCA synthesis and subsequent polymerization of polypeptoids. The same polypeptoids as obtained from the ROP of R-NCA monomers can be obtained via the ROP of their thio analogs.

Scheme 1.26. Ring-opening polymerization of *N*-Me NTA with PEGylated amines



Scheme 1.27. Homopolymerization (A) and random copolymerization (B) of sarcosine and *N*-butyl NTAs using rare earth borohydride initiators



## **CHAPTER II. MULTIVALENT BINDING INTERACTIONS OF MANNOSE FUNCTIONALIZED GLYCOPOLYPEPTIDES WITH CONCANAVALIN A**

### **2.1 Objectives**

Chapter I gave a broad overview on the background of polypeptides. Because of their resemblance to proteins, polypeptides are good candidates for use as biomaterials as they have been demonstrated to display minimal cytotoxicity.<sup>23</sup> One main feature that distinguishes polypeptides from other polymers is their ability to self-assemble into well-defined secondary structures, most notably  $\alpha$ -helices and  $\beta$ -sheets without any necessary chemical modification to induce such behavior. These well-defined secondary structures are formed via intramolecular hydrogen bonding interactions. The  $\alpha$ -helix, especially that of poly( $\gamma$ -benzyl-L-glutamate) has been noted to have a high persistence length rendering the structure rod-like, which maximizes side chain display to the environment compared with that of random coil polymers. The latter is prevalent in many glycopolymer systems, which have been used as synthetic substrates to study multivalent binding effects to lectins, proteins which bind to specific carbohydrates. The goal of this study is to synthesize a series of glycopolypeptides whose chain lengths, backbone conformations, and binding epitope densities can be systematically tuned, and investigate the effects of these molecular characteristics on interactions with lectin in particular with respect to the binding kinetics, binding stoichiometry, and binding efficiency. It is proposed that the enhanced side chain display observed in helical glycopolypeptides will enhance the binding activity of a lectin to the carbohydrate side chains.

### **2.2 Multivalent binding, glycopolymers, and glycopolypeptides**

The primary structure of a protein is defined by its specific amino acid sequence. In nature, many of these amino acid derivatives bear side chains functionalized with

carbohydrates or sugars and are known as glycopolypeptides. One example is glycosaminoglycans connected to a protein via a serine residue. Glycopolypeptides occur in the extracellular matrices of living systems as proteoglycans. Proteoglycans are involved in a number of biological processes such as regulating the growth of collagen fibrils, controlling the activities of growth factor-beta, and serving as an anionic source in glomerular filtration.<sup>193</sup> One problem encountered in working with proteoglycans is their heterogeneity in vivo often requiring multiple separations.<sup>194</sup> Synthetic models, glycopolymers, have been developed to gain a better understanding the behavior of proteoglycans. Many glycopolymers are based on backbones that cannot be degraded by proteolysis such as acrylates. Polystyrene and polyethylene have been shown to illicit immune response in mice, making them poor candidates as biomaterials.<sup>195</sup> Recent developments have been focused on the synthesis of glycopolypeptides, which have a main chain polymer backbone composed of amino acid repeat units. Glycopolypeptides provide a number of advantages such as tunable backbone conformation and proteolytic degradability.<sup>36-41</sup> These attributes would make glycopolypeptides an ideal model to investigate multivalent carbohydrate-lectin interactions.

### 2.2.1 Multivalent carbohydrate-lectin interactions

There are numerous processes that are governed by multivalent interactions between two different components in living systems. These interactions can occur between proteins and small molecules, proteins and cell membranes, antibodies and cells, and between viruses and cells. One of the most widely studied multivalent interactions are those between proteins and carbohydrates as carbohydrates play a vital role in controlling cell-cell signaling<sup>196-197</sup>, protein and cell interactions<sup>198-200</sup>, and the targeting of antibodies, and toxins.<sup>201-204</sup> One notable example is the triggering of apoptosis on human T-cells by the binding of galectin-1 to external galactose residues of T-cells.<sup>198-199</sup>



These processes are mediated by the binding of carbohydrate to lectins, which are proteins that have binding affinity for specific carbohydrates. Some examples of lectins are Concanavalin A, Ricin, and Ulex europaeus agglutinin, which bind to mannose, galactose, and fucose respectively. Lectins often bind to glycosylated cellular membranes, which contain the necessary carbohydrates for the specific interaction. The relationship between carbohydrate and lectin serves as a method of cellular recognition between the many components of biological processes.

Individual binding interactions between monosaccharides and individual protein receptors are weak as their association constants are rarely beyond  $10^{-6} \text{ M}^{-1}$ .<sup>205</sup> This value must be significantly higher in order to achieve any control over the specific biological process dictated by the binding interaction. These weak binding interactions between monosaccharides and protein receptors have been overcome by nature through multivalent interactions; carbohydrate binding proteins (lectins) tend to exist as highly ordered or multivalent species where multiple copies of a particular protein receptor are present. The weak binding interactions that do exist between proteins and carbohydrates can be overcome through what has become known as the glycoside cluster effect<sup>206</sup> where the binding of multiple lectins to a carbohydrate substrate greatly improves the binding strength and affinity versus that of a monovalent lectin and receptor system. The glycoside cluster effect can be best realized in the binding of viruses to target cells; viruses often contain hundreds of copies of a specific lectin used to bind to target cells. The influenza virus contains approximately 300 copies of hemagglutinin used to bind to *N*-acetyl neuraminic acid found on the extracellular matrices.<sup>207</sup> The synthesis of various glycopolymers and glycopolypeptides has allowed these systems of multivalent carbohydrate-lectin interactions to be better characterized and understood.

## 2.2.2 Glycopolymers

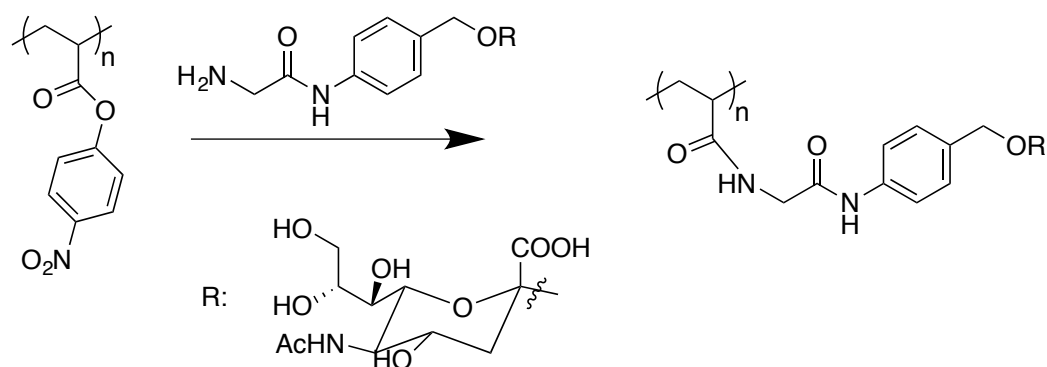
The synthesis of glycopolymers is motivated by the need to create synthetic analogs of proteoglycans and to serve as polysaccharide mimics in therapeutic applications such as drug delivery.<sup>208-210</sup> In this work, glycopolymers refer to those polymers containing carbohydrate moieties and non-polypeptide backbones.

**Glycopolymer synthesis.** Glycopolymers are composed of backbones that cannot be enzymatically degraded such as those based on carbon-carbon bonds. Poly(methacrylate)s<sup>211-214</sup> and styrenes<sup>215-216</sup> are among the most commonly used polymers in the synthesis of glycopolymers. There are numerous methods used to synthesize well-defined poly(methacrylate) and poly(styrene) polymers and they will not be covered here. Post-polymerization modification reactions using functionalized carbohydrate moieties are often used for their selectivity to couple with the desired functional groups in a “grafting to” approach. One of the earliest reports by Bovin et al used the amidation (*vide infra*) of an aminobenzyl functionalized sialic acid to the polymer pendant side chain.<sup>217</sup> This is summarized in Scheme 2.1. The biggest issues that can be seen with amidation reactions are that there is the possibility of disfavored equilibria, which may lead to incomplete side chain grafting. More chemoselective post-polymerization methods include copper mediated alkyne-azide cycloaddition (*vide infra*) and reactions with thiolated species either in thiol-ene, thiol-yne, or para-substitution of a fluorophenyl species.<sup>214, 216, 218-220</sup>

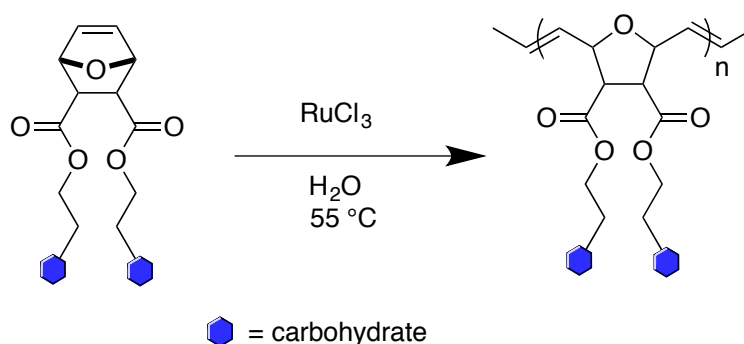
Alternatively, one could synthesize glycopolymers directly through the synthesis and polymerization of glycosylated monomers. However, accessing these monomers can be synthetically challenging. One notable example is the synthesis and polymerization of a glycosylated norbornene.<sup>221</sup> The derivatized norbornene is polymerized through ring-

opening metathesis polymerization (ROMP) to generate a fully glycosylated glycopolymer through what is known as a “grafting through” method (Scheme 2.2).

Scheme 2.1. Synthesis of sialic acid based glycopolymers via amidation



Scheme 2.2. ROMP of glycosylated norbornene



Influenza virus inhibition with glycopolymers. One prominent example of the study of the synthesis and application of glycopolymers to therapeutics is the inhibition of the binding activities of the influenza virus. The virus binds to target cells via a key lectin, hemagglutinin. Hemagglutinin is present on the virus with approximately 300 copies of the protein in a trimeric form. The virus uses these 300 copies of the lectin to bind to *N*-acetyl neuraminic acid residues on the target cells. Once bound to the target cell, the virus enters the cell and releases its RNA, beginning the viral replication cycle.<sup>207</sup> As previously discussed, multivalent binding is an occurrence where the association constant of the

substrate gradually increases with additional binding interactions to a ligand through the glycoside cluster effect. In the case of the influenza virus, multivalent binding occurs between the trimeric complex of hemagglutinin and the *N*-acetyl neuraminic acid residues of the target cell. Each monomeric binding event between *N*-acetyl neuraminic acid and hemagglutinin generates a weak binding interaction ( $K_d = 2 \text{ mM}$ ).<sup>222</sup> This single interaction is not strong enough for the virus to adhere to the cell. However, multiple binding interactions of the hemagglutinin onto additional copies of the *N*-acetyl neuraminic acid greatly increase the association constant and thus contribute to the adhesion that is observed when a virus binds to the cell in order to begin the lytic cycle to produce more viruses.

The first reported example that used glycopolymers as inhibitors of the influenza virus was reported by Bovin et al.<sup>217</sup> Aminobenzyl functionalized sialic acid were reacted with poly(4-nitrophenylacrylate)s in an amidation reaction in order to generate the desired glycopolymer (Scheme 2.1). The content of sialic acid was varied between samples and monomeric glycoside was also investigated as a potential inhibitor of the virus. It was found that increasing the content of the sugar on the glycopolymers increased the measured inhibition. The maximum inhibition was determined at 20% glycosylation; increasing the sugar content above 20% actually led to decreased levels of inhibition. Minimal, if any, inhibition of the virus was observed in monomeric sugar species and those glycopolymer species bearing low levels of glycosylation supporting the observations of weak binding interactions between monosaccharides and lectins.

The Whitesides group has made significant foray into the application of glycopolymers in therapeutics with respect to influenza virus inhibition.<sup>222-229</sup> Whitesides et al expanded upon the findings made by Bovin, who previously determined that intermediate levels of glycosylation on the polymer side chains provide the maximum

levels of virus binding inhibition due to competition between cooperative binding interactions of adjacent carbohydrate moieties. Overcrowding the glycopolymer backbone leads to increased steric bulk of the binding epitopes amongst each other. This results in reduced access by the lectin to the binding epitopes. One report explored the effects of side chain sterics and charge on inhibition.<sup>223</sup> It was determined that the addition of bulky groups or charged species decreased the observed binding with the influenza virus and thus lowered the observed inhibition levels. These studies involved the use of O-linked sialic acid moieties, which can be cleaved by neuraminidases, producing monomeric sialic acid, and potentially lowering the inhibitory potential of the glycopolymer systems. A C-linked sialic acid acrylate monomer was synthesized and demonstrated to be resistant to the effects of neuraminidases yet the level of viral inhibition paralleled that of the O-linked glycopolymers.<sup>225</sup>

One issue observed with these earlier studies is that copolymerization of functionalized comonomers was used to obtain the resulting glycopolymers and provide the spacing between the functional sialic acid moieties. Because it is known that the maximum inhibitory potential can be achieved by spacing out the binding epitopes from each other, copolymerization has allowed for the insertion of spacers. However, because two different acrylic monomers were used, there is the potential for the reactivity ratios of the monomers to differ significantly, possibly resulting in a gradient distribution and may contribute to overcrowding of the polymer side chains. Additionally, the use of post-polymerization modification allows polymers from a single reaction batch to be used comparatively in inhibition studies; the polymer species from a specific reaction batch would have similar polydispersity, molecular weights, and degrees of polymerization unlike those obtained from copolymerization.

A number of works by the Whitesides group have attempted to address these issues through post-polymerization modification strategies. A number of strategies that were explored in order to obtain a more statistical distribution of binding epitopes along the polymer chains was through the functionalization of poly[(*N*-acryloxy)succinimide]<sup>227</sup> or poly(acrylic anhydride)<sup>229</sup> with a variety of primary amines in addition to the sialic acid binding epitopes. From these studies, it was revealed that sub-nano molar levels of influenza virus inhibition could be achieved and that there was a dependence on the observed inhibitory potential with the sterics of the primary amines used; sterically bulkier side chains contributed to decreased inhibition.

Investigation of multivalent binding with Concanavalin A. It is interesting that increased epitope density actually led to decreased binding interactions between hemagglutinin and the influenza virus leading to decreased inhibition. A number of studies by Kiessling et al have investigated the effects of multivalency on the binding of the carbohydrate side chains of glycopolymers with Concanavalin A (ConA), a plant lectin derived from the jackbean, which has binding affinities for both glucose and mannose.<sup>230-234</sup>

Kiessling et al investigated the effects of multivalent binding of monovalent glucose and mannose and glycopolymeric scaffolds bearing glucose and mannose side chains to ConA. Glycopolymers used in the studies were synthesized by ring-opening metathesis polymerization (ROMP) of a glycosylated norbornene monomer (Scheme 2.2).<sup>221, 230</sup> Compared to previous methods which involved the radical polymerization of acrylic monomers<sup>217, 223</sup>, a ROMP based strategy would allow for improved control over the size, and epitope density of the resulting glycopolymers.<sup>221</sup> These early studies demonstrated that compared with monosaccharide species of glucose and mannose, the polyvalent glycopolymers exhibited at most, a 50000-fold improvement in inhibitory potential in the investigation of agglutination of erythrocytes.<sup>230</sup> The specificity of ConA

towards mannose versus glucose was also investigated. Previous studies have found that the free energies of binding of glucose and mannose to ConA only differ from approximately 0.2-0.8 kcal/mol.<sup>235</sup> This difference was clearly observed in the comparison of glycopolymers bearing glucose versus mannose side chains; glycopolymers bearing mannosides exhibited 160-fold lower inhibitory concentrations versus the glucoside analogues suggesting the improved binding affinity of ConA for mannose over glucose.

Subsequent studies investigated the effects of binding epitope density with respect to the rate of clustering (kinetics), and binding stoichiometry.<sup>234</sup> Glycopolymers were synthesized via ROMP bearing either mannose or galactose moieties on the side chains, the latter of which does not bind to ConA. The relative loadings of the mannoside or galactoside monomer were adjusted in order to obtain a series of glycopolymers with varying binding epitope densities. With respect to the rate of clustering, glycopolymers with higher percentages of mannosides on the side chains exhibited faster rates of clustering ( $k_i$ ) than those glycopolymers with lower degrees of mannosides. As expected, minimal clustering was observed in the species bearing all galactosides. Thus, the number of receptors is important when fast kinetics are desired. Higher binding epitope densities also led to higher observed binding stoichiometry, which is a measure of the number of ConA tetramers bound per chain. However, those glycopolymers with lower binding epitope densities tend to bind more ConA residues per mannose residue present on the chain due to the increased spacing between binding residues, requiring only 2 mannose residues per binding interaction with ConA versus 9 mannose residues in the fully glycosylated species.<sup>234</sup> Thus, although the former species binds the slowest, it benefits from the most use of the available mannose residues (Figure 2.1).

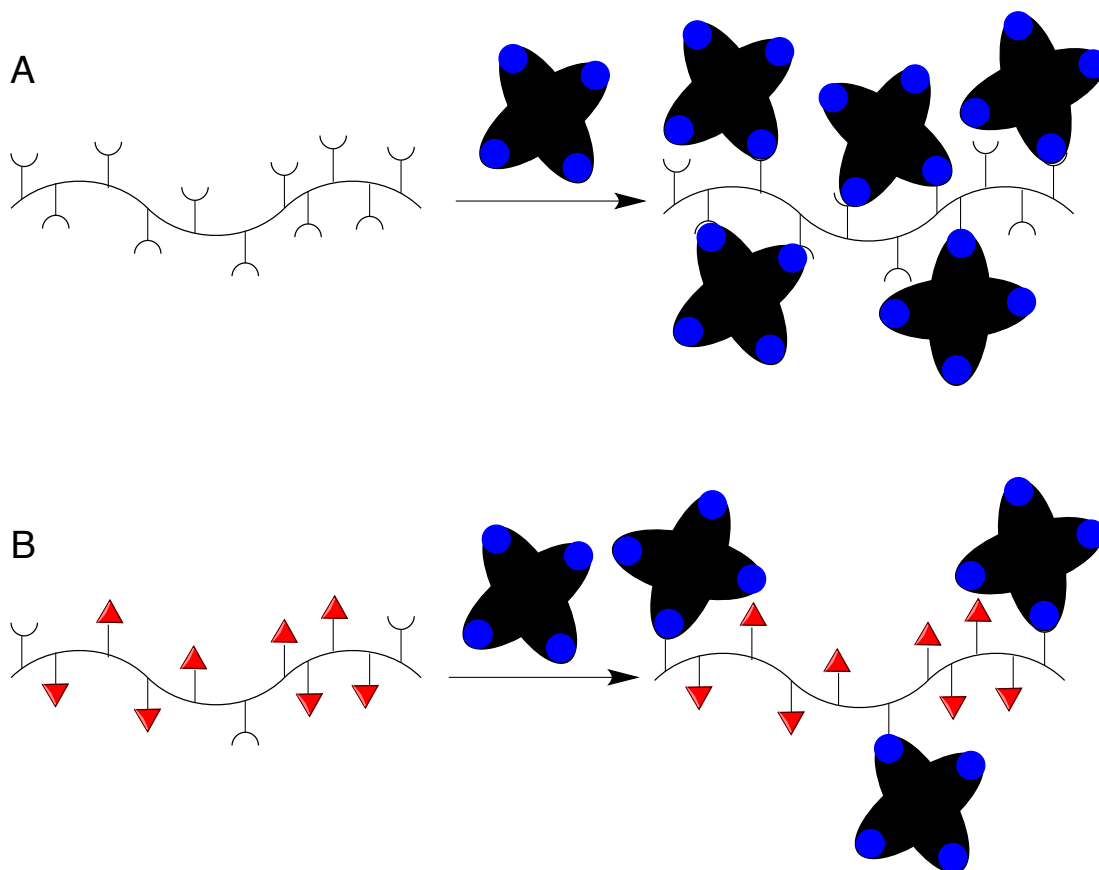


Figure 2.1. (A) Binding of ConA to a glycopolymer with maximum binding epitope density. Mannose binding epitopes are represented by the semicircles. (B) Binding of ConA to a glycopolymer with lower binding epitope density and spacing in between each of the binding species. Though example A binds more ConA, the example in B displays more effective binding with respect to a per mannose residue basis (mannose/ConA) due to usage of all of the available mannose receptors versus that of A where a number of mannosides are rendered inaccessible due to sterics.

Drug delivery. Another application that has been explored with glycopolymers is in drug delivery. There are a number of obstacles that must be overcome in the development of an efficient drug delivery system. One such roadblock is overcoming the blood brain barrier (BBB), which regulates the diffusion and transport of molecules into the brain. Unlike the rest of the body, the area surrounding the BBB does not contain pores known as fenestrae, which allow the two-way diffusion of molecules between the bloodstream and the tissue. Transport across the BBB must be via the lipid membrane. Interestingly it has been found that glycosylation allows molecules to pass through the BBB, thus



inspiring a potential application of glycopolymers as site specific drug delivery vessels which target the brain.

With respect to drug delivery methods, a commonly used method is one developed by Ringsdorf where a polymer is functionalized with the drug to be delivered, a solubilizing agent, and a targeting ligand.<sup>236</sup> Carbohydrate moieties are in this case able to assist as a targeting ligand, solubilizing agent, or both simultaneously. One example of a drug delivery system involving glycopolymers using the Ringsdorf method was developed by Cameron and Davis et al which involved the targeting of boar spermatozoa which display a galactose binding lectin. Site specific delivery could be achieved through the application of a galactose targeting ligand on the respective polymeric drug delivery platform. To demonstrate the site specific capabilities of their system, acrylic terpolymers composed of galactose, 2-diaminoethyl groups, and  $\alpha$ -tocopherol were synthesized.  $\alpha$ -tocopherol is an antioxidant, designed to repair oxidative damage of the spermatozoa brought on by storage and transport. The  $\alpha$ -tocopherol functionalized moiety was also replaced with a fluorescent marker, hostasol, to allow visualization of the spermatozoa.<sup>237</sup>

### 2.2.3 Glycopolypeptides

Each example of a glycosylated polymer species previously discussed was composed of a non-degradable polymer backbone, which may present problems with respect to biocompatibility. Poly(methyl methacrylate) has been shown to trigger an immune response in patients who have received methyl methacrylate based prostheses.<sup>238-</sup>  
<sup>239</sup> Glycopolypeptides have a number of distinct properties that may render them advantageous over glycopolymers. Most importantly, polypeptides have the potential to be enzymatically degraded, allowing for their removal from living systems. Secondly, polypeptides can self-assemble into well-defined secondary structures, (i.e.  $\alpha$ -helices,  $\beta$ -

sheets) which enhance side chain display and may allow for improved access to the pendant side chains.

Glycopolyptide synthesis. As with the synthesis of oligopeptides with exact sequencing of the amino acid repeat units, glycopolyptides have been synthesized using solid phase peptide methods using amino acid starting material that has been glycosylated.<sup>240-241</sup> Similarly, high molecular weight species are difficult to access and the quantities by which syntheses can be conducted are also limited.

A more unusual method to access glycopolyptides, DNA recombinant techniques, combine aspects of chemical and biological syntheses. Kiick et al have produced a series of sequence specific oligopeptides where the exact spacing of the glycosylated species can be controlled.<sup>242-243</sup> Following the synthesis of the peptide, the glutamic acid residues on the chain were functionalized with galactose through amidation reactions. The exact sequencing of the sugar moieties in these studies was designed in order to mimic the distance between the galactose binding sites of the cholera toxin so that the inhibition of the toxin using the glycopeptide could be further investigated. The main disadvantages with recombinant DNA techniques for polypeptide synthesis are the multiple steps required and that the process is time consuming.<sup>244</sup>

Glycopolyptides can also be accessed via the products of the ROP of amino acid based NCAs. There are a number of strategies that could be used with respect to NCA ROP to access the desired glycopolyptides. The carbohydrate moieties could be added onto the pendant side chains during monomer preparation to produce glycosylated amino acid based NCAs. Alternatively, carbohydrate moieties could be grafted onto the side chains using one of many post-polymerization modification reactions. A generic diagram outlining these synthetic strategies is shown in Figure 2.2.

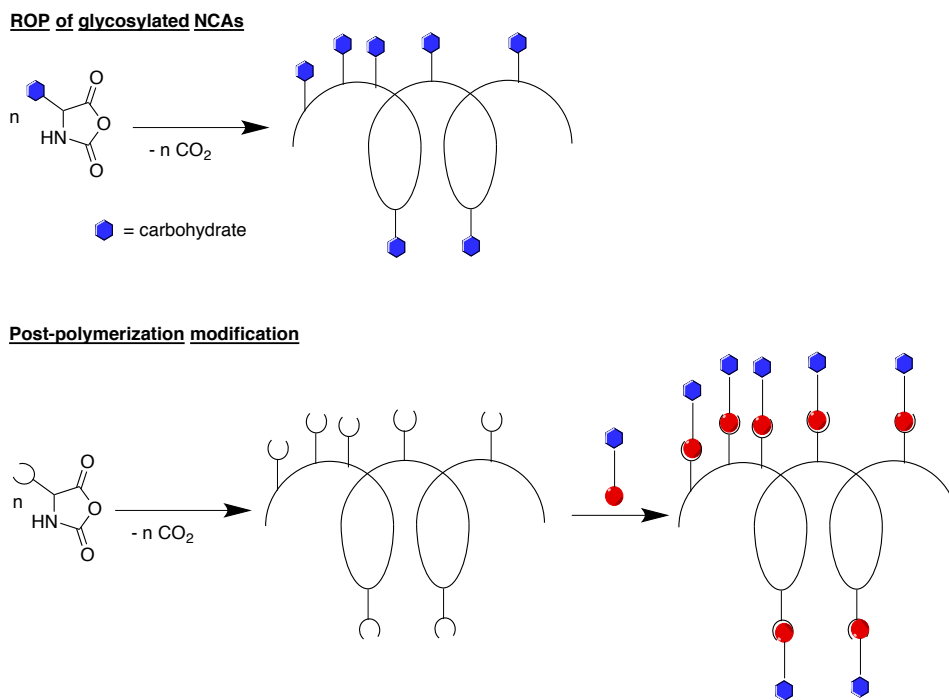
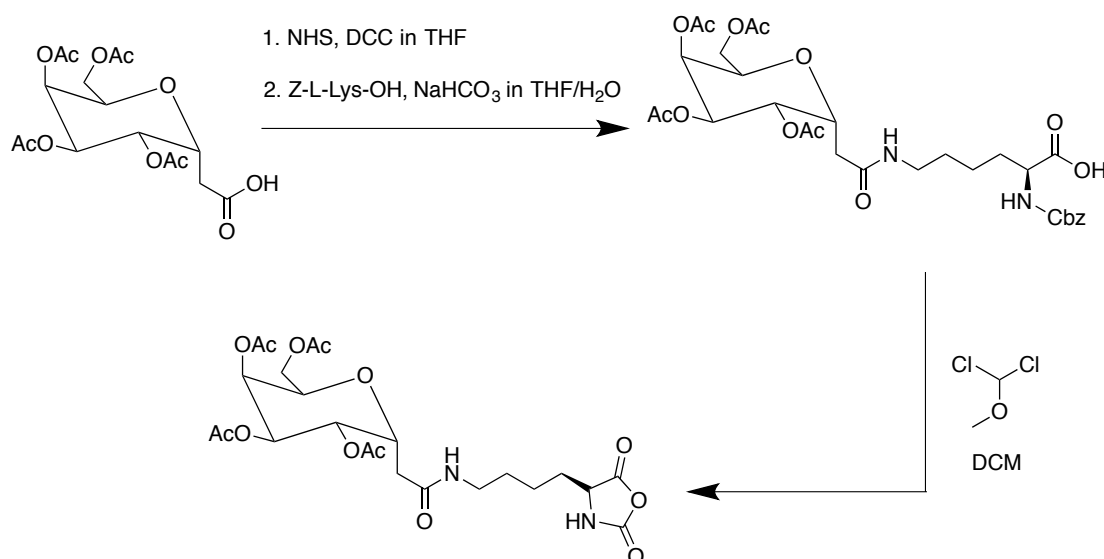


Figure 2.2. Diagrams outlining the various synthetic strategies to access glycopolypeptides in the ROP of NCAs.

The earliest reports of glycopolypeptide synthesis via the synthesis of glycosylated NCAs were made by Rude et al. O-linked glyco-serine NCAs were synthesized but it was noted that synthetic yields of the glyco-serine NCAs were poor and polymerization of these NCAs only yielded small oligomeric products, which was suggested to be due to hydrogen bonding interactions between the NCA monomer and the sugar substituents.<sup>245-246</sup> An additional drawback in the synthesis reported by Rude is the use of toxic mercuric cyanide in the Koenigs-Knorr reaction, a substitution reaction between a glycosyl halide and an alcohol. This was used to link the carbohydrate to the serine. An improvement of the synthetic yield of O-linked glyco-serine NCA and the synthesis of other glycosylated NCAs such as S-linked glyco-serine and glyco-threonine NCAs has also been reported by Cameron but the monomers were unable to be polymerized because of insufficient purity.<sup>247</sup> The method by Cameron also avoided use of mercury salts. Deming et al first reported the controlled ROP of a series of

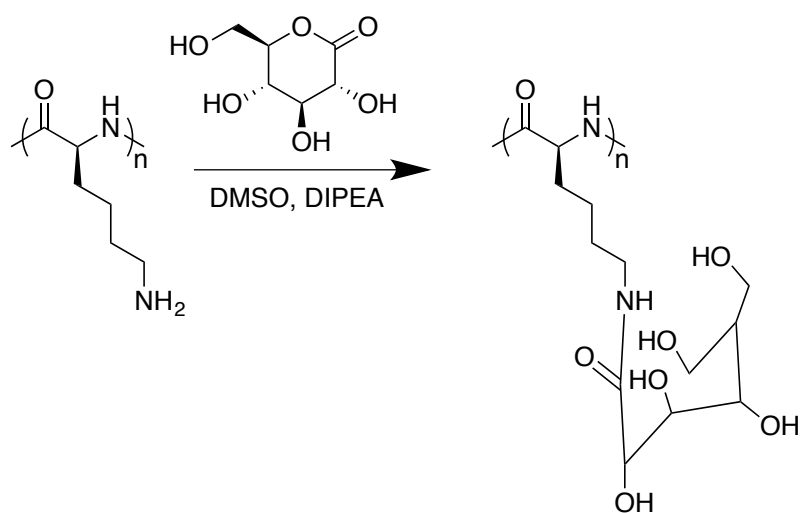
glycosylated lysine based NCAs.<sup>248</sup> Three different carbohydrates, glucose, mannose, and galactose were used in the preparation of three glyco-lysine NCAs (galactose example shown in Scheme 2.3). Through the use of  $\text{Co}(\text{PMe}_3)_4$  catalyst<sup>100</sup>, it was demonstrated that glycopolypeptides of varying chain lengths could be synthesized through the controlled ROP of NCAs. A glyco-cysteine derivative was also reported by Deming et al which displayed the ability to undergo a conformation switch to a random coil via aqueous oxidation in the presence of hydrogen peroxide.<sup>249</sup> Gupta et al also reported a series of glycopolypeptides that could be obtained from the ROP of pre-functionalized NCAs using primary amine initiators.<sup>250-251</sup> The biggest advantages to starting with functionalized, or glycosylated monomer, are that there is no need for post-polymerization modification in order to graft the carbohydrate moieties onto the side chains and that 100% glycosylation is guaranteed. However, glycosylated NCA monomers can be synthetically challenging to access.

Scheme 2.3. Synthesis of galactose functionalized L-lysine NCA as reported by Deming et al



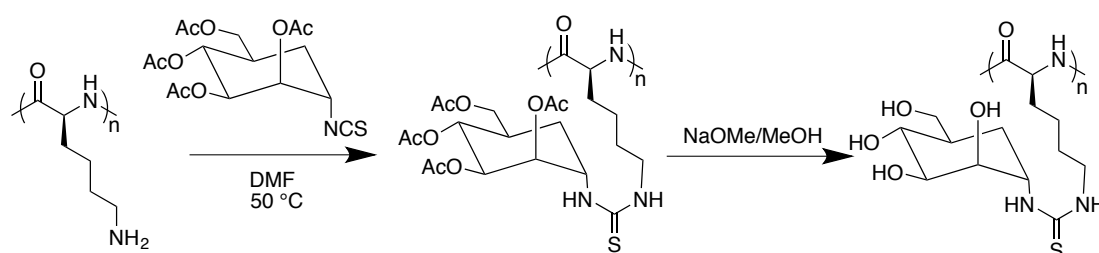
Post-polymerization modification reactions are another strategy used in the synthesis of glycopolypeptides. The main advantage of post-polymerization modification is the avoidance of the synthesis of complex monomers but grafting efficiency may be limited using post-polymerization modification reactions. Grafting efficiency may vary depending on a number of factors such as starting material solubility, sterics, and functional group compatibility. Thus quantitative grafting of carbohydrates in the synthesis of glycopolypeptides is not necessarily ensured. A number of the earliest reports by Feng et al relied on the formation of amide linkages between poly(L-lysine) and gluconolactone or lactobionolactone under basic conditions (Scheme 2.4) to produce a series of glycopolypeptides functionalized with linear carbohydrates.<sup>252-253</sup> While the feed ratios of ring-opened, linear carbohydrates could be adjusted in order to tune the sugar grafting densities, the highest reported grafting percentage was reported to be 75% due to the steric blockage of other available binding sites by the already grafted carbohydrate moieties.

Scheme 2.4. Post-polymerization synthesis of a glycopolypeptide via the reaction between poly(lysine) and gluconolactone as described by Feng et al



Another post-polymerization strategy that has been explored is the formation of thiourea linkages by Li et al. Deprotected poly(L-lysine) is reacted with isothiocyanate functionalized carbohydrates in order to generate the thiourea linkage between the poly(L-lysine) side chain and functional moiety (Scheme 2.5).<sup>254-255</sup> The biggest disadvantage of this method was the inefficiency of grafting; the maximum observed glycosylation density was only 36%, even if an excess of isothiocyanate sugar was used in the glycosylation reaction. This low grafting percent is possibly due to steric blockage of the side chains. Thus, this method is not robust and alternative methods need to be sought out to achieve higher grafting densities.

Scheme 2.5. Glycopolypeptide synthesis via thiourea linkage formation as described by Li et al



Chapter I gave a brief overview on the common post-polymerization reactions that can be carried out on the polypeptide side chains, especially those of glutamic acid derivatives. The biggest advantages to these reactions are their high chemoselectivity and functional group tolerance. Perhaps the most popular of these reactions is copper mediated alkyne/azide cycloaddition (CuAAC). The reaction is a Cu(I) catalyzed Huisgen 1,3-dipolar cycloaddition. CuAAC was reported in 2002 by the Sharpless<sup>256</sup> and Meldal<sup>257</sup> groups independently and has been<sup>257</sup> dubbed “the cream of the crop” of “click” chemistry reactions by the former due to its high chemoselectivity. The reaction has also been demonstrated to proceed in water. CuAAC has been used in multiple reports in the

synthesis of glycopolypeptides via post-polymerization modification.<sup>58, 123, 126-127, 258-259</sup>

While CuAAC allows for the grafting of the desired moieties, Cu ions could be introduced into living systems, possibly inducing cytotoxicity. Thus, extensive purification is required following a CuAAC reaction to ensure that Cu is completely removed. Common methods used to remove Cu ions following CuAAC include column chromatography<sup>260</sup>, ion exchange resin<sup>123, 212</sup>, and dialysis against water using EDTA.<sup>58</sup>

Other post-polymerization modification methods used in the synthesis of glycopolypeptides include thioether alkylation of poly(L-methionine) via alkyl halides or triflates.<sup>132</sup> The thioether alkylation has a unique advantage in forming cationic charge via a sulfonium cation upon completion of the reaction, which may allow uptake by cells but may also induce cytotoxicity. Glycosylated poly(L-methionine) derivatives were demonstrated to show potential as viable cell penetrating peptides because of adequate uptake as evidenced by fluorescence imaging and the minimal cytotoxicity exhibited by the cationic glycopolypeptide systems.<sup>261</sup> One disadvantage of this system is the insolubility of poly(L-methionine) in common solvents, making characterization of the parent polypeptide difficult.

Thiol-ene coupling was used by Schlaad in the synthesis of glycopolypeptides from poly(DL-allyl glycine) and poly(DL-propargyl-glycine).<sup>137</sup> Unlike CuAAC, thiol-ene coupling is copper free and requires minimal purification and does not have the potential to introduce cytotoxic Cu ions into living systems. However, it was reported that quantitative grafting of carbohydrate moieties to the alkene or alkyne side chains could not be accomplished except when 1-thio- $\beta$ -D-glucopyranose was used versus the *O*-acetyl protected analog. The low grafting efficiency was perhaps due to solvent choice as DMF appeared to be a poor solvent for poly(DL-allyl glycine). The thiol-ene reaction using 1-

thio- $\beta$ -D-glucopyranose was run in trifluoroacetic acid, which could be potentially hazardous.

Self-assembly of glycopolypeptides into more complex aggregates has been observed in a number of amphiphilic systems. Amphiphilic glycopolypeptide systems could be synthesized via CuAAC as demonstrated by Lecommandoux where the self-assembly of the “tree-like” glycopolypeptides into micelles was observed.<sup>262</sup> Gupta et al used a different approach to synthesizing amphiphilic glycopolypeptides via CuAAC, using azido functionalized mannose moieties bearing hydrophobic alkyl chains.<sup>258</sup> These species were also observed to self-assemble into spherical micelles.

Investigations of multivalent binding in glycopolypeptides. It is expected that backbone conformation would have an effect on the binding of the carbohydrate side chains to lectins. Based on the relative side chain presentation of a helical rod versus a compact coil, it would be expected that there would be enhanced binding activity in the former species. Unfortunately, previous studies show conflicting reports as to the effect of backbone conformation on the observed binding interactions of carbohydrates with lectins. Although helical species are expected to behave similarly to rigid rods, good and efficient binding of a lectin will only occur if the distance between two sugar moieties matches that of the distance between two lectin binding sites. This was observed in a report by Kobayashi et al where the binding activity of a series of stiff poly(glycosyl phenyl isocyanate)s was compared with that of a more flexible phenylacrylamide analog.<sup>263</sup> The former rigid rod species showed minimal activity towards lectin binding whereas enhanced binding of the lectins used in the study (Concanavalin A and RCA<sub>120</sub>) to the glycopolymers was observed in the latter flexible species, suggesting that the flexibility of the polymer chain allows for the spacing between sugar moieties on the side chains to conform to the spacing between the binding sites of the lectin. In turn this will



induce binding between carbohydrate and lectin. In contrast, Kiick et al have demonstrated that helical glycopolypeptides demonstrate superior binding activity in the investigation of the binding of galactose to cholera toxin in comparison to those of random coil species.<sup>264</sup> Thus, further investigation is required with respect to the effects of backbone conformation on the observed binding interactions between carbohydrates and lectins.

Chen<sup>123</sup> and Gupta<sup>251</sup> et al have investigated the effect of multivalent binding to ConA using glycopolypeptide scaffolds. The study by Chen et al investigated the effects of binding epitope density on the observed lectin-carbohydrate interactions. Synthesis of the glycopolypeptides was accomplished using post-polymerization modification of poly( $\gamma$ -propargyl-L-glutamate) via CuAAC. It was found that for a series of glycopolypeptides with decreasing mannose density that binding activity to ConA decreased with decreasing mannose content. Binding stoichiometry was determined to be much less than a previous report where a flexible glycopolymer synthesized via ATRP was investigated<sup>211</sup> suggesting that the sterics of the rigid rod helix contributed towards steric overcrowding of the chain, even with enhanced side chain display. Steric overcrowding ultimately affects access to the mannose side chains by the lectin resulting in decreased binding activity.

Gupta et al investigated a series of glycopolypeptides synthesized from the ROP of glycosylated lysine NCA. The monomer used in this study consisted of both enantiomerically pure (i.e. L) and racemic (DL) NCA. Polymerization of DL or racemic NCA monomers versus enantiomerically pure monomers (i.e. D or L) produces random coil species due to the introduction of disorder along the polypeptide backbone.<sup>265-266</sup> These random coil species would allow for a control species in the analysis of the effects of backbone conformation in synthetic glycopolypeptides. It was reported that backbone

conformation does not drastically affect carbohydrate-lectin binding interactions in experiments using ConA.

These works however are limited in scope as only a narrow range of DP<sub>n</sub> were studied, ranging from 35 to 66. Although it has been established in the study of glycopolymer interactions with ConA that chain length affects the observed binding due to the presence of more available binding sites<sup>232, 234, 267</sup>, this has not been elaborated upon in studies with glycopolypeptides. Further investigation is required with respect to the effect of varying chain lengths on multivalent lectin-carbohydrate interactions in glycopolypeptides. We have developed a series of glycopolypeptides of varying DP<sub>n</sub> from DP<sub>n</sub>=12 to 174 and of varying backbone conformations and will further explore the effects of these properties on the binding of ConA to these multivalent glycopolypeptides.

## **2.3 Results and discussion**

### **2.3.1 Synthesis and characterization of glycopolypeptides**

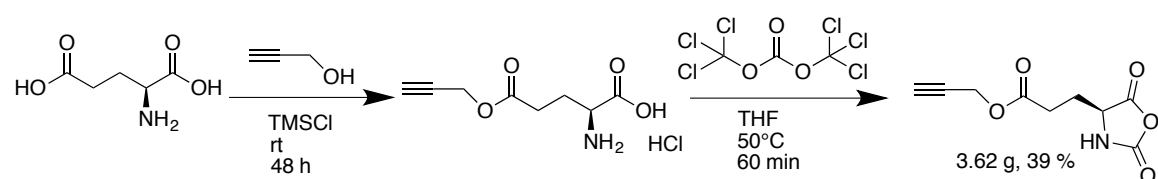
The synthetic methodology used to synthesize the helical and random coil glycopolypeptides was adopted from previous methods.<sup>58</sup> For the sake of brevity, schemes that are shown in this chapter will only show the L enantiomer although the racemic analogs are synthesized using parallel methods.

L-glutamic acid can be functionalized via an esterification reaction between the  $\gamma$ -carboxylic acid and a respective alcohol under acidic conditions. The versatility of this esterification can be demonstrated through a variety of monomer precursor glutamates that can be synthesized via this method such as  $\gamma$ -benzyl-L-glutamate<sup>211</sup>,  $\gamma$ -allyl-L-glutamate<sup>125</sup>,  $\gamma$ -3-chloropropyl-L-glutamate<sup>58</sup>, and  $\gamma$ -propargyl-L-glutamate.<sup>57</sup> The latter three glutamate derivatives have the potential to be functionalized in post-polymerization reactions, allowing for a variety of functionalities to be grafted to the side chains.

Esterification of L-glutamic acid with propargyl alcohol (Scheme 2.6) yielded the monomer precursor in good yield (81 %) thus allowing for larger scale reactions.

The NCA cyclization reaction was carried out via the Fuchs-Farthing method using triphosgene which has been shown to be easier to handle as a solid when compared with phosgene (gas) or diphosgene (liquid).<sup>51</sup> Three equivalents of phosgene are evolved for each mole of triphosgene thus the NCA synthesis uses a glutamic acid precursor to triphosgene ratio of 1:0.34. HCl is evolved during this reaction, which has been shown to contribute to early termination and the lowering of  $M_n$  and subsequent broadening of PDI. Thus, high purity of the  $\gamma$ -propargyl-L-glutamate *N*-carboxyanhydride (PLG-NCA) and its racemic analogue  $\gamma$ -propargyl-DL-glutamate *N*-carboxyanhydride (PDLG-NCA) is necessary in order to maintain polymerization control and prevent early termination, lowering of  $M_n$ , and subsequent broadening of PDI. Purification of PLG and PDLG-NCA was achieved using dry flash chromatography methods previously reported by Deming et al, which have been shown to be successful in the purification of amino acid based NCAs.<sup>60</sup>

Scheme 2.6. Synthesis of PLG-NCA from L-glutamic acid



ROP of PLG and PDLG NCAs was achieved using benzylamine initiator (Scheme 2.7). The molecular weights of the resulting polypeptide species could be controlled through variation of the initial monomer to initiator loadings ( $[M]_0:[BnNH_2]_0=10-200:1$ ), allowing for the synthesis of a series of propargyl functionalized polypeptides at varying  $M_n$  (2.0-29.0 kg·mol<sup>-1</sup>) with adequate PDI (1.05-1.15). These polymerization data of the

resulting poly( $\gamma$ -propargyl-L-glutamate) (PPLG) and poly( $\gamma$ -propargyl-DL-glutamate) (PPDLG) are shown in Table 2.1 and Table 2.2 respectively. Monomer conversion was analyzed using FTIR monitoring the disappearance of the carbonyl stretching bands at 1852 and 1785  $\text{cm}^{-1}$ . It can be seen from the polymerization data that the obtained molecular weights are comparable with theoretical values based on single-site initiation by benzylamine initiator and that the obtained molecular weight distributions are also adequate. This demonstrates that a series of well-defined polypeptides of varying chain lengths and backbone conformations can be obtained from the ROP of enantiomerically pure PLG NCA and its racemic counterpart PDLG NCA.

Scheme 2.7. Polymerization of PLG-NCA via benzylamine initiator

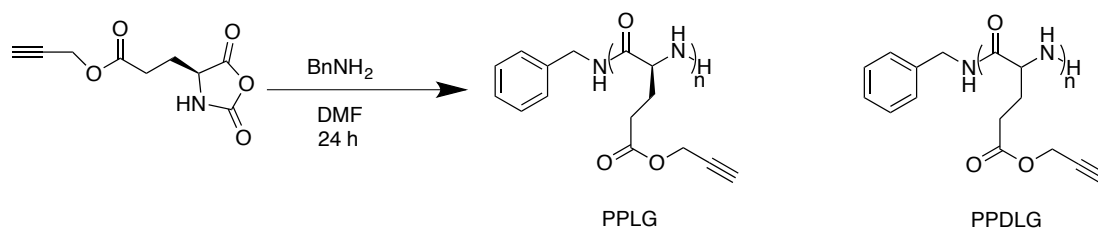


Table 2.1 Molecular weight characterization data for a series of PPLG obtained from the ROP of PLG NCA using benzylamine initiator <sup>a</sup>

$[M]_0:[\text{BnNH}_2]_0$	$M_n$ (theo.) ( $\text{kg}\cdot\text{mol}^{-1}$ ) <sup>b</sup>	$M_n$ (SEC) ( $\text{kg}\cdot\text{mol}^{-1}$ ) <sup>c</sup>	PDI	$\text{DP}_n$	Percent helicity
10:1	1.7	2.2	1.05	13	6.15
25:1	4.2	3.8	1.15	23	41.5
50:1	8.4	8.9	1.06	53	47.7
100:1	16.7	17.5	1.09	105	63.5
200:1	33.4	29.0	1.13	174	67.9

<sup>a</sup> All polymerizations were performed at  $[M]_0 = 1.0$  M in DMF for 24 h; <sup>b</sup> based on conversion calculated from FTIR analysis; <sup>c</sup> absolute molecular weights were calculated using previously determined  $\text{dn}/\text{dc} = 0.0844$  mL/g.

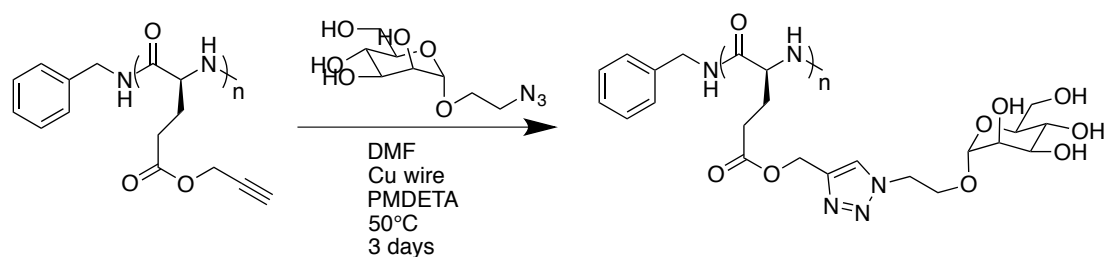
Table 2.2. Molecular weight characterization data for a series of PPDLG obtained from the ROP of PDLG NCA <sup>a</sup>

$[M]_0:[BnNH_2]_0$	$M_n$ (theo.) ( $kg \cdot mol^{-1}$ ) <sup>b</sup>	$M_n$ (SEC) ( $kg \cdot mol^{-1}$ ) <sup>c</sup>	PDI	DP
10:1	1.6	2.0	1.11	12
25:1	4.2	3.1	1.12	19
50:1	8.4	6.7	1.07	40
100:1	16.7	17.2	1.15	103

<sup>a</sup> All polymerizations were performed at  $[M]_0 = 1.0$  M in DMF for 24 h; <sup>b</sup> based on conversion calculated from FTIR analysis; <sup>c</sup> absolute molecular weights were calculated using previously determined  $dn/dc = 0.0872$  mL/g.

The side chains of PPLG and PPDLG contain propargyl groups, which can undergo post-polymerization modification via CuAAC. Synthesis of the glycopolypeptides was completed via CuAAC using 2-azidoethyl mannose (Scheme 2.8), which was performed under an oxygen free atmosphere in the glovebox in order to prevent possible oxidation of the Cu(I) to Cu(II). Oxidation would quench the reaction as Cu(I) is necessary for the reaction to occur. Unlike other CuAAC systems whose copper source was either copper(I)bromide<sup>58</sup> or copper(I)sulfate<sup>123</sup>, freshly shaved copper wire was used the copper source.<sup>268</sup> The copper wire can be used multiples times using this method.

Scheme 2.8. Glycosylation of PPLG via CuAAC using copper wire method



The formation of the triazole heterocycle is observed in the  $^1\text{H}$  NMR spectrum of the resulting glycopolyptide with the formation of a singlet at 8.04 ppm. There is also an observed downfield shift in the chemical shift of the methylene proton of the propargyl group from 4.68 to 5.13 ppm. The percentage of glycosylation can be determined via the integration of the triazole singlet peak with those of the aliphatic backbone. One issue that has plagued previous glycopolymer systems is the inability to reach quantitative grafting on the side chains. Based on the relative integrations of the newly observed triazole peak with those of the aliphatic backbone, it was suggested that quantitative grafting of mannose was achieved in both PPLG and PPDLG to yield their fully glycosylated glycopolyptide counterparts. Exemplary  $^1\text{H}$  NMR spectra of PPLG parent polymer, PPLG mannose, and PPLG mannose-galactose where the binding epitope densities were varied (vide infra) are shown in Figure 2.3.

### 2.3.2 Circular dichroism of glycopolyptides

Circular dichroism (CD) is a commonly used technique in the study of the secondary structures of proteins (i.e.  $\alpha$ -helix,  $\beta$ -sheet, random coil) and how changes in the environment such as pH, sample concentration, and temperature can affect the observed secondary structures. In this study, we hypothesize that helical glycopolyptides are near rod-like thus having enhanced surface area for side chain presentation whereas random coil glycopolyptides have a much more compact form, suppressing side chain exposure. The  $\alpha$ -helix shows distinct minima at 208 and 222 nm on the CD spectrum. Random coil species display only a distinct maximum at 215 nm. Percent helicity in the glycopolyptides was calculated using the formula  $((-[\theta_{222}] + 3000) / 39000)$ .<sup>269</sup> It was found that as  $\text{DP}_n$  increased from 13 to 174, the helicity increased from 6.15 to 67.9% (Figure 2.4, Table 2.1). This increase in observed helicity

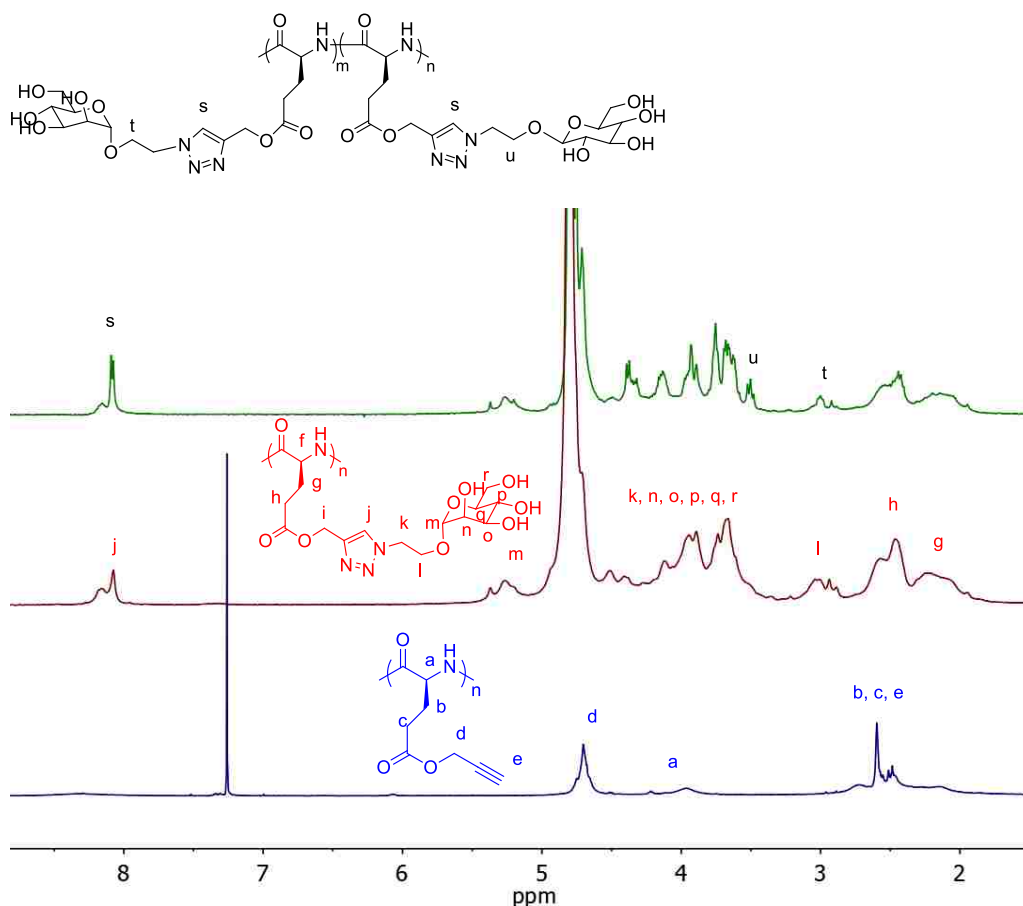


Figure 2.3.  $^1\text{H}$  NMR spectrum of PPLG ( $[M]_0:[I]_0=100:1$ ) (blue) collected in  $\text{CDCl}_3$  and subsequent PPLG mannose (red) and PPLG mannose-galactose (green) collected in  $\text{D}_2\text{O}$ .

with respect to  $\text{DP}_n$  may be due to improved H-bonding cooperation in samples with higher  $\text{DP}_n$ . However it was also observed that none of the samples are 100% helical suggesting that the observed polypeptides are not true rods. However, in contrast, there is a clear distinction in the measured CD spectra of helical samples versus those of random coil samples demonstrating that random coil analogs could be accessed using racemic starting material to introduce disorder in the hydrogen bonding interactions along the polypeptide backbone (Figure 2.5). The CD data obtained will allow for a better understanding of how a multivalent ligand will bind to the glycopolymer substrate with respect to the general backbone architecture of the polymer and the relative percent helicity.

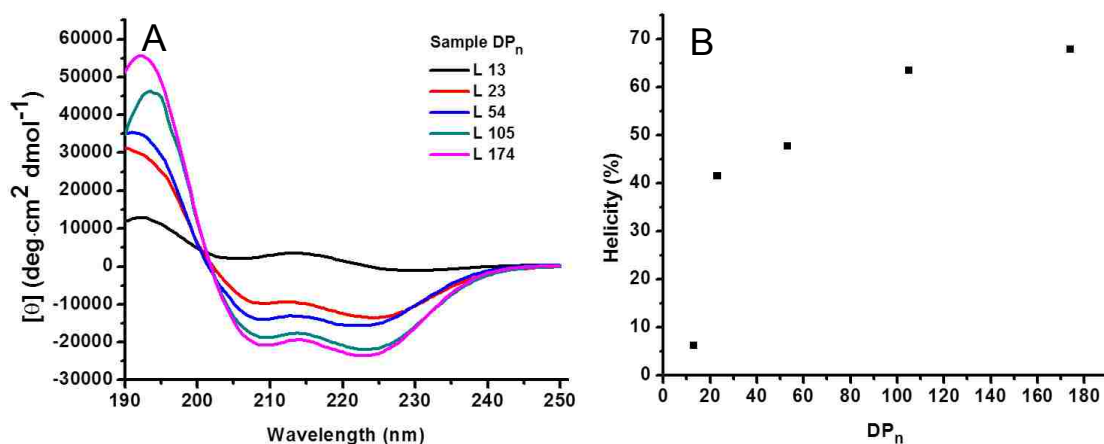


Figure 2.4. (A) CD spectra for a series of PPLG mannose glycopolypeptides. Samples were prepared at 1.0 mg/mL in HEPES buffered saline. Each curve is the average of three runs. (B) Plot of percent helicity versus DP<sub>n</sub>. Percent helicity values were calculated using the formula  $(([\theta]_{222}] + 3000) / 39000)$ .

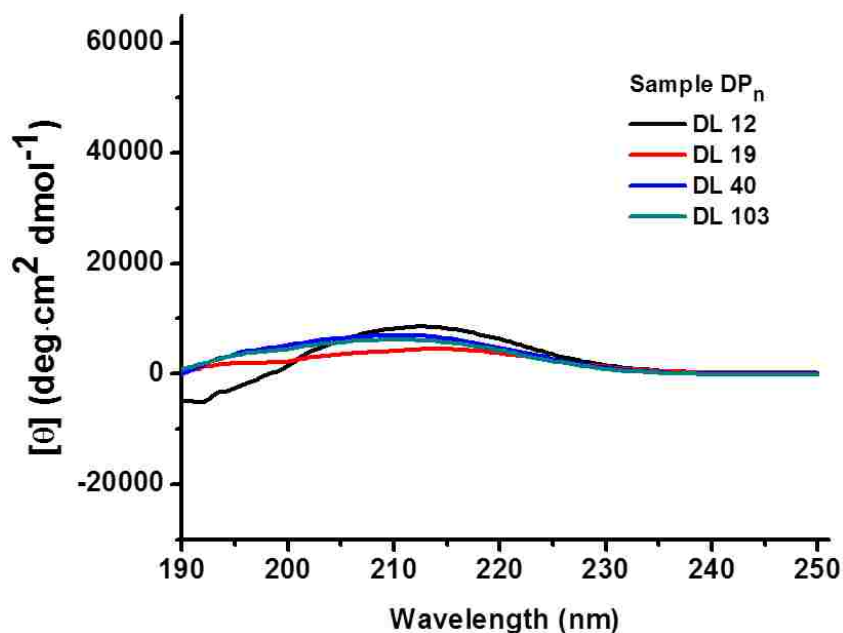


Figure 2.5. CD spectra for a series of PPDLG mannose glycopolypeptides. Samples were prepared at 1.0 mg/mL in HEPES buffered saline. Each curve is the average of three runs.

### 2.3.3 Binding studies of PPLG and PPDLG mannose with ConA

Concanavalin A (ConA) is a plant lectin with a binding affinity for mannose and glucose derived from the jackbean and is commonly used as a model ligand to investigate



the binding activities of synthetic carbohydrate functionalized systems. At neutral pH, ConA exists as a tetramer thus allowing for four possible binding sites which are spaced 65 Å apart.<sup>270</sup> Figure 2.6 shows a generic diagram of ConA and the effect of glycoclustering that occurs between ConA and the glycopolypeptides upon binding. We will investigate specific aspects of the binding of ConA to mannose, namely the initial binding rate constant ( $k_i$ ), the binding stoichiometry, and the mannose/ConA ratio and how  $DP_n$  and backbone architecture affect these parameters.

### 2.3.3.1 Binding kinetic study

One factor that may be influenced by the chain length, backbone architecture, or binding epitope density is the initial rate of aggregation that is observed when the glycopolypeptides are exposed to ConA. The glycoclustering that occurs during the

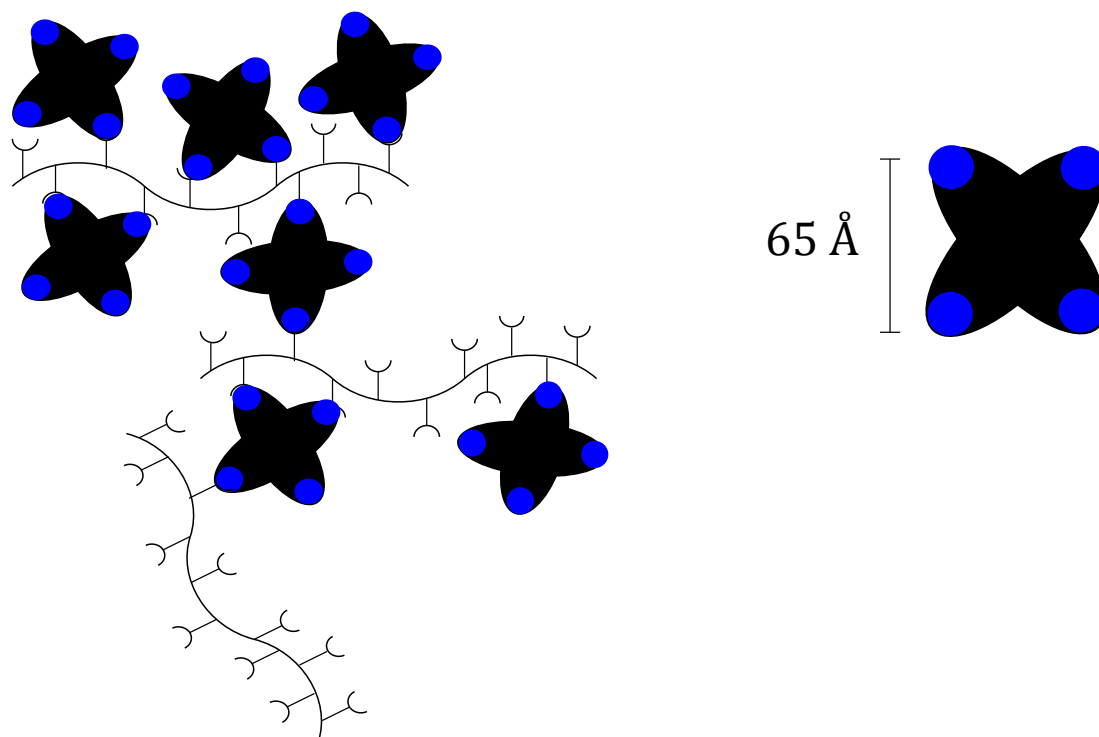


Figure 2.6. Glycoclustering due to ConA and the glycopolypeptide forming highly ordered species and a diagram of ConA indicating the distance between binding sites.

binding between the glycopolyptide and ConA results in an increase in the turbidity of the solution due to the insoluble aggregates that form, possibly due to the formation of higher ordered species from the crosslinking between ConA and the glycopolyptides. The turbidity further increases with more binding events, indicating that larger clusters are formed, until all of the binding sites have been exhausted either through occupation of all of the available sites or via steric inhibition. The former is the ideal scenario and the latter is the most likely case with respect to ConA binding due to its size.

To investigate the initial rate of clustering that occurs between ConA and the glycopolyptides, ConA (1  $\mu\text{M}$ ) was mixed with a fiftyfold excess of glycopolyptide solution in HEPES buffered saline resulting in clustering as evidenced by the change in turbidity by UV-vis spectroscopy over the course of time (Figure A1, A2). The initial rate of cluster formation ( $k_i$ ) was determined by a linear fit to the steepest part of each

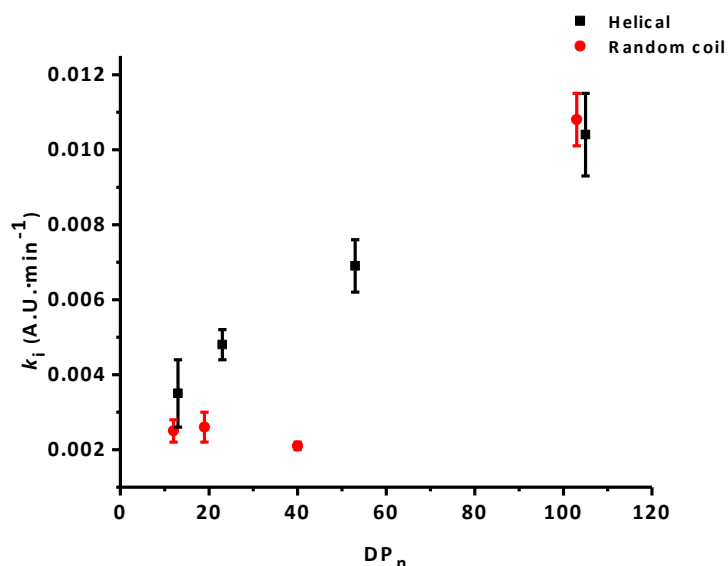


Figure 2.7. Plot of  $k_i$  versus  $\text{DP}_n$  obtained from turbidity assay experiments for helical (black) and random coil (red) glycopolyptides. The  $k_i$  for L 174 is not plotted. Some error bars are smaller than the plot markers.

Table 2.3. Initial binding rate constants ( $k_i$ ) for a series of PPLG and PPDLG mannose

Entry <sup>a</sup>	$k_i$ (A.U. min <sup>-1</sup> ) <sup>b</sup>
L 13	0.0035(9)
L 23	0.0048(4)
L 53	0.0069(7)
L 105	0.0104(11)
L 174	0.161(11)
DL 12	0.0025(3)
DL 19	0.0026(4)
DL 40	0.0021(1)
DL 103	0.0108(7)
ConA alone	-
Methyl mannose	-

<sup>a</sup> Each entry is listed with the backbone followed by the DP<sub>n</sub> as determined by SEC-MALS-DRI of the PPLG or PPDLG precursor. DL samples represent random coil samples whereas L samples are used to designate helical polypeptides; <sup>b</sup> the reported  $k_i$  were determined by a linear fit to the steepest part of each curve and are the average of three independent runs.

displayed curve. These results are shown in Figure 2.7 and Table 2.3. A control experiment using methyl mannose demonstrated the lack of clustering due to the low binding constants of monosaccharides. ConA alone was also measured to demonstrate that the observed changes in turbidity were not due to ConA potentially being unstable and insoluble in aqueous solution. A number of trends were observed. It can be observed from the data shown in Figure 2.7 that the observed  $k_i$ s increase with increasing DP<sub>n</sub>. As DP<sub>n</sub> increased from 13 to 174 in PPLG mannose samples, the measured  $k_i$  increased from 0.0035(9) to 0.161(1) A.U.·min<sup>-1</sup>, a 46-fold increase. Similarly, as PPDLG mannose DP<sub>n</sub> increased from 12 to 103, the measured  $k_i$  increased fourfold from 0.0025(3) to 0.0108(7)

A.U. $\cdot$ min<sup>-1</sup>. These observations are perhaps due to the higher availability of binding sites, which increases the likelihood for a binding event to occur due to the exposure of the additional mannose moieties. Secondly, those samples with higher DP<sub>n</sub> are less likely to experience steric hindrance of the binding sites in the early stages of the binding interactions due to the additional space afforded by possessing more binding sites. This allows for larger clusters to form much more quickly in those samples than in glycopolypeptides with lower DP<sub>n</sub>. These demonstrate that sample DP<sub>n</sub> contributes significantly to  $k_i$  as binding occurs fastest in glycopolypeptides where there are more binding epitopes and can accommodate more ConA due to the increased size of the multivalent glycopolypeptides. There does appear to be an effect on the observed  $k_i$  with respect to backbone architecture as evidenced in Figure 2.7. Helical glycopolypeptides in general appeared to bind faster than their random coil counterparts at lower DP<sub>n</sub>. This observed higher  $k_i$  of helical glycopolypeptides versus random coil polymers is suggested to be due to the enhanced side chain display in the former. Interestingly, the observed  $k_i$  of a helical and random coil glycopolypeptide at similar DP<sub>n</sub> (DP<sub>n</sub>= 105, 103 for PPLG and PPDLG mannose respectively) were comparable ( $k_i$ = 0.0104(11), 0.0108(7) A.U. $\cdot$ min<sup>-1</sup> for PPLG and PPDLG mannose respectively). A random coil glycopolypeptide at similar DP<sub>n</sub> to the L 174 sample was not successfully synthesized by the described method; accessing a random coil polypeptide of similar DP<sub>n</sub> to that of the L 174 sample could be helpful in the study of the effect of backbone architecture on the observed  $k_i$  at higher DP<sub>n</sub>.

### 2.3.3.2 Binding stoichiometry from quantitative precipitation assay

Another aspect of carbohydrate-lectin interactions that has been studied is the binding stoichiometry of the system. The binding stoichiometry refers to the number of ligands bound per polymer chain; the higher the binding stoichiometry the greater number

of ConA tetramers bound per chain. The binding efficiency could also be determined via the ratio of the average number of mannose residues available on the side chains (i.e.  $DP_n$ ) to binding stoichiometry (mannose/ConA). This value quantifies the number of mannose residues required for each observed binding event. Lower mannose/ConA values indicate more effective binding as less mannose moieties are required for each observed binding event as suggested by the measured binding stoichiometry. Higher mannose/ConA values reveal less effective binding and may indicate that effects due to sterics may be hindering access to the mannose side chains. This shows a less effective use of all of the available binding epitopes.

Quantitative precipitation assays were performed in order to measure the binding stoichiometry of the glycopolyptide series. Methods for quantitative precipitation assay were adopted from previous methods<sup>234, 271</sup> where a series of glycopolyptide samples were prepared at various concentrations and mixed in equal volume ratios with a solution of ConA of known concentration in order to induce clustering and the observation of precipitation in the samples. Samples were allowed to incubate until no additional precipitation was observed in the systems (48 h). Following the collection and washing of the precipitated ConA, the ConA content is measured by dissolving the obtained precipitate in a solution of competing ligand, methyl mannose and analyzing for absorption by UV-vis spectroscopy at 280 nm. From quantitative precipitation assay, the concentration for the half-maximal precipitation of ConA from the solution can be determined from sigmoidal fits to the resulting curves. From this concentration, the binding stoichiometry can be determined. These results are shown in Table 2.4 and Figure 2.8, 2.9.

Similar to the turbidity experiments to determine binding kinetics, the measured binding stoichiometry was found to be correlated with the degree of polymerization or

chain length. As  $DP_n$  increased in PPLG mannose from 13 to 174, the binding stoichiometry increased from  $1.19 \pm 0.16$  to  $7.49 \pm 1.18$ . This is not surprising as substrates with higher valency have a larger number of binding sites available and thus have the ability to bind additional tetramers of ConA and lower the effective concentration required to precipitate ConA. This has been previously demonstrated in glycopolymers that have been produced via ring-opening metathesis polymerization.<sup>232</sup> The obtained Not every mannose binding site on the glycopolypeptides can be accessed, especially in those with low degrees of polymerization as ConA is a large molecule and sterics would prevent side chain access, even in helical samples. This is evident in the reduced binding stoichiometry observed in short glycopolypeptides. However, the obtained binding stoichiometry values agree well with theoretical prediction based on the ConA binding site distance of 65 Å and the peptide unit length of 3.8 Å. This indicates that 17 repeat units are required for each possible binding event. For example, the PPLG mannose sample of  $DP_n=105$  can theoretically accommodate 6 individual ConA ligands. The observed binding stoichiometry of  $DP_n=105$  ( $5.30 \pm 0.17$ ) is comparable to theoretical value. The mannose/ConA ratio also increases with increasing  $DP_n$  indicating that binding efficiency decreases with increasing  $DP_n$  because more mannose residues are required to bind to each ConA tetramer. This would suggest that the steric hindrance of the binding sites is dominant and ultimately affects the binding efficiency.

The backbone architecture of the glycopolypeptides also affects the observed binding stoichiometry. The high concentrations required for half-maximal precipitation of PDDLG mannose lead to the observed low binding stoichiometries. The obtained binding stoichiometries at higher  $DP_n$  were determined to be much lower than those of their helical counterparts. Even as  $DP_n$  increased from 12 to 103, binding stoichiometry only increased from  $0.96 \pm 0.10$  to  $2.74 \pm 0.09$ . These results are in contrast to those reported

by Gupta et al, where the glycopolyptide backbone conformation did not affect binding stoichiometry. The obtained results support the argument of Kiick et al in that helical glycopolyptides are more effective in the binding of lectins. The continual increase of mannose/ConA of fully glycosylated helical glycopolyptide species indicate that the effects of sterics and chain overcrowding limit access to the mannose moieties in these systems and thus the effects of longer chain length and a more favorable side chain presentation due to helical backbone architecture are insufficient to further improve upon the binding efficiency. However, even in PPDLG mannose experiments, the mannose/ConA ratio still increased with increasing  $DP_n$  suggesting that similar steric limitations influence the observed binding.

A control sample of methyl mannose was prepared similarly to the glycopolyptide samples. The results from quantitative precipitation assay of methyl mannose with ConA indicate that monomeric mannose is unable to precipitate out ConA and clustering does not occur in such samples due to the inability for crosslinking to occur between the methyl mannose substrates even though it is possible that all of the binding sites in the ConA tetramers are occupied due to the much smaller size of methyl mannose versus a glycopolyptide, whose influence on the observed binding is greatly affected by sterics.

#### 2.3.4 Varying binding epitope density

One factor that could further influence the effects of the multivalent binding of ConA to the mannose glycopolyptides is the variation of binding epitope density. Decreasing the binding epitope density decreases the number of binding sites but increases the likelihood that they will be spaced out farther apart from each other, possibly overcoming steric crowding along the polymer backbone. Previous studies have noted that decreasing binding epitope density leads to slower binding kinetics but may

improve the overall binding efficiency by decreasing the number of sugar residues necessary for each measured binding event (mannose/ConA) by quantitative precipitation assay determination of binding stoichiometry. It was previously stated that ConA has a binding specificity for mannose and glucose; ConA does not recognize and bind to galactose. Incorporating galactose at various ratios will space out the mannose binding epitopes along the polypeptide backbone and may aid in overcoming steric blockage of the binding sites. 2-azidoethyl galactose was used in conjunction with 2-azidoethyl mannose in CuAAC to obtain a series of glycopolypeptides with varying epitope densities (Scheme 2.9). An exemplary  $^1\text{H}$  NMR spectrum of the glycopolypeptide containing both mannose and galactose residues was shown in Figure 2.3 (vide supra). Galactose and mannose content were determined via the relative integration of the methylene protons of galactose (3.4 ppm) and mannose (3.0 ppm).

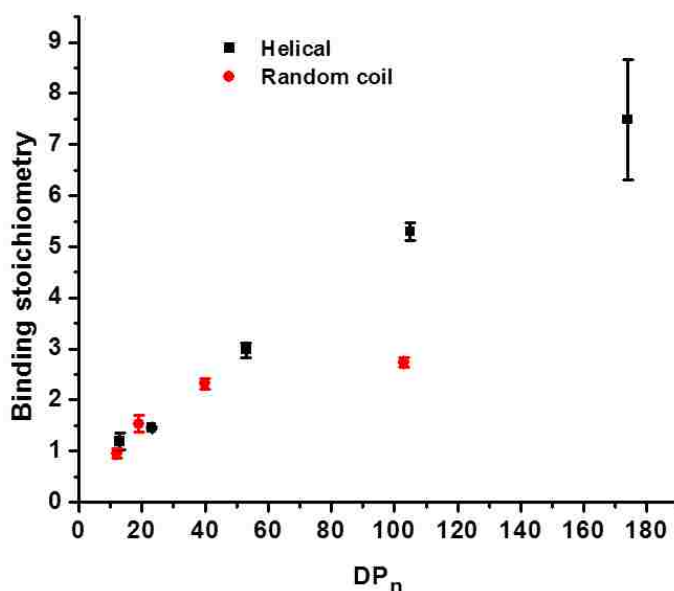


Figure 2.8. Plot of binding stoichiometry versus  $\text{DP}_n$  obtained from quantitative precipitation assay experiments for helical (black) and random coil (red) glycopolypeptides. Some error bars are smaller than the plot markers.



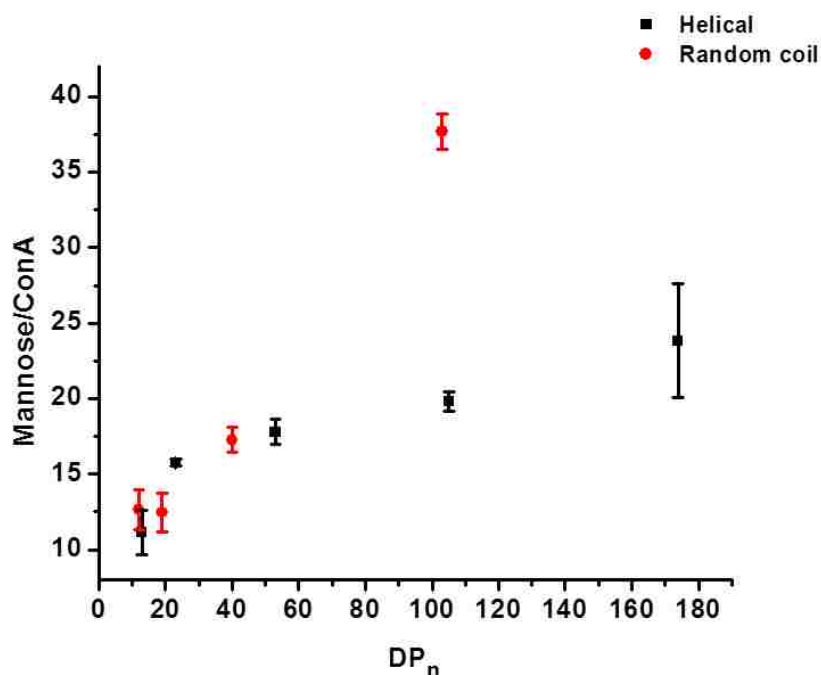


Figure 2.9. Plot of mannose/ConA versus DP<sub>n</sub> obtained from quantitative precipitation assay experiments for helical (black) and random coil (red) glycopolypeptides. Some error bars are smaller than the plot markers.

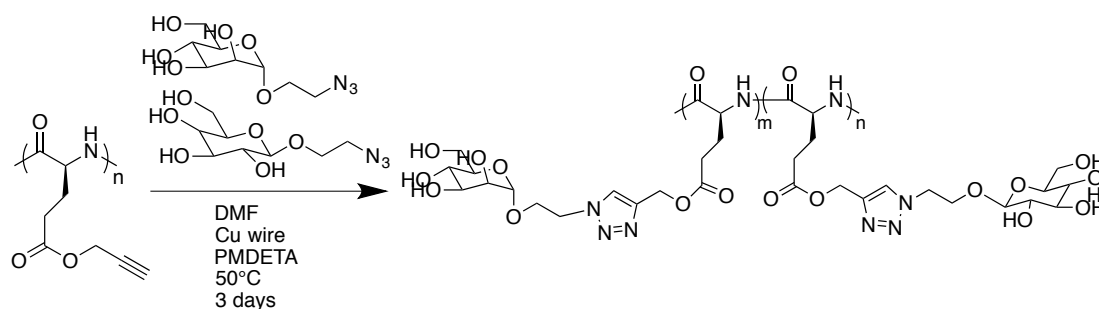
Table 2.4. Binding stoichiometry data for a series of helical and random coil glycopolypeptides

Sample DP <sub>n</sub> <sup>a</sup>	Binding stoichiometry <sup>b</sup>	Mannose/ConA <sup>c</sup>
L 13	1.19 ± 0.16	11.16 ± 1.46
L 23	1.46 ± 0.02	15.76 ± 0.21
L 53	2.98 ± 0.14	17.80 ± 0.82
L 105	5.30 ± 0.17	19.83 ± 0.64
L 105 68% mannose	2.72 ± 0.37	29.43 ± 3.94
L 174	7.49 ± 1.18	23.83 ± 3.76
DL 12	0.96 ± 0.10	12.64 ± 1.32
DL 19	1.54 ± 0.16	12.47 ± 1.29
DL 40	2.32 ± 0.11	17.28 ± 0.82
DL 103	2.74 ± 0.09	37.70 ± 1.17
Methyl mannose	-	-

<sup>a</sup> Each entry is listed with the backbone followed by the DP<sub>n</sub> as determined by SEC-MALS-DRI of the PPLG or PDDLG parent polypeptide; <sup>b</sup> binding stoichiometry was determined at the half maximal concentration required to completely precipitate out ConA <sup>c</sup> mannose/ConA was determined by [(percent mannose × DP<sub>n</sub>) / binding stoichiometry].

Interestingly, we found that altering the mannose epitope density drastically affected the observed binding kinetics (Figure 2.11). By decreasing the mannose percent by approximately one third (68 % mannose by <sup>1</sup>H NMR), the observed initial rate of

Scheme 2.9. Glycosylation of PPLG with varying mannose and galactose loadings



clustering as determined by turbidity assay was determined to be  $k_i = 0.0012(1) \text{ A.U.} \cdot \text{min}^{-1}$ , which is drastically lower than any of the previously observed  $k_i$ . Further decreasing the mannose density on the glycopolypeptide side chain led to further decreased in  $k_i$  as indicated by the lack of increase of turbidity within the experimental timeframe as shown in Figure 2.10 suggesting that the presence of galactose residues has negative effects on the observed carbohydrate-lectin interactions. The increase in galactose content may have contributed to additional difficulty of ConA accessing the mannose binding sites, contrary to previous reports where spacing out mannose improves the binding efficiency. The mannose residues may be too far apart in glycopolypeptides with low mannose densities, not allowing for an effective binding interaction between lectin and carbohydrate. This is also evident in the determined binding stoichiometry (Table 2.4) as the sample with 68 % mannose which was nearly half that of the 100 % mannose analog. A larger mannose/ConA was also observed compared with that of the fully glycosylates species suggesting that binding efficiency was decreasing. Thus, increasing the spacing between binding epitopes in glycopolypeptides appears to lower the observed binding efficiency of ConA than previous reports where a more effective use of the binding epitopes was observed through a decrease in mannose/ConA, suggesting and increase in efficiency.

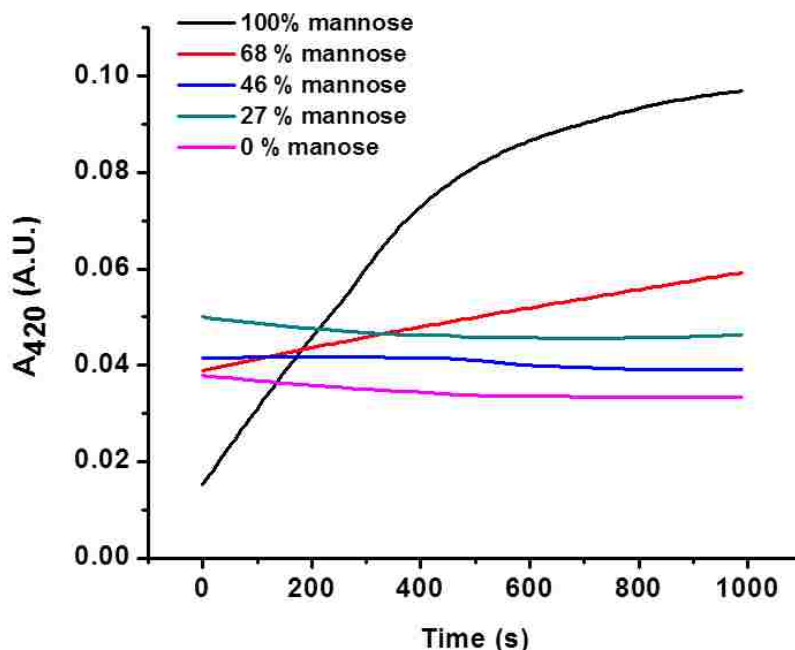


Figure 2.10. Turbidity curves obtained from the analysis of a series of PPLG mannose/galactose at varying epitope densities ( $DP_n=105$ ) in the presence of ConA (mannose:ConA=50:1) at 420 nm. The shown curves are the averages of three independent runs.

#### 2.4 Dynamic light scattering of glycopolypeptides

Dynamic light scattering (DLS) was used in order to investigate the relative size of the glycopolypeptides and may give some insight into the slower observed  $k_i$ , lower binding stoichiometry, and higher mannose/ConA observed in the glycopolypeptides in comparison with their previously reported glycopolymer counterparts. Significant aggregation was observed in all of the glycopolypeptide samples. Exemplary DLS spectra of a helical glycopolypeptide (Figure 2.11) and a random coil glycopolypeptide (Figure 2.12) are shown. This has a number of implications. It is possible that the observed aggregation contributes to the steric hindrance that leads to the lower  $k_i$ , lower binding stoichiometry, and higher mannose/ConA. The contribution of other glycopolypeptides to the observed aggregation may be blocking additional mannose binding sites that could potentially partake in binding activity with ConA to increase  $k_i$ , binding stoichiometry, and decrease mannose/ConA.

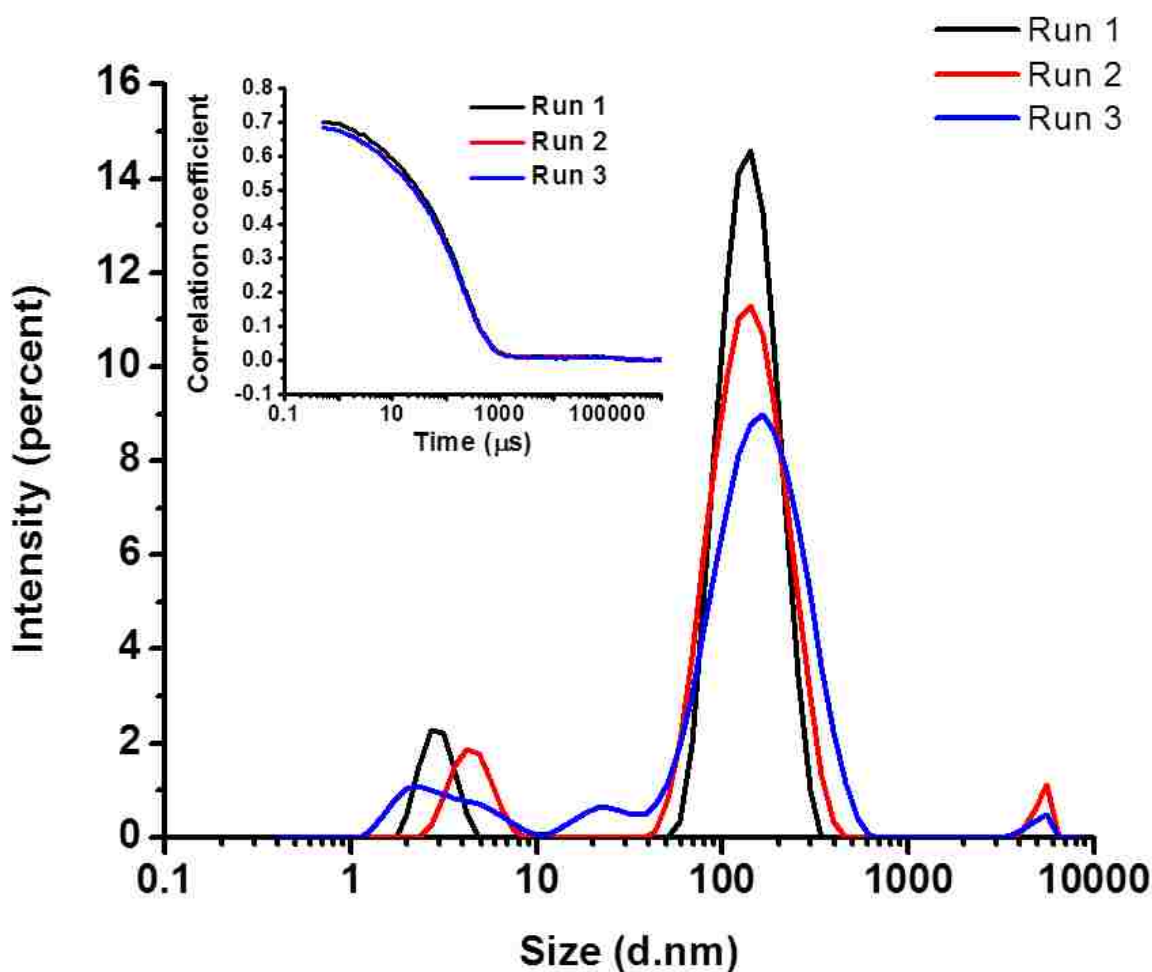


Figure 2.11. DLS results of three separate runs of PPLG mannose ( $DP_n=13$ ) taken in HEPES buffered saline at a concentration of 1 mg/mL. Correlograms for each respective run are shown in the inset.

We hypothesized that the addition of cationically charged species to the side chains could potentially break up the aggregates due to electrostatic repulsion. However, the addition of charge could potentially disrupt the observed helicity. Cheng et al have reported that moving the charge at least eleven carbons away from the main polypeptide backbone does not affect the helicity. A terminal azide functionalized six carbon quaternary amine was used in CuAAC reactions together with 2-azidoethyl mannose order to investigate the effects of placing charge on the side chains (Scheme 2.10). DLS

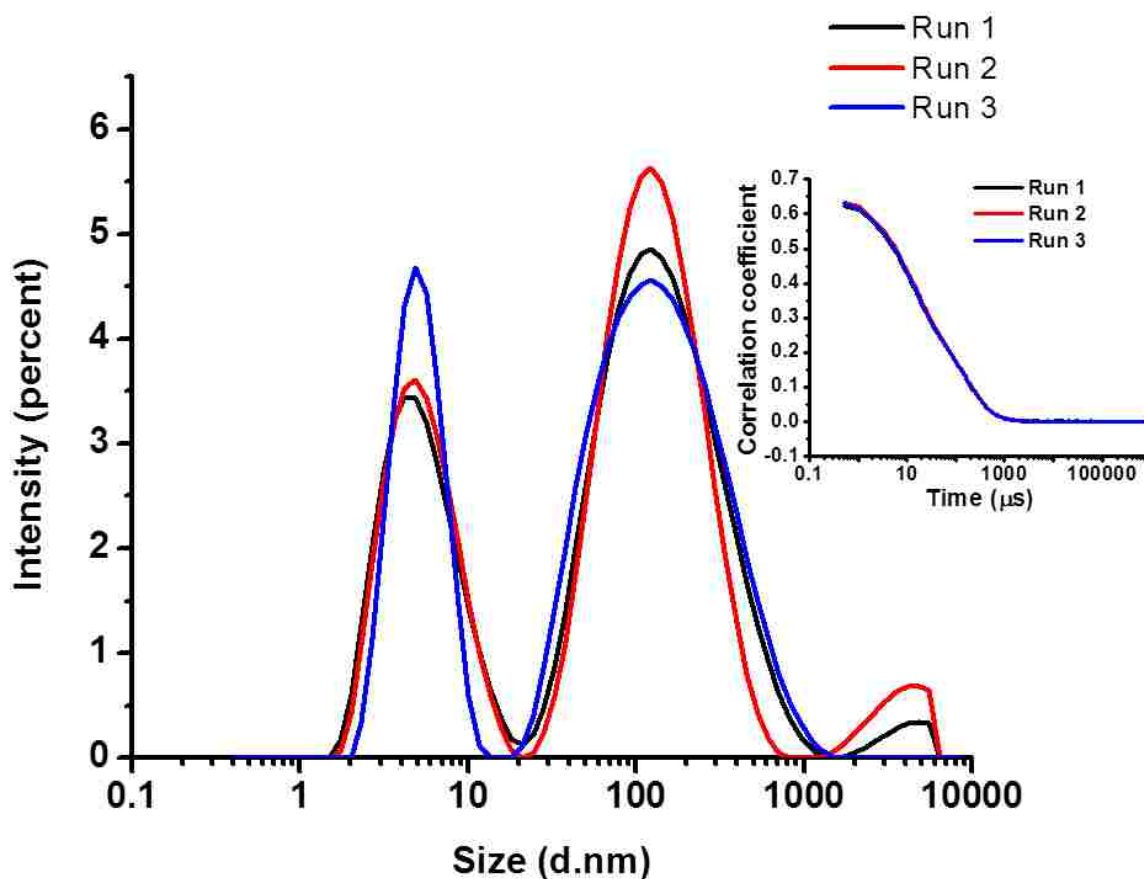


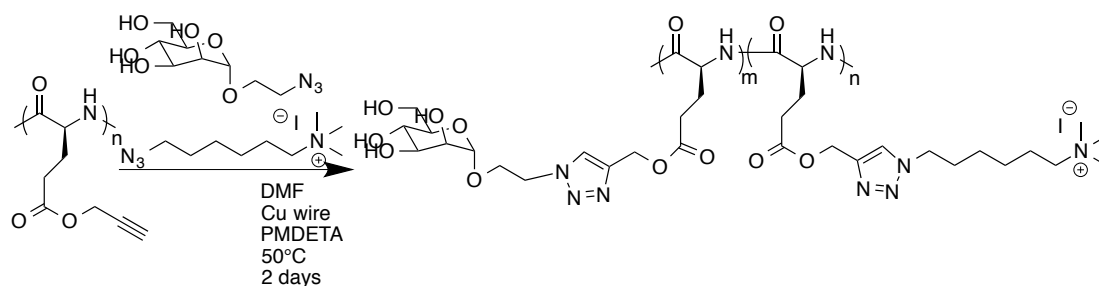
Figure 2.12. DLS results of three separate runs of PPDLG mannose ( $DP_n=103$ ) taken in HEPES buffered saline at a concentration of 1 mg/mL. Correlograms for each respective run are shown in the inset.

analysis of the resulting glycopolyptide (Figure 2.13) coupled with the quaternary amine indicates that there is still significant aggregation and the addition of charge has little to no effect on mitigating the effects of aggregation.

## 2.5. Conclusions

A series of glycopolyptides have been synthesized from the ROP of their corresponding propargyl-L-glutamate and propargyl-DL-glutamate NCAs using benzylamine initiator followed by post-polymerization grafting of mannose moieties via the highly efficient CuAAC. The former series adopt helical conformations and the latter adopt random coil conformations according to CD analysis. Helicity was found to decrease with decreasing  $DP_n$ . In binding studies with ConA, it was found that  $DP_n$  has

Scheme 2.10. Synthesis of cationically charged glycopolypeptide species via CuAAC



the greatest contribution with respect to the initial observed binding kinetics as the presence of additional binding sites promotes the faster binding of ConA to the glycopolypeptide substrates resulting in a much faster observed change in turbidity. As expected, glycopolypeptides possessing random coil conformations had lower observed  $k_i$  and lower binding stoichiometry suggesting the more restricted side chain presentation and access in random coil species. This is much more apparent at low  $DP_n$ . However, at higher  $DP_n$ , the initial rate of binding was found to be comparable to that of a helical glycopolypeptide of comparable  $DP_n$ . This may suggest more compact coil conformations at low  $DP_n$  and more extended conformations at high  $DP_n$ . Steric hindrance is still suggested to be the biggest limiting factor in the number of ConA tetramers that could possibly be bound to the glycopolypeptide samples as evidenced in quantitative precipitation assays. Although increasing  $DP_n$  allows for additional binding sites and additional space for binding events, the increasing mannose/ConA ratios indicate binding efficiency decreases with increasing  $DP_n$ . Significant aggregation was revealed by DLS analysis, which may also have an effect on the slower observed  $k_i$ , lower binding stoichiometry, and higher mannose/ConA observed in the glycopolypeptides in comparison with their previously reported glycopolymer counterparts. The installation of cationic charge did not appear to contribute to breakup of the observed aggregates. Although trends can be observed in the observed binding activity to ConA with respect to

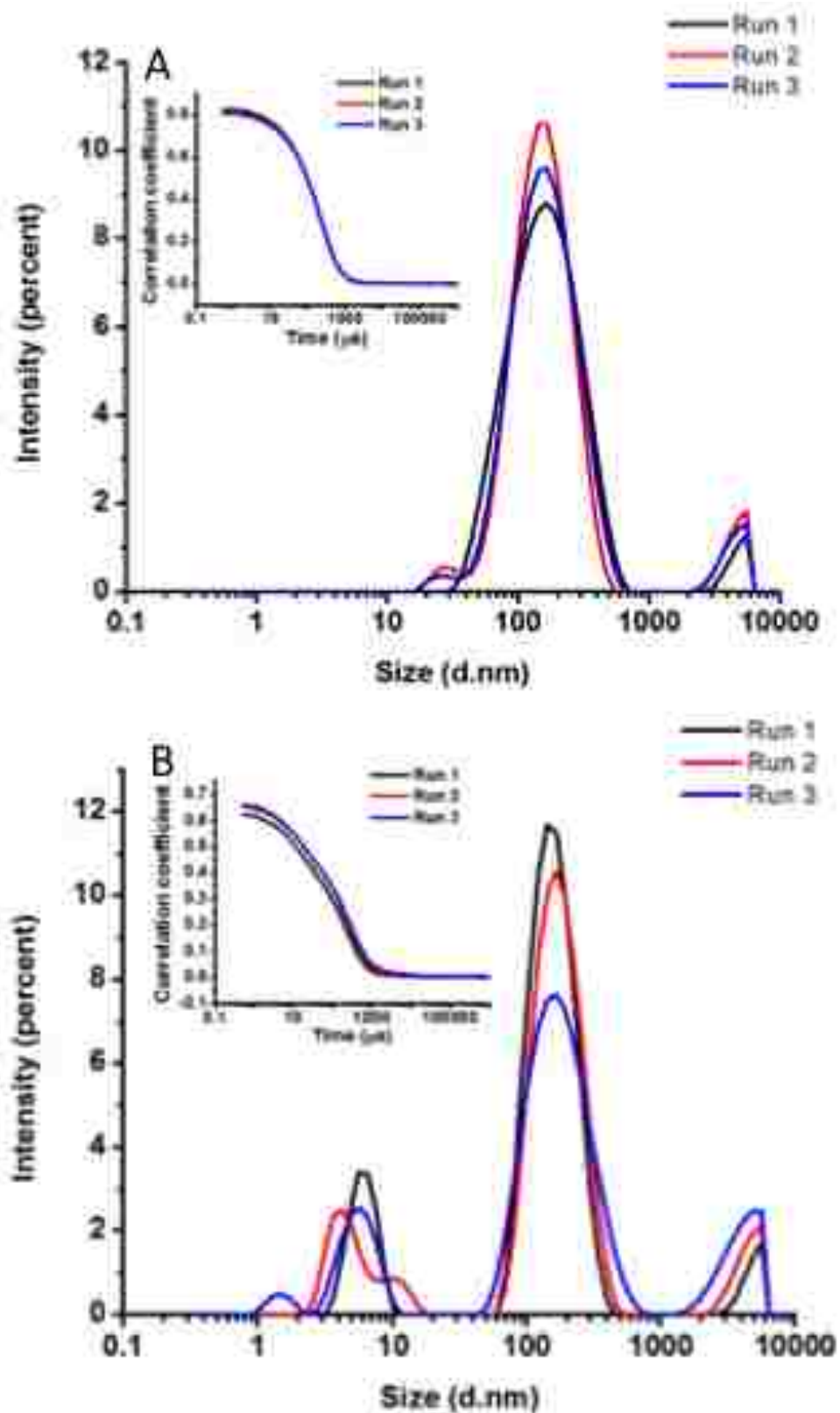


Figure 2.13. DLS results of three separate runs for PPLG mannose ( $DP_n=23$ ) bearing no cationic charge on the side chains (A) and 9% cationic charge (B) as determined by  $^1\text{H}$  NMR. Samples were prepared at concentrations of 1 mg/mL in HEPES buffered saline. Correlograms for each respective run are shown in the insets.

changing  $DP_n$  and backbone conformation, the results are still dwarfed by those of glycopolymers. Thus, helical glycopolypeptides with superior side chain presentation may not necessarily be the most efficient multivalent materials.

## 2.6 Experimental

### 2.6.1 Instrumentation and general considerations

All chemicals were used as received unless otherwise noted. Anhydrous THF, and *N,N*-dimethylformamide (DMF) for monomer synthesis and polymerizations respectively were purified by passing through activated alumina columns under an argon atmosphere (Innovative Technology, Inc.).  $^1\text{H}$  NMR spectra were recorded on a Bruker AV-400 and AVIII-400. Chemical shifts were determined in reference to the protio impurities of the deuterated solvents ( $\text{CDCl}_3$ , or  $\text{D}_2\text{O}$ ) Size exclusion chromatography (SEC) analysis was carried out on an Agilent 1200 system (Agilent 1200 series degasser, isocratic pump, auto sampler, and column heater) equipped with three Phenomenex 5  $\mu\text{m}$ , 300  $\text{\AA}$   $\times$  7.8 mm columns [100  $\text{\AA}$ , 1000  $\text{\AA}$ , and Linear (2)], Wyatt DAWN EOS multiangle light scattering (MALS) detector (GaAs 30 mW laser at  $\lambda$ ) 690 nm], and Wyatt Optilab rEX differential refractive index (DRI) detector with a 690 nm light source. DMF containing 0.1 M LiBr was used as the eluent at a flow rate of 0.5  $\text{mL} \cdot \text{min}^{-1}$ . The column and the MALS and DRI detector temperatures were all maintained at ambient temperature (21  $^\circ\text{C}$ ). Data from SEC-MALS-DRI was processed using Wyatt Astra v 6.0 software. Circular dichroism (CD) data were collected on a Jasco J810 CD spectrometer (Japan Spectroscopic Corporation) using a cell with a path length of 0.1 cm and a band width of 1.0 nm at 20  $^\circ\text{C}$ . Three scans were collected and averaged between 190 nm and 250 nm at a scanning rate of 50  $\text{nm} \cdot \text{min}^{-1}$  with a data pitch of 0.5 nm. UV-vis spectroscopy experiments were carried out on a Cary 50 Bio UV-vis spectrometer equipped with a xenon flash lamp at a scan rate of 50 nm/s. Dynamic light scattering (DLS) experiments were conducted on a



Malvern Zetasizer Nano-ZS instrument using Zetasizer software 6.12. Each sample was measured three times.

The random coil analogues used in this study can be similarly synthesized to the enantiomerically pure (i.e. L) species using DL-glutamic acid in place of L-glutamic acid. The respective polypeptide is abbreviated as PPDLG throughout the text. For the sake of brevity, only the “L” designation is used in the experimental details.

#### 2.6.2 Synthesis of $\gamma$ -propargyl-L-glutamate *N*-carboxyanhydride

Synthesis of  $\gamma$ -propargyl-L-glutamate. L-glutamic acid (23.44 g, 159 mmol) was suspended in propargyl alcohol (400 mL, 4.8 mol) and the flask was purged with nitrogen for 20 minutes. Chlorotrimethylsilane (45 mL, 355 mmol) was added dropwise to the flask via an addition funnel. The suspension was stirred at ambient temperature until the solution became homogenous. The obtained dark brown homogenous solution was decanted into diethyl ether (1 L). The product precipitated out as an off white solid and was collected via filtration and dried under vacuum (23.85 g, 81 %).

Synthesis of  $\gamma$ -propargyl-L-glutamate *N*-carboxyanhydride.  $\gamma$ -Propargyl-L-glutamate (8.04 g, 43.9 mmol) and triphosgene (4.43 g, 14.9 mmol) were charged into an oven dried flask and suspended in anhydrous THF (200 mL). The reaction suspension was heated at 55 °C during which the reaction slowly became homogeneous. THF was then removed under vacuum leaving the product as a crude viscous liquid. The NCA monomer was purified via dry column chromatography using silica gel dried in the vacuum oven for 48 h at 120 °C. The mobile phase used first was anhydrous hexanes followed by a gradient of 9:1–1:1 anhydrous THF:hexanes ( $R_f=0.23$  in 1:1 THF:hexanes). Fractions containing the NCA were collected and concentrated to yield the NCA as a viscous orange liquid (3.62 g, 39 %).

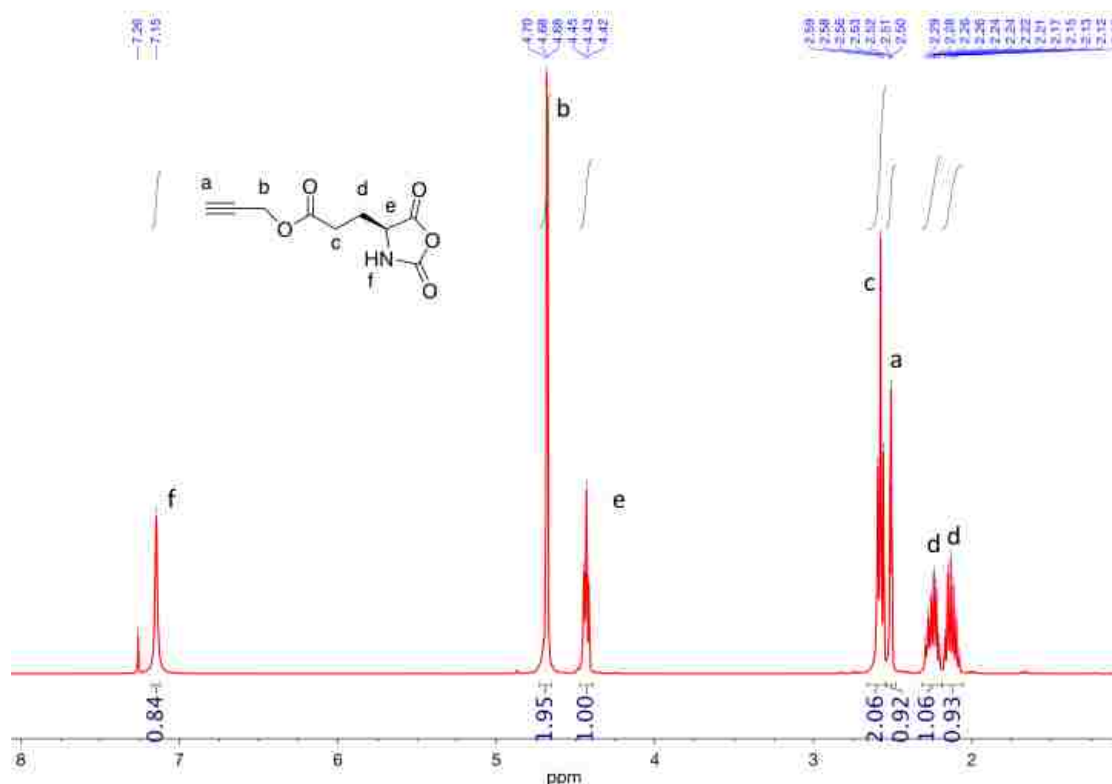


Figure 2.14. <sup>1</sup>H NMR spectrum of PLG-NCA collected in CDCl<sub>3</sub>.

### 2.6.3. General procedure for the polymerization of $\gamma$ -propargyl-L-glutamate *N*-carboxyanhydride

In the glovebox, PLG-NCA (275 mg, 1.3 mmol,  $[M]_0 = 1.0$  M) was weighed into a vial and dissolved in DMF (1265  $\mu$ L). A known volume of a benzylamine stock solution (37  $\mu$ L, 13  $\mu$ mol, 0.35 M) was then added to the solution. The reaction was stirred for 24 h at ambient temperature under a nitrogen atmosphere. Monomer conversion was calculated via FTIR. DMF was removed via vacuum distillation at 50 °C, 100 mTorr leaving a crude solid film. Purified PPLG was obtained by dissolving the crude solid film in minimal dichloromethane, reprecipitation from excess hexanes as a white solid, and subsequently collected via filtration, and dried under vacuum (153 mg 70%).

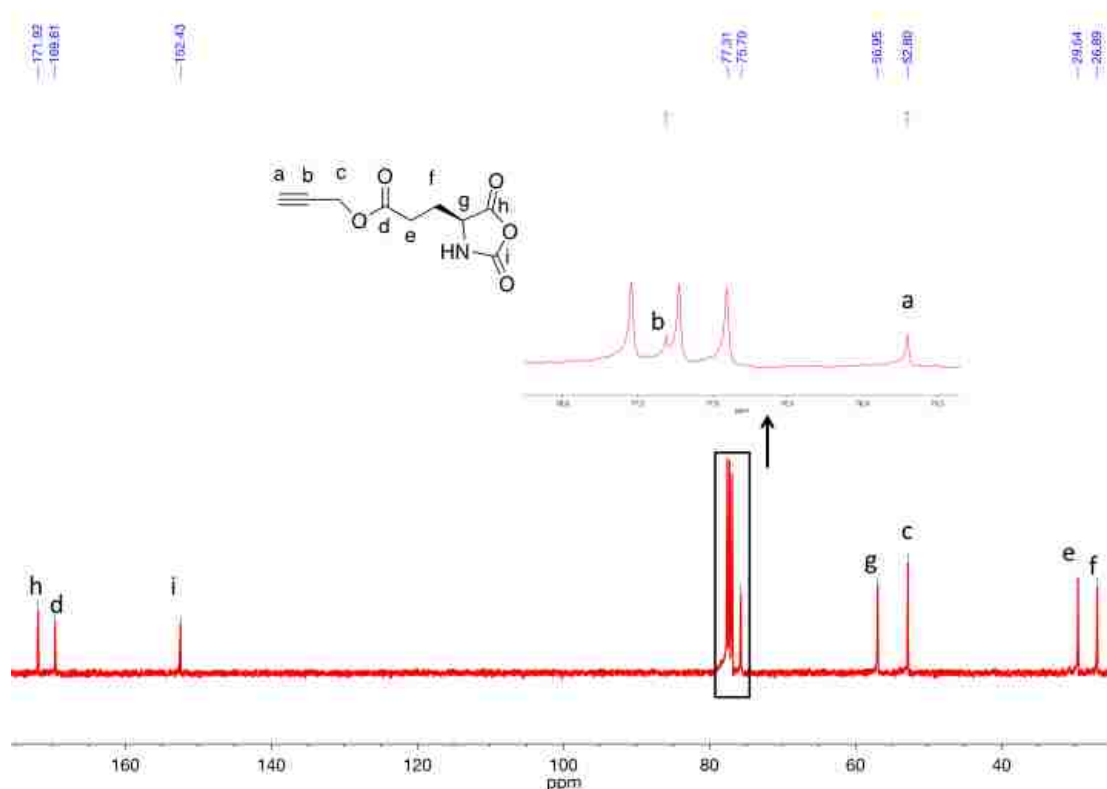


Figure 2.15.  $^{13}\text{C}\{^1\text{H}\}$  NMR spectrum of PLG NCA collected in  $\text{CDCl}_3$ .

#### 2.6.4 Glycosylation of poly( $\gamma$ -propargyl-L-glutamate) via CuAAC

2-azidoethyl mannose was previously synthesized from a known procedure.<sup>211</sup> 2-azidoethyl galactose can be synthesized using the same procedure. PPLG (22 mg, 0.132 mmol) and 2-azidoethyl mannose (66 mg, 0.264 mmol) were weighed into a vial. A piece of copper wire (~0.5 g) was freshly shaved with sandpaper and placed in the vial with PPLG and mannose. The polypeptide and sugar moiety were dissolved in DMF (5 mL) and PMDETA (4  $\mu\text{L}$ , 20  $\mu\text{mol}$ ) was subsequently added to the vial. The reaction was stirred at 50  $^\circ\text{C}$  for 3 days. DMF was removed via vacuum distillation leaving crude glycopolypeptide in the flask, which was dissolved in water (5 mL) and dialyzed against distilled water for 3 days (MWCO=6000-8000 Da) with the water being changed twice daily. The contents of the dialysis bag were emptied into a vial and lyophilized to yield the glycopolypeptide as an off white solid (32 mg, 58%). In cases where 2-azidoethyl

galactose is involved in the glycosylation, the relative loadings of 2-azidoethyl mannose and 2-azidoethyl galactose can be adjusted accordingly in order to vary the binding epitope densities in the resulting glycopolypeptides.

#### 2.6.5 Circular dichroism

Glycopolypeptide samples were dissolved at concentrations of 1 mg/mL in HEPES buffered saline and measured from 250 – 190 nm (0.5 nm data pitch) at a scanning rate of 50 nm/s on the CD instrument. Shown plots are the average of three runs following background subtraction of HEPES buffered saline. Conversion to mean residue molar ellipticity was accomplished using the concentration of the glycopolypeptide solution and the mass of the repeat unit of the glycopolypeptide ( $416 \text{ g}\cdot\text{mol}^{-1}$ ).

#### 2.6.6 Turbidity assay

Concanavalin A (ConA) was dissolved in HEPES buffered saline (HBS) at a concentration of 1  $\mu\text{M}$ . Solutions of glycopolypeptide were prepared in HBS so that the concentration of mannose residues was 50  $\mu\text{M}$ . In a polystyrene cuvette, the ConA and glycopolypeptide solutions were mixed (1:1 v/v) and placed into the UV-vis spectrometer running “cycle mode” where the absorption at 420 nm was analyzed every 10 s. Initial rates of aggregation and clustering were determined from the steepest part of the obtained plots.

#### 2.6.7 Quantitative precipitation assay

A series of glycopolypeptide solutions were made at varying concentrations from 0.01  $\mu\text{M}$  to 100  $\mu\text{M}$ . The glycopolypeptide solutions were mixed in an equal volume ratio with a stock solution of ConA (60  $\mu\text{M}$ ) so that the final concentration of ConA was 30  $\mu\text{M}$ . The samples were allowed to incubate at room temperature overnight. The precipitates were collected via centrifugation for 10 minutes and washed with additional cold HBS. The centrifugation and washing steps were repeated twice. An aqueous solution of methyl

mannopyranose (1 mL, 1.0 M) was added to dissolve the obtained precipitate and the content of precipitated ConA per sample was determined via UV-vis spectroscopy at 280 nm.

## 2.7 Supplemental data for Chapter II

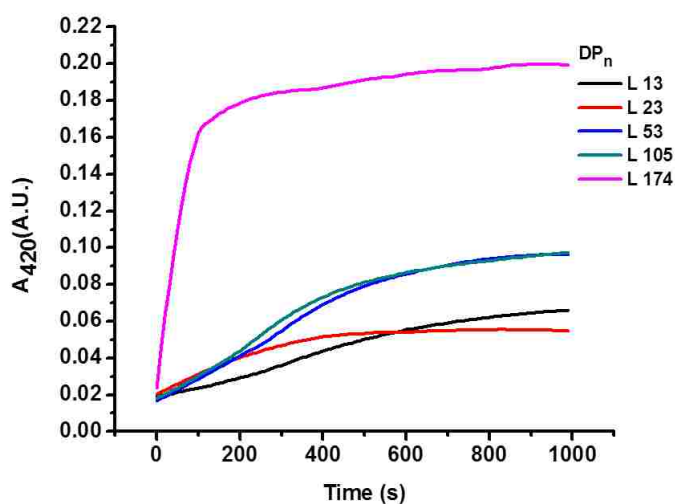


Figure A1. Plots of absorption at 420 nm versus time obtained from turbidity assay experiments with helical glycopolypeptides. The shown curves are the averages of three runs.

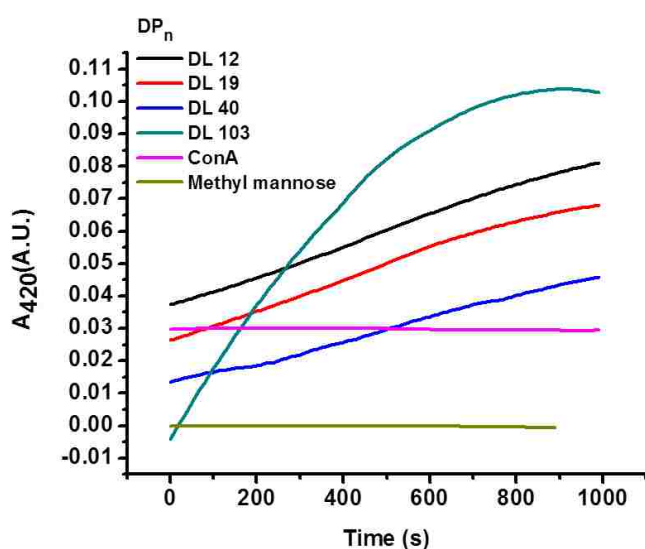


Figure A2. Plots of absorption at 420 nm versus time obtained from turbidity assay experiments with random coil glycopolypeptides. The shown curves are the averages of three runs.

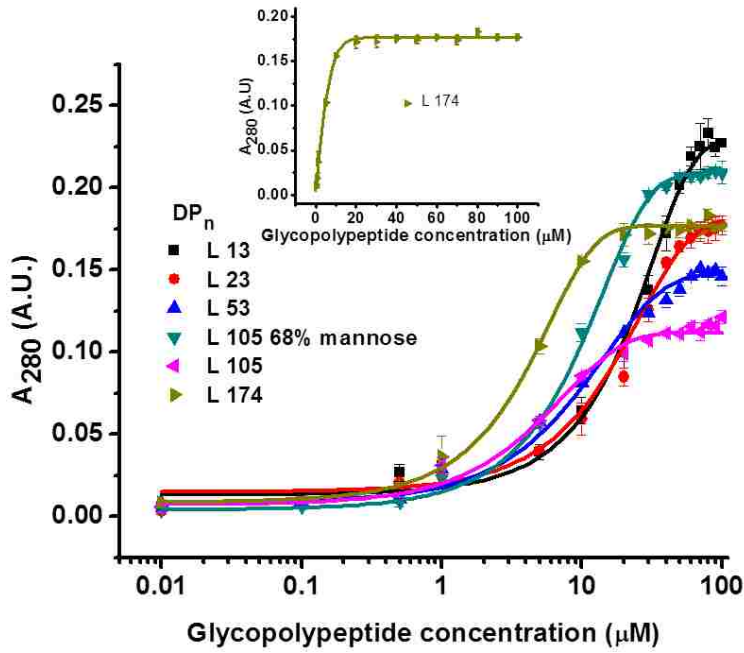


Figure A3. Sigmoidal plots obtained from quantitative precipitation assay experiments with helical glycopolyptides. The shown curves are the averages of two independent experiments. An inset of an exemplary curve plotted in the linear scale is included for reference. Some error bars are smaller than the plot markers.

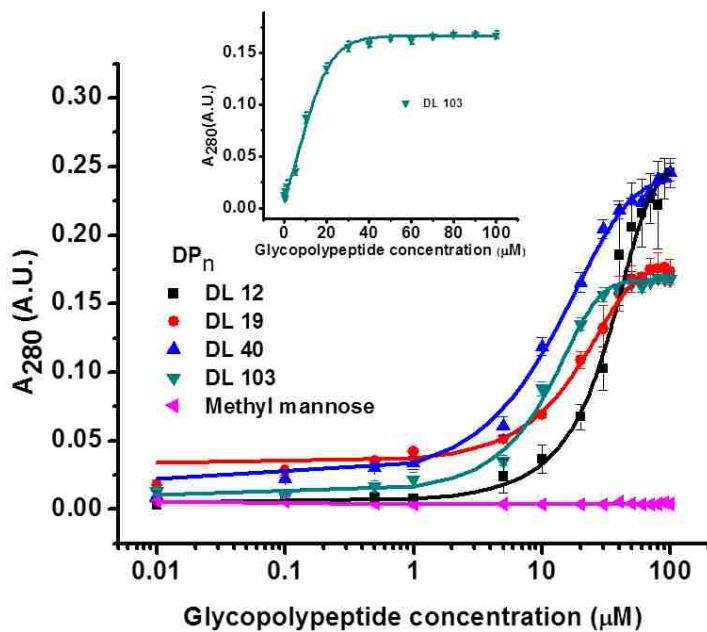


Figure A4. Sigmoidal plots obtained from quantitative precipitation assay experiments with random coil glycopolyptides. The shown curves are the averages of two independent experiments. An inset of an exemplary curve plotted in the linear scale is included for reference. Some error bars are smaller than the plot markers.

## CHAPTER III. 1,1,3,3-TETRAMETHYLGUANIDINE PROMOTED RING-OPENING POLYMERIZATION OF *N*-BUTYL *N*-CARBOXYANHYDRIDE USING ALCOHOL INITIATORS\*

### 3.1 Objectives

Chapter I gave a brief introduction to nucleophilic ROP of both polypeptide and polypeptoid based NCAs, which is commonly accomplished using primary amine initiators. The hydroxyl group is one of the most common functional groups found in nature but is a weak nucleophile. Hydroxyl groups can be found at the termini of numerous polymer species (i.e. polyesters, polyethers) which could potentially be hybridized with polypeptoids to create new materials. In a straightforward polymerization reaction of Bu-NCA with benzyl alcohol initiator, it was observed that no polymerization had occurred, thus affirming that hydroxyls are poorer initiators than amines. We reasoned that if the nucleophilicity of alcohols could be improved through the development of a catalytic system, they could be made into viable initiators. We were inspired by a number of reports by Waymouth et al, which used organocatalysts to improve the nucleophilicity of the hydroxyl group of alcohols through hydrogen bonding interactions, and used them in the ROP of various polyesters. In addition to being able to possibly synthesize new polypeptoid based materials, ROP of NCAs using alcohol initiators may also eliminate the need for chain end functionalization in order to convert the hydroxyl to the more labile primary amine. This chapter details our study of the organocatalytic ROP of Bu-NCA using alcohol initiators.

---

\* This chapter previously appeared as Chan, B. A.; Xuan, S.; Horton, M.; Zhang, D., 1,1,3,3-Tetramethylguanidine-Promoted Ring-Opening Polymerization of *N*-Butyl *N*-Carboxyanhydride Using Alcohol Initiators. *Macromolecules* **2016**, *49* (6), 2002-2012. It is reprinted with permission by the American Chemical Society. Copyright 2016 American Chemical Society.

### 3.2 Introduction to organocatalysis in polymerization

Organo-mediated polymerization has gained traction due to the need for metal-free polymers for certain applications (e.g., biomedical uses and microelectronics) and the successful development of catalytic systems that enable efficient controlled polymerizations under relatively mild reaction conditions. One of the earliest accounts of organo-mediated polymerization involved the acid-catalyzed (*p*-toluene sulfonic acid) polymerization between adipic acid and diethylene glycol.<sup>273</sup> Neutral organic bases have recently been shown to mediate the ring-opening polymerizations (ROPs) of a variety of heterocycles (e.g., lactones, epoxides, cyclic carbonates, and cyclic siloxanes) to form polyester, polyether, polycarbonate, and polysiloxane polymers in the presence of alcohol initiators. Among the myriad of neutral organic bases used in organocatalytic ROP systems are guanidines,<sup>274-279</sup> amidines,<sup>173, 275</sup> phosphazenes,<sup>280-281</sup> phosphines,<sup>282</sup> pyridines,<sup>282-283</sup> tertiary amines,<sup>282-285</sup> isothioureas,<sup>174</sup> imidazoles,<sup>286</sup> and *N*-heterocyclic carbenes (NHC).<sup>166, 287-289</sup> It has been proposed that these organo-bases mediate the polymerizations of the heterocycles by either nucleophilic activation of the monomers or alcohol/chain-end activation via hydrogen bonding interaction.<sup>275-276, 278-279, 281, 288, 290,291</sup>

Polypeptoids are structural mimics of polypeptides featuring an *N*-alkyl substituted polyglycine backbone. Without intramolecular hydrogen bonding interactions along the backbone, polypeptoids exhibit enhanced protease-resistance<sup>292</sup> and can be thermally processed in bulk, in contrast to polypeptides.<sup>141</sup> In addition, the physicochemical properties of polypeptoids (e.g., crystallinity,<sup>141, 159, 293</sup> solubility,<sup>160-161</sup> and conformation)<sup>27, 294</sup> are highly tailorable by controlling the side chain structure. These combined attributes make polypeptoids an emerging class of biomimetic polymers useful for various biomedical applications.<sup>3, 5-6, 153, 295-296</sup> Polypeptoids can be prepared by solid phase synthesis either by the conventional techniques developed by Merrifield<sup>45</sup> which



involve coupling the successive amino acid unit in a protected (commonly Fmoc) form to a growing chain anchored on a resin. The Fmoc protecting group is then removed, exposing an amine on which the next coupling step to form the peptide bond can occur.<sup>145</sup> This method requires the synthesis of various *N*-substituted glycines which is time consuming and costly. A different approach by Zuckermann known as the “sub-monomer” method<sup>146</sup> does not require protecting groups but uses successive acylation and nucleophilic displacement with bromoacetic acid and secondary amines to build the sequence-specific polypeptoid. While the solid phase synthetic methods ensure a precise control over chain length and sequence, they have the disadvantages of being inefficient and difficult to access high molecular weight species. Alternatively, high molecular weight polypeptoids have been synthesized through controlled ROPs of *N*-substituted *N*-carboxyanhydride monomers (R-NCAs)<sup>27, 142, 147, 155, 157, 160-161</sup> or *N*-thiocarboxyanhydrosulfides.<sup>111, 182, 190-191</sup> For the controlled NCA polymerization, primary amines or NHCs are the commonly used initiators. The former initiates the ROP of R-NCAs via the generation of a linear propagating species bearing a secondary amino chain end, whereas the latter initiates the chain growth by the formation of a cyclic zwitterionic propagating intermediate.<sup>84, 147, 150</sup>

While hydroxyl groups are one of the most common functionalities found in small organic compounds and polymers alike (e.g., the chain ends of polyester and polyether), alcohol-initiated polymerization of R-NCAs has never been reported. One early study showed that  $\alpha$ -amino acid derived *N*-carboxyanhydrides can be converted into high molecular weight polypeptides in the presence of alcohol in high yield.<sup>48</sup> The solution pH was found to affect the reaction product. Reactions in acidic conditions produce amino acid esters via alcoholysis,<sup>297-300</sup> whereas neutral or basic conditions favor oligo or polypeptide products. Under basic conditions, alkoxide species can initiate the

polymerization of NCAs by an activated monomer mechanism which involves the deprotonation of the N-H protons of the NCA monomer and addition of the deprotonated (“activated”) monomer to a neutral monomer to initiate the chain growth.<sup>78</sup> In contrast to  $\alpha$ -amino acid-based NCAs, we have found that R-NCAs do not react with alcohols alone.

Early work by Waymouth and Hedrick has revealed that the nucleophilicity of alcohols can be enhanced by hydrogen bonding interaction with bifunctional thioureas, diazabicycloundecene, and triazabicyclodecene (TBD), enabling alcohol-initiated controlled ROPs of various cyclic esters. We reason that R-NCAs can potentially be polymerized using a suitable combination of alcohol initiators and organic bases. Herein, we report the investigation of the ROPs of *N*-butyl *N*-carboxyanhydride using various alcohol initiators and 1,1,3,3-tetramethylguanidine (TMG) as an organocatalyst. The polymerization behavior is strongly dependent on the sterics of the alcohols. With primary alcohols such as BnOH, MeOH, EtOH, 2-methoxyethanol, and *n*-PrOH, the polymerizations proceed in a controlled manner, producing well-defined poly(*N*-butyl glycine) (PNBG) polypeptoids with controlled molecular weight and narrow molecular weight distribution in the low to moderate molecular weight range ( $M_n = 3\text{-}23 \text{ kg}\cdot\text{mol}^{-1}$ ). The reaction has also been extended towards the synthesis of amphiphilic hetero-block copolymers consisting of PEG and PNBG segments by using a hydroxyl-ended PEG macroinitiator. This method can potentially enable the facile access to a variety of hetero-block copolymers comprised of polypeptoid segments without the need of chain-end derivation to install primary amine functionalities.<sup>301</sup>

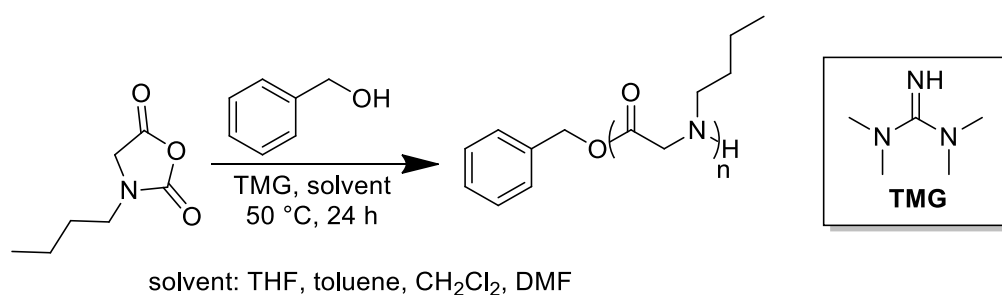
### 3.3 Results and discussion

#### 3.3.1 Initial results

*N*-butyl *N*-carboxyanhydride (Bu-NCA) was chosen as the model monomer in this study, as the monomer can be readily synthesized in high purity and good yield, and the

resulting poly(*N*-butyl glycine)s (PNBGs) have been well characterized previously.<sup>147</sup> Polymerization of Bu-NCA was carried out in the presence of 1,1,3,3-tetramethylguanidine (TMG) and benzyl alcohol in various solvents (i.e., THF, toluene, CH<sub>2</sub>Cl<sub>2</sub>, and DMF) at 50 °C under a nitrogen atmosphere (Scheme 3.1). The initial monomer to alcohol ratios ([M]<sub>0</sub>:[BnOH]<sub>0</sub>) were systematically varied between 25:1 and 400:1, while the initial TMG and monomer concentration ([TMG]<sub>0</sub>=0.6 mM, [M]<sub>0</sub>=1.0 M) were kept constant. All reactions reached quantitative conversion within 24 h. This is verified by the FTIR analysis of reaction aliquots showing the complete disappearance of carbonyl stretching bands at 1851 cm<sup>-1</sup> and 1777 cm<sup>-1</sup> that are characteristic of the Bu-NCA monomers. The resulting polypeptoids were obtained by precipitation into excess hexanes (or diethyl ether in the case of reactions conducted in DMF), collected by filtration, and drying under vacuum.

Scheme 3.1. ROP of Bu-NCA via BnOH initiator and TMG organocatalyst



<sup>1</sup>H NMR spectroscopic analysis confirms the formation of the desired PNBG polymers.<sup>147</sup> An exemplary <sup>1</sup>H NMR spectrum of the obtained PNBG is shown in Figure 3.1. MALDI-TOF MS analysis of a low MW polymer obtained from a reaction in THF ([M]<sub>0</sub>:[BnOH]<sub>0</sub>=25:1) indicates that the polypeptoids mainly contain one benzyl ester and one secondary amino end groups, in agreement of benzyl alcohol initiating the ROP of the Bu-NCAs (Figure 3.2). Polypeptoids containing TMG moieties were also observed in

the MS spectra, although in a low apparent quantity. This suggests the potential occurrence of TMG-initiated polymerization of Bu-NCA to some extent (vide infra). Analysis of all polymers obtained from polymerizations in THF by size-exclusion chromatography equipped with multiangle light scattering and differential refractive index detectors (SEC-MALS-DRI) revealed mono-modal peaks with molecular weight

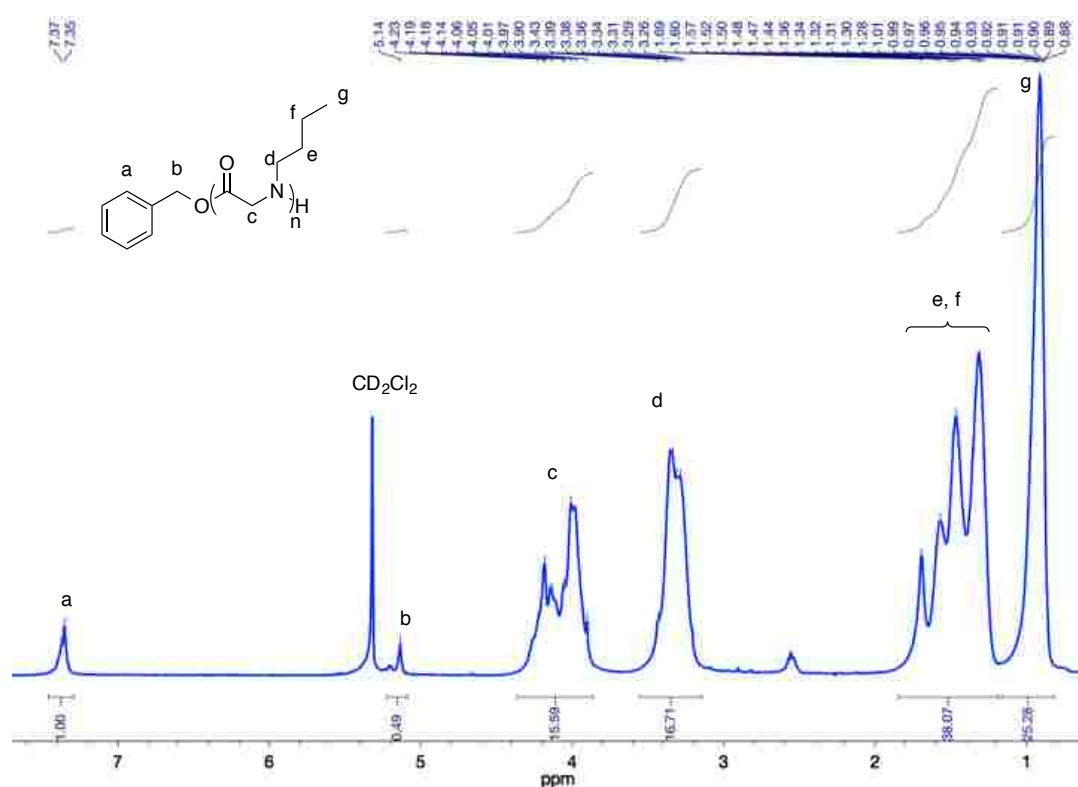


Figure 3.1.  $^1\text{H}$  NMR spectrum of PNBG obtained via ROP of Bu-NCA with benzyl alcohol initiator and TMG promotor ( $[\text{M}]_0:[\text{BnOH}]_0=25:1$ ). Polymerization was performed at  $[\text{M}]_0=1.0$  M,  $50$   $^\circ\text{C}$ , in THF for 24 h.  $[\text{TMG}]_0$  was held at  $0.6$  mM. The spectrum was collected in  $\text{CD}_2\text{Cl}_2$ .

( $M_n$ ) in the  $2.9\text{-}20.5$   $\text{kg}\cdot\text{mol}^{-1}$  range and narrow molecular weight distribution (PDI=1.03-1.08) (Figure 3.3). It was found that the control over  $M_n$ s is strongly dependent on the solvent (Table 3.1). For polymerization conducted in THF and toluene, the polymer molecular weight increases as the initial monomer to benzyl alcohol ratio is systematically increased. The polymer molecular weights agree with the theoretical

values based on single-site initiation by the benzyl alcohol at low molecular range and become lower than the theoretical values at the higher molecular weight range ( $[M]_0:[BnOH]_0 > 100:1$ ). The deviation becomes more pronounced as the  $[M]_0:[BnOH]_0$  ratio is further increased. In contrast to reactions in THF and toluene, polypeptoids obtained from polymerization in  $CH_2Cl_2$  and DMF have comparable molecular weights regardless of the  $[M]_0:[BnOH]_0$  ratio, indicating a lack of controlled polymerization in these solvents.

It was also noted that for the polymers obtained from reactions in THF and toluene, the  $M_n$ s determined by  $^1H$  NMR spectroscopy via integration of protons due to the PNBG repeating units relative to the benzyl ester end-groups (Figure 3.3) are higher than those determined by the SEC-MALS-DRI method and the discrepancy becomes more pronounced at the high MW range. This suggests that some of the high molecular weight polymers may contain chain ends other than benzyl ester groups, in accordance with MALDI-TOF MS results.

### 3.3.2 Competition with TMG initiation

To assess whether TMG may initiate the polymerization of Bu-NCA, a series of polymerizations of Bu-NCA with varying initial TMG loadings were conducted under the standard conditions (i.e.,  $[M]_0:[TMG]_0 = 25:1-200:1$ ,  $[M]_0 = 1.0$  M,  $50$  °C, THF, 24 h). It was found that the molecular weight of the resulting PNBG polymers increases proportionally with the  $[M]_0:[TMG]_0$  ratio until the ratio exceeds 200:1 at which point the  $M_n$  becomes lower than the theoretical value (Table 3.2 and Figure 3.4).  $^1H$  NMR and MALDI-TOF MS analyses of the resulting polymers (Figure 3.5 and 3.6) also indicate the attachment of TMG to the polymers. These results indicate that TMG indeed can efficiently initiate the polymerization of Bu-NCAs on its own. This may contribute to the deviation of the polymer molecular weight of the PNBGs from the theoretical values in

the TMG-promoted polymerization of Bu-NCA using benzyl alcohol initiators, as the theoretical values are based on the single-site initiation with alcohol alone. For reactions with low loading of alcohol initiators (e.g.,  $[M]_0:[I]_0=400:1$ ), the TMG concentration (0.6 mM) becomes comparable to that of benzyl alcohol (2.5 mM), resulting in competitive initiating pathways that would lower the polymer molecular weight. To further investigate the effect of TMG concentration on the polymer molecular weight control, a series of polymerizations of Bu-NCAs where  $[TMG]_0$  was increased to equimolar concentration relative to that of benzyl alcohol was conducted under the standard conditions (i.e.,  $[M]_0=1.0$  M,  $[M]_0:[BnOH]_0=25:1-100:1$ , 50 °C, THF, 24 h). The resulting polymer molecular weights ( $M_n$ s) were approximately half of the theoretical values based on initiation by benzyl alcohol alone when the  $[M]_0:[BnOH]_0$  ratio exceeded 25:1 (Entry 2-3, Table 3.3). These results further support that TMG can compete with alcohols to initiate the polymerization of Bu-NCA on its own. As a result, the control of TMG concentration relative to that of the alcohol is important in order to ensure the efficient and predominant initiation by alcohols, yielding well-defined polypeptoids with controlled polymer molecular weight and chain-end structures.

### 3.3.3 Demonstration of a living polymerization

Polymerizations of Bu-NCA in the presence of BnOH and TMG exhibit living polymerization characteristics, evidenced by the linear increase of polymer molecular weight and decreasing molecular weight distribution ( $PDI=1.22-1.05$ ) with increasing conversion (Figure 3.7A). A chain extension experiment was also conducted to further verify the living nature of the polymerization. Specifically, a polymerization ( $[M]_0:[BnOH]_0:[TMG]_0=50:1:0.03$ ) was conducted under standard conditions in 50 °C THF for 24 h to reach full conversion. A second batch of monomer

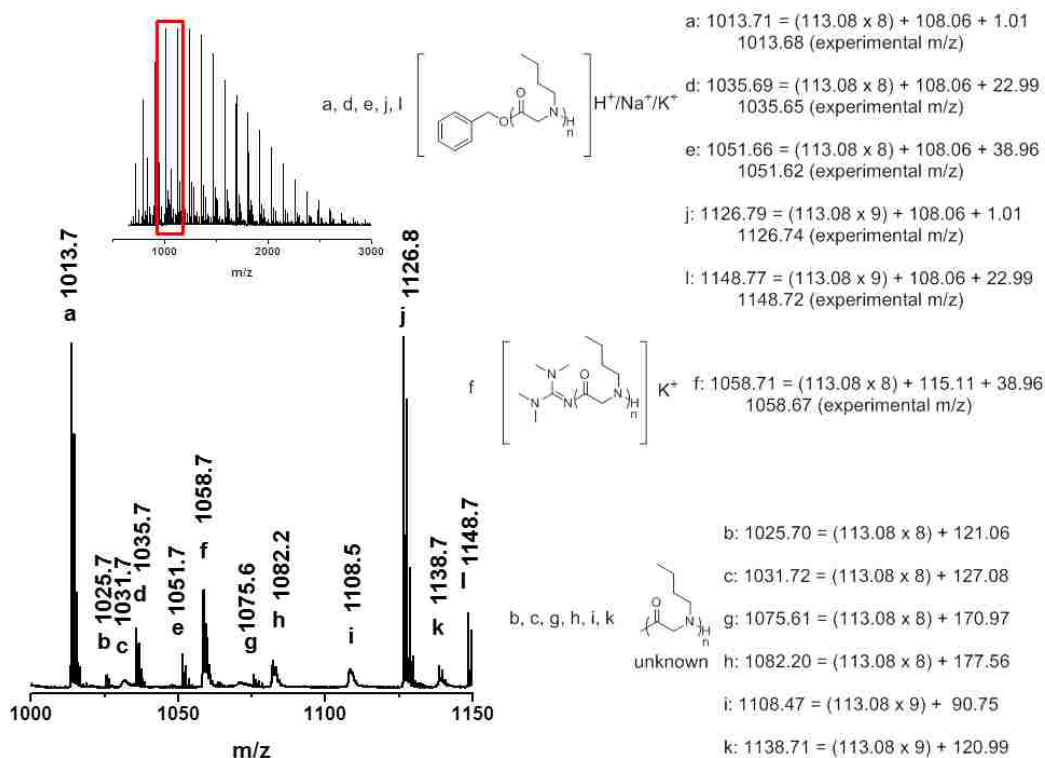


Figure 3.2. MALDI-TOF MS spectra of a low molecular weight PNBG obtained by BnOH-initiated polymerization of Bu-NCA in the presence of TMG under the standard conditions ( $[M]_0=1.0$  M,  $[TMG]_0=0.6$  mM,  $[M]_0:[BnOH]_0=25:1$ , THF, 50 °C) and the PNBG polymer structures corresponding to the respective mass ions. CHCA was used as the matrix.

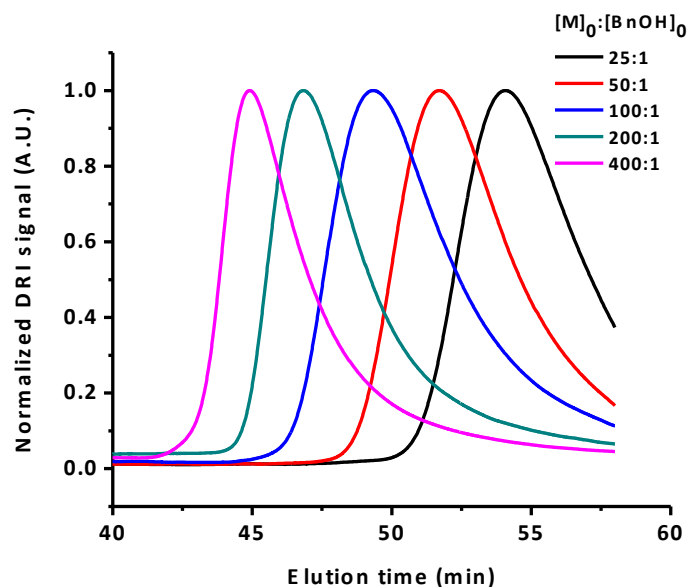


Figure 3.3. SEC-DRI chromatograms of PNBG polymers obtained by ROP of Bu-NCAs in the presence of benzyl alcohol and TMG with increasing  $[M]_0:[BnOH]_0$  ratio and a constant initial monomer and TMG concentration ( $[M]_0=1.0$  M and  $[TMG]_0=0.6$  mM) in 50 °C THF.

Table 3.1. TMG-mediated polymerization of Bu-NCAs to afford poly(*N*-butyl glycine)s in the presence or absence of benzyl alcohol in different solvents.<sup>a</sup>

Solvent	[M] <sub>0</sub> : [BnOH] <sub>0</sub>	[TMG] <sub>0</sub> (mM)	<i>M</i> <sub>n</sub> (theo.) <sup>b</sup>	<i>M</i> <sub>n</sub> (SEC) <sup>c</sup>	<i>M</i> <sub>n</sub> (NMR) <sup>d</sup>	PDI <sup>c</sup>	DP <sup>e</sup>	Conv. (%) <sup>f</sup>
THF	25:1	no TMG	-	-	-	-	-	0
	no BnOH	0.6	-	42.9	- <sup>g</sup>	1.03	380	100
	25:1	0.6	2.8	2.9	3.8	1.08	26	100
	50:1	0.6	5.7	5.6	5.5	1.04	50	100
	100:1	0.6	11.3	8.9	14.5	1.08	79	100
	200:1	0.6	22.6	13.1	15.7	1.05	116	100
Toluene	400:1	0.6	45.2	20.5	42.5	1.04	181	100
	25:1	0.6	2.8	4.0	5.3	1.13	35	100
	50:1	0.6	5.7	4.8	6.7	1.09	42	100
	100:1	0.6	11.3	8.2	9.3	1.04	72	100
	200:1	0.6	22.6	11.1	19.4	1.02	98	100
CH <sub>2</sub> Cl <sub>2</sub>	400:1	0.6	45.2	15.4	25.2	1.02	136	100
	25:1	0.6	2.8	5.3	2.2	1.23	47	100
	50:1	0.6	5.7	6.1	4.2	1.18	54	100
DMF	100:1	0.6	11.3	6.5	6.3	1.04	57	100
	25:1	0.6	2.8	3.1	3.5	1.09	27	100
	50:1	0.6	5.7	4.1	5.2	1.19	36	100
	100:1	0.6	11.3	5.3	6.1	1.03	47	100

<sup>a</sup> All polymerizations were conducted at [M]<sub>0</sub>=1.0 M at 50 °C and were allowed to reach full conversion in 24 h. The initial TMG concentration ([TMG]<sub>0</sub>) was held constant at 0.6 mM; <sup>b</sup> theoretical molecular weights in the unit of kg·mol<sup>-1</sup> are calculated from [M]<sub>0</sub>: [BnOH]<sub>0</sub> ratio and conversion; <sup>c</sup> polymer molecular weights (kg·mol<sup>-1</sup>) are determined by the SEC-MALS-DRI method using dn/dc = 0.0815 ± 0.0012 mL·g<sup>-1</sup>; <sup>d</sup> polymer molecular weights (kg·mol<sup>-1</sup>) are determined by end group analysis using <sup>1</sup>H NMR spectroscopy, assuming all polymers are terminated with benzyl end-groups; <sup>e</sup> calculated from the *M*<sub>n</sub> determined by SEC-MALS-DRI method; <sup>f</sup> determined by FTIR analysis of reaction aliquots after 24 h; <sup>g</sup> end groups were not observed in the <sup>1</sup>H NMR spectrum.

Table 3.2. Molecular weight analysis of PNBGs obtained by ROP of Bu-NCAs using TMG initiators at varying [M]<sub>0</sub>: [TMG]<sub>0</sub> ratio <sup>a</sup>

[M] <sub>0</sub> : [TMG] <sub>0</sub>	<i>M</i> <sub>n</sub> (theo.) (kg·mol <sup>-1</sup> ) <sup>b</sup>	<i>M</i> <sub>n</sub> (SEC) (kg·mol <sup>-1</sup> ) <sup>c</sup>	<i>M</i> <sub>n</sub> (NMR) (kg·mol <sup>-1</sup> ) <sup>d</sup>	PDI <sup>c</sup>	Conv. <sup>e</sup> (%)
25:1	2.8	2.7	2.5	1.11	100
50:1	5.6	4.3	5.3	1.02	100
125:1	12.0	11.7	10.7	1.10	85
200:1	16.5	9.2	8.8	1.04	73

<sup>a</sup> All polymerizations were conducted at [M]<sub>0</sub>=1.0 M in THF at 50 °C for 24 h; <sup>b</sup> theoretical molecular weights were calculated from the [M]<sub>0</sub>: [TMG]<sub>0</sub> ratio and conversion; <sup>c</sup> polymer molecular weights and the molecular weight distribution were determined by SEC-MALS-DRI method using dn/dc = 0.0815 ± 0.0012 mL·g<sup>-1</sup>; <sup>d</sup>



polymer molecular weights were determined by end group analysis using  $^1\text{H}$  NMR assuming that all polymers were terminated with TMG amide groups;  $^e$  conversions were determined by FTIR analysis of the reaction aliquots after 24 h.

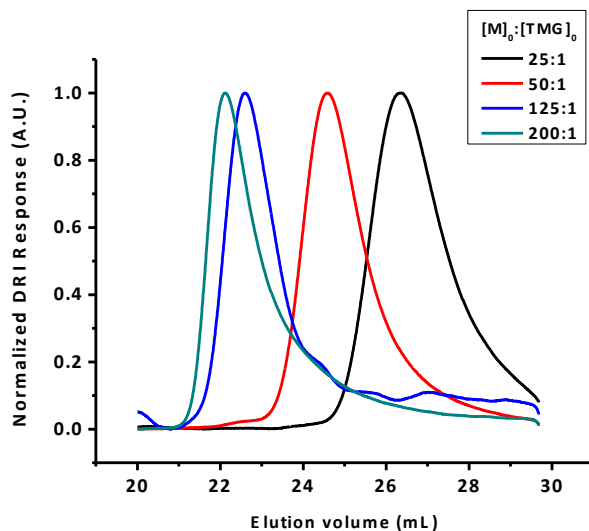


Figure 3.4. SEC-DRI chromatograms of PNBG polymers obtained from the ROP of Bu-NCA using TMG as initiators ( $[\text{M}]_0=1.0$  M,  $50^\circ\text{C}$ , THF).

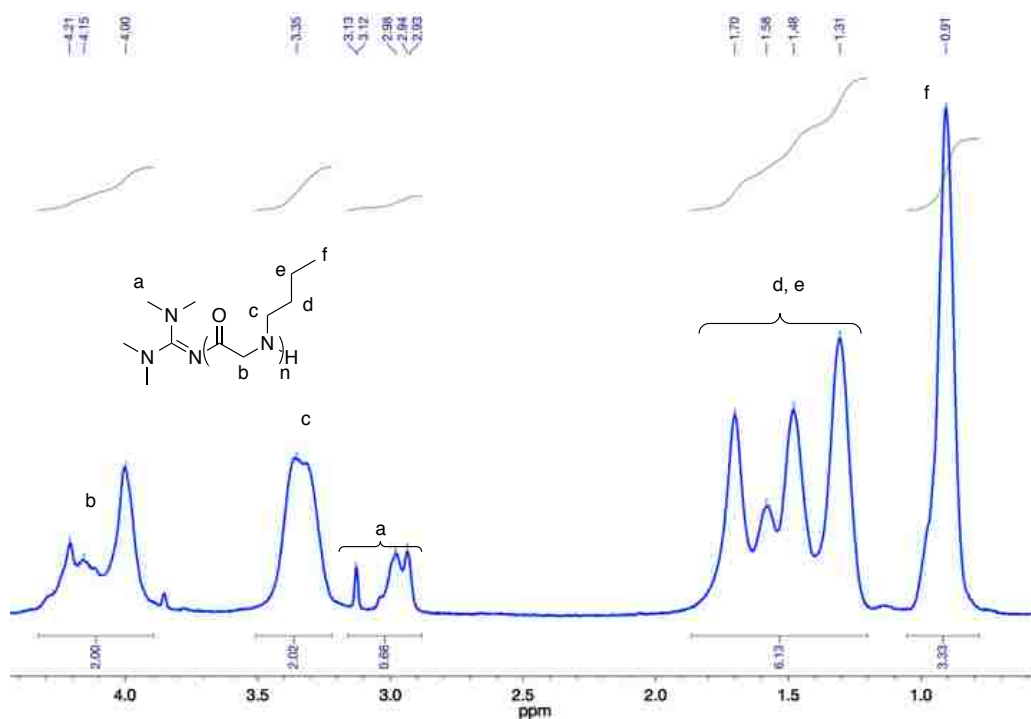


Figure 3.5.  $^1\text{H}$  NMR spectrum of PNBGs obtained via ROP of Bu-NCA with TMG initiator ( $[\text{M}]_0:[\text{TMG}]_0=25:1$ ). Polymerization was performed at  $[\text{M}]_0=1.0$  M,  $50^\circ\text{C}$ , in THF for at least 24 h. The spectrum was collected in  $\text{CDCl}_3$ .

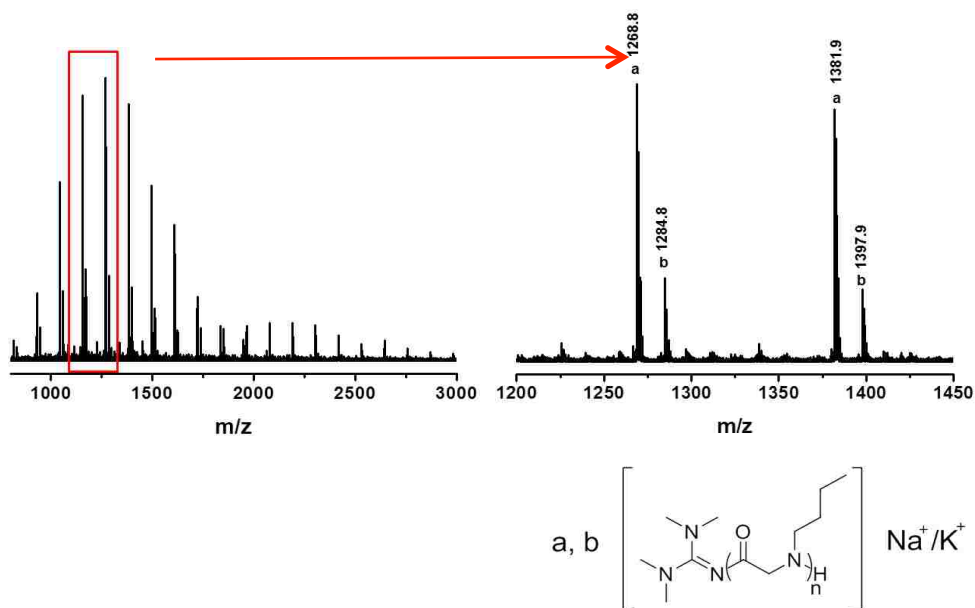


Figure 3.6. MALDI-TOF MS spectra of PNBGs obtained from ROP of Bu-NCA using TMG initiator alone ( $[M]_0:[TMG]_0=25:1$ ,  $[M]_0=1.0$  M,  $50$  °C, THF). CHCA matrix was used in sample preparation.

Table 3.3. Polymerization of Bu-NCA in the presence of equimolar BnOH and TMG <sup>a</sup>

$[M]_0:[BnOH]_0:$ $[TMG]_0$	$M_n$ (theo.) ( $\text{kg}\cdot\text{mol}^{-1}$ ) <sup>b</sup>	$M_n$ (SEC) ( $\text{kg}\cdot\text{mol}^{-1}$ ) <sup>c</sup>	PDI <sup>c</sup>	DP	Conv. <sup>d</sup> (%)
25:1:1	2.8	2.2	1.03	19	100
50:1:1	5.6	3.0	1.08	27	100
100:1:1	11.3	5.8	1.03	51	100

<sup>a</sup> All polymerizations were conducted at  $[M]_0=1.0$  M in THF at  $50$  °C for 24 h; <sup>b</sup> theoretical molecular weights were calculated from the  $[M]_0:[BnOH]_0$  ratio and conversion; <sup>c</sup> polymer molecular weights and the molecular weight distribution were determined by SEC-MALS-DRI method using  $dn/dc = 0.0815 \pm 0.0012$   $\text{mL}\cdot\text{g}^{-1}$ ; <sup>d</sup> conversions were determined by FTIR analysis of the reaction aliquots after 24 h.

( $[M]_0:[BnOH]_0=100:1$ ) was subsequently introduced to the reaction mixture to allow for further chain propagation. SEC-MALS-DRI analysis of the PNBG polymers obtained from the first and second polymerization (Figure 3.7B) revealed an increase of polymer  $M_n$  that agrees well with the theoretical predictions for a controlled enchainment where all propagating chains remain active for monomer addition (Table 3.4).

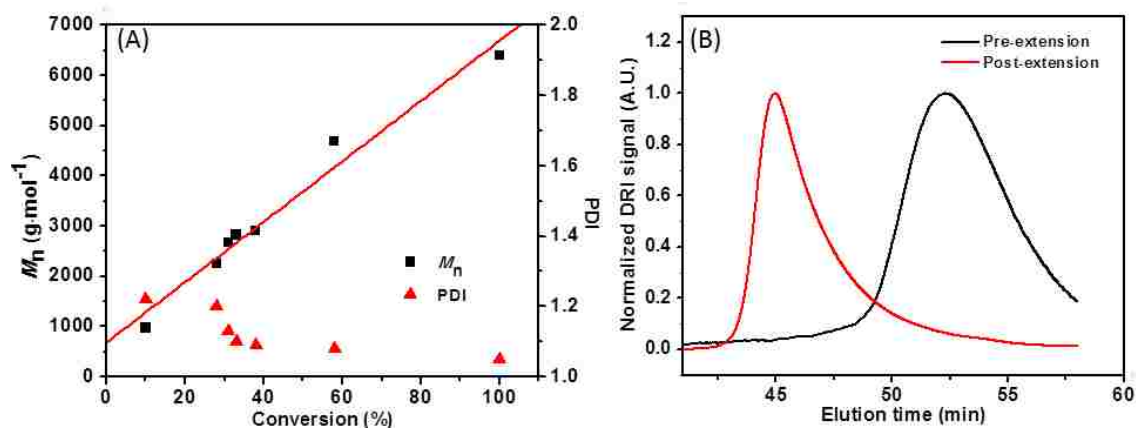


Figure 3.7. (A) Plots of polymer molecular weight ( $M_n$ ) and molecular weight distribution (PDI) versus conversion for the TMG-mediated polymerization of Bu-NCA using BnOH initiators ( $[M]_0:[BnOH]_0:[TMG]_0=50:1:0.03$ ,  $[M]_0=1.0$  M, THF, 50 °C)  $R^2=0.98$ . (B) SEC-MALS-DRI chromatograms from the chain extension experiment (first reaction:  $[M]_0:[BnOH]_0:[TMG]_0=50:1:0.03$ ,  $[M]_0=1.0$  M, THF, 50 °C; chain extension reaction:  $[M]_0:[BnOH]_0=100:1$ ).

Table 3.4. Chain extension of PNBG polymers prepared by TMG-mediated polymerization of Bu-NCA using BnOH initiators <sup>a</sup>

	$[M]_0:[BnOH]_0$	$M_n$ (theo.) <sup>b</sup> ( $\text{kg}\cdot\text{mol}^{-1}$ )	$M_n$ (SEC) <sup>c</sup> ( $\text{kg}\cdot\text{mol}^{-1}$ )	PDI <sup>c</sup>	DP <sup>d</sup>
Pre-extension	50:1	5.6	6.4	1.13	57
Post-extension	150:1	17.0	16.2	1.09	143

<sup>a</sup> All polymerizations were conducted at  $[M]_0=1.0$  M in 50 °C THF and were allowed to react for at least 24 h to reach quantitative conversion.  $[TMG]_0$  was held constant at 0.6 mM; <sup>b</sup> theoretical molecular weights in  $\text{kg}\cdot\text{mol}^{-1}$  are calculated from  $[M]_0:[BnOH]_0$  ratio and conversion; <sup>c</sup> determined by the SEC-MALS-DRI method using  $dn/dc = 0.0815 \pm 0.0012 \text{ mL}\cdot\text{g}^{-1}$ ; <sup>d</sup> number average degree of polymerization was calculated from the  $M_n$  determined by SEC-MALS-DRI method.

### 3.3.4 Kinetic study of the polymerization

Kinetic experiments were conducted for the polymerization of Bu-NCAs under standard conditions using deuterated solvent (50 °C, THF- $d_8$ ), where the initial loading of BnOH loading is systematically varied ( $[M]_0:[BnOH]_0=25:1-100:1$ ) and the initial monomer and TMG concentrations are kept constant ( $[M]_0=0.15$  M,  $[TMG]_0=90 \mu\text{M}$  (0.06 mol% relative to  $[M]_0$ )). The progression of the reaction was monitored using  $^1\text{H}$  NMR spectroscopy. The polymerization exhibits a first-order dependence on the monomer and

benzyl alcohol concentration respectively with a propagating rate constant ( $k_p=0.59 \pm 0.01 \text{ M}^{-1}\text{h}^{-1}$ ) (Figure 3.8A and 3.8C, Table 3.5). To determine the effect of  $[\text{TMG}]_0$  on the propagation rate, polymerization of Bu-NCA with varying loadings of TMG and constant initial monomer and BnOH concentrations ( $[\text{M}]_0=0.15 \text{ M}$ ,  $[\text{M}]_0:[\text{BnOH}]_0=50:1$ ) were conducted in  $50 \text{ }^\circ\text{C}$  THF- $d_8$ . The polymerization still exhibited pseudo-first order kinetics (Figure 3.8B) and the propagating rate did not appear to be significantly affected by the variation of  $[\text{TMG}]_0$  in the  $45\text{-}180 \text{ }\mu\text{M}$  range (i.e.,  $0.03\text{-}0.12 \text{ mol.}\%$  relative to  $[\text{M}]_0$ ) (Table 3.6). This suggests that TMG does not affect the chain propagation and only acts cooperatively with BnOH to initiate the polymerization.

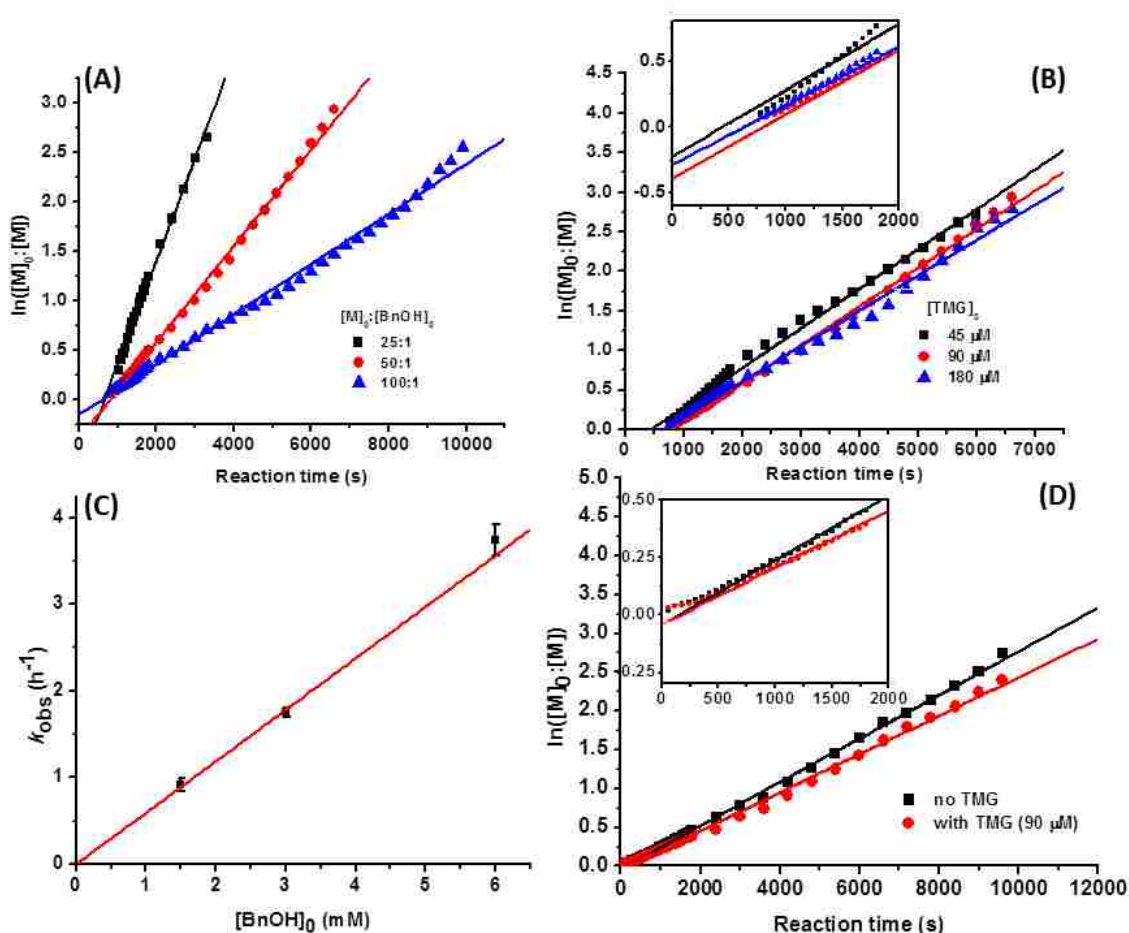


Figure 3.8. (A) Plots of  $\ln([\text{M}]_0/[\text{M}])$  versus reaction time for the TMG-promoted polymerization of Bu-NCA using BnOH initiators at various initial BnOH loading ( $[\text{M}]_0:[\text{BnOH}]_0=25:1\text{-}100:1$ ,  $[\text{M}]_0=0.15 \text{ M}$ ,  $[\text{TMG}]_0=90 \text{ }\mu\text{M}$ , THF- $d_8$ ,  $50 \text{ }^\circ\text{C}$ ); (B) plots of  $\ln([\text{M}]_0/[\text{M}])$  versus reaction time for the TMG-promoted polymerization of Bu-NCA using BnOH initiators at various initial TMG loading; (C) plots of  $k_{\text{obs}}$  versus  $[\text{BnOH}]_0$

for the TMG-promoted polymerization of Bu-NCA using BnOH initiators; (D) plots of  $\ln([M]_0/[M])$  versus reaction time for the BnNH<sub>2</sub>-initiated polymerization of Bu-NCA with (red) or without TMG present (black) ( $[M]_0:[BnNH_2]_0=50:1$ ,  $[M]_0=0.15$  M,  $[TMG]_0=90$  or  $0$   $\mu$ M, THF-d<sub>8</sub>, 50 °C).

Table 3.5. The observed polymerization rate constant ( $k_{obs}$ ) for BnOH-initiated polymerization of Bu-NCA with varying BnOH loadings and constant initial monomer and TMG concentrations <sup>a</sup>

Entry number	$[M]_0:[BnOH]_0$	$k_{obs}$ (h <sup>-1</sup> )
1	25:1	$3.74 \pm 0.18$
2	50:1	$1.75 \pm 0.05$
3	100:1	$0.91 \pm 0.08$

<sup>a</sup> For all reactions, the initial monomer and TMG concentrations were held constant at  $[M]_0=0.15$  M and  $[TMG]_0=90$   $\mu$ M, respectively. All kinetic experiments were repeated at least twice.

Table 3.6. The observed polymerization rate constant ( $k_{obs}$ ) for a series of BnOH-initiated polymerization of Bu-NCA with varying TMG loadings and constant initial monomer and BnOH concentrations <sup>a</sup>

Entry number	$[M]_0:[BnOH]_0:[TMG]_0$	$[TMG]_0$ (mM)	$k_{obs}$ (h <sup>-1</sup> )
1	50:1:0.015	45	$1.62 \pm 0.02$
2	50:1:0.030	90	$1.75 \pm 0.05$
3	50:1:0.060	180	$1.81 \pm 0.01$

<sup>a</sup> For all reactions, the initial monomer and BnOH concentrations were held constant at  $[M]_0=0.15$  M and  $[BnOH]_0=3$  mM, respectively. All kinetic experiments were repeated at least twice.

Benzylamine has been previously shown to initiate the controlled polymerization of various R-NCAs.<sup>153</sup> To further compare the relative polymerization efficiency, Bu-NCAs were also polymerized using benzylamine with or without TMG present under identical conditions to those reactions using BnOH and TMG ( $[M]_0:[BnNH_2]_0=50:1$ ,  $[M]_0=0.15$  M,  $[TMG]_0=90$  or  $0$   $\mu$ M, 50 °C, THF-d<sub>8</sub>). The BnOH-initiated ROP of Bu-NCAs in the presence of TMG ( $k_{obs}=1.75 \pm 0.05$  h<sup>-1</sup>, Figure 3.8B) is only slightly faster than that with benzylamine initiator alone ( $k_{obs}=1.01 \pm 0.12$  h<sup>-1</sup>, Figure 3.8D). Addition of a catalytic amount of TMG (90  $\mu$ M) to the benzylamine initiated polymerization has no significant

effect on the polymerization rate ( $k_{\text{obs}} = 0.89 \pm 0.06 \text{ h}^{-1}$ , Figure 3.8D). These results strongly suggest that TMG can promote the polymerization of Bu-NCAs by activating the benzyl alcohol initiator but not the primary amine initiator or the propagating species bearing secondary amino chain ends.

### 3.3.5 Expanding the breadth of alcohol initiators and their dependence on sterics and electronics

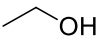
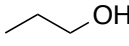
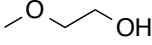
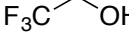
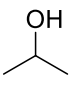
Encouraged by these initial findings, we set to investigate the general applicability of the polymerization method toward the synthesis of polypeptoids using a series of alcohol initiators having different structures in conjunction with TMG. Polymerization of Bu-NCAs using methanol, ethanol, 2-methoxyethanol, *n*-propanol, isopropyl alcohol, and *tert*-butyl alcohol in conjunction with TMG were conducted under identical conditions to those where benzyl alcohol was employed as initiators. It was found that the primary alcohol (i.e., methanol, ethanol, 2-methoxyethanol, and *n*-propanol)-initiated ROPs of Bu-NCAs produced PNBG polymers with controlled molecular weights in the 2.8-23.2  $\text{kg}\cdot\text{mol}^{-1}$  range and narrow molecular weight distributions (PDI=1.02-1.16) (Table 3.7). The polymer molecular weights and end-group structures of the resulting PNBG polymers agree reasonably well with the theoretical prediction of controlled polymerizations with alcohol as initiators (Figure B1-4), up until the  $[\text{M}]_0:[\text{ROH}]_0$  ratio reaches approximately 200:1 when the molecular weight begins to deviate. In stark contrast, polymerization of Bu-NCAs using a more sterically hindered secondary alcohol (e.g., isopropyl alcohol) together with TMG yielded polypeptoids whose molecular weights were substantially higher than the theoretical values, suggesting that initiation is significantly inefficient and slower relative to propagation. To our surprise, when *tert*-butyl alcohol was used, no polymerization was observed regardless of the initial monomer to alcohol ratios under standard conditions. The pKa of these alcohols are comparable and differ within 2 units (Table 3.8). We also investigated 2,2,2-

trifluoroethanol and phenol that are more electron deficient and have much lower pK<sub>a</sub>s (Table 3.8) than all other alcohols that have been studied as initiators. It was found that 2,2,2-trifluoroethanol in conjunction with TMG produced PNBGs whose  $M_n$ s were significantly higher than the theoretical values, whereas phenol in conjunction with TMG failed to initiate the polymerization regardless of the initial monomer to alcohol ratios (Table 3.7). Similarly, when benzylmercaptan (BnSH) in conjunction with TMG was used, no polymerization was observed under standard conditions regardless of the initial monomer to initiator loadings. These results clearly indicate that the electronic and steric characteristics of hydroxyl-containing nucleophiles strongly impact the initiation efficiency and the polymerization behavior. To understand the observed polymerization behavior, it is appropriate to consider the possible modes of initiation by alcohols in the presence of TMG.

### 3.3.6 Elucidation of an initiating pathway

TMG is a strong base (pK<sub>a</sub>=15.5 for TMG-H<sup>+</sup> in THF, 23.37 in CH<sub>3</sub>CN)<sup>302-304</sup> and good nucleophile similarly to triazabicyclodecene (TBD) (pK<sub>a</sub>=21.0 for TBD-H<sup>+</sup> in THF, 26.03 in CH<sub>3</sub>CN)<sup>302, 304-305</sup> which has been widely studied in the ROPs of various cyclic esters.<sup>274-275, 277, 279, 291, 306-309</sup> As a result, three possible mechanisms of initiation that differ from that of the normal primary amine-initiated polymerization of R-NCAs (Scheme 3.2)<sup>48, 153</sup> can be envisioned for the role of TMG in the alcohol-initiated polymerization of Bu-NCAs with TMG present (Scheme 3.3). The first mechanism involves the formation of hydrogen bonding complexes (Scheme 3.3, Mechanism I) between TMG and alcohols, resulting in enhanced nucleophilicity of the alcohol initiators similarly to what was proposed for the TBD-catalyzed ROP of various cyclic esters.<sup>275</sup> This results in rapid initiation by ring-opening addition of the Bu-NCAs with the activated alcohols. The subsequent chain propagation proceeds by conventional

Table 3.7. Polymerization of Bu-NCA in the presence of TMG and different alcohols <sup>a</sup>

Alcohol	[M] <sub>0</sub> : [I] <sub>0</sub>	<i>M<sub>n</sub></i> (theo.) <sup>b</sup> (kg·mol <sup>-1</sup> )	<i>M<sub>n</sub></i> (SEC) <sup>c</sup> (kg·mol <sup>-1</sup> )	<i>M<sub>n</sub></i> (NMR) <sup>d</sup> (kg·mol <sup>-1</sup> )	PDI <sup>c</sup>	DP <sup>e</sup>	Conv. (%) <sup>f</sup>
CH <sub>3</sub> OH	25:1	2.8	3.9	- <sup>g</sup>	1.04	34	100
	50:1	5.6	6.7	- <sup>g</sup>	1.05	59	100
	100:1	11.3	11.3	- <sup>g</sup>	1.04	100	100
	200:1	22.6	13.9	- <sup>g</sup>	1.10	123	100
	400:1	45.2	14.8	- <sup>g</sup>	1.04	131	100
	25:1	2.8	3.5	- <sup>g</sup>	1.03	31	100
	50:1	5.6	6.3	- <sup>g</sup>	1.09	58	100
	100:1	11.3	10.1	- <sup>g</sup>	1.02	89	100
	200:1	22.6	16.9	- <sup>g</sup>	1.04	150	100
	400:1	45.2	19.9	- <sup>g</sup>	1.04	176	100
	25:1	2.8	4.3	- <sup>g</sup>	1.06	38	100
	50:1	5.6	6.3	- <sup>g</sup>	1.09	56	100
	100:1	11.3	13.3	- <sup>g</sup>	1.06	118	100
	200:1	22.6	18.1	- <sup>g</sup>	1.05	160	100
	400:1	45.2	23.2	- <sup>g</sup>	1.04	205	100
	25:1	2.8	2.8	1.9	1.09	25	100
	50:1	5.6	5.6	5.4	1.16	50	100
	100:1	11.3	8.5	7.9	1.03	75	100
	200:1	22.6	12.9	- <sup>g</sup>	1.12	114	100
	400:1	45.2	13.3	- <sup>g</sup>	1.05	118	100
F <sub>3</sub> C- 	25:1	2.8	14.5	- <sup>g</sup>	1.06	128	100
	50:1	5.6	19.9	- <sup>g</sup>	1.04	176	100
	100:1	11.3	23.3	- <sup>g</sup>	1.01	206	100
	25:1	2.8	13.6	- <sup>g</sup>	1.08	120	100
	50:1	5.6	22.0	- <sup>g</sup>	1.05	194	100
	100:1	- <sup>h</sup>	- <sup>h</sup>	- <sup>h</sup>	- <sup>h</sup>	- <sup>h</sup>	0

<sup>a</sup> All polymerizations were conducted at [M]<sub>0</sub>=1.0 M in 50°C THF for 24 h. [TMG]<sub>0</sub> was held constant at 0.06 mol % with respect to the molar amount of monomer; <sup>b</sup> theoretical polymer molecular weights were determined by [M]<sub>0</sub>: [I]<sub>0</sub> and conversion; <sup>c</sup> polymer molecular weight and the molecular weight distribution are determined by the SEC-MALS-DRI method using dn/dc = 0.0815 ± 0.0012 mL·g<sup>-1</sup> for the PNBG polymer; <sup>d</sup> polymer molecular weight are determined by end group analysis using <sup>1</sup>H NMR spectroscopy; <sup>e</sup> calculated from the *M<sub>n</sub>* determined by the SEC analysis; <sup>f</sup> determined by FTIR analysis of reaction aliquots after 24 h; <sup>g</sup> end group protons cannot be unambiguously distinguished in the respective <sup>1</sup>H NMR spectra; <sup>h</sup> no polymerization was observed in the respective experiment.



Table 3.8. Change of imine and hydroxyl proton chemical shifts upon formation of hydrogen bonding complexes between TMG and various alcohols/phenol/acids and the pKa of the alcohols/phenol/acid.

Nucleophilic initiators	$\Delta d_1$ (ppm) <sup>a</sup>	$\Delta d_2$ (ppm) <sup>b</sup>	pK <sub>a</sub>	
			DMSO <sup>310-</sup> <sub>311</sub>	H <sub>2</sub> O <sup>311-</sup> <sub>312</sub>
BnOH	0.07	1.42	-	15.4
MeOH	0.82	1.46	29.0	15.5
EtOH	0.57	1.39	29.8	16.0
2-Methoxyethanol	0.40	2.39	-	14.8
2,2,2-Trifluoroethanol	0.40	1.40	23.5	12.5
<i>n</i> -PrOH	0.03	2.07	-	16.1
<i>i</i> -PrOH	0.08	0.72	30.3	16.5
<i>t</i> -BuOH	0.04	0.01	32.2	17.0
Phenol	1.96 <sup>c</sup>	0.75 <sup>c</sup>	18.0	9.95
Benzoic acid	3.38 <sup>c</sup>	1.73 <sup>d</sup>	11.1	4.2

<sup>a</sup>  $\Delta\delta$ , refers to the chemical shift difference between the imine proton of TMG and the protons forming the hydrogen bonding between the TMG and various alcohols; <sup>b</sup>  $\Delta\delta$ , refers to the chemical shift difference between the hydroxyl proton of various alcohols and the protons forming the hydrogen bonding between the TMG and the alcohols; <sup>c</sup> for phenol and benzoic acid,  $\Delta\delta$ , refers to the chemical shift difference between the imine proton of TMG and the iminium protons ( $=NH_2^+$ ) of the TMG-H<sup>+</sup> species; <sup>d</sup> for phenol or benzoic acid,  $\Delta\delta$ , refers to the chemical shift difference between the hydroxyl proton of phenol or carboxyl proton of benzoic acid and the iminium protons ( $=NH_2^+$ ) of the TMG-H<sup>+</sup> species. The pKa of BnSH = 15.3 in DMSO.

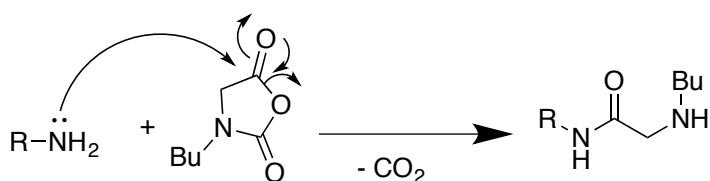
nucleophilic addition of the Bu-NCA monomers to the secondary amino chain ends of the growing polymer chains (Scheme 3.4). The second proposed mechanism of initiation involves the direct nucleophilic addition of the Bu-NCA monomers by the TMG to form a zwitterionic species (Scheme 3.3, Mechanism II), which can be displaced by the alcohol to form a neutral initiating species bearing secondary amino end-groups from which enchainment ensues. The third mechanism of initiation involves the deprotonation of alcohols by TMG to form an alkoxide species, which initiate the polymerization by nucleophilic addition of Bu-NCAs to form the anionic carbamate initiating species with 1,1,3,3-tetramethylguanindinium counter ions (TMG-H<sup>+</sup>) (Scheme 3.3, Mechanism III).

The subsequent chain propagation occurs by ring-opening addition of Bu-NCAs with the carbamate species followed by decarboxylation of the mixed anhydride intermediate (Scheme 3.4). Early studies of small molecular compounds revealed that the mixed anhydride linkages are kinetically labile, readily yielding amide linkages accompanied by CO<sub>2</sub> liberation.<sup>95, 313-314</sup>

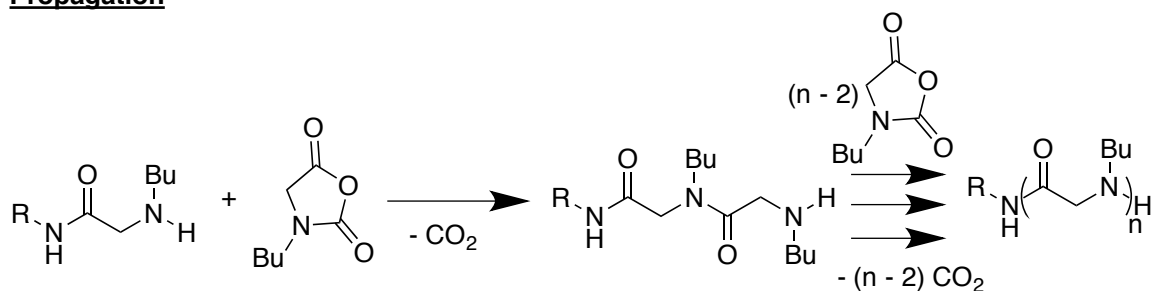
We have shown that TMG alone can initiate the polymerization of Bu-NCAs to produce the PNBGs bearing the neutral TMG end-groups (*vide supra*). Addition of an excess of benzyl alcohol to the PNBGs bearing the neutral TMG end-group failed to produce any PNBGs bearing benzyl ester end-groups, verified by the MALDI-TOF MS analysis. This result suggests that benzyl alcohol was not able to substitute the neutral TMG moiety on the TMG *N*-butyl glycine amide to initiate the polymerization of Bu-NCA (Mechanism II, Scheme 3.3). We also conducted a 1:1 reaction of TMG and Bu-NCA as well as a 1:1:1 reaction of TMG, Bu-NCA and BnOH in 50 °C, THF. The ESI-MS and <sup>1</sup>H NMR analysis of the former reaction product revealed the formation of *N*-butyl glycine cyclic dimer (i.e., diketopiperazine), *N,N*-dimethyl *N*-butyl glycine, *N*-butyl glycine derived hydroimidazolone, and TMG (Figure 3.9 and 3.10). The latter reaction also produced benzyl *N*-butyl glycine ester (Figure 3.11 and 3.12), the proposed initiating species (Mechanism II, Scheme 3.3), in addition to the four identical compounds that were also observed in the 1:1 reaction of TMG and Bu-NCA in THF. These results are consistent with the formation of a zwitterionic intermediate (Mechanism II, Scheme 3.3), which may react with alcohols to yield the initiating species (Scheme 3.5). As a result, Mechanism II is a possible mode of initiation for the alcohol-initiated polymerization of Bu-NCA in the presence of TMG.

Scheme 3.2. The mechanism of the primary amine-initiated ROP of Bu-NCA.

### Initiation



### Propagation



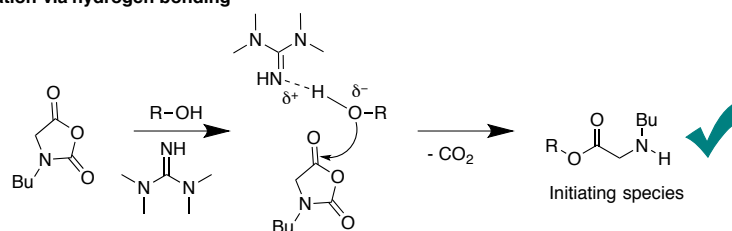
To investigate whether TMG can activate the alcohols and thus promote the initiation through hydrogen bonding interactions or deprotonation (Mechanism I and II, Scheme 3.3),  $^1\text{H}$  NMR spectra were collected for equimolar mixtures of various alcohols and TMG at 27 °C in THF- $d_8$ .  $^1\text{H}$  NMR analysis of an equimolar mixture of TMG and BnOH revealed that the disappearance of the hydroxyl proton of BnOH at 4.13 ppm and the imine proton of TMG at 5.38 ppm and the appearance of a new broad peak at 5.45 ppm that is integrated to two protons (Figure 3.14). The new peak is indicative of the formation of a TMG-BnOH complex by hydrogen bonding which has been previously shown to mediate the Baylis-Hillman reaction.<sup>315</sup> The broadness of the new peaks is indicative of the dynamic exchange of the two protons in the hydrogen bonding complexes. The TMG-BnOH complex formed by hydrogen bonding is also suggested to be present during polymerization as formation of the complex was observed via  $^1\text{H}$  NMR at 50 °C (Figure 3.15) This observation is in contrast to a complete proton transfer to TMG that would result in the formation of a guanidinium species exhibiting a more

significant downfield chemical shift at 8.76 ppm (Figure B5) for the iminium protons, as demonstrated in the 1:1 equimolar reaction between TMG and benzoic acid that is

Scheme 3.3. Three proposed initiation mechanisms of the TMG-promoted ROP of Bu-NCA using alcohol initiators.

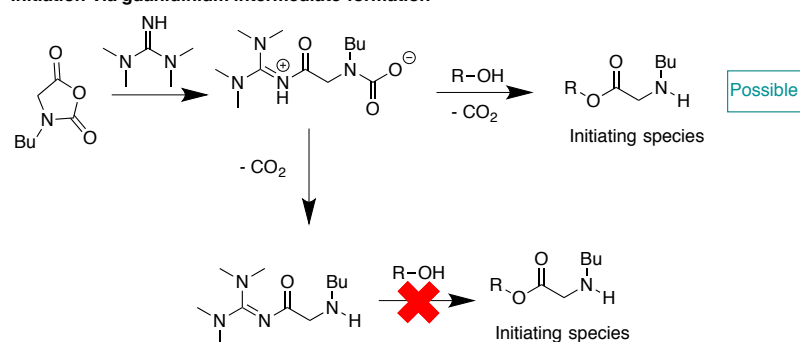
**Mechanism I**

Initiation via hydrogen bonding



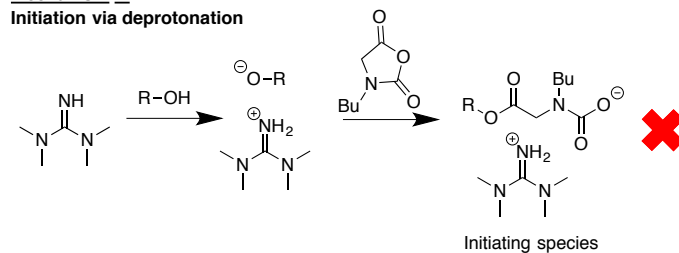
**Mechanism II**

Initiation via guanidinium intermediate formation



**Mechanism III**

Initiation via deprotonation

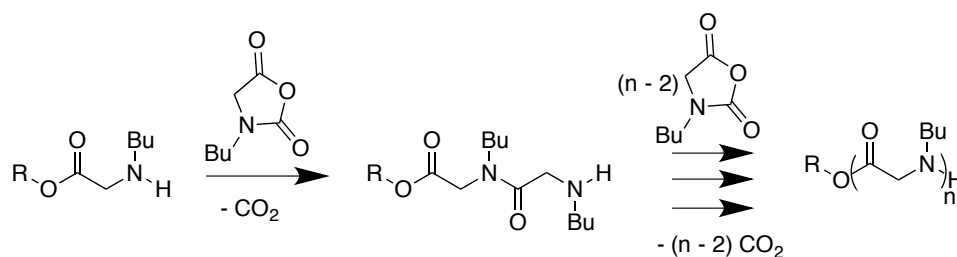


significantly more acidic than alcohols (Table 3.8).  $^1\text{H}$  NMR analyses of equimolar mixtures of TMG and methanol, ethanol, 2-methoxyethanol, 2,2,2-trifluoroethanol, and *n*-propanol also revealed the hydrogen bonding interaction between the TMG and the respective alcohol (Figures B6-10, Table 3.8), evidenced by the appearance of a new broad peak in the 4.56 - 5.78 ppm range in their respective  $^1\text{H}$  NMR spectra. By contrast,  $^1\text{H}$  NMR analysis of the equimolar reaction mixture between isopropyl alcohol (or *tert*-

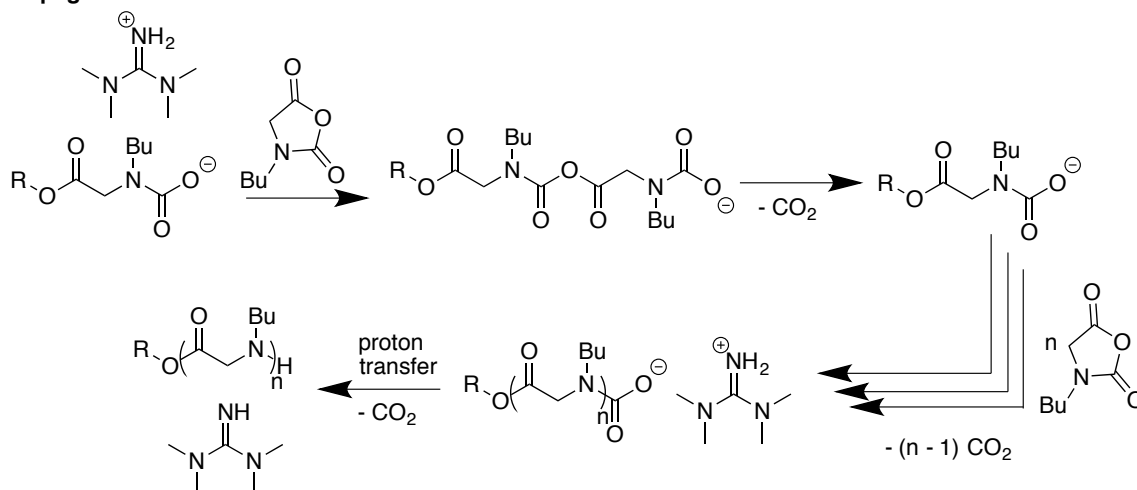
butyl alcohol) and TMG revealed the presence of two separate and distinct peaks (Figures B11 and B12) where each peak was integrated to one proton. These two peaks are

Scheme 3.4. Proposed propagation pathways following different initiating mechanisms shown in Scheme 3.3

**Propagation from Mechanisms I and II**



**Propagation from Mechanism III**



somewhat broadened but minimally shifted relative to the hydroxyl proton peak of the alcohol or imine proton peak of the TMG on their own in the  $^1H$  NMR spectra. This clearly indicates the presence of interactions between these alcohols and TMG through hydrogen bonding. However, the structures of the hydrogen bonding complexes of the secondary or tertiary alcohols with TMG are significantly different from those of primary alcohols with TMG. For primary alcohols that do not have strong electron withdrawing substituents (EWS), the hydrogen bonding interactions between the alcohols and TMG promote the initiation by enhancing the nucleophilicity of the alcohols towards the ring-

opening addition to the Bu-NCAs. For primary alcohols (e.g., 2,2,2-trifluoroethanol) that bear strong EWS, the initiation by the hydrogen bonding complex is inefficient due

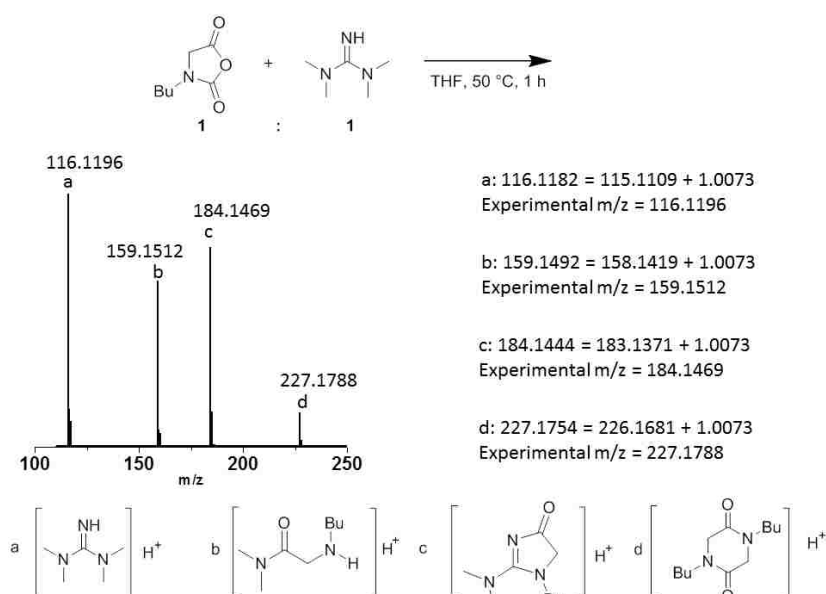


Figure 3.9. ESI-MS spectrum of the reaction product from the 1:1 (molar ratio) reaction of Bu-NCA and TMG in 50 °C THF. The spectrum was obtained in positive ionization mode.

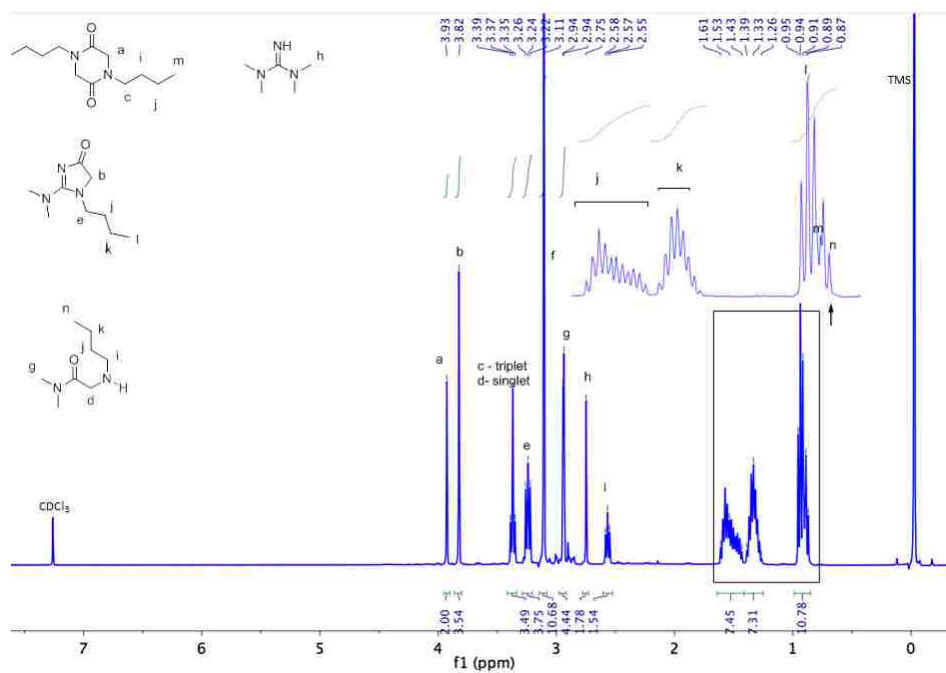


Figure 3.10. <sup>1</sup>H NMR spectrum of the reaction product from the 1:1 (molar ratio) reaction of Bu-NCA and TMG in 50 °C THF. The spectrum was collected in CDCl<sub>3</sub> solvent.

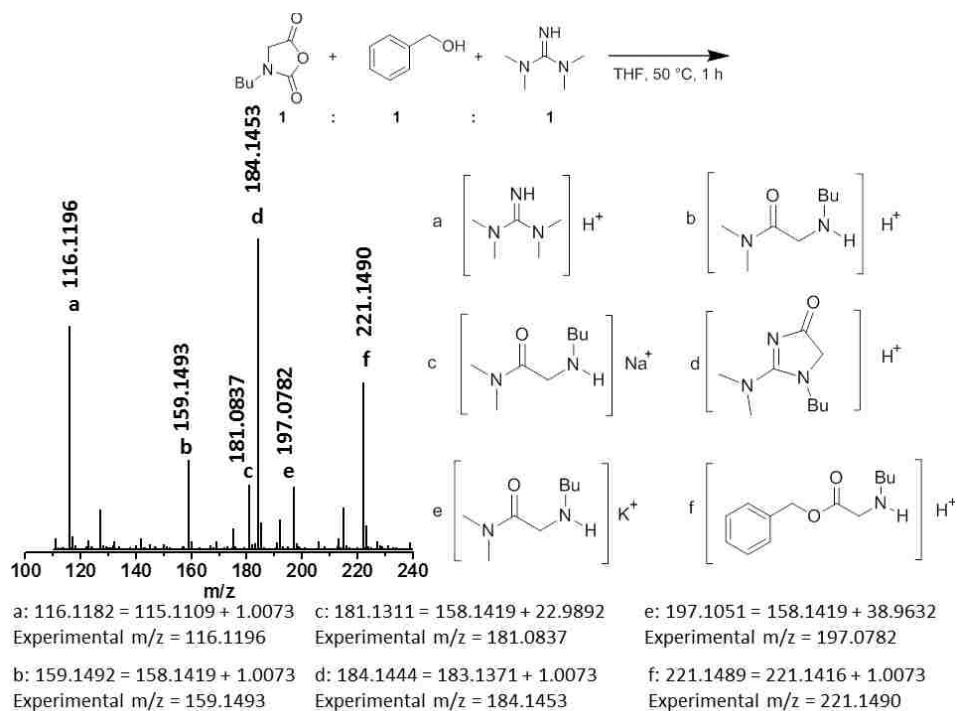


Figure 3.11. ESI-MS spectrum of the reaction product from the 1:1:1 (molar ratio) reaction of Bu-NCA, TMG and BnOH in 50 °C THF. The spectrum was obtained in positive ionization mode.

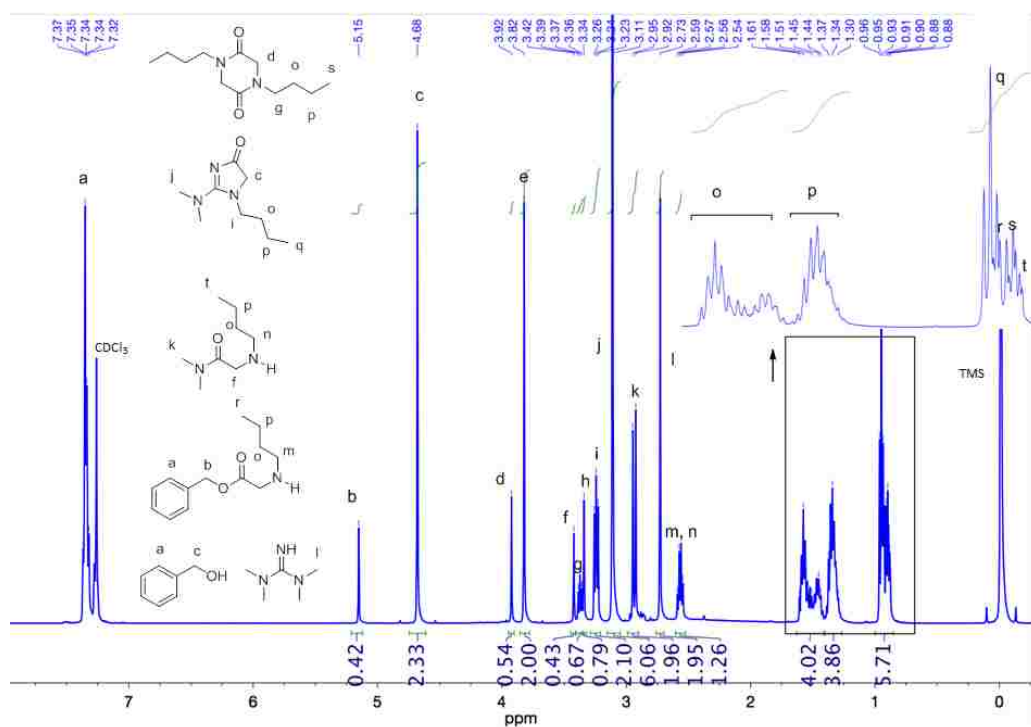
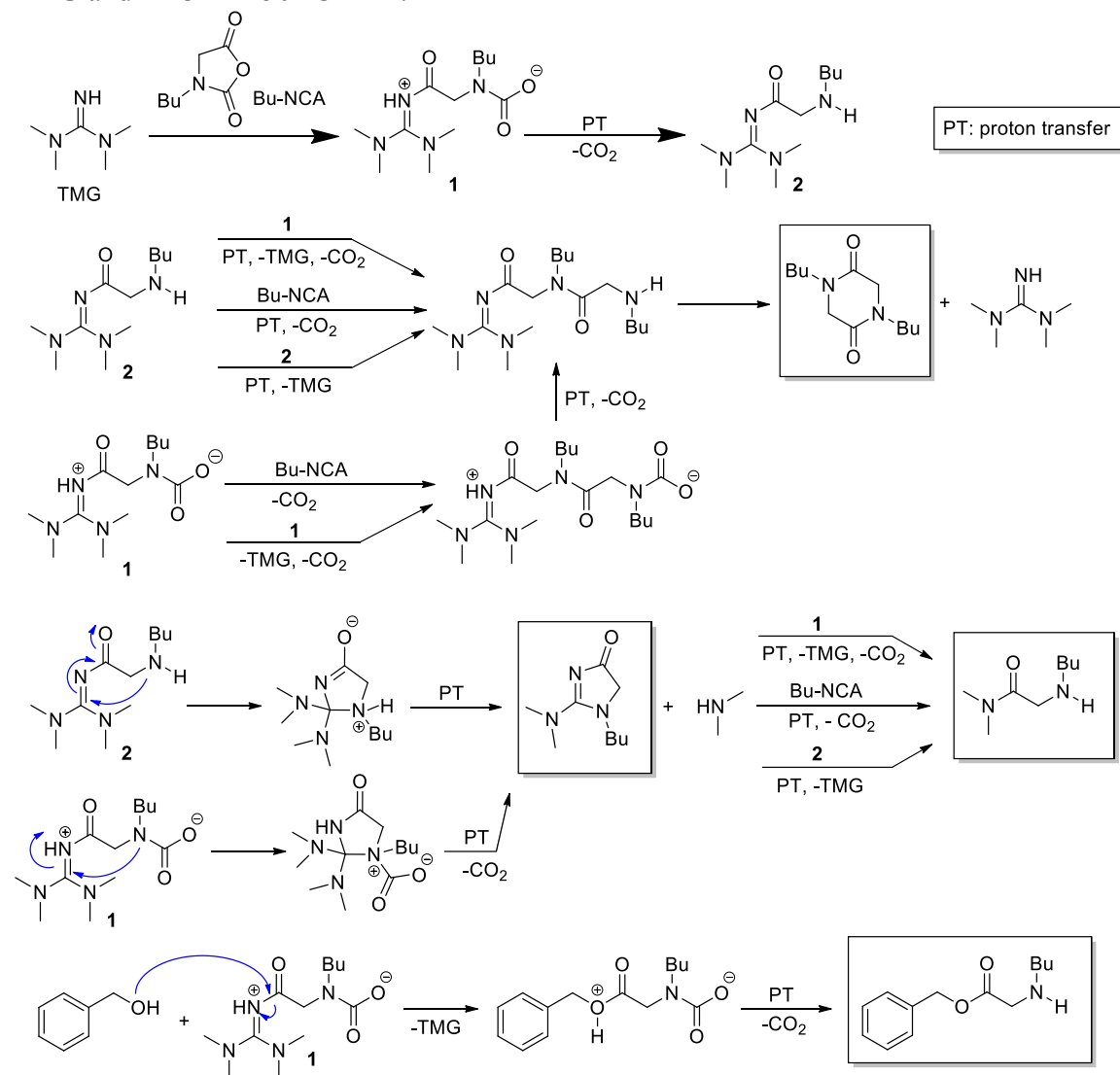


Figure 3.12.  $^1\text{H}$  NMR spectrum of the reaction product from the 1:1:1 (molar ratio) reaction of Bu-NCA, TMG and BnOH in 50 °C THF. The spectrum was collected in  $\text{CDCl}_3$  solvent.

Scheme 3.5. Proposed reaction pathways for the formation of the reaction products from the 1:1 (molar ratio) reaction of Bu-NCA and TMG or the 1:1:1 reaction of Bu-NCA, TMG and BnOH in 50 °C THF.



to the significantly reduced nucleophilicity of the alcohol moiety in the complex. The complexes involving secondary or tertiary alcohols (e.g., isopropyl alcohol or *tert*-butyl alcohol) have increasing steric hindrance, resulting in either inefficient initiation or failure to initiate the polymerization.



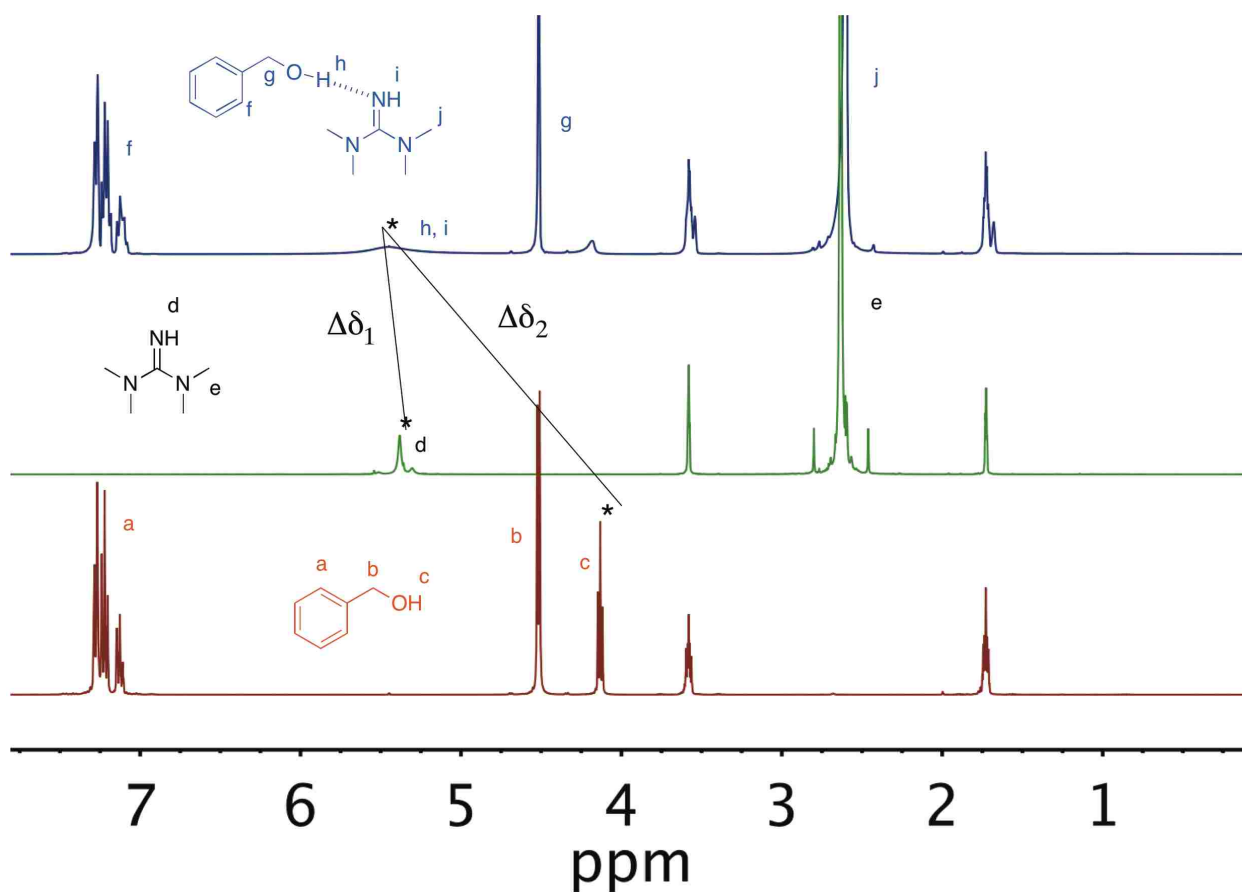


Figure 3.13. Overlaid <sup>1</sup>H NMR spectra of benzyl alcohol (red), TMG (green), and an equimolar mixture of benzyl alcohol and TMG (blue) in THF-d<sub>8</sub>. The spectra were collected at 0.5 M concentration for the respective compounds.

In contrast to alcohol-TMG complexes, <sup>1</sup>H NMR analysis of the equimolar mixture of TMG and phenol showed a large downfield chemical shift of the imine protons to 7.34 ppm (Figure B13), consistent with the formation of guanidinium species by proton transfer rather than a hydrogen bonding complex. This is attributed to the much higher acidity of phenol relative to other aliphatic alcohols (Table 3.8). The higher acidity of BnSH (pK<sub>a</sub>=15.3 in DMSO) also likely contributed to the absence of polymerization. The resulting phenoxide having a TMG-H<sup>+</sup> counter-ion does not effectively initiate the polymerization of Bu-NCA presumably due to steric hindrance imposed by the tightly associated TMG-H<sup>+</sup>

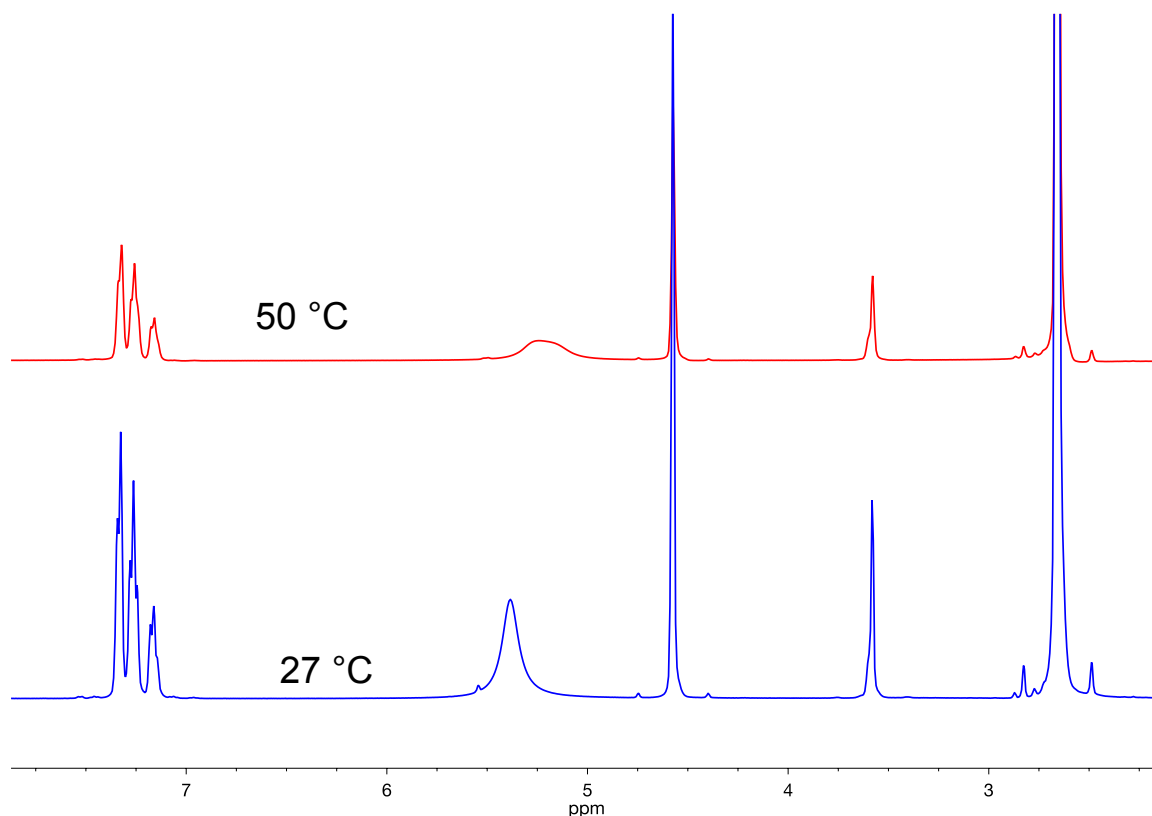


Figure 3.14. Overlaid  $^1\text{H}$  NMR spectra of the 1:1 mixture of benzyl alcohol and TMG at 27 °C (blue) and 50 °C (red) in  $\text{THF-d}_8$ . The spectra were collected at 0.5 M concentration.

counter-ions in the low polarity solvents. In contrast, sodium phenoxide has the potential to initiate polymerization of Bu-NCA (Table 3.9) suggesting that the choice of counter-ion does matter. It is possible that the  $\text{TMG-H}^+$  counter-ion versus that of sodium is better solvated in THF, leading to a tighter association with the oxygen anion which leads to the observed significantly reduced polymerization activity.

The formation of hydrogen bonding complexes between alcohols and TMG appears to be the most likely mode of initiation for the polymerization of Bu-NCA (Scheme 3.3, Mechanism I), although the initiation via the zwitterionic intermediate remains a possibility (Mechanism II, Scheme 3.3). Regarding the chain propagation, kinetic studies have shown that TMG has negligible effect on the observed rate of propagation in the alcohol-initiated polymerization of Bu-NCA (*vide supra*). This is consistent with the

proposed propagating species bearing secondary amino end-groups (Scheme 3.4), which is unlikely to be activated by TMG via hydrogen bonding in view of the high pKa of secondary amines (pKa ~44 in DMSO).<sup>316</sup>

Table 3.9. Polymerization of Bu-NCA by sodium phenoxide <sup>a</sup>

[M] <sub>0</sub> :[PhONa] <sub>0</sub>	M <sub>n</sub> (theo.) (kg·mol <sup>-1</sup> ) <sup>b</sup>	M <sub>n</sub> (SEC) (kg·mol <sup>-1</sup> ) <sup>c</sup>	PDI	DP	M <sub>n</sub> (NMR) (kg·mol <sup>-1</sup> ) <sup>d</sup>	DP (NMR)
25	2.8	4.1	1.06	36	1.9	17
50	5.6	6.9	1.14	61	4.4	44
100	11.3	13.5	1.26	119	8.1	72
200	22.6	18.3	1.26	162	- <sup>e</sup>	- <sup>e</sup>
400	45.2	24.6	1.07	218	- <sup>e</sup>	- <sup>e</sup>

<sup>a</sup>All polymerizations were conducted at [M]<sub>0</sub>=1.0 M in 50 °C THF for 24 h. <sup>b</sup> theoretical polymer molecular weights were determined by [M]<sub>0</sub>:[PhONa]<sub>0</sub> and conversion determined by FTIR; <sup>c</sup> polymer molecular weight and the molecular weight distribution are determined by the SEC-MALS-DRI method using dn/dc = 0.0815 ± 0.0012 mL·g<sup>-1</sup> for the PNBG polymer;<sup>147</sup> <sup>d</sup> polymer molecular weights are determined by end group analysis using <sup>1</sup>H NMR spectroscopy; <sup>e</sup> end group protons cannot be unambiguously distinguished in the respective <sup>1</sup>H NMR spectra.

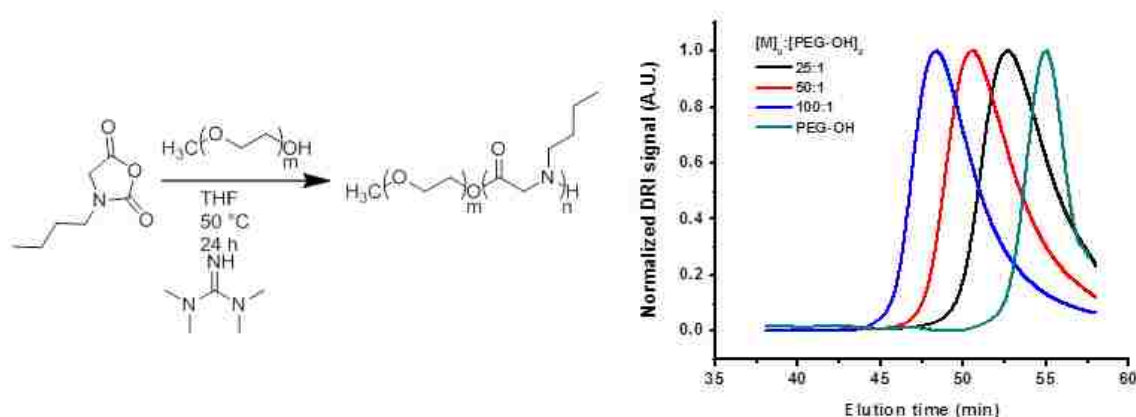


Figure 3.15. Reaction scheme of TMG-promoted ROP of Bu-NCA using a PEG-OH ( $M_n = 550 \text{ g}\cdot\text{mol}^{-1}$ ) macroinitiator and SEC chromatograms of the PEG-OH precursor and the PEG-*b*-PNBG hetero-block copolymers obtained from the reaction ( $[M]_0:[\text{PEG-OH}]_0=25:1-100:1$ ).

### 3.3.7 Macroinitiation of Bu-NCA using poly(ethylene glycol) monomethyl ether

The nature of the alcohols clearly affects the initiation efficiency and hence the controlled polymerization of Bu-NCAs. To assess the potential use of the TMG-promoted ROPs of Bu-NCAs towards the synthesis of hetero-block copolymers containing polypeptoid segments, we investigated the polymerization of Bu-NCA using a hydroxyl-terminated poly(ethylene glycol) macroinitiator (PEG-OH). Low molecular weight poly(ethylene glycol) methyl ether ( $M_n = 550 \text{ g}\cdot\text{mol}^{-1}$ , PDI=1.04) was used in the TMG-promoted polymerization of Bu-NCA under the standard conditions as for the reactions using small alcohol initiators (Figure 3.15). The reaction reached high conversion in 24 h, evidenced by FTIR spectroscopic analysis of reaction aliquots. SEC analysis of the resulting polymers revealed mono-modal peaks with increasing polymer molecular weight as the  $[M]_0:[\text{PEG-OH}]_0$  ratio is increased (Figure 3.15). This confirms the formation of hetero-block copolymers consisting of polyether and polypeptoid segments (PEG-*b*-PNBG). The molecular weight distribution (PDI) is modest in the 1.12-1.22 range. MALDI-TOF MS analysis of a low molecular weight block copolymer product (Entry 1, Table 3.10) revealed the exclusive formation of PEG-*b*-PNBG block copolymers and the absence of any unreacted PEG macroinitiators (Figure 3.16). As a result, polymer molecular weights were also determined by integration of the methyl protons of PNBG segments (0.88 – 0.96 ppm) relative to the methylene protons of PEG segments (3.64 ppm) by  $^1\text{H}$  NMR spectroscopy (Figure 3.17). The  $M_n$ s of the resulting block copolymers are slightly higher than the theoretical prediction based on sole initiation by the hydroxyl-ended PEGs, suggesting initiation of Bu-NCAs is somewhat slower relative to propagation when the PEG-OH macroinitiator is used. In spite of the high molecular

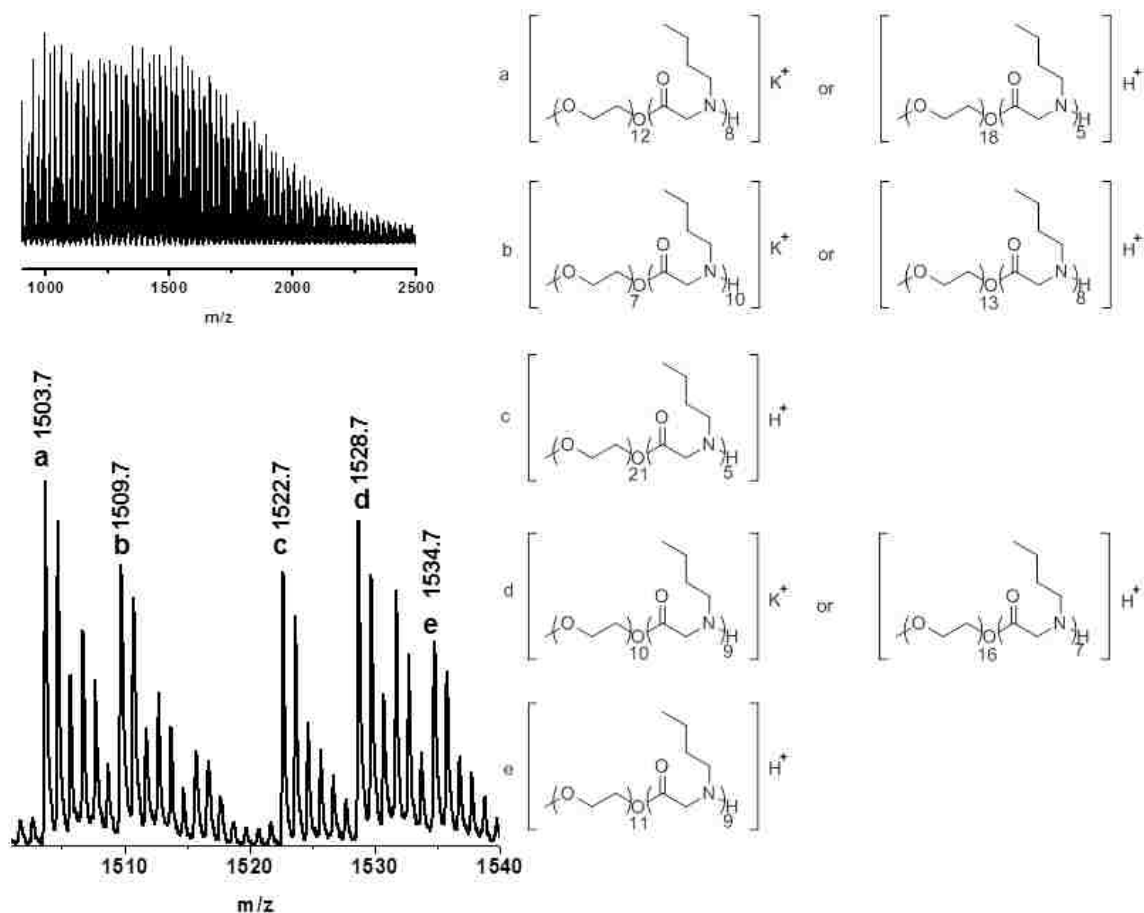


Figure 3.16. Representative MALDI-TOF MS spectra of the PEG-*b*-PNBG block copolymers obtained from the TMG-promoted ROP of Bu-NCAs using PEG ( $M_n = 550 \text{ g}\cdot\text{mol}^{-1}$ , PDI=1.04) macroinitiator ( $[M]_0:[\text{PEG-OH}]_0 = 25:1$ ,  $[M]_0 = 1.0 \text{ M}$ ,  $[\text{TMG}]_0 = 0.6 \text{ mM}$ ).

weight of the PEG-OH relative to isopropyl alcohol or *tert*-butyl alcohol, the hydroxyl termini on the PEG chains are not sterically restricted as in the case of the secondary and tertiary alcohols. As a result, the hydrogen bonding complex involving PEG-OH and TMG can initiate the chain growth by nucleophilic ring-opening addition of Bu-NCAs, in contrast to the isopropyl alcohol or *tert*-butyl alcohol-TMG complexes which are too sterically hindered to initiate the polymerization of Bu-NCA efficiently (Table 3.8).

### 3.4 Conclusions

We have demonstrated that 1,1,3,3-tetramethylguanidine (TMG) can effectively promote the controlled polymerization of Bu-NCA monomers when appropriate alcohols

Table 3.10. TMG-promoted polymerization of Bu-NCA using a hydroxyl-terminated PEG ( $M_n = 550 \text{ g}\cdot\text{mol}^{-1}$ , PDI=1.04) macroinitiator <sup>a</sup>

$[M]_0:[\text{PEG-OH}]_0$	$M_n$ (theo.) <sup>b</sup> ( $\text{kg}\cdot\text{mol}^{-1}$ )	$M_n$ (NMR) <sup>c</sup> ( $\text{kg}\cdot\text{mol}^{-1}$ )	$M_n$ (SEC) <sup>d</sup> ( $\text{kg}\cdot\text{mol}^{-1}$ )	PDI <sup>d</sup>	DP <sup>e</sup> (PNBG)	Conv. <sup>f</sup> (%)
25:1	3.7	4.3	6.6	1.22	32	100
50:1	6.3	8.5	11.3	1.12	69	100
100:1	11.0	14.2	17.2	1.14	120	91

<sup>a</sup> All polymerizations were conducted at 1.0 M in THF at 50 °C.  $[\text{TMG}]_0$  was held constant at 0.06 mol % relative to  $[M]_0$ . <sup>b</sup> Determined from the  $[M]_0:[\text{PEG-OH}]_0$  ratio and conversion. <sup>c</sup> Calculated by end group analysis using  $^1\text{H}$  NMR spectroscopy. <sup>d</sup> Determined by SEC-DRI method using polystyrene standards. <sup>e</sup> Number average degree of polymerization of the PNBG segments was calculated from  $M_n$ s determined by end-group analysis using  $^1\text{H}$  NMR spectroscopy. <sup>f</sup> Determined by FTIR analysis of a reaction aliquot after 24 h.

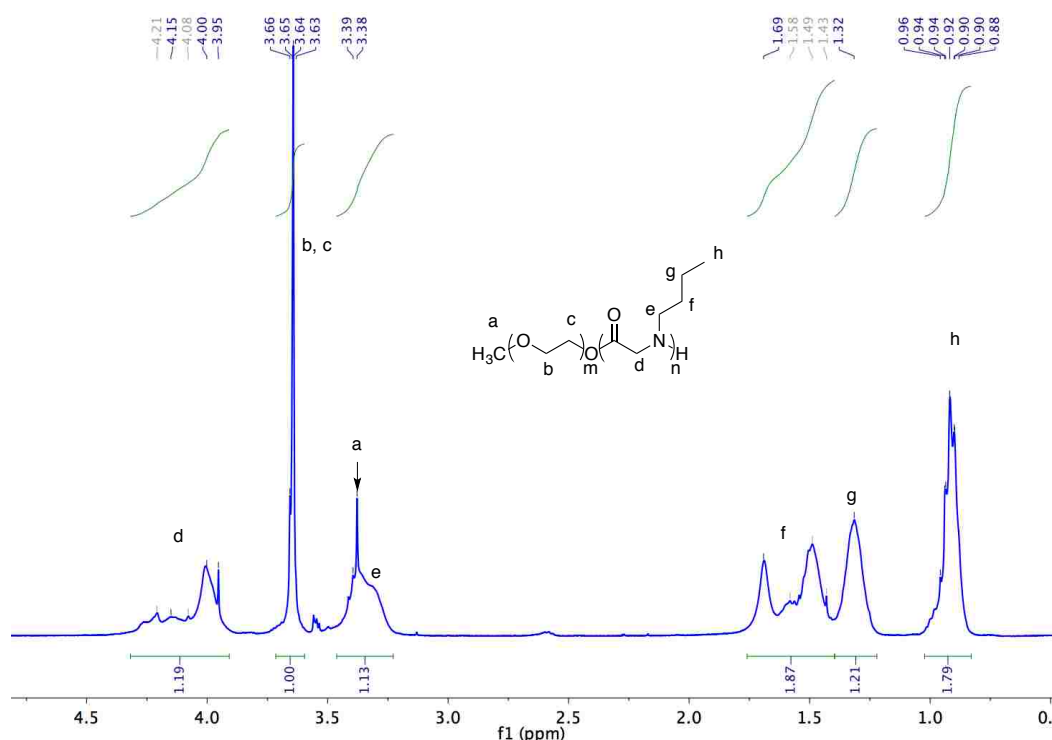


Figure 3.17. Representative  $^1\text{H}$  NMR spectrum of the PEG-*b*-PNBG block copolymers obtained from the TMG-promoted ROP of Bu-NCAs using PEG ( $M_n = 550 \text{ g}\cdot\text{mol}^{-1}$ , PDI=1.04) macroinitiator ( $[M]_0:[\text{PEG-OH}]_0 = 25:1$ ,  $[M]_0 = 1.0 \text{ M}$ ,  $[\text{TMG}]_0 = 0.6 \text{ mM}$ ).

(e.g., BnOH, MeOH, EtOH,  $\text{MeOCH}_2\text{CH}_2\text{OH}$ , *n*-PrOH) are used as initiators, in sharp contrast to no polymerization activity when TMG is absent. In these reactions, TMG interacts with the alcohols via hydrogen bonding interaction, resulting in enhanced nucleophilicity of the alcohols towards the ring-opening addition of the Bu-NCA

monomers and thereby initiation of the chain growth. The steric and electronic characteristics of the alcohols have been found to strongly influence the polymerization behavior. Hydrogen bonding complexes involving secondary or tertiary alcohols (e.g., isopropyl alcohol and *tert*-butyl alcohol) and TMG are too sterically hindered to efficiently initiate the polymerization. Primary alcohols (e.g., 2,2,2-trifluoroethanol) that are strongly electron deficient are also poor initiators in spite of the hydrogen bonding interaction with TMG. This resulted in either no polymerization activity or polymerization characteristics that are significantly deviated from those of controlled polymerizations. Furthermore, it was demonstrated that the TMG-promoted ROPs of Bu-NCA can be used to produce well-defined amphiphilic hetero-block copolymers consisting of hydrophilic PEG and hydrophobic PNBG blocks with tunable molecular weight and moderate molecular weight distribution by using hydroxyl-ended PEG macroinitiators. One distinct advantage of the method is that the activation of the alcohol initiators occurs under mild conditions via hydrogen bonding interaction with TMG. This can reduce many potential side reactions (e.g., substitution, elimination, epimerization) that may occur to monomers bearing functional side chains when activation of alcohol is rendered by deprotonation to form strongly nucleophilic and basic alkoxide species. It is a potentially convenient method to access hetero-block copolymers containing polypeptoid segment by using hydroxyl-terminated macro-initiators (e.g., polyether, polyester, or polyol).

### **3.5 Experimental**

#### 3.5.1 Instrumentation and general considerations

All chemicals were used as received unless otherwise noted. 1,1,3,3-tetramethylguanidine (TMG) and benzylamine were stirred over CaH<sub>2</sub> and alcohols over anhydrous MgSO<sub>4</sub> prior to being purified via vacuum distillation. Anhydrous deuterated

tetrahydrofuran (THF-d<sub>8</sub>) was obtained by stirring THF-d<sub>8</sub> (Sigma-Aldrich) over CaH<sub>2</sub> overnight followed by vacuum transfer. Benzylamine for kinetics experiments was purified similarly to THF. Anhydrous THF, dichloromethane, toluene, and *N,N*-dimethylformamide (DMF) for polymerizations were purified by passing through activated alumina columns under an argon atmosphere (Innovative Technology, Inc.). *N*-butyl *N*-carboxyanhydride (Bu-NCA) was synthesized from a previously reported method.<sup>147</sup> <sup>1</sup>H NMR spectra were recorded on a Bruker AV-400 and AVIII-400. Chemical shifts were determined in reference to the protio impurities of the deuterated solvents (CDCl<sub>3</sub>, CD<sub>2</sub>Cl<sub>2</sub>, or THF-d<sub>8</sub>) <sup>1</sup>H NMR spectra for kinetics experiments were also recorded on a Bruker AVIII-400. Size exclusion chromatography (SEC) analysis was carried out on an Agilent 1200 system (Agilent 1200 series degasser, isocratic pump, auto sampler, and column heater) equipped with three Phenomenex 5 μm, 300 Å×7.8 mm columns [100 Å, 1000 Å, and Linear (2)], Wyatt DAWN EOS multiangle light scattering (MALS) detector (GaAs 30 mW laser at λ) 690 nm], and Wyatt Optilab rEX differential refractive index (DRI) detector with a 690 nm light source. DMF containing 0.1 M LiBr was used as the eluent at a flow rate of 0.5 mL·min<sup>-1</sup>. The column and the MALS and DRI detector temperatures were all maintained at ambient temperature (21 °C). Data from SEC-MALS-DRI was processed using Wyatt Astra v 6.0 software. The MALDI-TOF MS experiments were carried out on a Bruker ultrafleXtreme tandem time-of-flight (TOF) mass spectrometer equipped with a smartbeam-II<sup>TM</sup> 1000 Hz laser (Bruker Daltonics, Billerica, MA). Prior to the measurement of each sample, the instrument was calibrated with Peptide Calibration Standard II consisting of a mixture of standard peptides Angiotensin I, Angiotensin II, Substance P, Bombesin, ACTH clip 1-17, ACTH clip 18-39, and Somatotatin 28 (Bruker Daltonics, Billerica, MA). Samples were measured in positive reflector mode. A saturated α-cyano-4-hydroxycinnamic acid (CHCA) in



methanol was used as the matrix in all measurements. Polymer samples were dissolved in THF at 10 mg/mL. The matrix and polymer samples were combined (v/v, 50/50) and vortexed. Samples (1  $\mu$ L) were deposited onto a 384-well ground-steel sample plate using the dry droplet method. Data analysis was conducted with flexAnalysis software. Electrospray ionization mass spectroscopy (ESI MS) was carried out on an ESI TOF 6210 (Electrospray Time-of-Flight) mass spectrometer (Agilent Technologies). The capillary voltage was 4200 V, drying gas (nitrogen) temperature was 325 °C delivered at 8 L/min. The fragmentor voltage was set to 150 V. Samples were prepared by dissolving ~10 mg of the sample in 200  $\mu$ L of THF. 20  $\mu$ L of the THF solution was then added to 200  $\mu$ L of acetonitrile solution containing 0.1% formic acid as the proton source. All samples were run in positive mode ionization.

### 3.5.2 Synthesis of *N*-butyl *N*-carboxyanhydride

Synthesis of *N*-butyl glycine hydrochloride. Glyoxylic acid monohydrate (25.12 g, 273 mmol) was suspended in 400 mL of dichloromethane and butylamine (13.5 mL, 136 mmol) was added. The reaction was stirred at ambient temperature for 24 h. Dichloromethane was removed via rotary evaporation and 1 N HCl (400 mL) was added to the residue and heated at reflux (85 °C) for 5 h. HCl was removed via rotary evaporation leaving a crude brown solid which was dissolved in minimal methanol and recrystallized from excess diethyl ether. The product was afforded as off-white crystals. (15.05 g, 66 %)

Synthesis of *N*-Boc *N*-butyl glycine. A round bottom flask was charged with *N*-butyl glycine hydrochloride (15.05 g, 89.8 mmol) and Boc anhydride (45.4 g, 224 mmol) and the contents were dissolved in 300 mL of distilled water. Triethylamine (63 mL, 449 mmol) was added and the reaction was stirred at ambient temperature for 24 h. The reaction solution was then extracted with hexanes (2  $\times$  200 mL). The aqueous layer was

saved and acidified with 4 N HCl. The acidified aqueous layer was further extracted with ethyl acetate ( $3 \times 200$  mL). The combined organic layers were dried over  $\text{MgSO}_4$ , filtered, and concentrated via rotary evaporation to yield the product as a clear liquid. (17.56 g, 85 %)

Synthesis of Bu-NCA. *N*-Boc *N*-butyl glycine (17.56 g, 75.9 mmol) was dissolved in dry dichloromethane (200 mL) and chilled on an ice bath. Phosphorus trichloride (8.3 mL, 94.9 mmol) was added dropwise over the course of 30 minutes to the dichloromethane solution. The ice bath was removed and the solution was allowed to warm up to ambient temperature and stirred for 2 hours. Dichloromethane was removed under vacuum leaving a crude white solid which was brought into the glovebox. The solid was extracted with dichloromethane, filtered, and stirred over NaH for 30 minutes. The solution was then refiltered and concentrated under vacuum to yield crude monomer as a white solid. Pure NCA was afforded via high vacuum sublimation at 50 °C, 120 mTorr. (2.71 g, 23 %)

### 3.5.3 General polymerization procedure

All polymerizations except for kinetics experiments were conducted in either THF, toluene, dichloromethane or DMF with initial monomer concentration  $[\text{M}]_0=1.0$  M at 50 °C for 24 h to reach high conversion. An aliquot of the reaction mixture was taken and analyzed by FTIR spectroscopy to determine the conversion. Polymers were precipitated into excess hexanes (or diethyl ether for reactions in DMF) and dried at room temperature under vacuum to yield the respective polymers as white solids. A representative polymerization procedure is as follows. In the glovebox, Bu-NCA monomer (88 mg, 0.56 mmol,  $[\text{M}]_0 = 1.0$  M) was weighed into an oven dried vial and dissolved in anhydrous THF (495  $\mu\text{L}$ ). A known volume of a benzyl alcohol/THF stock solution (59  $\mu\text{L}$ , 5.6  $\mu\text{mol}$ , 95 mM) was then added to the solution followed by a known volume of a 1,1,3,3-tetramethylguanidine stock solution (6  $\mu\text{L}$ , 0.33  $\mu\text{mol}$ , 54.5 mM) The reaction was

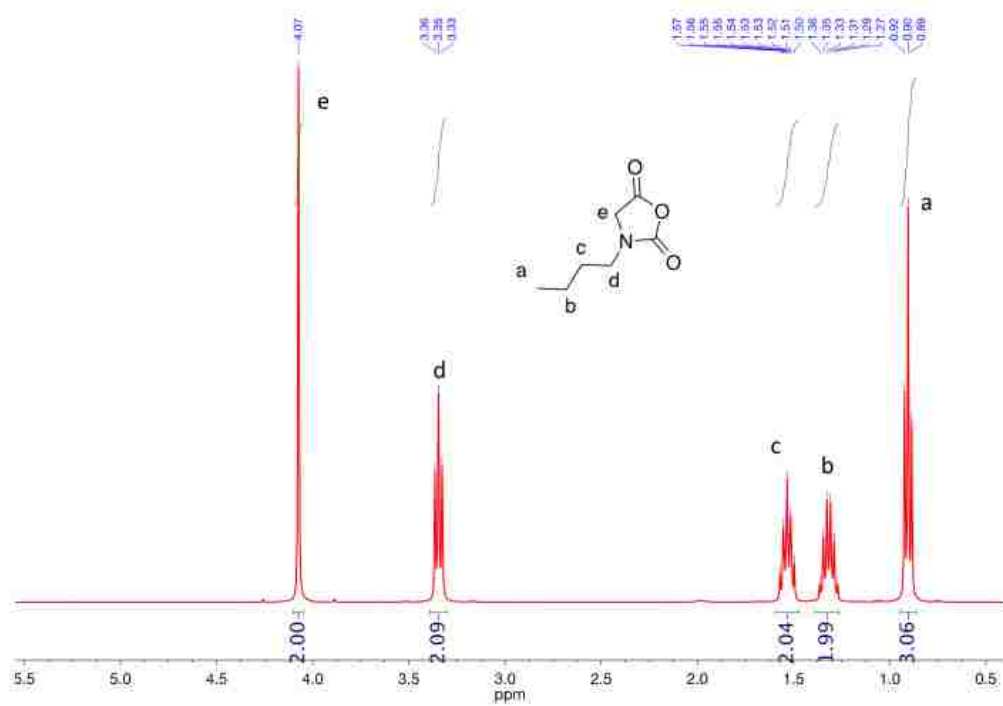


Figure 3.18.  $^1\text{H}$  NMR spectrum of Bu-NCA collected in  $\text{CDCl}_3$ .

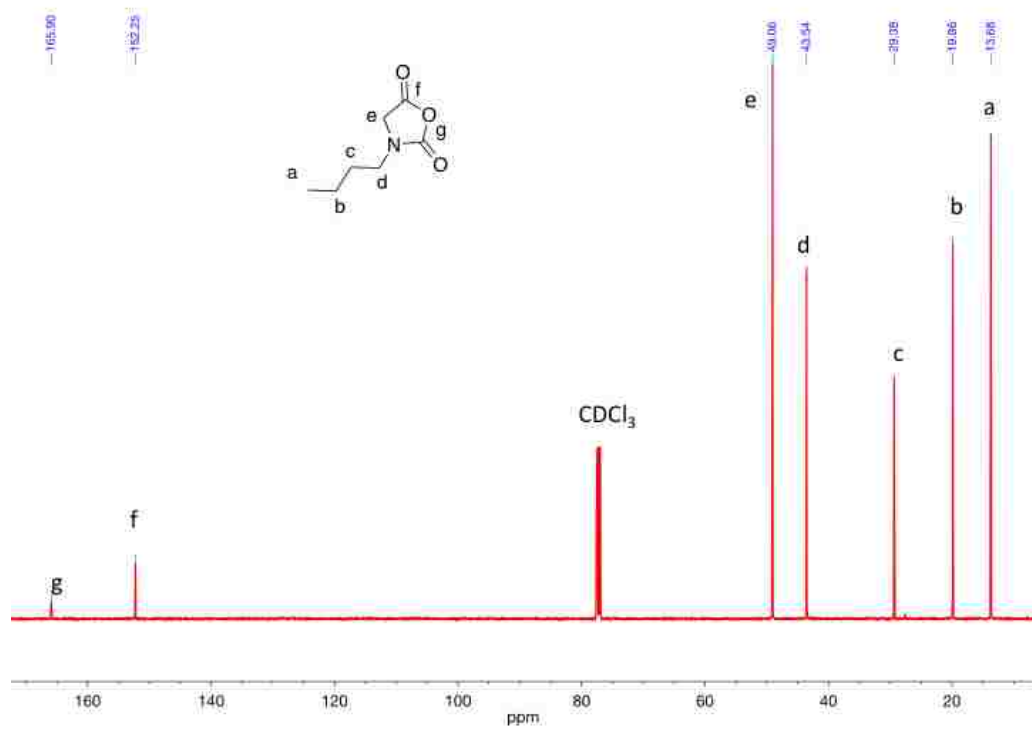


Figure 3.19.  $^{13}\text{C}\{^1\text{H}\}$  NMR spectrum of Bu-NCA collected in  $\text{CDCl}_3$ .

stirred for 24 h at 50°C under a nitrogen atmosphere and then quenched by the addition of excess hexanes. The white precipitate was isolated by careful removal of the supernatant and drying under vacuum.  $^1\text{H}$  NMR and  $^{13}\text{C}$  NMR data of high molecular weight poly(*N*-butyl glycine) (PNBG) have previously been reported.<sup>147</sup>

### 3.5.4 General kinetics procedure

A predetermined amount of BnOH (or BnNH<sub>2</sub>) and TMG stock solutions in toluene-d<sub>8</sub> (50 mM each) were added to a THF-d<sub>8</sub> solution of Bu-NCA (500 μL, 0.075 mmol, 150 mM) at room temperature. The contents were transferred into a resealable J. Young NMR tube.  $^1\text{H}$  NMR spectra were collected every 20 s at 50 °C over the course of four half-lives. Monomer conversion was calculated from the relative integration of the methylene proton resonance of the monomer and polymer respectively. In kinetic experiments involving TMGs, it was determined that by the time the first spectra were taken, approximately 5.9-13.8% of the monomer was converted into polymer. Kinetics experiments were repeated at least twice under identical conditions for each set of polymerization conditions.

### 3.6 Supplemental data for Chapter III

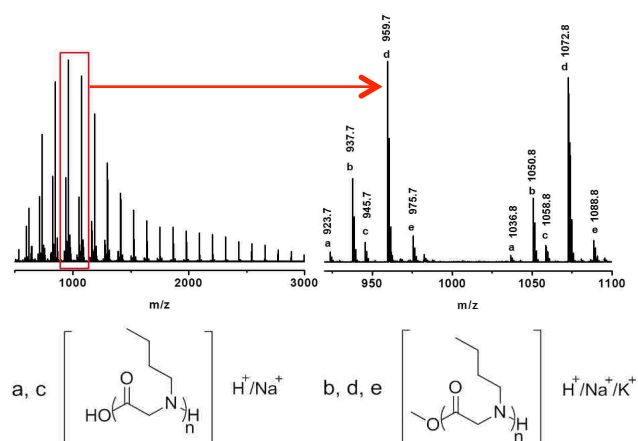


Figure B1. MALDI-TOF MS spectra of the PNBG polymers obtained via TMG-promoted ROP of Bu-NCA with methanol initiators ( $[\text{M}]_0:[\text{MeOH}]_0 = 25:1$ ,  $[\text{M}]_0 = 1.0 \text{ M}$ ,  $[\text{TMG}]_0 = 0.6 \text{ mM}$ ).

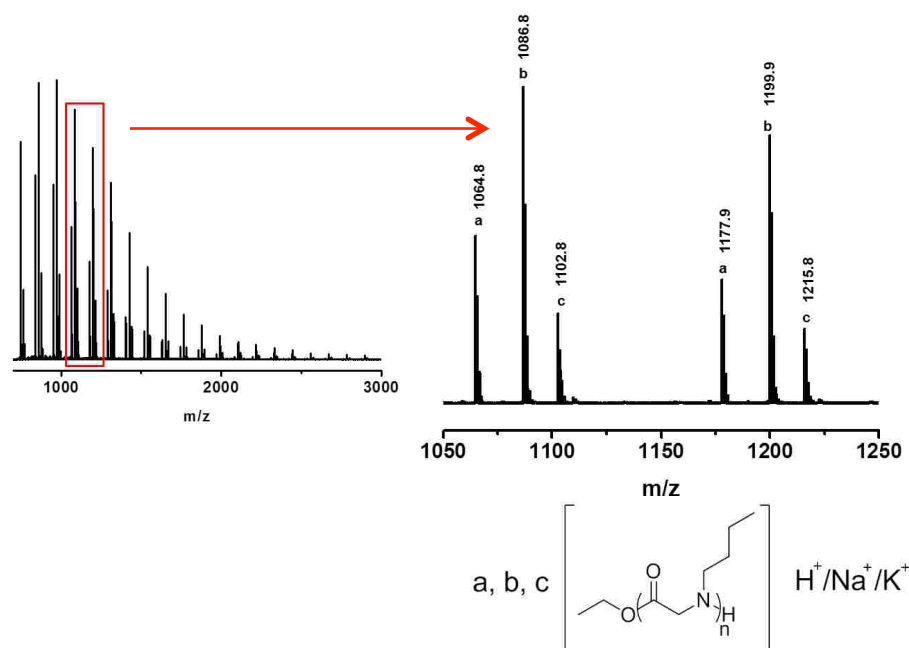


Figure B2. MALDI-TOF MS spectra of the PNBG polymers obtained by TMG-promoted ROP of Bu-NCAs using ethanol initiators ( $[M]_0:[EtOH]_0 = 25:1$ ,  $[M]_0 = 1.0$  M,  $[TMG]_0 = 0.6$  mM).

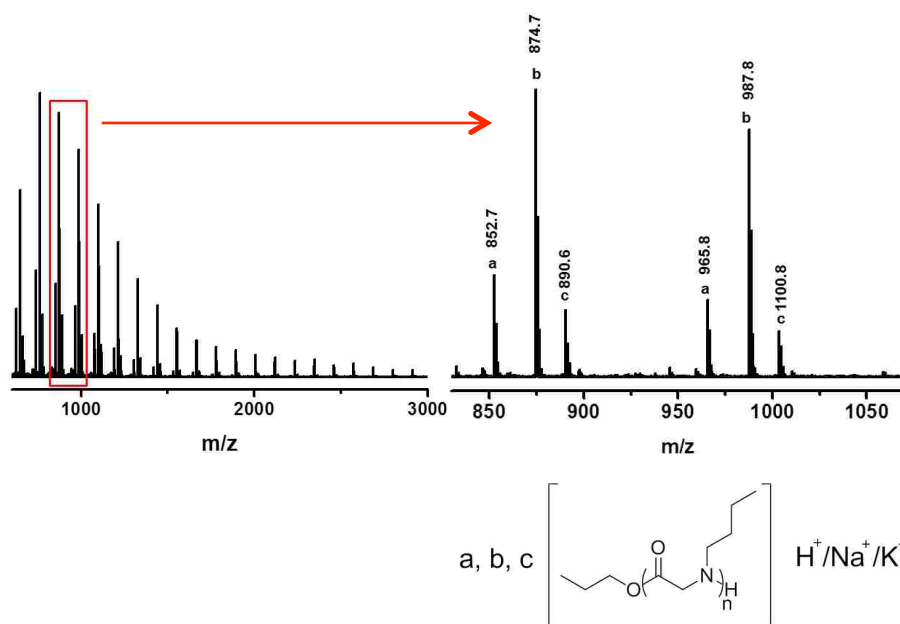


Figure B3. MALDI-TOF MS spectra of the PNBG polymers obtained by TMG-promoted ROP of Bu-NCAs using *n*-propanol initiators ( $[M]_0:[n\text{-PrOH}]_0 = 25:1$ ,  $[M]_0 = 1.0$  M,  $[TMG]_0 = 0.6$  mM).

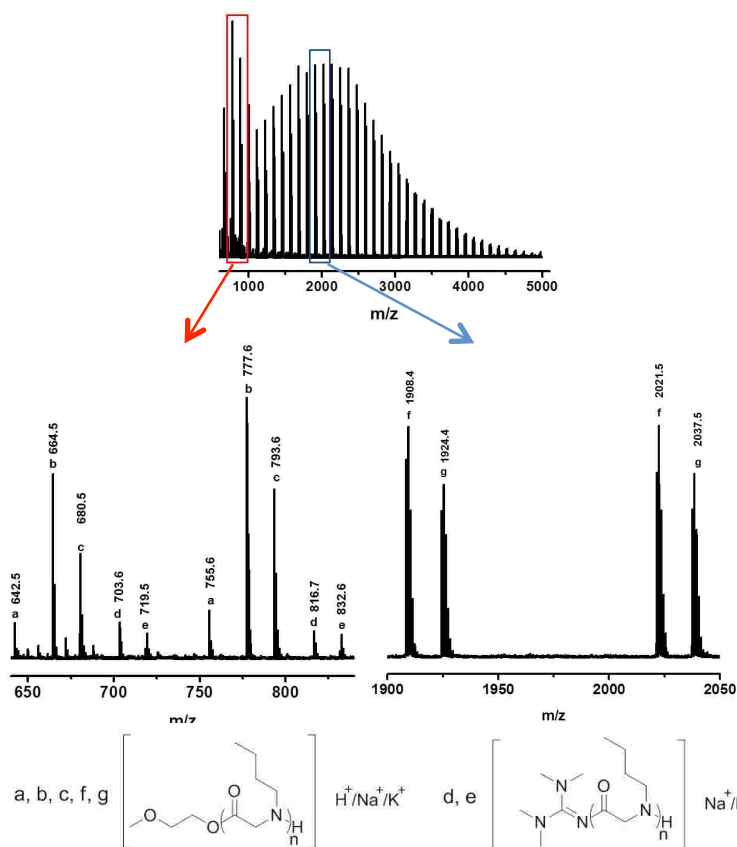


Figure B4. MALDI-TOF MS spectra of the PNBG polymers obtained by TMG-promoted ROP of Bu-NCAs using 2-methoxyethanol initiators ( $[\text{M}]_0:[2\text{-MeOEtOH}]_0 = 25:1$ ,  $[\text{M}]_0 = 1.0 \text{ M}$ ,  $[\text{TMG}]_0 = 0.6 \text{ mM}$ ). TMG-terminated polymeric species are present at low m/z.

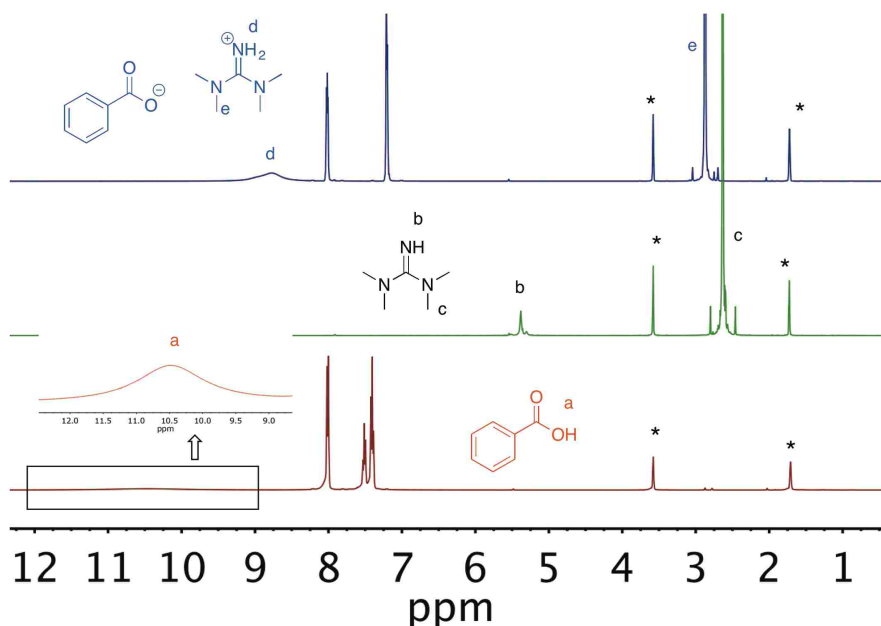


Figure B5. Overlaid  $^1\text{H}$  NMR spectra of TMG (red), TMG (green), and the 1:1 mixture of benzoic acid and TMG (blue). Spectra were collected in THF- $\text{d}_8$  at 0.5 M concentrations for the respective compounds. THF- $\text{d}_8$  is denoted by the asterisks (\*).

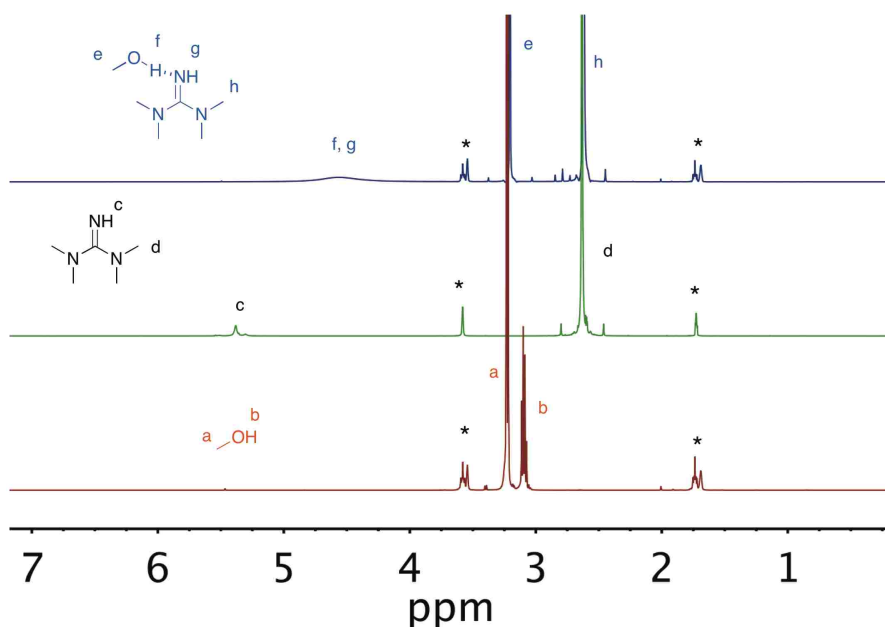


Figure B6. Overlaid <sup>1</sup>H NMR spectra of methanol (red), TMG (green), and the 1:1 mixture of both compounds (blue) in THF-d<sub>8</sub>. Spectra were collected at 0.5 M concentrations for the respective compounds. THF-d<sub>8</sub> is denoted by the asterisks (\*).

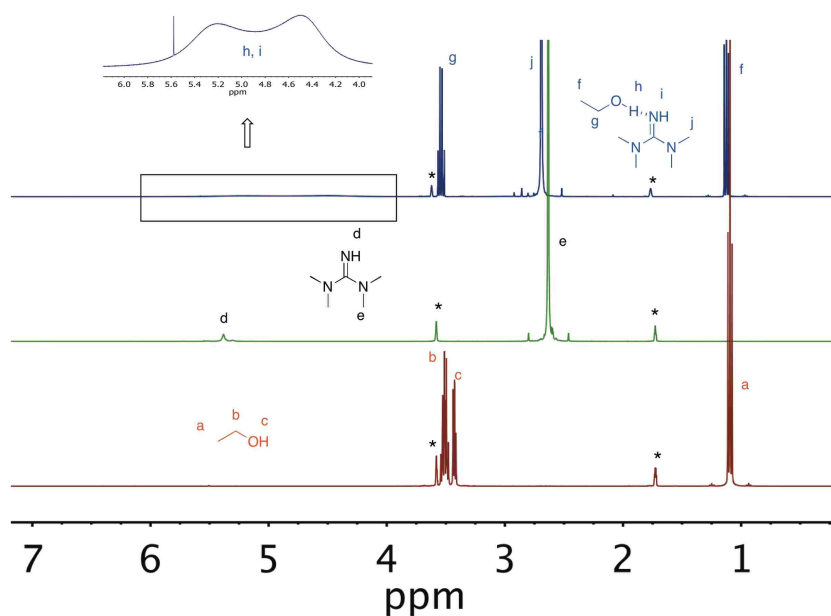


Figure B7. Overlaid <sup>1</sup>H NMR spectra of ethanol (red), TMG (green), and the 1:1 mixture of both compounds (blue) in THF-d<sub>8</sub>. Spectra were collected at 0.5 M concentrations for the respective compounds. THF-d<sub>8</sub> is denoted by the asterisks (\*).

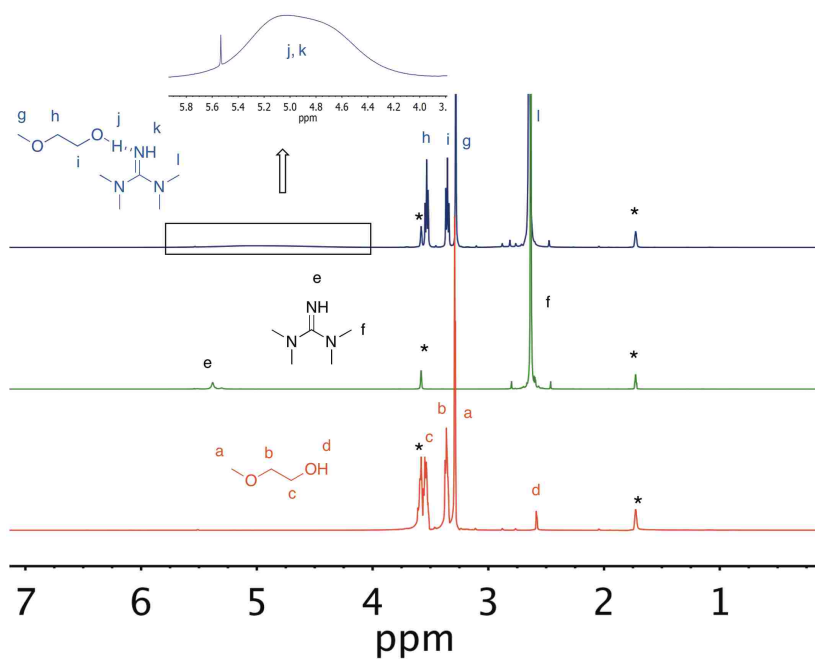


Figure B8. Overlaid  $^1\text{H}$  NMR spectra of 2-methoxyethanol (red), TMG (green), and the 1:1 mixture of both compounds (blue) in  $\text{THF-d}_8$ . Spectra were collected at 0.5 M concentrations for the respective compounds.  $\text{THF-d}_8$  is denoted by the asterisks (\*).

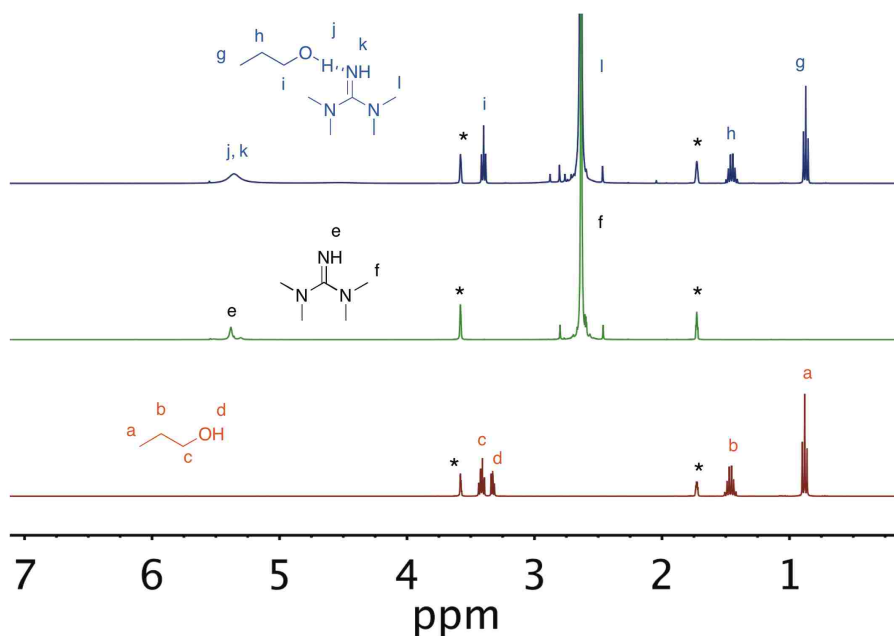


Figure B9. Overlaid  $^1\text{H}$  NMR spectra of *n*-propanol (red), TMG (green), and the 1:1 mixture of both compounds (blue) in  $\text{THF-d}_8$ . Spectra were collected at 0.5 M concentrations for the respective compounds.  $\text{THF-d}_8$  is denoted by the asterisks (\*).



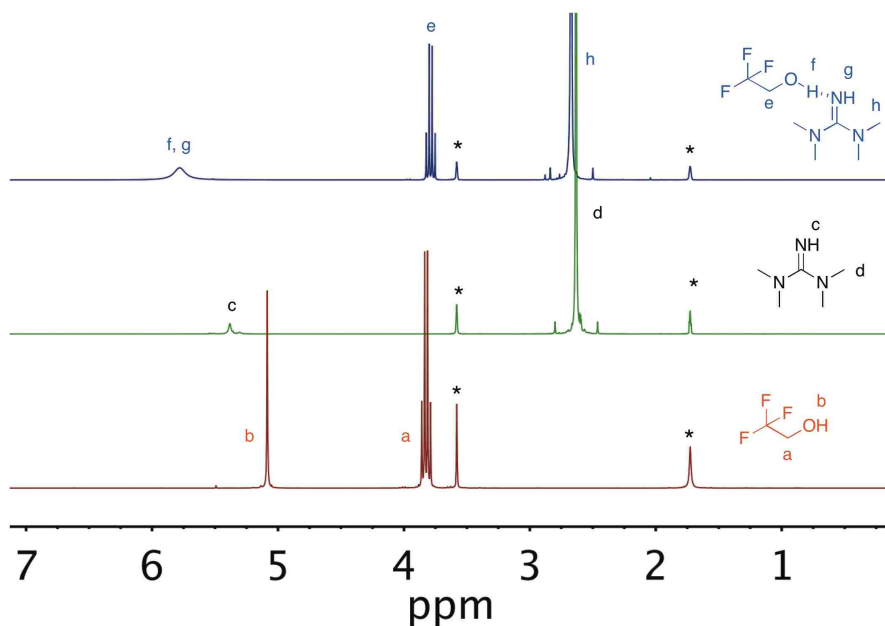


Figure B10. Overlaid <sup>1</sup>H NMR spectra of 2,2,2-trifluoroethanol (red), TMG (green), and the 1:1 mixture of both compounds (blue) in THF-d<sub>8</sub>. Spectra were collected at 0.5 M concentrations for the respective compounds. THF-d<sub>8</sub> is denoted by the asterisks (\*).

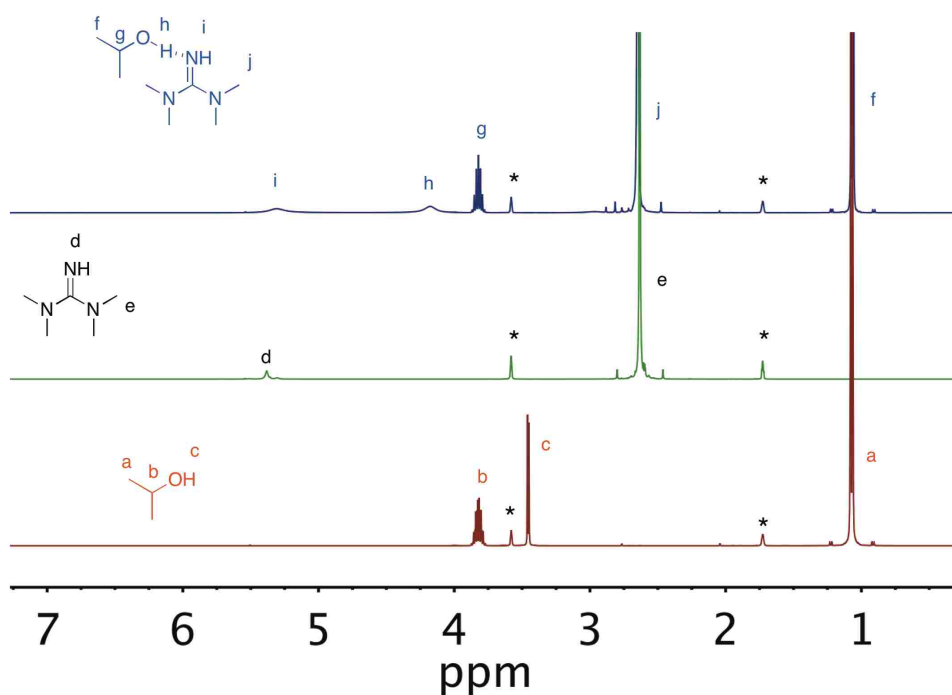


Figure B11. Overlaid <sup>1</sup>H NMR spectra of isopropyl alcohol (red), TMG (green), and the 1:1 mixture of both compounds (blue) in THF-d<sub>8</sub>. Spectra were collected at 0.5 M concentrations for the respective compounds. THF-d<sub>8</sub> is denoted by the asterisks (\*).

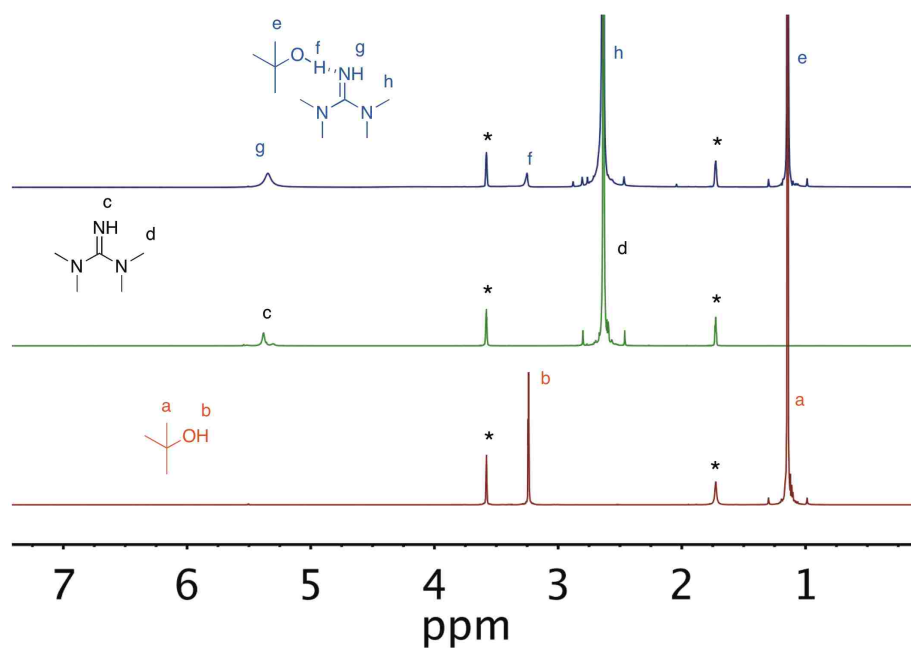


Figure B12. Overlaid <sup>1</sup>H NMR spectra of *tert*-butyl alcohol (red), TMG (green), and the 1:1 mixture of both compounds (blue) in THF-d<sub>8</sub>. Spectra were collected at 0.5 M concentrations for the respective compounds. THF-d<sub>8</sub> is denoted by the asterisks (\*).

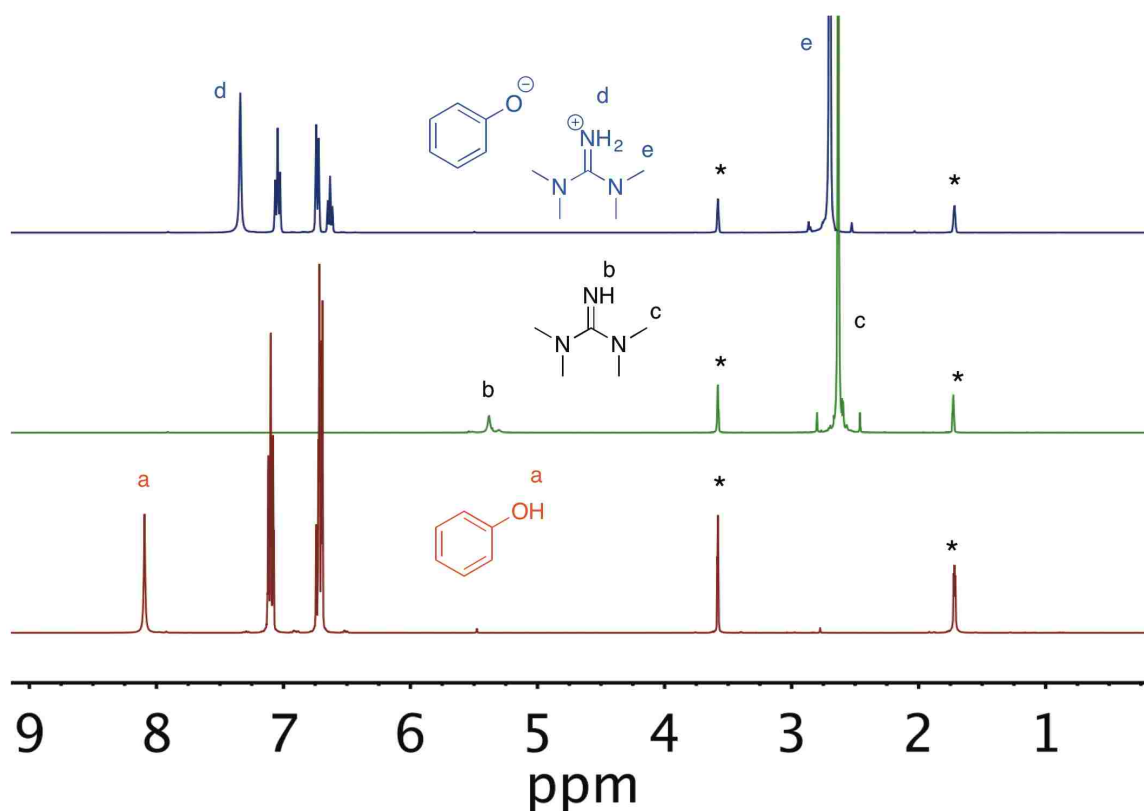


Figure B13. Overlaid <sup>1</sup>H NMR spectra of phenol (red), TMG (green), and the 1:1 mixture of both compounds (blue) in THF-d<sub>8</sub>. Spectra were collected at 0.5 M concentrations for the respective compounds. THF-d<sub>8</sub> is denoted by the asterisks (\*).

## CHAPTER IV. *N*-THIOCARBOXYANHYDROSULFIDES AS POTENTIAL ALTERNATIVES TO *N*-CARBOXYANHYDRIDE MONOMERS IN THE SYNTHESIS OF PEPTIDOMIMETIC POLYMERS

### 4.1 Objectives

The syntheses of amino acid and *N*-alkyl glycine based NCA monomers have been discussed in Chapter I and it was noted that extreme care needs to be taken in the final steps in carrying out the cyclization and purification of NCAs because the NCAs are sensitive to moisture, potentially leading to self-initiation; a moisture-free atmosphere is essential. Additionally, purification of NCAs has to be performed under moisture-free conditions using dry solvent column chromatography, distillation, or vacuum sublimation in order to reduce the risk of introducing moisture and other impurities. There has been increasing interest in developing more robust and operationally simpler methods to obtain well-defined systems of polypeptides and polypeptoids. One such avenue explored by Endo et al is the polymerization of urethane derivatives of amino acids, which generates the respective NCA monomers in situ.<sup>317</sup> While this avoids the synthesis of NCAs, the method did not allow for controlled polymerization and was limited to polypeptides whose  $DP_n$ s < 100. Doriti et al have improved the method reported by Endo et al and recently reported the synthesis of well-defined polysarcosines (up to  $20 \text{ kg}\cdot\text{mol}^{-1}$ ) from in situ generation of *N*-methyl glycine NCA from the polycondensation of *N*-phenoxy carbonyl sarcosine.<sup>318</sup> Another viable strategy is the synthesis of structurally similar monomers to NCAs that demonstrate improved stability towards moisture and impurities but possess similar reactivity to NCAs in the presence of an initiator. Kricheldorf reported the ROP of amino acid based *N*-thiocarboxyanhydrides, thioanhydride analogs to NCAs, but displayed some skepticism<sup>190, 319</sup> about the

robustness of their use in the polymerization of high molecular weight polypeptides; the reactions did not reach quantitative conversion and polymer molecular weights deviated from theory. We have explored the organo-mediated ROP of a number of *N*-substituted glycine NTAs. In contrast to Kricheldorf's findings, we have found that well-controlled systems of high molecular weight polysarcosine can be synthesized using conventional initiators that have previously been used in the ROP of R-NCAs. Additionally, we have synthesized a number of new amino acid based NTA monomers, namely those of  $\gamma$ -benzyl-L-glutamate and DL-methionine, the former of which is well-studied and known to be well-soluble in organic solvents. We have found that NTA monomers show potential to serve as viable alternatives to NCAs in the synthesis of well-controlled and well-defined polypeptides and polypeptoids.

#### **4.2 Background of *N*-thiocarboxyanhydrosulfides**

Synthesis of polypeptides and polypeptoids often involves the ring-opening polymerization (ROP) of the corresponding *N*-carboxyanhydride monomers (NCA) as these reactions proceed faster than solid phase methods and allow access to high molecular weight species. From these methods, polypeptides and polypeptoids with predictable molecular weights and adequate polydispersities could be obtained.

NCA monomers have been prepared under moisture-free conditions (under nitrogen atmosphere), using oven-dried glassware with dry solvents due to the fact that the anhydride group is easily susceptible to moisture. Successful controlled polymerizations also depend on obtaining NCA monomer of the utmost purity as the introduction of nucleophilic impurities (e.g. Cl<sup>-</sup>) can lead to self-initiation. Chapter I gave an overview of various purification methods for NCAs, which have ranged from recrystallization<sup>48, 51, 58</sup>, cold base wash<sup>53, 57-58</sup>, sublimation<sup>147</sup>, column chromatography<sup>42</sup>,

<sup>59-61</sup>, celite filtration<sup>62</sup>, and rephosgenation<sup>55</sup>, all of which can be tedious, and time consuming.

The general structure of *N*-thiocarboxyanhydrosulfides (NTA) only differs from NCAs in the anhydride functional group where a sulfur atom is substituted for oxygen (Figure 4.1). Originally, NTAs were used in the synthesis of small peptides and have been explored as potential monomers for use in stepwise methods.<sup>183-184</sup> NTAs have also seen application in textile development.<sup>189</sup> They are ideal alternatives to NCAs due to the fact that the thioanhydride has been observed to be less reactive towards nucleophiles than that of anhydrides, leading to increased stability under ambient conditions.<sup>48, 319</sup> The main drawback with NTA monomers is that the improved stability of NTAs leads to low polymerization activity. It has also been suggested that NTAs are less reactive than NCAs because of the increased delocalization of the sulfur atom electrons in NTAs compared with those of the oxygen atom in NCAs.<sup>48</sup>

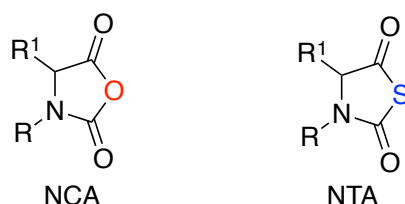


Figure 4.1. Generic chemical structures of NCA and NTA monomers.

The use of NTAs as monomers in polymerization reactions was first reported by Kricheldorf in 1974 where the ROPs of glycine-NTA and sarcosine-NTA were studied in parallel with the ROPs of their respective NCAs. These early studies showed that the obtained molecular weights from NTA polymerizations were significantly lower versus those of the polymerizations of their corresponding NCA monomers, suggesting the lack of adequate control over the polymerization.<sup>319-320</sup> Kricheldorf et al reinvestigated NTAs as potential alternatives to NCAs in 2008 where the polymerizations of sarcosine, DL-

phenylalanine, and DL-leucine NTAs were studied using hexylamine initiator.<sup>190</sup> It was observed that quantitative conversions in the polymerization reactions were never reached except in the case of the ROP of sarcosine-NTA when  $[M]_0:[I]_0 = 20:1$ . Likewise, the observed molecular weights for the polymers obtained from the ROPs of NTAs were much lower than expected, regardless of  $[M]_0:[I]_0$ . A positive outcome of this study however confirmed the formation of the amide end group via initiation with a primary amine and a reactive amine terminus via NAM as determined by MALDI TOF MS. Two reasons were hypothesized for the observed low conversions and low molecular weights. The first was due to the steric hindrance of the active chain end via hydrogen bonding based aggregation in polypeptides. It was suggested that the intramolecular hydrogen bonding of the formed oligopeptides during the ROP of DL-leucine and DL-phenylalanine NTAs contributes to a physical chain death due to the formation of  $\beta$ -sheet lamellae hindering access of the reactive amine terminus to successive NTAs via sterics. In the case of the ROP of sarcosine-NTA, the thiocarbonate intermediate was proposed to be stabilized via solvation with those of other polysarcosine chains, thus preventing additional propagation events. It was noted by Kricheldorf that NTAs appear to be poor candidates for the synthesis of polypeptides and polypeptoids<sup>190</sup> and that the ROP of NTAs was not a viable and reliable method to obtain high molecular weight polypeptide species.

On the contrary, interest in R-NTA monomers as alternatives to R-NCAs in the synthesis of polypeptoids has increased recently. Ling and coworkers synthesized two R-NTA monomers, *N*-methyl and *N*-butyl *N*-thiocarboxyanhydrosulfides (Me-NTA and Bu-NTA respectively) and developed two catalytic systems to obtain well-controlled molecular weight species of polysarcosine, and poly(*N*-butyl glycine) respectively.<sup>182, 191</sup> The first system uses primary amine mediated polymerization via NAM. It was noted in

the ROP of Me-NTA by NAM that high reaction temperatures (60 °C) and long reaction times (48 h) in a relatively poor solvent for polysarcosine, dioxane, are necessities for improved yields and molecular control.<sup>182</sup> Polysarcosine is insoluble in dioxane resulting in a heterogeneous polymerization system, which may ultimately affect polymerization kinetics. Other solvents which are good solvents for polysarcosine, namely DMF, *N*-methyl pyrrolidone, DMSO, and *N,N*-dimethylacetamide were all screened as potential polymerization solvents, but yielded uncontrollable polymerizations and low yields compared with those polysarcosines obtained from the ROP of the respective NCAs. This demonstrates the importance of solvent choice in the ROP of R-NTAs. The second catalytic system developed by Ling et al used rare earth borohydride initiators, which were previously explored as catalysts in the ROP of BLG-NCA.<sup>111</sup> Similarly, polymerization conditions required high temperatures (60 °C), and longer reaction times (48 h) in acetonitrile in order to reach quantitative conversions. Rare earth borohydride initiators also have to be synthesized unlike those of the commercially available primary amines.<sup>191</sup>

We studied the organo-mediated ROP of a series of *N*-alkyl glycine NTAs and show that one initiator, 1,1,3,3-tetramethylguanidine, can be used to obtain well-defined polysarcosines with predictable molecular weights and narrow PDI. Benzylamine was also demonstrated to be a viable initiator for the ROP of R-NTAs. Secondly, we expanded the scope of amino acid based NTA monomers which bear N-H proton. It was demonstrated that although notable challenges still remain in achieving solution phase polymerization of amino acid based NTAs in a controlled manner, polymerization of the corresponding NTAs in the solid state can produce well-controlled polypeptides and further demonstrate that NTAs are viable alternatives to NCAs in the synthesis of polypeptides and polypeptoids.

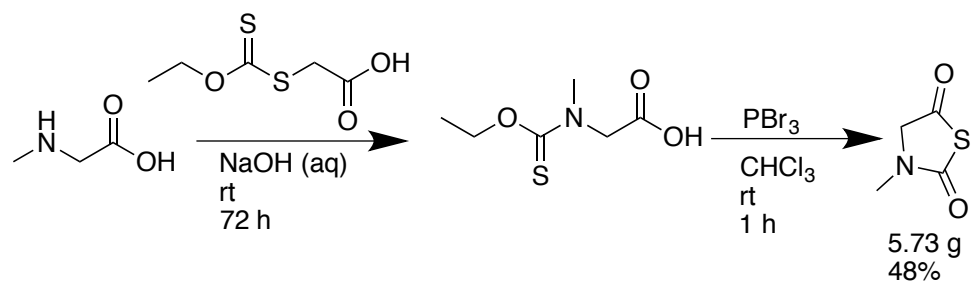
## 4.3 Results and discussion

### 4.3.1 Synthesis and ROP of R-NTAs

Sarcosine or *N*-methyl NTA (Me-NTA) was prepared using published methods<sup>182, 190</sup> and was characterized by <sup>1</sup>H NMR analysis, <sup>13</sup>C NMR, and electrospray ionization mass spectrometry.<sup>190</sup> All synthetic steps were carried out in open air, using regular solvent, in contrast to the syntheses of R-NCAs, where dry solvent was used in the cyclization of the R-NCA.

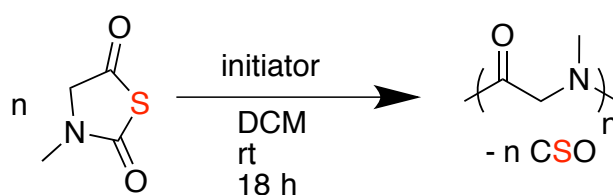
The synthesis of XAA using commercially available potassium ethyl xanthogenate and chloroacetic acid under basic conditions was relatively straightforward and can be carried out at large scales (~ 25 g) with adequate yield (78%). XAA is coupled to commercially available sarcosine under basic conditions followed by cyclization with phosphorus tribromide to form the NTA heterocycle. Crude NTA was obtained following a base wash with saturated sodium bicarbonate and concentration of the organic layer. Overall yield was adequate (48%) following the vacuum distillation of the NTA monomer as a colorless liquid which solidifies when stored at -30 °C and melts at ambient temperature. Scheme 4.1 shows a generic synthetic scheme for the synthesis of Me-NTA.

Scheme 4.1. Synthesis of Me-NTA





Scheme 4.2. Generic polymerization of Me-NTA



Mechanistically, the polymerization of NTAs should parallel those of NCAs except that carbonyl sulfide gas is lost versus that of carbon dioxide as shown in Scheme 4.2. We screened a number of initiators, which have been previously demonstrated to participate in the ROP of R-NCAs. An obvious choice is the screening of primary amine initiator as it has been demonstrated on numerous occasions that polypeptoids with predictable molecular weights can be obtained from primary amine mediated ROP of R-NCAs via the normal amine mechanism. A number of organobases, namely amidines, guanidines, and NHCs, have previously been investigated in the ROP of cyclic esters into their corresponding polyesters.<sup>166, 173, 275-276, 278, 287, 321</sup> Within this category of initiators, NHCs and diazabicycloundecene (DBU) have been studied in the ZROP of R-NCAs to obtain polypeptoids with well-defined cyclic architectures, making them viable candidates for further investigation in the ROP of R-NTAs.<sup>19, 147, 150</sup> 1,1,3,3-tetramethylguanidine (TMG) was also reported to participate as an initiator in the ROP of Bu-NCA to obtain adequately controlled PNBG species.<sup>272</sup> Organosilyl amine mediated ROP of sarcosine-NCA was briefly mentioned by Cheng et al in the mechanistic study of organosilyl amine mediated ROP of amino acid based NCAs.<sup>104</sup> These initiators are summarized in Figure 4.2.

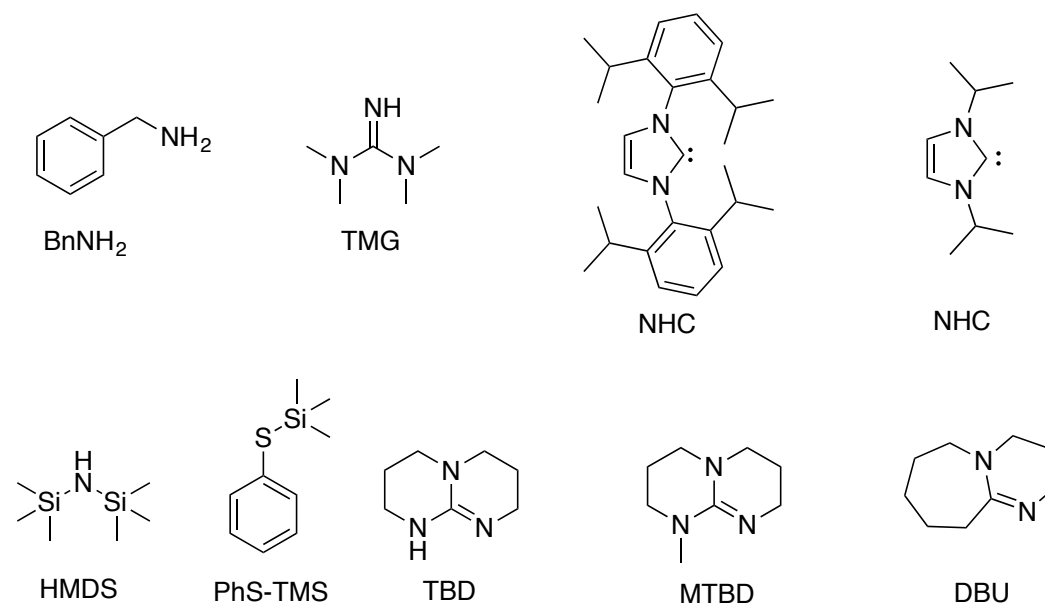


Figure 4.2. Chemical structures of the various initiators investigated in the ROP of Me-NTA.

The general reaction scheme for the ROP of Me-NTA is shown in Scheme 4.2. One observation from previous reports on the ROP of Me-NTA is that the choice of polymerization solvent (i.e. dioxane, THF, CH<sub>3</sub>CN) often leads to heterogeneous polymerization reactions as monomer conversion increases, which may affect polymerization kinetics. It was reported that polysarcosine can remain solubilized in polymerization reactions with dichloromethane.<sup>84</sup> This was confirmed in our own polymerization experiments with Me-NTA and is the solvent of choice for this investigation.

To our surprise, TMG performed the best out of the initiators we investigated in the ROP of Me-NTA. Polymerization reactions were observed to reach quantitative conversion in 18 h, nearly threefold faster than previous reports (48 h). Additionally, polymerization reactions were carried out at ambient temperature versus 60 °C in previous reports. Polysarcosine was recovered through precipitation of the reaction solution into excess hexanes, and subsequent filtration and drying under vacuum.

Molecular weight characterization data from the ROP of Me-NTA using TMG initiators are shown in Table 4.1. It can be seen from the molecular weight characterization data that molecular weights increase with decreasing monomer to initiator loadings, suggesting that the ROP of Me-NTA exhibits living character. The obtained PDIs were also relatively narrow (1.04-1.11). The SEC-DRI-MALS traces however exhibited significant aggregation, evidenced by the presence of high molecular weight shoulders. Direct injection of the reaction solution containing unpurified polysarcosine did not remedy the observed high molecular weight shoulders in SEC-DRI-MALS analysis. Ling et al previously reported that  $DP_n$  of up to 150 could be reached in the ROP of Me-NTA using benzylamine initiator.<sup>192</sup> The  $DP_n$  at low monomer to initiator loadings ( $[M]_0:[TMG]_0=400:1$ ) obtained using TMG initiator was observed to be more than double of the previously reported  $DP_n$  based on SEC-DRI-MALS analysis (Figure 4.3, Table 4.1). This demonstrates that high molecular weight polysarcosine can be obtained from the ROP of Me-NTA under significantly milder conditions and in less reaction time, showing potential for Me-NTA as an alternative monomer to synthesize high molecular weight polysarcosines. MALDI TOF MS and <sup>1</sup>H NMR analyses indicated the presence of a TMG end group (Figure 4.4, 4.5). FTIR analysis of polysarcosine obtained from the ROP of Me-NTA initiated by TMG ( $[M]_0:[TMG]_0=25:1$ ) also suggests the presence of the TMG end group as indicated by the broadened stretching band at 1632 cm<sup>-1</sup> possibly corresponding to the imine (C=N) and carbonyl (C=O) stretching of the resulting polysarcosine (Figure 4.6).

We wanted to further investigate the possible living character of the polymerization. A chain extension experiment using TMG initiator was performed in order to demonstrate that there are no termination events and that the polymer chains remain active for additional propagation. A polymerization was conducted using Me-

NTA ( $[M]_0:[TMG]_0=100:1$ ) under standard conditions ( $[M]_0=1.0$  M, 22 °C, in dichloromethane) to achieve quantitative conversion of monomer. A second batch of monomer was subsequently introduced so additional chain propagation could occur ( $[M]_0:[TMG]_0=200:1$ ).

Table 4.1. Molecular weight characterization data for TMG initiated ROP of Me-NTA <sup>a</sup>

$[M]_0:[TMG]_0$	$M_n$ (theo.) ( $\text{kg}\cdot\text{mol}^{-1}$ ) <sup>b</sup>	$M_n$ (GPC) ( $\text{kg}\cdot\text{mol}^{-1}$ ) <sup>c</sup>	PDI	$DP_n$ <sup>d</sup>
25	1.8	1.9	1.11	27
50	3.6	4.1	1.07	58
100	7.1	6.0	1.04	85
150	10.7	9.1	1.04	128
250	17.8	12.6	1.05	177
400	28.4	27.9	1.04	393

<sup>a</sup> All polymerizations were performed at  $[M]_0 = 1.0$  M, 22 °C in dichloromethane for 18 h; <sup>b</sup> based on conversion calculated from FTIR analysis; <sup>c</sup> absolute molecular weights were calculated using previously determined  $dn/dc = 0.0987$  mL/g; <sup>d</sup> based on  $M_n$  obtained from SEC-DRI-MALS and the repeat unit of PNMG= $71$   $\text{g}\cdot\text{mol}^{-1}$ .

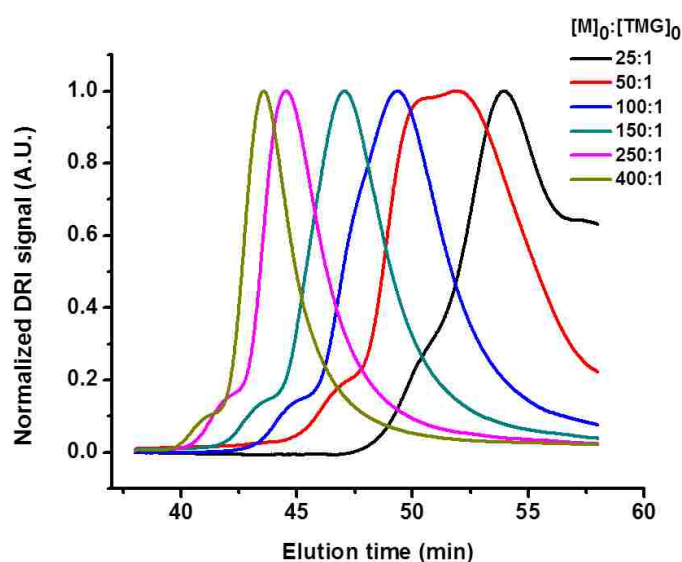


Figure 4.3. SEC-DRI-MALS traces from the ROP of Me-NTA ( $[M]_0=1.0$  M) in the presence of TMG initiator with increasing  $[M]_0:[TMG]_0$  ratios in  $\text{CH}_2\text{Cl}_2$  at ambient temperature.

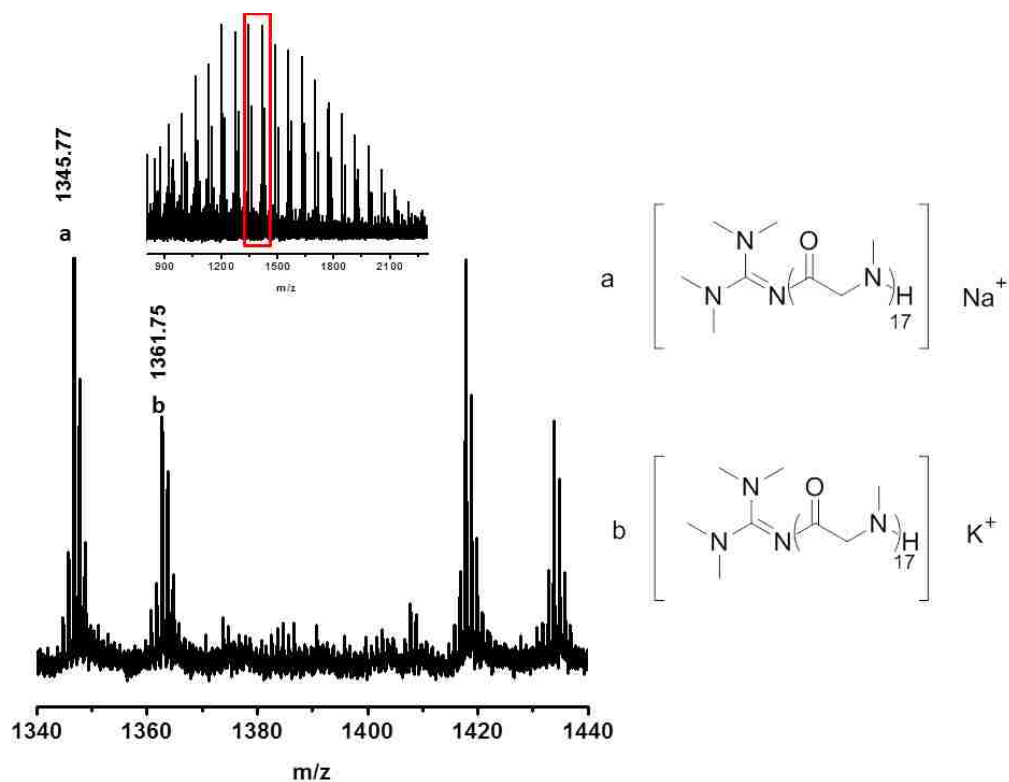


Figure 4.4. MALDI TOF MS spectrum of TMG initiated ROP of Me-NTA ( $[M]_0:[TMG]_0 = 25:1$ ,  $[M]_0 = 1.0$  M).

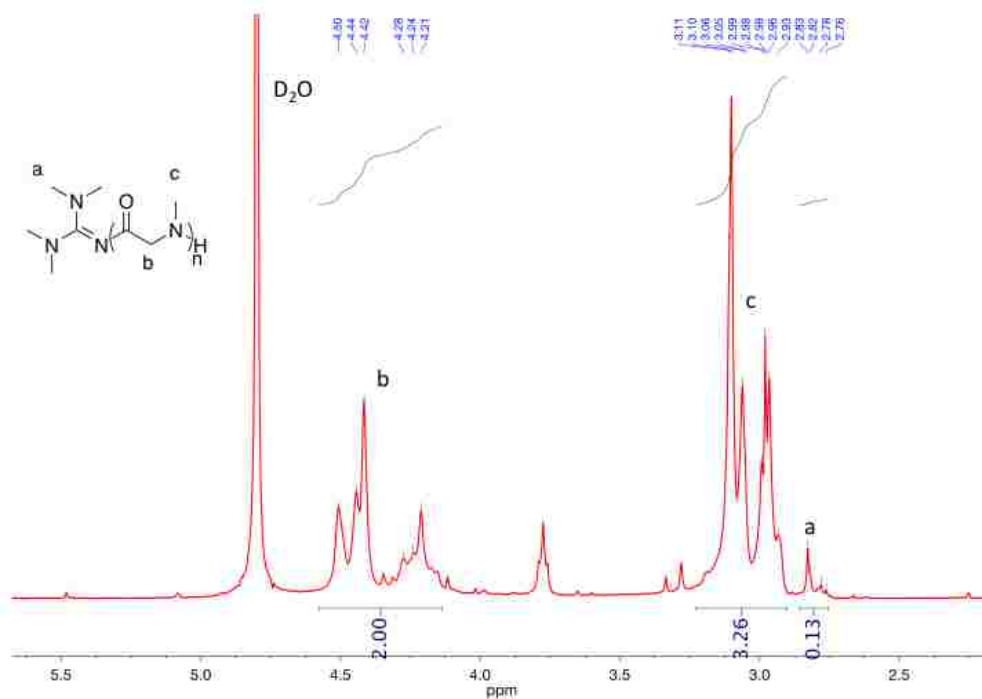


Figure 4.5. <sup>1</sup>H NMR spectrum of polysarcosine obtained from the ROP of Me-NTA with TMG initiator ( $[M]_0:[TMG]_0=25:1$ ,  $[M]_0=1.0$  M in CH<sub>2</sub>Cl<sub>2</sub>). The spectrum was collected in D<sub>2</sub>O.

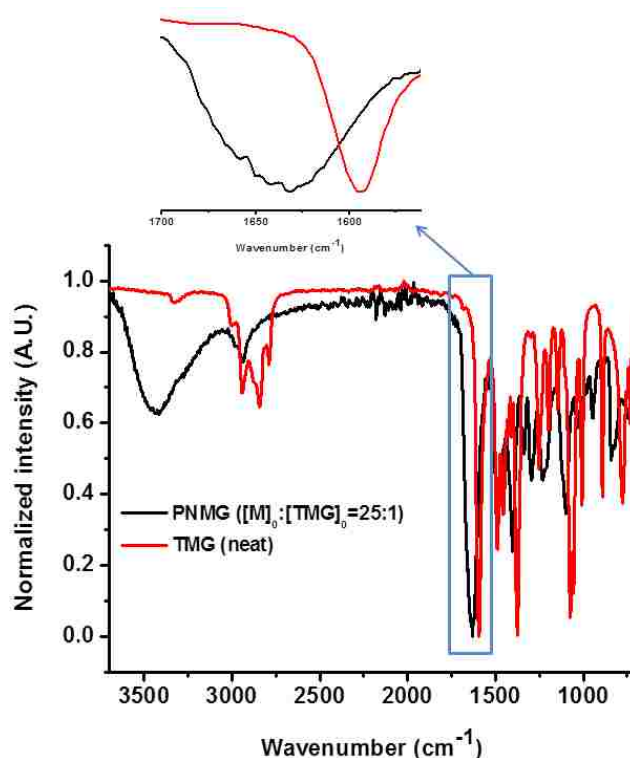


Figure 4.6. FTIR spectra of a low molecular weight polysarcosine synthesized via the ROP of Me-NTA using TMG initiator ( $[M]_0:[TMG]_0=25:1$ ) and TMG.

SEC-MALS-DRI analysis of the polysarcosines obtained before and after the introduction of the second batch of Me-NTA indicate an increase in polymer molecular weight that agrees well with theoretical values supporting the living character of the ROP of Me-NTA and that enchainment is possible (Figure 4.7A, Table 4.2). The living character of the polymerization was further supported through the linear increase in  $M_n$  with respect to increasing monomer conversion (Figure 4.7B)

Table 4.2. Chain extension of polysarcosine prepared by TMG-mediated polymerization of Me-NTA <sup>a</sup>

Entry	$M_n$ (theo.) ( $\text{kg}\cdot\text{mol}^{-1}$ ) <sup>b</sup>	$M_n$ (GPC) ( $\text{kg}\cdot\text{mol}^{-1}$ ) <sup>c</sup>	PDI <sup>c</sup>	DP <sup>d</sup>
Pre-extension	7.1	7.2	1.06	101
Post-extension	14.2	15.5	1.05	218

<sup>a</sup>. All polymerizations were conducted at  $[M]_0=1.0$  M in dichloromethane at 22 °C and were allowed to react for at least 18 h to reach quantitative conversion; <sup>b</sup>. theoretical molecular weights in  $\text{kg}\cdot\text{mol}^{-1}$  are calculated from  $[M]_0:[TMG]_0$  ratio and conversion; <sup>c</sup>. determined by the SEC-MALS-DRI method using  $dn/dc = 0.987(17)$   $\text{mL}\cdot\text{g}^{-1}$ ; <sup>d</sup>. number average degree of polymerization was calculated from the  $M_n$  determined by SEC-MALS-DRI method.

Ling et al recently reported using benzylamine initiator in the random copolymerization of *N*-methyl and *N*-butyl glycine NTA monomers to obtain thermoresponsive copolypeptoids whose cloud point temperatures can be tuned by varying the sarcosine content in order to vary the hydrophilic character of the copolypeptoid and affect the observation of hydrophobic collapse.<sup>192</sup> However,  $DP_n$  of up to only 150 were reported (vide supra). Using the prescribed reaction conditions outlined in Scheme 1.2, we investigated the extent to which benzylamine (or primary amines in general) initiator could be used to synthesize homopolypeptoids. A series of polymerizations were set up at  $[M]_0=1.0$  M with monomer to initiator loadings ranging from 25-400:1. Similar to TMG initiated ROP of Me-NTA, quantitative conversion was observed after approximately 18 h, suggesting that the polymerization reactions proceeded much faster in dichloromethane under mild conditions. These reactions remained homogeneous and precipitation of polysarcosine was not observed, contrary to previous reports.<sup>182, 191</sup> Molecular weights of the resulting polysarcosines were characterized by SEC-DRI-MALS whose results are shown in Figure 4.8 and Table 4.3.

Table 4.3 suggests that the  $M_n$ s of polysarcosine could also be controlled through varying the initial monomer to benzylamine loadings and that the PDI obtained from SEC-DRI-MALS are relatively narrow. SEC-DRI-MALS traces (Figure 4.6) also indicated high molecular weight shoulders, which may be due to aggregation of polysarcosine. Similar to TMG initiated polymerizations of Me-NTA, direct injection of unprecipitated and unpurified polysarcosine into the SEC-DRI-MALS instrument did not remedy the observation of high molecular weight aggregate shoulder peaks. The obtained  $M_n$ s begin to deviate when  $[M]_0:[BnNH_2]_0 > 200:1$  suggesting that there are upper limits to the polymerization control. MALDI TOF MS analysis was conducted in order to assess

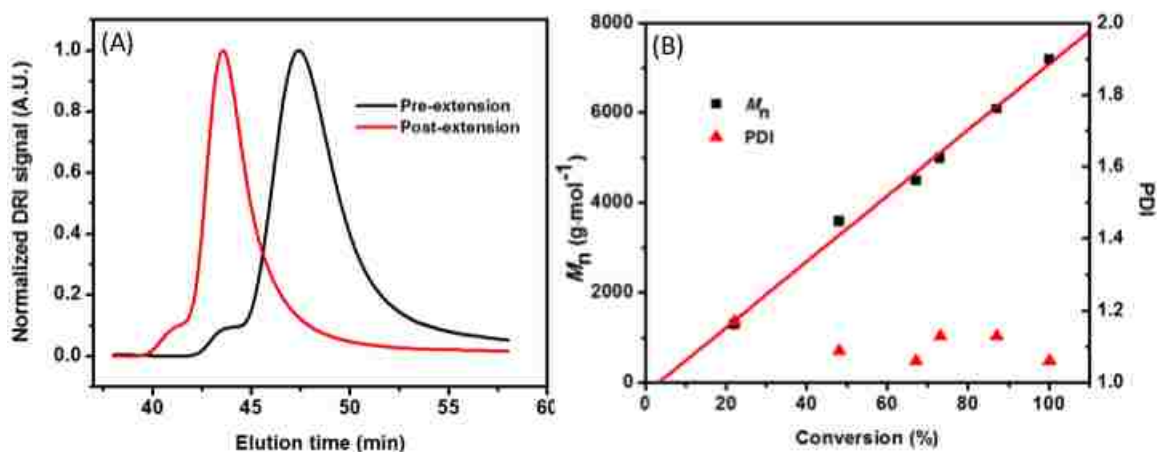


Figure 4.7. (A) SEC-MALS-DRI chromatograms from the chain extension experiment (first reaction:  $[M]_0:[TMG]_0=100:1$ ,  $[M]_0=1.0$  M, DCM, 22 °C; chain extension reaction:  $[M]_0:[TMG]_0=200:1$ ) (B) Plots of  $M_n$  and PDI versus conversion for the ROP of Me-NTA using TMG initiator ( $[M]_0:[TMG]_0=100:1$ ,  $[M]_0=1.0$  M, 22°C in DCM).

the end group structures. Kricheldorf had previously reported that in the case of the ROP of DL-phenylalanine and DL-leucine NTAs that the reaction pathway exclusively follows a C5 attack. MALDI TOF MS analysis of a low molecular weight benzylamine initiated species of polysarcosine (Figure 4.9) also suggested that the reaction follows an exclusive C5 attack. The major species observed were the benzyl amide terminated species with sodium or potassium counterions. The presence of benzyl terminated species was also verified by  $^1H$  NMR (Figure 4.10). The presence of thiocarbamic acid terminated species was also suggested in MALDI TOF MS, possibly lending some support to the stabilization of the thiocarbonate through enhanced solvation as previously proposed by Kricheldorf. Nonetheless, these results indicate that the ROP of Me-NTA follows the expected NAM pathway.

Cheng et al have previously demonstrated the aspects of organosilicon amine mediated ROP of amino acid based NCAs.<sup>102-104</sup> It was reported that HMDS was able to initiate the ROP of sarcosine-NCA during mechanistic studies but the concept was not



Table 4.3. Molecular weight characterization data for benzylamine initiated ROP of Me-NTA<sup>a</sup>

$[M]_0:[BnNH_2]_0$	$M_n$ (theo.) (kg·mol <sup>-1</sup> ) <sup>b</sup>	$M_n$ (GPC) (kg·mol <sup>-1</sup> ) <sup>c</sup>	PDI	DP <sup>d</sup>
25	1.8	2.5	1.14	35
50	3.6	3.8	1.04	54
100	7.1	6.2	1.06	87
200	14.2	12.7	1.03	179
400	28.4	19.2	1.03	270

<sup>a</sup> All polymerizations were performed at  $[M]_0 = 1.0$  M, 22 °C in dichloromethane for 18 h; <sup>b</sup> based on conversion calculated from FTIR analysis; <sup>c</sup> absolute molecular weights were calculated using previously determined  $dn/dc = 0.0987(17)$  mL/g<sup>147</sup>; <sup>d</sup> based on  $M_n$  obtained from SEC-DRI-MALS and the repeat unit of PNMG=71 g·mol<sup>-1</sup>.

further explored. We also investigated whether or not Me-NTA could be polymerized using HMDS. Reaction conditions used were similar to those of benzylamine and TMG. While quantitative conversions were reached under similar conditions to previous reactions, HMDS failed to obtain higher molecular weight species (Table C1) and is therefore suggested to be a poor candidate for the ROP of NTAs. This is further supported by our use of phenyl trimethylsilyl sulfide (PhS-TMS), which was recently reported to participate in faster initiation of the ROP of polypeptide based NCAs than HMDS.<sup>105</sup> PhS-TMS initiated reactions produced no observable conversion of NTA thus suggesting that organosilicon amines are ineffective initiators in the ROP of R-NTAs.

A number of organobases which include NHCs, DBU, TBD, and MTBD have all been explored as organocatalysts in the ROP of cyclic esters into their corresponding polyesters. The former two species were also demonstrated to proceed through ZROP of both cyclic ester and R-NCA monomers. Under similar conditions to previous reactions, a

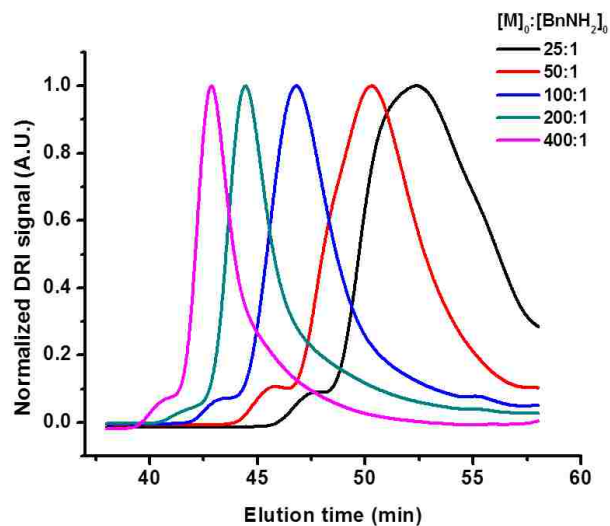


Figure 4.8. SEC-DRI-MALS traces from the ROP of Me-NTA ( $[M]_0=1.0$  M) in the presence of benzylamine initiator with increasing  $[M]_0:[BnNH_2]_0$  ratios in  $CH_2Cl_2$  at ambient temperature for 18 h.

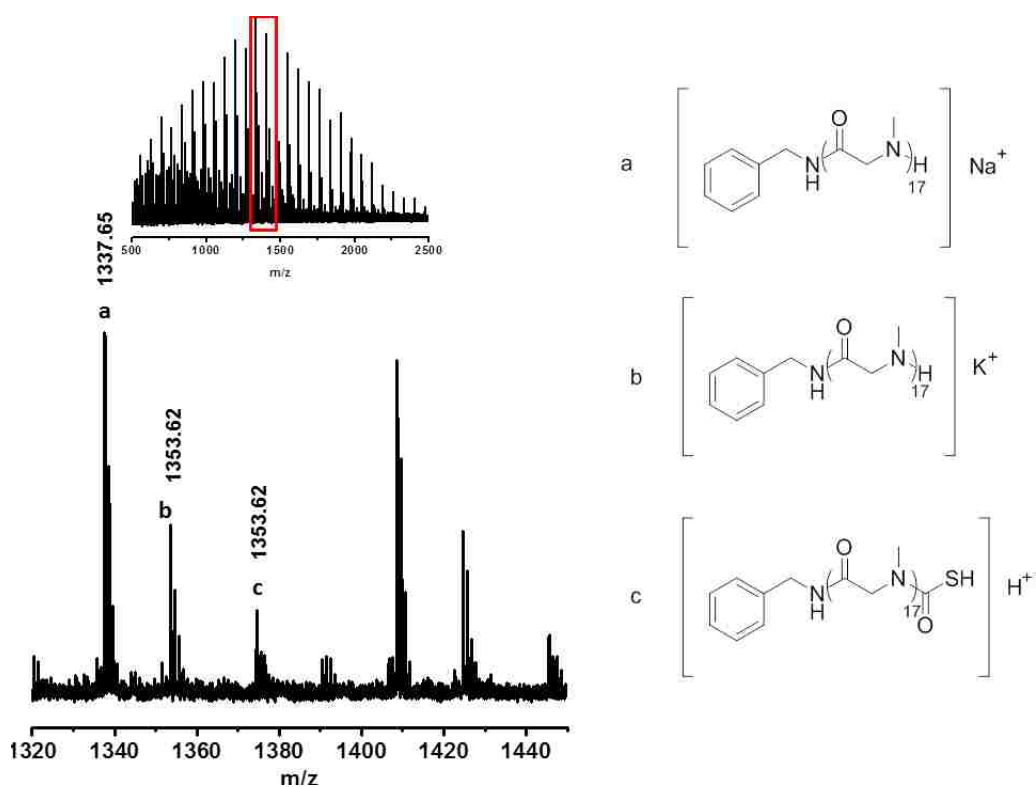


Figure 4.9. MALDI TOF MS spectrum of benzylamine initiated ROP of Me-NTA ( $[M]_0:[BnNH_2]_0 = 25:1$ ,  $[M]_0 = 1.0$  M).

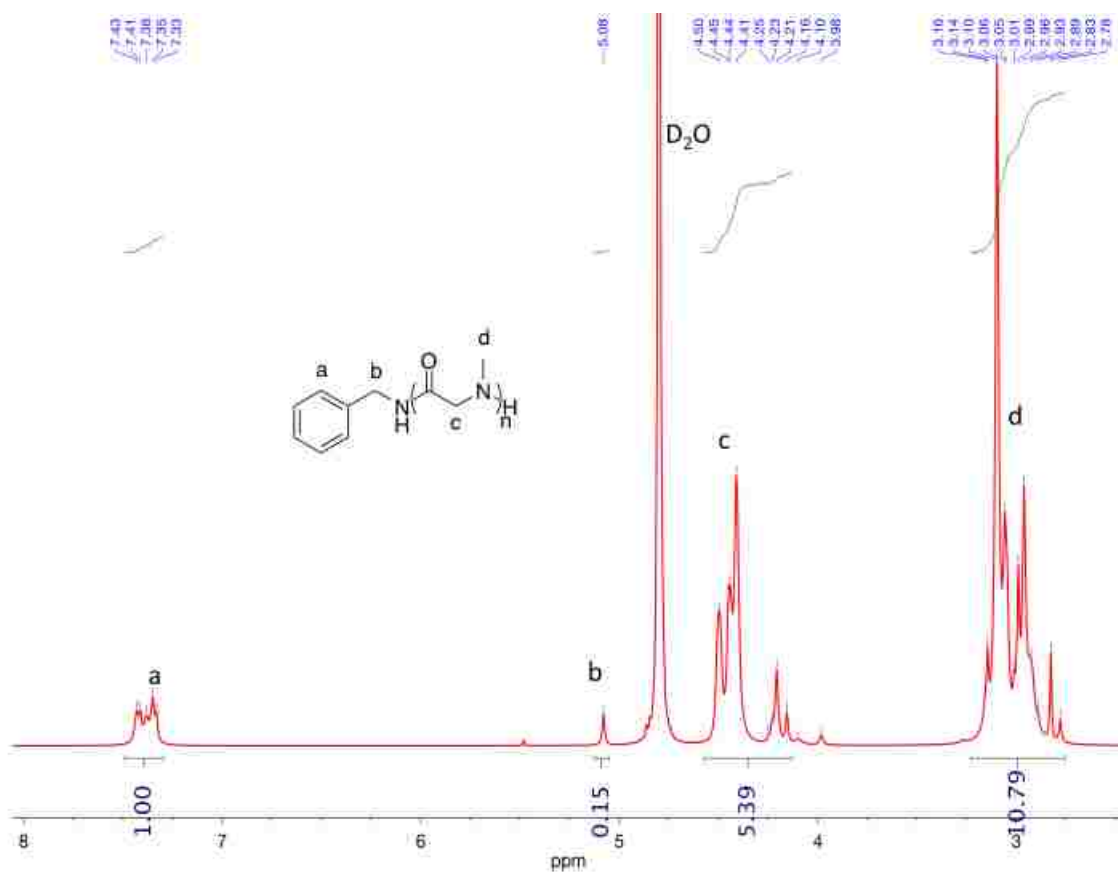


Figure 4.10.  $^1\text{H}$  NMR spectrum of polysarcosine obtained from the ROP of Me-NTA with benzylamine initiator ( $[\text{M}]_0:[\text{BnNH}_2]_0=25:1$ ,  $[\text{M}]_0=1.0$  M in  $\text{CH}_2\text{Cl}_2$ ). The spectrum was collected in  $\text{D}_2\text{O}$ .

series of polymerizations using two NHCs of varying steric hindrance, DBU, TBD and MTBD initiators. Molecular weight characterization of the resulting polysarcosine species are tabulated in Table C2. An exemplary spectrum of NHC terminated polysarcosine is shown in Figure C1. A small singlet at 9.64 ppm can be observed in Figure C1 suggesting that the NHC initiator exists partially in the protonated state.<sup>150</sup> In turn, this lowers the effective initiator concentration, which may have contributed to the slightly higher deviations in obtained  $M_n$  by SEC-DRI-MALS. Although end group analysis suggests the presence of the desired end groups, polymerization via amidine, and NHC is not as robust as those reactions obtained from those of benzylamine and TMG. The obtained  $M_n$ s deviate even at low monomer to initiator loadings suggesting the relatively poor polymerization behavior of these organobases as initiators. For

polymerizations where  $[M]_0:[I]_0 < 100$ , it was observed that the more sterically hindered NHC and MTBD displayed adequate molecular weight control. This may be due to the reaction center being more electron rich due to contributions from the additional aliphatic groups.

NTAs are noted for their stability and longer shelf life than that of NCAs, especially under inert atmospheres (e.g. argon).<sup>182</sup> A sample of Me-NTA was left exposed to the ambient atmosphere for one month. <sup>1</sup>H NMR spectra were taken at  $t_0$  (time of synthesis and purification), 2 weeks, and 4 weeks as shown in Figure 4.11. Over the course of one month, the monomer did not appear to degrade in air and merely absorbed ambient moisture from the atmosphere as indicated by the formation of a small singlet at approximately 1.6 ppm. An aliquot was removed and polymerized in dichloromethane at  $[M]_0 = 1.0$  M, and ambient temperature over a course of 18 h using TMG as the initiator with  $[M]_0:[I]_0 = 250:1$ . The reactivity of the slightly aged monomer did not appear to be affected as the reaction displayed quantitative conversion by FTIR analysis and the absolute molecular weight obtained by SEC-DRI-MALS was comparable to the theoretical value ( $M_n(\text{SEC-DRI-MALS}) = 17.9 \text{ kg}\cdot\text{mol}^{-1}$ ,  $M_n(\text{theo.}) = 17.8 \text{ kg}\cdot\text{mol}^{-1}$ , PDI = 1.04, DP = 252). This shows that Me-NTA has adequate shelf life even if left exposed to the ambient environment for one month and its polymerization activity is unaffected.

Inspired by the reactivity of Me-NTA towards a number of initiators, we desired to further investigate their application to the ROP of other R-NTAs. The synthesis of Bu-NTA was reported by Ling et al<sup>191-192</sup> and used as the hydrophobic component in the synthesis of thermoresponsive polypeptoids. Although the synthesis of Bu-NTA requires the synthesis of the corresponding *N*-butyl glycine precursor, the procedure to access Bu-NTA parallels that of Me-NTA. Purification of Bu-NTA was achieved via column chromatography. Bu-NTA also solidifies when stored at -30 °C, similar to its Bu-NCA.

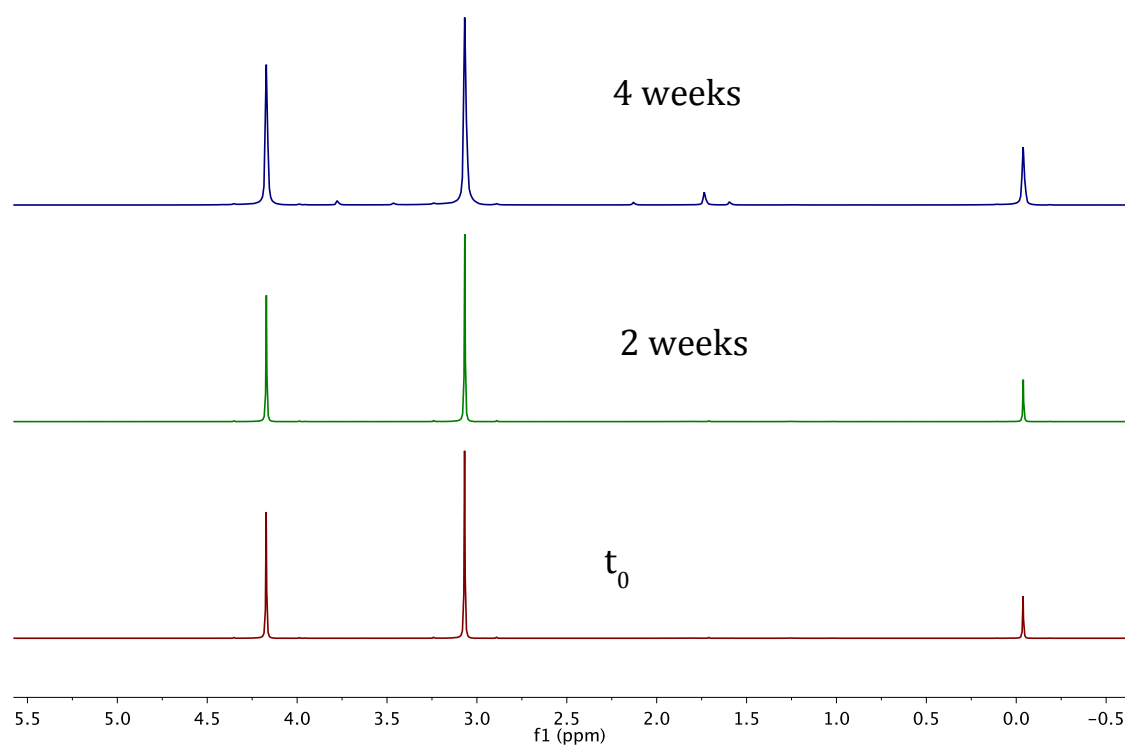
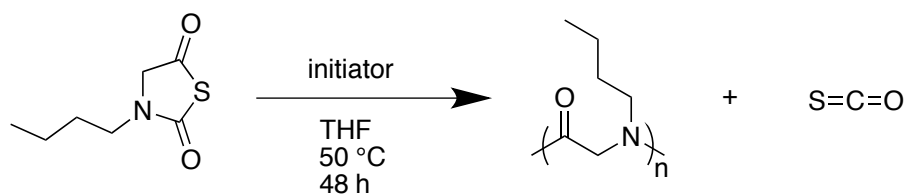


Figure 4.11.  $^1\text{H}$  NMR spectra taken in  $\text{CDCl}_3$  of Me-NTA at  $t_0$ , 2 weeks, and 4 weeks exposed to the ambient air. “ $t_0$ ” refers to the time at which the synthesis and purification of the particular batch of monomer used in the study was complete.

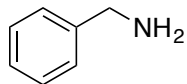
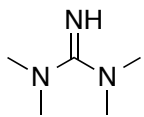
Scheme 4.3. Polymerization of Bu-NTA



Polymerization of Bu-NTA (Scheme 4.3) was carried out at  $[\text{M}]_0 = 1.0 \text{ M}$ , in THF at  $50 \text{ }^\circ\text{C}$  using a variety of initiators. Surprisingly, the reactivity of Bu-NTA is much less than that of Me-NTA; unlike the 18 h required for the polymerizations of Me-NTA to reach quantitative conversion, much higher reaction times (48 h) are required in the ROP of Bu-NTA to reach quantitative conversion. Changing the polymerization solvent to dichloromethane did not speed up the reaction as observed in the ROP of Me-NTA. Only

benzylamine and TMG initiators were demonstrated to be able to reach quantitative conversion. Table 4.4 shows the molecular weight characterization data for the obtained PNBGs from the ROP of Bu-NTA. Although the obtained molecular weights somewhat agree with theoretical values and the PDI are adequate, synthesis of PNBGs via the ROP of Bu-NTA is inefficient compared with those from the ROP of Bu-NCA. One drawback is that zero monomer conversion is observed when  $[M]_0:[I]_0 > 100:1$ , hindering access to high molecular weight PNBGs. Secondly, the ROP of the NTA is much slower than that of the NCA; PNBGs of comparable  $M_n$  and  $DP_n$  could be synthesized within 24 h via the ROP of Bu-NCA.

Table 4.4. Molecular weight characterization data for the ROP of Bu-NTA using benzylamine and TMG initiators <sup>a</sup>

Initiator	$[M]_0:[I]_0$	$M_n$ (theo) ( $\text{kg}\cdot\text{mol}^{-1}$ ) <sup>b</sup>	$M_n$ (SEC) ( $\text{kg}\cdot\text{mol}^{-1}$ ) <sup>c</sup>	PDI	DP
	25:1	2.8	2.3	1.05	20
	50:1	5.6	4.8	1.08	42
	100:1	11.3	14.5	1.05	128
	25:1	2.8	2.4	1.15	21
	50:1	5.6	6.2	1.12	55
	100:1	11.3	16.7	1.21	148

<sup>a</sup> All polymerizations were carried out at  $[M]_0 = 1.0$  M in THF, 50 °C for 48 h; <sup>b</sup> calculated from conversion determined by FTIR analysis; <sup>c</sup> absolute  $M_n$ s were determined using the  $dn/dc$  value of PNBG = 0.0815(12) mL/g.<sup>147</sup>

There are a number of possible explanations for the reduced reactivity of Bu-NTA. Bu-NTA is sterically bulkier than Me-NTA thus it is possible that the steric bulk of the butyl aliphatic chain blocks nucleophilic attack at the C5 position. However, this is not observed in the ROP of Bu-NCA as polymerizations have been observed to occur relatively rapidly upon the addition of initiator. It is possible that Bu-NTA is more stable than Me-NTA due to the presence of additional aliphatic chains making the NTA more electron rich, thus improving the delocalization of the sulfur atom electrons, which

contribute to the stability and reduced polymerization activity in NTAs. Benzylamine and TMG initiators were possibly not nucleophilic enough to reliably initiate the ROP of Bu-NTA. Benzyl alkoxide initiator was used in order to investigate whether a stronger nucleophile would be able to improve upon the polymerization activity of Bu-NTA. SEC-MALS-DRI results are summarized in Table 4.5 and traces are shown in Figure 4.12. It can be observed from the molecular weight characterization data that well-controlled PNBGs can be obtained via the ROP of Bu-NTA up until  $[M]_0:[I]_0 > 200:1$ , a small improvement over the activity of benzylamine and TMG initiators. End group analysis via  $^1\text{H}$  NMR (exemplary spectrum shown in Figure 4.13) supports the absolute  $M_n$  obtained via SEC-DRI-MALS (Figure 4.12). Although the same PNBGs can be obtained through the ROP of Bu-NTA, the reaction is overall inefficient when compared with that of the ROP of Bu-NCA. This is due to the low yield of monomer synthesis and markedly reduced reactivity of Bu-NTA versus those of Bu-NCA and Me-NTA. Thus, the ROP of Bu-NTA is an inefficient pathway to obtain well-defined high molecular weight PNBGs.

Table 4.5. Molecular weight characterization data for a series of PNBGs obtained via benzyl alkoxide initiator <sup>a</sup>

$[M]_0:[I]_0$	$M_n$ (theo.) ( $\text{kg}\cdot\text{mol}^{-1}$ ) <sup>b</sup>	$M_n$ (GPC) ( $\text{kg}\cdot\text{mol}^{-1}$ ) <sup>c</sup>	$M_n$ (NMR) ( $\text{kg}\cdot\text{mol}^{-1}$ )	PDI	DP
25:1	2.8	3.5	3.4	1.03	31
50:1	5.6	5.4	6.2	1.13	48
100:1	11.3	10.4	10.9	1.07	92
200:1	22.6	19.2	- <sup>d</sup>	1.24	170

<sup>a</sup> All polymerizations were carried out at  $[M]_0 = 1.0$  M in THF, 50 °C for 48 h; <sup>b</sup> calculated from conversion determined by FTIR analysis; <sup>c</sup> absolute  $M_n$ s were determined using the  $dn/dc$  value of PNBG = 0.0815(12) mL/g<sup>147</sup>; <sup>d</sup> end groups could not be distinguished in  $^1\text{H}$  NMR.

#### 4.3.2 Amino acid based NTA monomers

To date, although a number of amino acid based NTAs have been synthesized<sup>185-186, 190, 319</sup>, polymerization activity via the ROP of amino acid based NTAs has been

demonstrated to be relatively poor compared to the ROP of R-NTAs.<sup>190</sup> We set out to synthesize a model monomer in order to demonstrate that well-defined polypeptides can be obtained from the ROP of their corresponding NTA monomers.

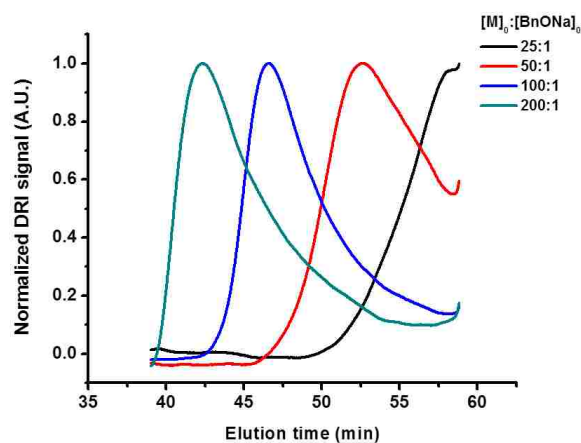


Figure 4.12. SEC-MALS-DRI traces from the ROP of Bu-NTA with BnONa initiator ( $[M]_0=1.0$  M) in 50 °C THF.

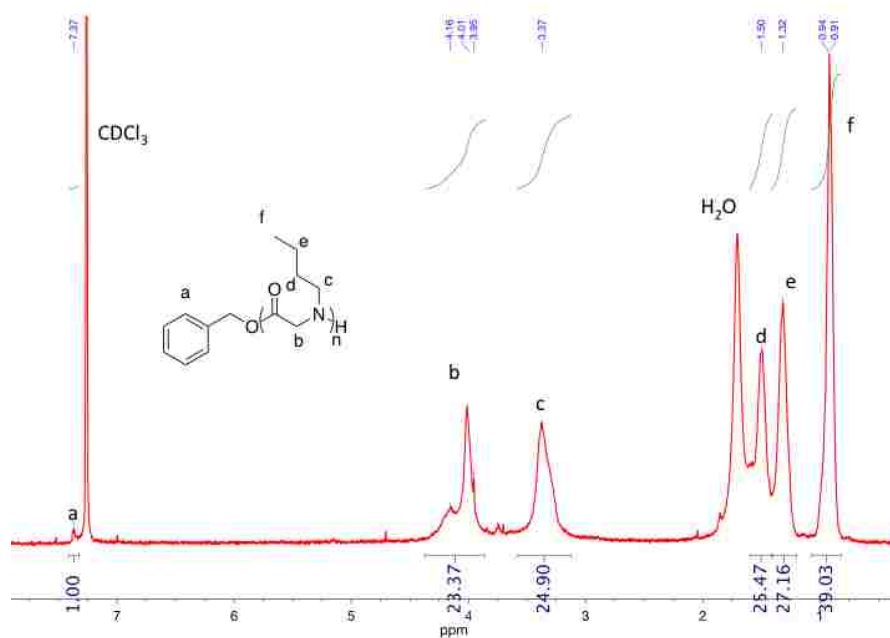


Figure 4.13.  $^1\text{H}$  NMR spectrum of PNBG obtained from the ROP of Bu-NTA with benzyl alkoxide ( $[M]_0:[\text{BnONa}]_0=50:1$ ,  $[M]_0=0.5$  M in THF, 50 °C). The spectrum was collected in  $\text{CDCl}_3$ .

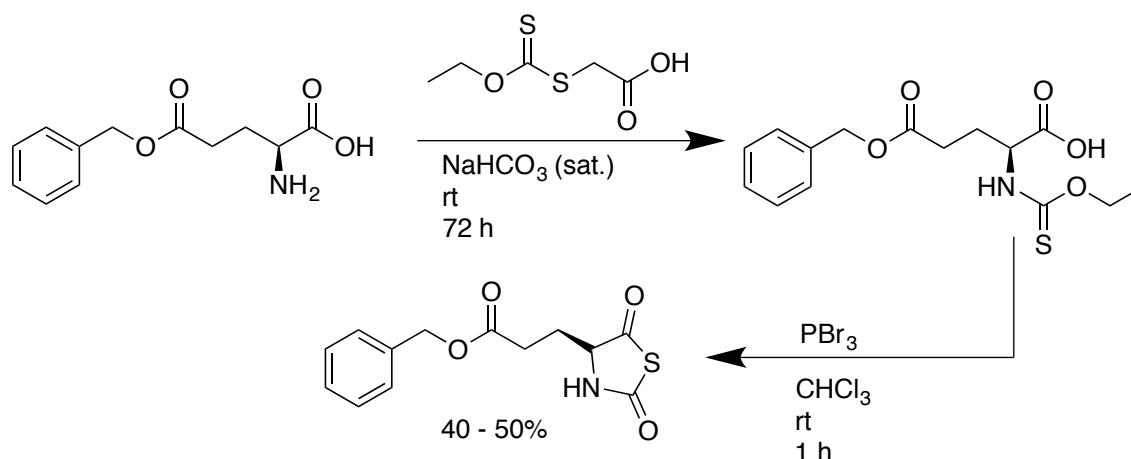


#### 4.3.2.1 ROP of amino acid based NTA monomers in solution state

$\gamma$ -Benzyl-L-glutamate *N*-thiocarboxyanhydrosulfide. One of the most extensively studied polypeptides is poly( $\gamma$ -benzyl-L-glutamate) (PBLG). PBLG has a number of well-defined characteristics such as its ability to self-assemble into  $\alpha$ -helical secondary structures and a well-studied persistence chain length.<sup>24</sup> PBLG is also soluble in many organic solvents and has been shown to not aggregate in solvents such as dioxane.<sup>24</sup> PBLG can be synthesized from the ROP of its respective NCA monomer, synthesized via cyclization of the parent amino acid derivative with triphosgene<sup>51</sup>, among other cyclizing agents. However, the synthesis of the NTA analogue of BLG NCA has yet to be reported and would make an interesting model polypeptide based NTA monomer to investigate for polymerization activity.

BLG-NTA synthesis. Synthesis of the monomer differs from that of the polypeptoid based NTAs. BLG contains a benzyl ester side chain, which is subject to hydrolysis at higher pH (>10). To avoid hydrolysis, milder basic conditions were used where the starting materials are reacted in the presence of saturated sodium bicarbonate, a weaker, non-nucleophilic base. Following the coupling reaction between XAA and BLG, the resulting intermediate is cyclized with phosphorus tribromide similar to the synthesis of Me-NTA (Scheme 4.4). Crude BLG NTA can be obtained after a base wash (saturate sodium bicarbonate) and concentration of the organic layer. BLG NTA is purified via column chromatography using 3:2 hexanes:ethyl acetate and was obtained in adequate yields (40-50%). The chemical structure of the NTA was verified via X-ray crystallography (Figure 4.14) using crystals grown via the slow evaporation of chloroform. X-ray crystallography revealed that racemization occurred during monomer

Scheme 4.4. Synthesis of BLG NTA

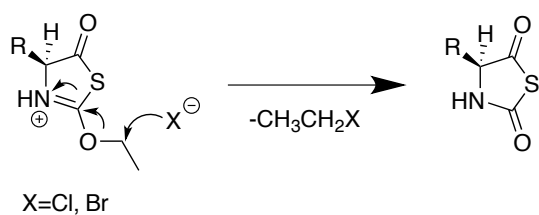


synthesis, consistent with previous syntheses of  $\alpha$ -amino acid NTAs.<sup>186</sup> While this does not appear to affect future polymerizations using such monomers, it does affect purity of the monomer, not being able to produce enantiomerically pure species. Possible solutions to remedy or reduce the amount of racemization could be to reduce the reaction time and temperature of cyclization reactions as was previously reported by Hirschmann.<sup>186</sup> Additionally, the steric bulk of the intermediate following the coupling reaction between XAA and benzyl-L-glutamate due to the ethyl group from XAA has been shown to potentially contribute to racemization.<sup>187</sup> This could be potentially remedied by using a less sterically hindered methyl xanthate for the intermediate coupling, which may improve the rate of dealkylation and prevention of enolization of the proposed azlactone intermediate during cyclization (Scheme 4.5). This in turn would prevent or reduce the amount of racemization observed in the synthesis of amino acid based NTAs.

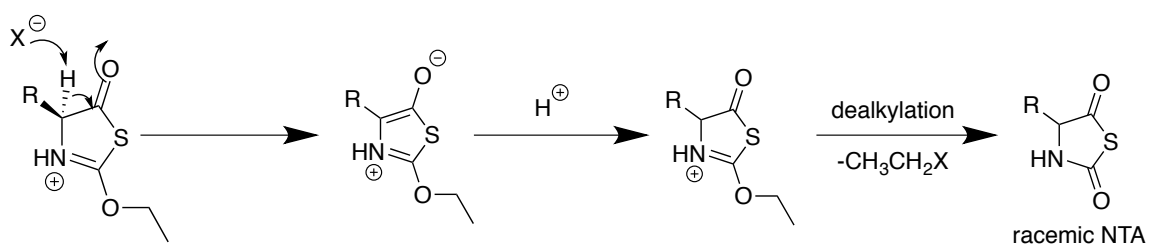
In contrast to the ROP of R-NTAs, polymerization activity of BLG-NTA was poor under solution phase conditions as polymerizations either exhibited poor molecular weight control based on the significant deviations of the obtained  $M_n$ s from theory, or that the polymerizations revealed low conversions, even after a number of days of reaction

Scheme 4.5. Proposed dealkylation and racemization mechanisms of amino acid based NTAs

**Proposed NTA dealkylation mechanism from azlactone intermediate**



**Racemization of azlactone intermediate via enolization**



time. For example, zero conversion was observed in polymerization reactions of BLG NTA using benzylamine initiator in contrast to the polymerization reactions of Me-NTA previously discussed. The addition of triazabicyclodecene organocatalyst (TBD) (5 mol. % with respect to monomer) in conjunction with benzylamine initiator allows the reaction to proceed to quantitative conversion as observed by FTIR within 48 h. The molecular weight characterization however shows significant deviation with adequate polydispersities (Table 4.6).

The rate of polymerization of BLG-NTA was also observed to be much slower than that of Me-NTA polymerization. It was found that polymerizations appeared to be concentration dependent. This was demonstrated in a series of polymerizations carried out in dioxane using hexylamine initiator where  $[M]_0:[I]_0= 80:1$  and the initial monomer concentrations varied from 0.5 to 2.0 M. Conversions were tracked by  $^1\text{H}$  NMR over the course of 48 h (Figure 4.15) and indicated that the rate of the ROP of BLG-NTA is

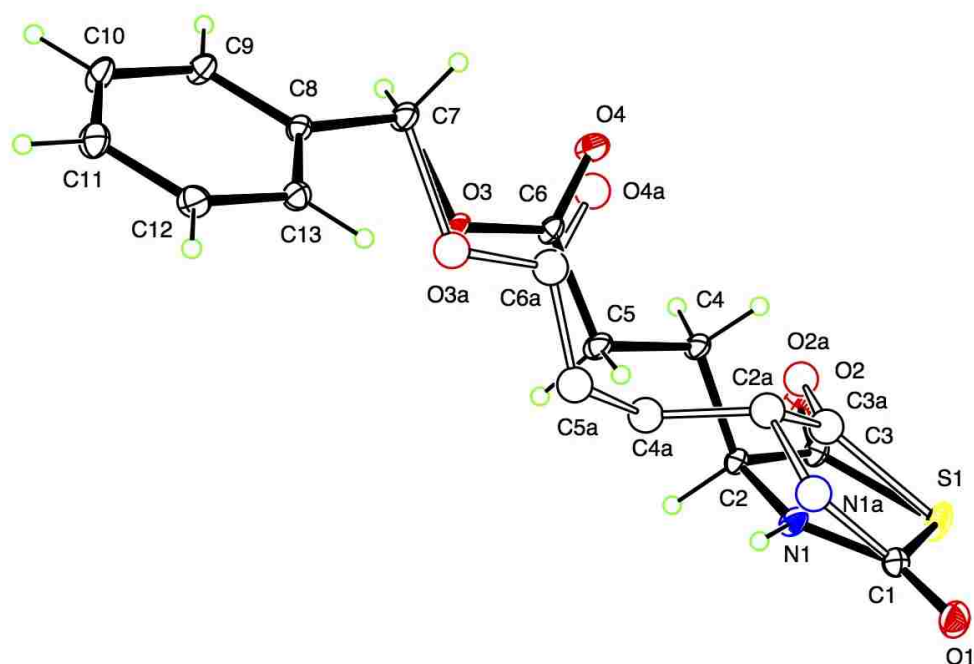


Figure 4.14. Crystal structure of BLG NTA as obtained via X-ray crystallography.

Table 4.6. Molecular weight characterization data for benzylamine/TBD initiated ROP of BLG NTA <sup>a</sup>

$[M]_0:[BnNH_2]_0$	$M_n$ (theo.) ( $\text{kg}\cdot\text{mol}^{-1}$ ) <sup>b</sup>	$M_n$ (SEC) ( $\text{kg}\cdot\text{mol}^{-1}$ ) <sup>c</sup>	PDI	DP
25	5.5	13.5	1.09	61
50	11.0	16.9	1.17	77
100	21.9	26.2	1.19	120

<sup>a</sup> All polymerizations were conducted at ambient temperature in DCM with  $[M]_0=0.5$  M; <sup>b</sup> calculated based on conversion determined by <sup>1</sup>H NMR; <sup>c</sup> absolute molecular weight was determined using  $dn/dc=0.1292$   $\text{mL}\cdot\text{g}^{-1}$ .<sup>97</sup>

concentration dependent. The resulting PBLGs were characterized by SEC-MALS-DRI in order to assess the polymerization control afforded by the slow, solution state ROP (Figure 4.16, Table 4.7). The obtained molecular weights from concentration dependent studies in solution state were comparable to determined theoretical values based on conversion.

DL-Methionine NTA. Although PBLG is a well-studied polypeptide, the polymer cannot be further modified except under hydrolytic conditions where there is ester exchange of the benzyl ester side chain with the desired moieties.<sup>322-325</sup> This process can be time consuming and does not guarantee that quantitative functionalization of the side chains as there could exist the possibility for disfavored equilibria for the desired end product. In general, orthogonal “click” chemistry reactions such as CuAAC, and thiol-ene coupling have arisen in order to accomplish efficient post-polymerization modification. One particular post-polymerization modification that has seen less attention than either CuAAC or thiol-ene coupling is the alkylation of a thioether. Deming reported the synthesis and polymerization of L-methionine NCA in order to access poly(L-methionine) and have demonstrated a wide range of compounds ranging from simple alkyl chains to carbohydrates that can be grafted onto the side chains via the alkylation of the thioether.<sup>132</sup> However, this system involves the use of NCA monomers and possesses the same drawbacks as all other NCA monomers. We sought out to synthesize an NTA monomer based on methionine that possesses the simplified synthesis, and ambient stability of previous NTAs but also possesses the opportunity for post-polymerization functionalization to demonstrate the versatility of the polypeptide platform.

Synthesis of DL-methionine NTA was analogous to that of Me and Bu-NTAs as there is no possibility for side chain hydrolysis as encountered in BLG-NTA synthesis (Scheme 4.6). Like previous NTA monomers, DL-methionine NTA was synthesized in open air, using regular solvent, and adequate yields (~66%) were obtained following simple recrystallization from dichloromethane and hexanes as a colorless solid.

Unlike the ROP of BLG-NTA, the solution state polymerization of DL-methionine showed promise as poly(DL-methionine)s ranging from 2.9-13.3 kg·mol<sup>-1</sup> were able to be obtained using a variety of initiators. The ROP of DL-methionine NTA

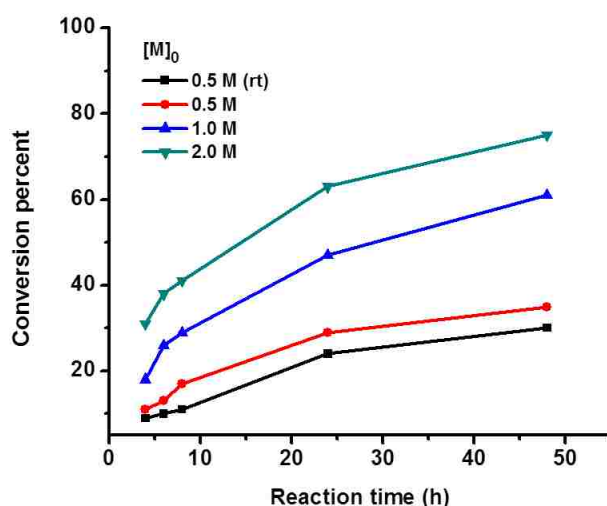


Figure 4.15. Plot of conversion percent versus reaction time in the solution state ROP of BLG-NTA at various  $[M]_0$ . All polymerizations were carried out at  $[M]_0:[I]_0=80:1$  at  $50\text{ }^\circ\text{C}$  in dioxane using hexylamine initiator unless otherwise noted. Conversions were analyzed  $^1\text{H}$  NMR.

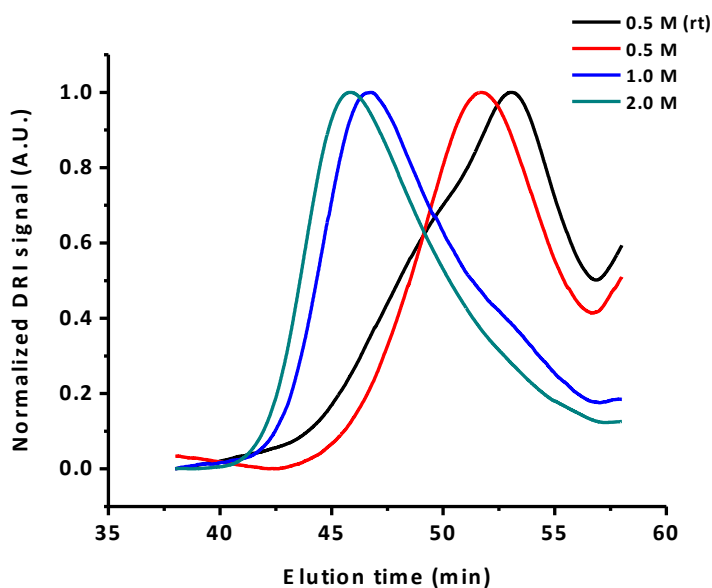


Figure 4.16. SEC-DRI-MALS traces of the ROP of BLG-NTA at varying monomer concentrations after 48 h ( $[M]_0:[I]_0=80:1$  at  $50\text{ }^\circ\text{C}$  in dioxane). Monomer conversion percentages at 48 h are shown in Table 4.7.

(Scheme 4.7) did not proceed as a homogeneous solution. Although it was observed that the monomer could be dissolved in THF (polymerization solvent), the reaction solution

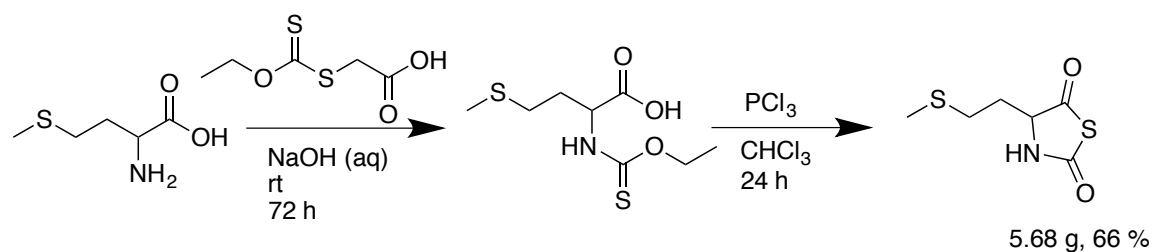
was observed to be heterogeneous following the addition of initiator (benzylamine or TMG). A control experiment containing monomer but no initiator in THF remained homogeneous and demonstrated that the observed precipitate in the heterogeneous

Table 4.7. Molecular weight characterization of PBLG polymerized at varying  $[M]_0$

$[M]_0$	$M_n$ (theo.) ( $\text{kg}\cdot\text{mol}^{-1}$ ) <sup>a</sup>	$M_n$ (SEC) ( $\text{kg}\cdot\text{mol}^{-1}$ ) <sup>b</sup>	PDI	DP	Conv. % at 48 h <sup>c</sup>
0.5 M (rt)	5.3	4.1	1.09	19	30
0.5 M	6.1	6.7	1.08	31	35
1.0 M	10.7	12.8	1.09	58	61
2.0 M	13.1	13.5	1.15	62	75

<sup>a</sup> Theoretical molecular weight was calculated based on conversion at 48 h as determined by <sup>1</sup>H NMR; <sup>b</sup> absolute molecular weights were determined using  $dn/dc=0.1292 \text{ mL/g}$ <sup>97</sup>; <sup>c</sup> reproduced from Figure 4.15.

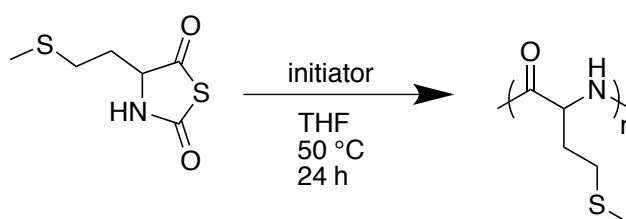
Scheme 4.6. Synthesis of DL-methionine NTA



solutions was that of an oligo/polymeric product and not precipitated monomer. The polypeptide is insoluble in common organic solvents but soluble in trifluoroacetic acid thus allowing for determination of molecular weight via end group analysis by <sup>1</sup>H NMR in deuterated trifluoroacetic acid (d-TFA) (Table 4.8). Monomer conversion was easily analyzed by <sup>1</sup>H NMR in deuterated trifluoroacetic acid as the peaks corresponding to the chiral center proton and methylene protons adjacent to the thioester were observed to shift downfield during the course of the polymerization. Polymerization activity was

investigated with either benzylamine or TMG initiator. At lower  $[M]_0:[I]_0$  ( $< 50:1$ ), benzylamine initiated polymerizations reached quantitative conversion within 24 h. However, at higher  $[M]_0:[I]_0$  (100:1, 200:1), the reactions reached approximately 66, 35% conversion respectively, even after allowing the reactions to proceed for 72 h. Based on theoretical  $M_n$  calculations from conversion, the 100, 200:1 reactions using benzylamine initiator would have terminated at similar molecular weight and  $DP_n$ .  $^1H$  NMR end group analysis of the resulting polypeptides revealed that the molecular weights were similar in those respective systems. In contrast, TMG initiated ROPs of DL-methionine NTA were able to reach quantitative conversion in reactions where  $[M]_0:[I]_0 = 100:1$  suggesting a more efficient polymerization using TMG initiator. Poly(DL-methionine) is insoluble in most common solvents and SEC-DRI-MALS analysis cannot be run on the resulting polymers from these ROPs to determine absolute  $M_n$  or PDI. Using  $^1H$  NMR end group analysis, it was determined that  $M_n$ s ranging from 2.9-7.9  $kg \cdot mol^{-1}$  and from 3.8 to 13.3  $kg \cdot mol^{-1}$  were able to be obtained by the ROP of DL-methionine NTA using benzylamine and TMG initiators respectively. Poly(DL-methionine) was obtained through stirring the heterogeneous reaction mixture with excess diethyl ether and collected via filtration, and drying under vacuum. The  $M_n$ s of the obtained polypeptides were characterized via  $^1H$  NMR end group analysis in deuterated trifluoroacetic acid (Figure 4.17).

Scheme 4.7. Polymerization of DL-methionine NTA



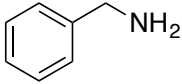
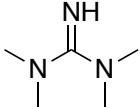


The versatility and flexibility of functionalizing the thioether side chains can be demonstrated through an alkylation of the thioether as was previously demonstrated by Kramer et al.<sup>132</sup> A simple methylation was carried out using poly(DL-methionine) and iodomethane in aqueous media (Scheme 4.8). After stirring for 48 h, the initial suspension of poly(DL-methionine) in water was observed to have become homogeneous suggesting that the iodomethane reacted with poly(DL-methionine). The alkylated polypeptide was purified via dialysis against NaCl (aq) (0.1 M) to perform anion exchange, and then against water to remove unreacted iodomethane. The final product was obtained from the lyophilization of the dialysis bag contents. Evidence for the successful methylation of poly(DL-methionine) was observed in the resulting <sup>1</sup>H NMR analysis in D<sub>2</sub>O (Figure 4.18) due to the change in chemical shift and relative peak intensity of the S-methyl thioether protons which integrated to six protons, relative to other protons of poly(DL-methionine). Additionally, the DP<sub>n</sub> of the resulting polypeptide from <sup>1</sup>H NMR end group analysis was comparable with respect to the parent polypeptide. This simple experiment only serves to demonstrate the possible post-polymerization functionalization of poly(DL-methionine) and serves to show that functional NTA monomers can be synthesized and subsequently polymerized in order to obtain the same polypeptides without the inherent disadvantages of NCA monomers. SEC-MALS-DRI analysis was attempted on the final methylated product but the polymer was insoluble in DMF/LiBr.

#### 4.3.2.2 Solid state ROP of amino acid based NTAs

Solid phase polymerization had previously been explored in the ROP of amino acid based NCAs noting that the overall molecular arrangement of the monomer molecules in a crystal have an effect on monomer reactivity.<sup>326</sup> We decided to further investigate the possibility of solid-state polymerization of BLG NTA because high local

Table 4.8. Molecular weight characterization data for the ROP of DL-methionine NTA initiated by BnNH<sub>2</sub> or TMG<sup>a</sup>

Initiator	[M] <sub>0</sub> : [I] <sub>0</sub>	<i>M</i> <sub>n</sub> (theo.) (kg·mol <sup>-1</sup> ) <sup>b</sup>	<i>M</i> <sub>n</sub> (NMR) (kg·mol <sup>-1</sup> ) <sup>c</sup>	DP	Conv. (%) <sup>d</sup>
	Control	-	-	-	0
	25	3.3	2.9	22	100
	50	6.6	6.0	46	100
	100	8.7	7.9	60	66
	25	3.3	3.8	29	100
	50	6.6	5.8	44	100
	100	13.2	13.3	101	100

<sup>a</sup> All polymerizations were conducted at [M]<sub>0</sub>=0.5 M, 50 °C, in THF for 24 h; <sup>b</sup> calculated based on conversion determined by <sup>1</sup>H NMR analysis and the repeat unit of poly(DL-methionine) (131 g·mol<sup>-1</sup>); <sup>c</sup> determined via end group analysis via <sup>1</sup>H NMR; <sup>d</sup> determined by <sup>1</sup>H NMR analysis of a crude reaction aliquot in d-TFA.

concentrations of the monomer molecules are afforded in the solid state. Solid-state polymerizations were carried out in hexanes, a poor solvent for BLG NTA, with hexylamine initiator ([M]<sub>0</sub>=0.5 M, 50 °C) (Scheme 4.9). Interestingly, polymerization control improved significantly in solid-state polymerizations with controllable molecular weights ranging from 6.4-22.0 kg·mol<sup>-1</sup> using hexylamine initiator and from 8.5-30.8 kg·mol<sup>-1</sup> using TMG initiator (up to approximately DP<sub>n</sub> =140, Table 4.9, 4.10). The obtained PDI from SEC-MALS-DRI analysis (Figure 4.19) were also adequate (1.24-1.29 using benzylamine initiator, 1.20-1.32 using TMG initiator) suggesting characteristics of a living polymerization in the solid state.

One aspect that has been previously discussed in preceding chapters is the living nature of the NCA ring-opening polymerization, which allows access to peptidomimetic

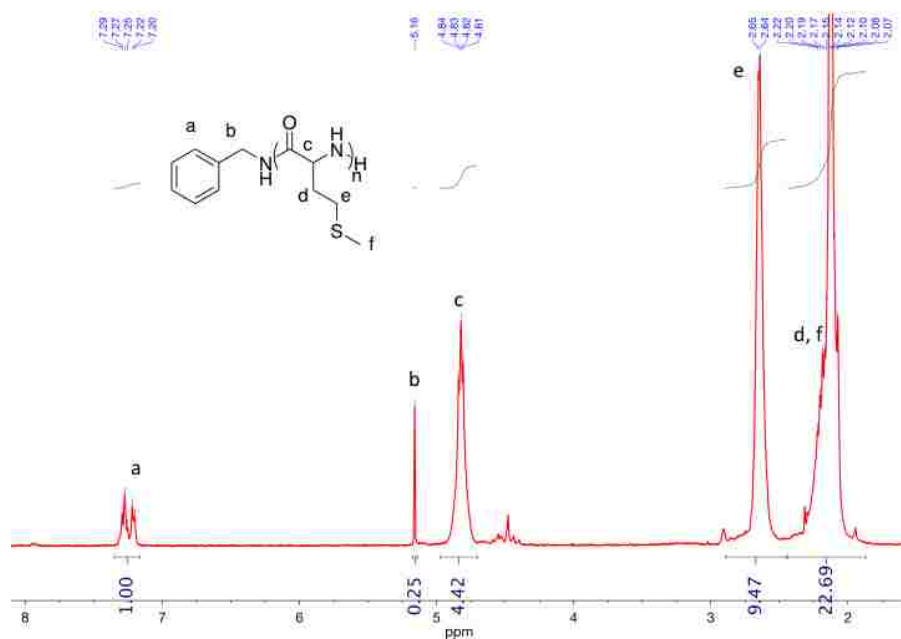
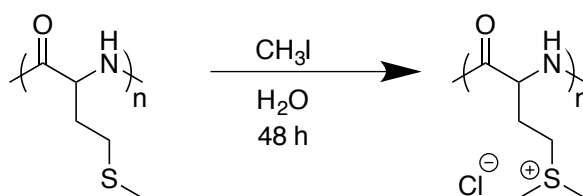


Figure 4.17.  $^1\text{H}$  NMR spectrum of benzylamine initiated poly(DL-methionine) ( $[\text{M}]_0:[\text{BnNH}_2]_0=25:1$ ,  $[\text{M}]_0=0.5$  M). The spectrum was collected in deuterated trifluoroacetic acid.

Scheme 4.8. Methylation of poly(DL-methionine) with iodomethane



polymers with predictable molecular weights and narrow PDI. To investigate the potential living nature of the solid-state polymerization of BLG NTA, a series of polymerizations ( $[\text{M}]_0:[\text{I}]_0=80:1$ ,  $[\text{M}]_0=0.5$  M, hexanes,  $50\text{ }^\circ\text{C}$ ) were carried out using hexylamine initiator with the reactions being quenched at various conversion percentages (Figure 4.19) as determined by  $^1\text{H}$  NMR. Molecular weights obtained from SEC-MALS-DRI analysis (Figure 4.20) were found to increase linearly based on conversion percent suggesting the living nature of the solid-state polymerization of BLG NTA.

Table 4.9. Molecular weight characterization data for the solid state ROP of BLG-NTA using hexylamine initiator <sup>a</sup>

$[M]_0:[I]_0$	$M_n$ (theo.) (kg·mol <sup>-1</sup> ) <sup>b</sup>	$M_n$ (SEC) (kg·mol <sup>-1</sup> ) <sup>c</sup>	PDI	DP
25	5.5	6.4	1.29	29
50	11.0	10.1	1.24	46
100	21.9	18.6	1.27	85
200	43.8	22.0	1.29	100
400	87.6	20.4	1.25	93

<sup>a</sup> All polymerizations were carried out at  $[M]_0 = 0.5$  M in hexanes at 50 °C for 24 h; <sup>b</sup> theoretical molecular weights were based on monomer conversion determined by <sup>1</sup>H NMR; <sup>c</sup> absolute molecular weights were determined using  $dn/dc = 0.1292$  mL/g.

It was also demonstrated that solid state polymerization methods using hexylamine initiator could also be extended to that of  $\epsilon$ -carbobenzyloxy-L-lysine NTA (Scheme 4.10) (Z-Lys NTA), which was unable to be polymerized to high conversion levels using conventional solution state ROP methods. The polymerization of Z-Lys NCA is a common route towards high molecular weight poly(lysine)s. The protection of the  $\epsilon$ -NH<sub>2</sub> of lysine is necessary as an exposed labile primary amine side chain could interfere with both the synthesis and polymerization of NCAs. Following polymerization, the carboxybenzyl protecting group can be removed either through acidolysis or hydrogenolysis, exposing the labile primary amine side chain.<sup>327</sup> Polymerization conversion was analyzed by removal of the solvent, dissolution of the remaining solid in a good solvent, and analyzed by <sup>1</sup>H NMR. Polymerizations of Z-Lys NTA via solid state revealed quantitative conversion was reached in approximately 45 h when  $[M]_0:[I]_0 < 100:1$ . From SEC-MALS-DRI, the obtained absolute molecular weights from SEC-DRI-MALS analysis ranged from 8.5-50.0 kg·mol<sup>-1</sup> and are comparable to those of theory up

Scheme 4.9. Solid-state polymerization of BLG NTA using hexylamine initiator

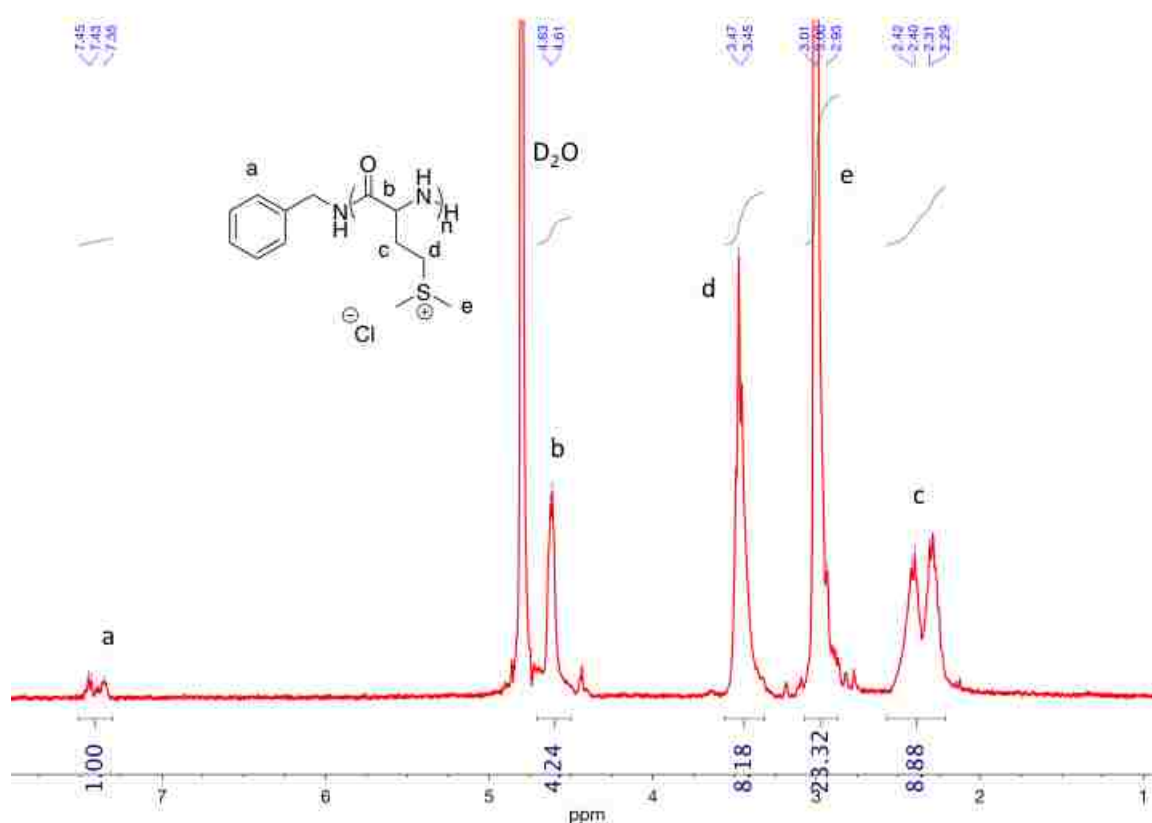
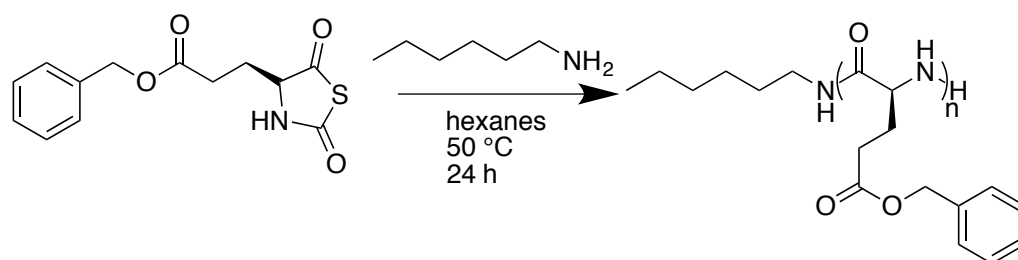


Figure 4.18.  $^1\text{H}$  NMR spectrum of poly(S,S-dimethyl-DL-methionine) obtained from the methylation of poly(DL-methionine) ( $[\text{M}]_0:[\text{I}]_0=25:1$ ,  $[\text{M}]_0=0.5\text{ M}$ ) with iodomethane followed by dialysis and lyophilization. The spectrum was collected in  $\text{D}_2\text{O}$ .

until  $[\text{M}]_0:[\text{I}]_0 > 200:1$  when the  $M_n$  is observed to deviate and PDI broadens (up to 1.60) (Table 4.11, Figure C2). This demonstrates both a slight expansion of the applicability of solid state polymerization methods of  $\alpha$ -amino acid NTAs and represents an alternative route to access high molecular weight poly(Z-lysine)s.

Table 4.10. Molecular weight characterization from the solid state ROP of BLG NTA using TMG initiator <sup>a</sup>

$[M]_0:[TMG]_0$	$M_n$ (theo.) ( $\text{kg}\cdot\text{mol}^{-1}$ ) <sup>b</sup>	$M_n$ (SEC) ( $\text{kg}\cdot\text{mol}^{-1}$ ) <sup>c</sup>	PDI	DP
25	5.5	8.5	1.20	39
50	11.0	11.5	1.32	52
100	21.9	21.8	1.30	99
200	43.8	30.8	1.27	140
400	87.6	30.4	1.27	139

<sup>a</sup> All polymerizations were conducted at 50 °C in hexanes at  $[M]_0=0.5$  M; <sup>b</sup> calculated based on conversion determined by <sup>1</sup>H NMR; <sup>c</sup> absolute molecular weight was determined using  $dn/dc=0.1292$   $\text{mL}\cdot\text{g}^{-1}$ .<sup>97</sup>

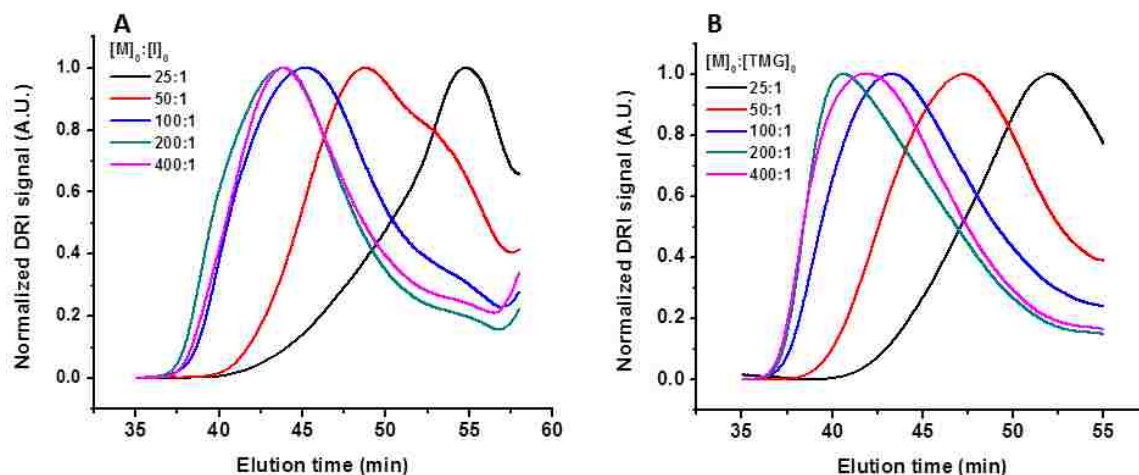


Figure 4.19. (A) SEC-DRI-MALS traces from the solid state polymerization of BLG-NTA using hexylamine initiator. (B) SEC-DRI-MALS traces from the solid state polymerization of BLG-NTA using TMG initiator.

#### 4.4 Conclusions

In this chapter, we have demonstrated that contrary to previous reports, the synthesis of well-defined high molecular weight polypeptides and polypeptoids can be accomplished via the ROP of their corresponding NTA monomers. The synthesis of both amino acid and R-NTAs is greatly simplified from their NCA counterparts as the

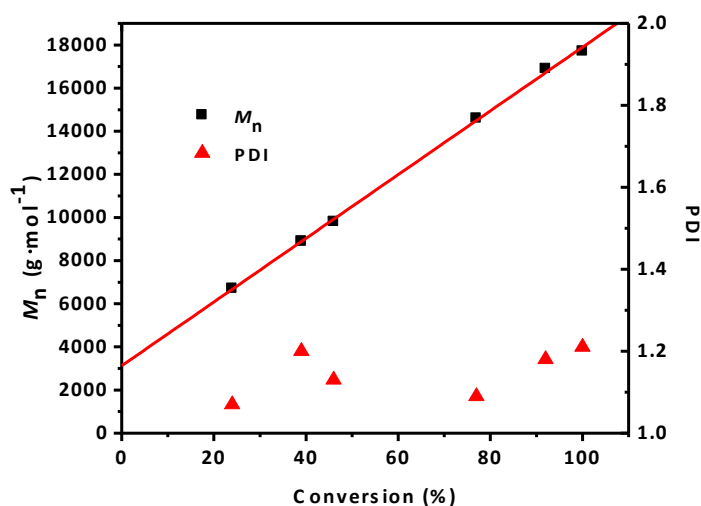


Figure 4.20. Plots of molecular weight ( $M_n$ ) and PDI versus conversion for the solid-state polymerization ( $[M]_0:[I]_0=80:1$ ,  $[M]_0=0.5$  M, hexanes,  $50$  °C,  $R^2=0.99$ ) of BLG NTA using hexylamine initiator. Absolute  $M_n$ s were determined using SEC-DRI-MALS with  $dn/dc=0.1292$  mL g<sup>-1</sup>.<sup>97</sup>

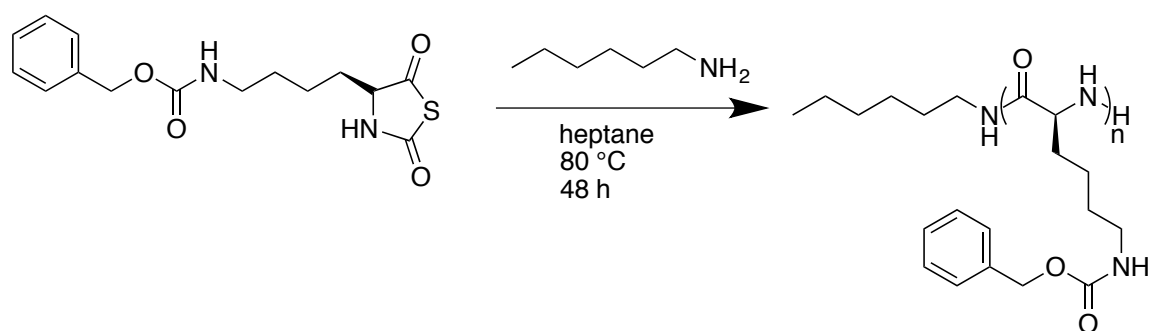
Table 4.11. Molecular weight characterization data for a series of poly(Z-lysine)s obtained from the solid state ROP of Z-lysine NTA<sup>a</sup>

$[M]_0:[I]_0$	$M_n$ (theo.) (kg·mol <sup>-1</sup> ) <sup>b</sup>	$M_n$ (GPC) (kg·mol <sup>-1</sup> ) <sup>c</sup>	PDI	DP	Conv. % (48 h) <sup>d</sup>
25:1	6.6	8.5	1.16	32	100
50:1	13.1	12.9	1.31	49	100
100:1	26.2	28.6	1.25	109	100
200:1	31.4	44.4	1.60	169	60
400:1	34.6	50.0	1.42	191	33

<sup>a</sup> All polymerizations were carried out at  $[M]_0=0.2$  M in heptane for 48 h; <sup>b</sup> calculated from conversion obtained from <sup>1</sup>H NMR and the repeat unit of poly(Z-lysine) = 262 g·mol<sup>-1</sup>; <sup>c</sup> absolute molecular weights were determined using previously measured  $dn/dc=0.123$  mL/g; <sup>d</sup> monomer conversion was analyzed by <sup>1</sup>H NMR.<sup>97</sup>

reactions can be carried out in open air and purification was accomplished under similar mild conditions. Me-NTA was demonstrated to be able to be polymerized using a small library of commercially available initiators. One initiator stood out, TMG, demonstrating promise in being able to achieve well-defined high molecular weight polysarcosines. The living character of TMG initiated polymerization was also demonstrated through enchainment. Although the ROP of Bu-NTA was also demonstrated, the monomer was

Scheme 4.10. ROP of Z-lysine NTA using hexylamine initiator via solid state methods



significantly less reactive than Me-NTA. We have reported the synthesis and characterization of a number of new amino acid based NTA monomers. It was found that the ROP of amino acid based NTA monomers proceeded poorly in solution state, obtaining polymer species whose molecular weights deviated significantly from theory or observing no monomer conversion at all. An improvement in polymerization activity was observed in the solid state polymerization of amino acid based NTAs as a series of well-controlled polypeptides could be synthesized up to approximately  $DP_n=140$ . However there seems to be an upper limit to the molecular weights obtainable by solid state methods. This work only represented a foray into the development of new monomers and polymerization systems to obtain the same polypeptides and polypeptoids previously obtained from the ROP of NCAs.

## 4.5 Experimental

### 4.5.1 Instrumentation and general considerations

All chemicals were used as received unless otherwise noted. Benzylamine, 1,1,3,3-tetramethylguanidine (TMG), hexamethyldisilazane (HMDS), *N*-heterocyclic carbenes (NHC), diazabicycloundecene (DBU), triazabicyclodecene (TBD), and *N*-methyl triazabicyclodecene (MTBD) initiators were also used as received. <sup>1</sup>H NMR spectra were recorded on a Bruker AV-400 and AVIII-400. Chemical shifts were



determined in reference to the protio impurities of the deuterated solvents ( $\text{CDCl}_3$ ). Size exclusion chromatography (SEC) analysis was carried out on an Agilent 1200 system (Agilent 1200 series degasser, isocratic pump, auto sampler and column heater) equipped with three Phenomenex 5  $\mu\text{m}$ , 300  $\text{\AA}$  $\times$ 7.8 mm columns [100  $\text{\AA}$ , 1000  $\text{\AA}$ , and Linear (2)], Wyatt DAWN EOS multiangle light scattering (MALS) detector (GaAs 30 mW laser at  $\lambda$ ) 690 nm], and Wyatt Optilab rEX differential refractive index (DRI) detector with a 690 nm light source. DMF containing 0.1 M LiBr was used as the eluent at a flow rate of 0.5  $\text{mL}\cdot\text{min}^{-1}$ . The column and the MALS and DRI detector temperatures were all maintained at ambient temperature (21  $^\circ\text{C}$ ). Data from SEC-MALS-DRI was processed using Wyatt Astra v 6.0 software.

#### 4.5.2 *N*-methyl *N*-thiocarboxyanhydrosulfide synthesis

*N*-methyl-NTA (Me-NTA) was synthesized according to previously reported literature.<sup>182,</sup>

190

Synthesis of *S*-ethoxythiocarbonyl mercaptoacetic acid (XAA). A typical synthesis of XAA is as follows. A round bottom flask was charged with potassium ethyl xanogenate (23.27 g, 145 mmol) and DI water (200 mL). A separate flask was charged with chloroacetic acid (13.72 g, 145 mmol), sodium hydroxide (5.80 g, 145 mmol) and distilled water (250 mL). The latter solution was subsequently added to the round bottom flask containing xanthate and stirred at ambient temperature for 24 h. The homogenous yellow solution was acidified with concentrated HCl, decanted into a separatory funnel, and extracted with chloroform (2  $\times$  200 mL). The combined organic layers were dried over  $\text{MgSO}_4$ , filtered, and concentrated to yield crude XAA as a yellow liquid. Purification via trituration in excess hexanes yielded XAA as a yellow crystals following filtration and drying under vacuum (20.28 g, 78%).

Synthesis of Me-NTA. A round bottom flask was charged with XAA (20.75 g, 115 mmol), sarcosine (10.26 g, 115 mmol), sodium hydroxide (9.21 g, 230 mmol), and DI water (200 mL). The contents were stirred at ambient temperature for 3 days. The solution was acidified with concentrated HCl and extracted with chloroform (200 mL). The organic layer was dried over MgSO<sub>4</sub>, filtered, and concentrated via rotary evaporation to give a crystalline intermediate. The intermediate was weighed (16.05 g, 90.6 mmol) and reconstituted in chloroform (200 mL). Phosphorus tribromide (4.3 mL, 45.3 mmol) was then added to the solution. The solution was allowed to stir at ambient temperature for 1 h. Saturated sodium bicarbonate (200 mL) was added to the solution and stirred vigorously. Violent bubbling was observed and when the bubbling subsided, the biphasic solution was decanted into a separatory funnel and further extracted via shaking and venting. The aqueous layer was discarded and the organic layer was further washed with distilled water (200 mL), and brine (200 mL), dried over MgSO<sub>4</sub>, filtered, and concentrated to yield crude NTA as a pale yellow liquid. Pure NTA was obtained via vacuum distillation at 120 °C, 100 mTorr as a clear liquid (5.73 g, 48 %).

#### 4.5.3 *N*-butyl *N*-thiocarboxyanhydrosulfide synthesis

Synthesis of *N*-butyl glycine hydrochloride. The synthetic procedure of *N*-butyl glycine hydrochloride was previously discussed in Chapter III.

Synthesis of *N*-butyl *N*-thiocarboxyanhydrosulfide. A round bottom flask was charged with *N*-butyl glycine hydrochloride (13.90 g, 82.9 mmol), XAA (14.95 g, 82.9 mmol), NaOH (9.95 g, 249 mmol), and DI water (300 mL). The resulting homogeneous yellow solution was stirred for 3 days at ambient temperature. The solution was acidified with concentrated HCl and the aqueous solution extracted with ethyl acetate (2 × 150 mL). The combined organic layers were dried over MgSO<sub>4</sub>, filtered, and concentrated to yield a yellow liquid, which was subsequently dissolved in chloroform (200 mL). Phosphorus

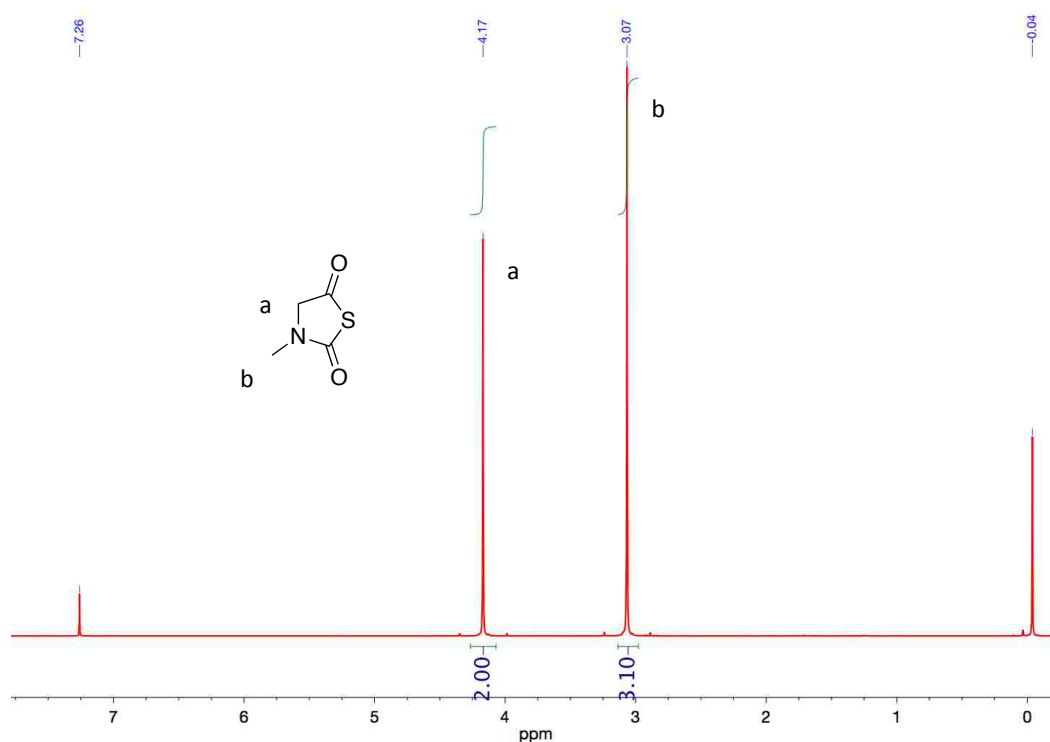


Figure 4.21.  $^1\text{H}$  NMR spectrum of Me-NTA in  $\text{CDCl}_3$ .

tribromide (3.96 mL, 41.5 mmol) was added via syringe all at once and the reaction was stirred at ambient temperature for 1 h. The reaction solution was subsequently washed with saturated sodium bicarbonate (200 mL), DI water (200 mL), and brine (200 mL). The chloroform layer was dried over  $\text{MgSO}_4$ , filtered, and concentrated to yield crude Bu-NTA as a yellow liquid. Bu-NTA was purified via column chromatography using a 1:7 ethyl acetate:petroleum ether as the mobile phase ( $R_f=0.24$ ). Bu-NTA solidifies when stored at  $-30\text{ }^\circ\text{C}$ , but liquefies at ambient temperature, similar to Bu-NCA (2.20 g, 15 %). ESI-MS: calc'd  $m/z$ : 174.0583, experimental  $m/z$ : 174.0582 ( $\text{M}+\text{H}^+$ )

#### 4.5.4 General polymerization procedure of Me-NTA

All polymerizations were conducted in either dichloromethane with initial monomer concentration  $[\text{M}]_0=1.0\text{ M}$  at ambient temperature for 18 h to reach high conversion. Polymers were precipitated into excess hexanes and dried at room temperature under

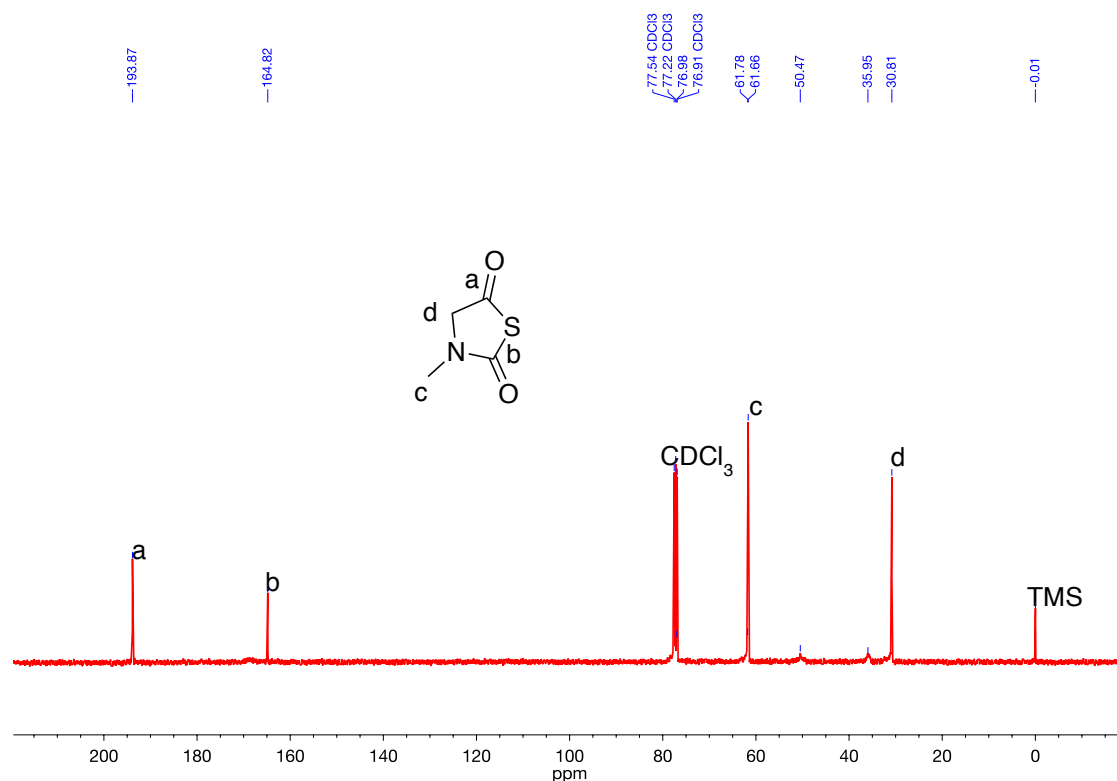


Figure 4.22.  $^{13}\text{C}^{23}$  NMR spectrum of Me-NTA in  $\text{CDCl}_3$ .

vacuum to yield the respective polymers as white solids. A representative polymerization procedure is as follows. In the glovebox, Me-NTA monomer (64 mg, 0.489 mmol,  $[\text{M}]_0 = 1.0 \text{ M}$ ) was weighed in an oven-dried vial and dissolved in anhydrous dichloromethane (440  $\mu\text{L}$ ). A known volume of a TMG/DCM stock solution (49  $\mu\text{L}$ , 4.89  $\mu\text{mol}$ , 0.1 M) was subsequently added. The reaction was stirred for 18 h at ambient temperature under a nitrogen atmosphere and then quenched by the addition of excess hexanes. Poly(sarcosine) as a white solid was isolated by suction filtration and drying under vacuum (26 mg, 76 %)

#### 4.5.5 General polymerization procedure of Bu-NTA

Bu-NTA was polymerized similarly to that of Me-NTA except that the reaction was carried out in THF at 50  $^\circ\text{C}$ .

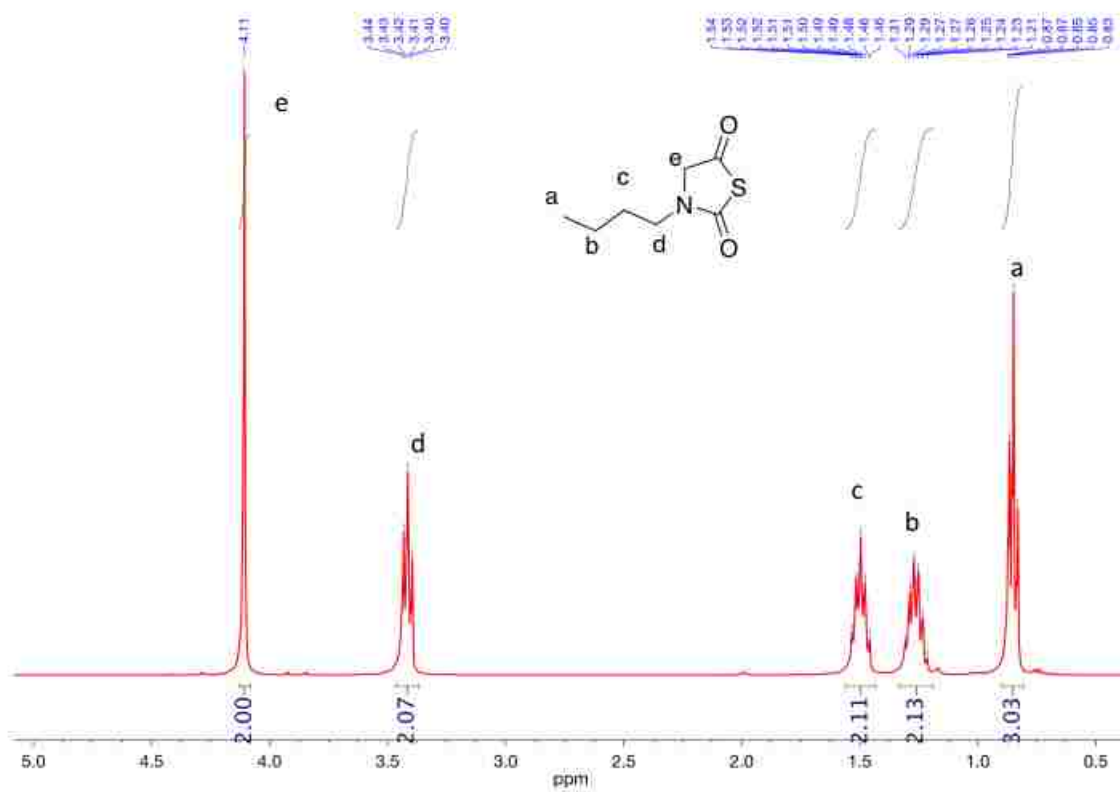


Figure 4.23.  $^1\text{H}$  NMR spectrum of Bu-NTA collected in  $\text{CDCl}_3$ .

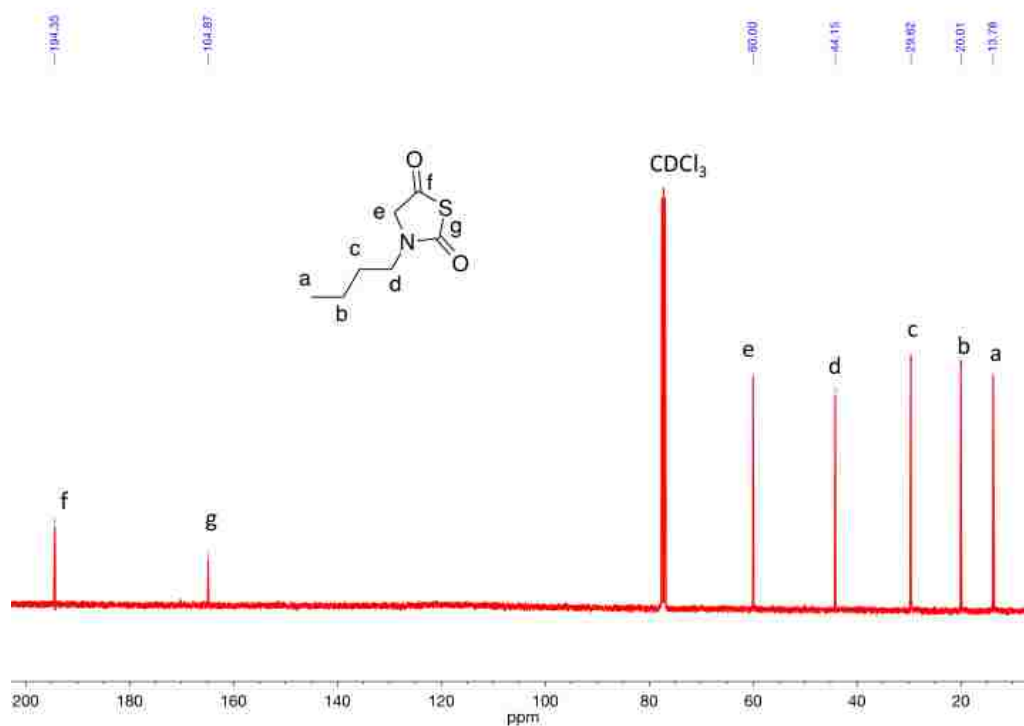


Figure 4.24.  $^{13}\text{C}$   $\{^1\text{H}\}$  NMR spectrum of Bu-NTA obtained in  $\text{CDCl}_3$ .

#### 4.5.6 DL-methionine *N*-thiocarboxyanhydrosulfide synthesis

DL-methionine NTA was synthesized similarly to Me-NTA. Unlike Me-NTA the intermediate compound isolated from the reaction between XAA and DL-methionine was cyclized in the presence of phosphorus trichloride (1.25 eq). The reaction solution was washed with saturated NaHCO<sub>3</sub> (200 mL), DI H<sub>2</sub>O (200 mL), and brine (200 mL). The organic layer was dried over MgSO<sub>4</sub>, filtered, and concentrated via rotary evaporation to yield a pale yellow liquid, which crystallized at room temperature to give the crude desired product. The product was recrystallized from dichloromethane and hexanes as an off white solid (5.68, 66 %).

ESI-MS: calc'd m/z: 192.0147, experimental m/z: 192.0148 (M+H<sup>+</sup>)

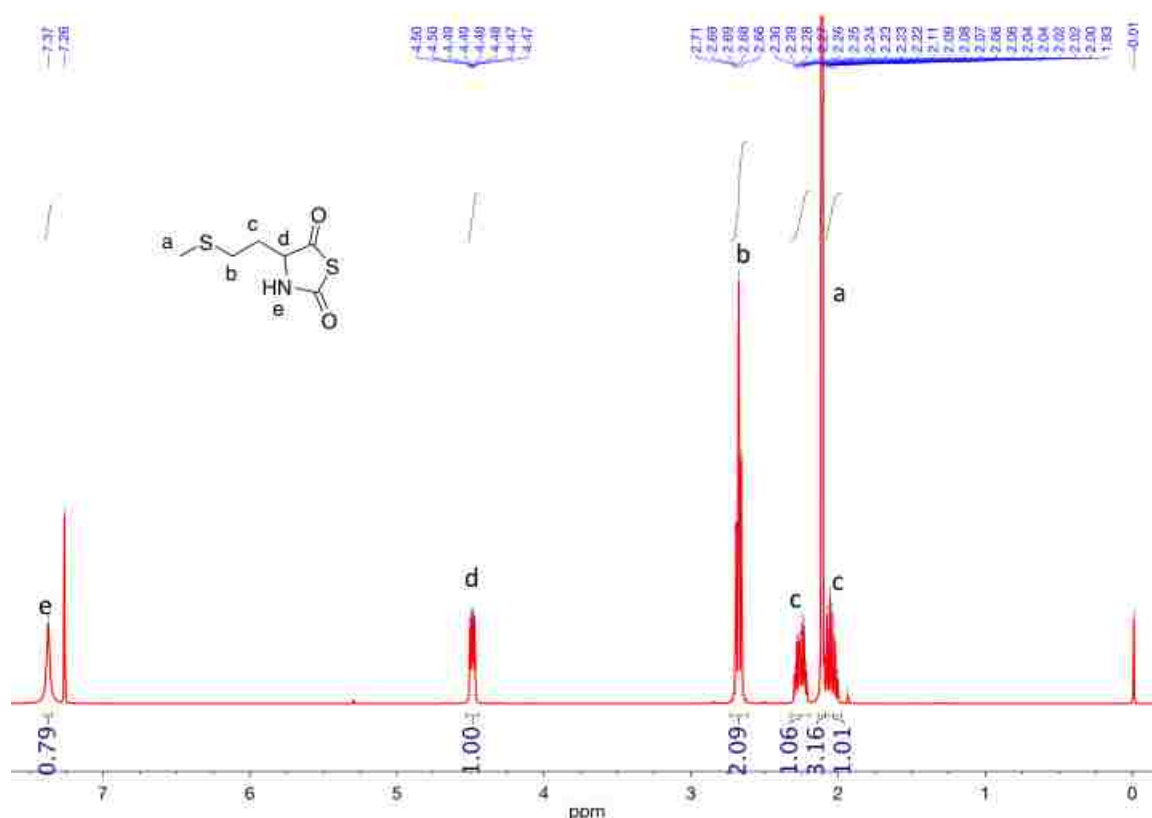


Figure 4.25. <sup>1</sup>H NMR spectrum of DL-methionine NTA collected in CDCl<sub>3</sub>.

#### 4.5.7 General polymerization procedure of DL-methionine NTA

All polymerizations were conducted in THF with initial monomer concentration  $[M]_0=0.5$  M at 50 °C. A representative polymerization procedure is as follows. In the glovebox, DL-methionine NTA (153 mg, 0.80 mmol) was weighed into an oven dried vial and dissolved in THF (754  $\mu$ L). A known volume of stock solution containing benzylamine in THF (46  $\mu$ L, 0.35 M,  $[M]_0:[BnNH_2]_0=50:1$ ) was added to the monomer solution. The contents were heated at 50 °C during which the reaction proceeded as a heterogeneous reaction. A control experiment set up under similar conditions but containing no initiator verified that DL-methionine NTA remained soluble in THF throughout the polymerization and the observed heterogeneity was due to polymerization activity. An aliquot of solution was removed and dissolved in deuterated trifluoroacetic acid for

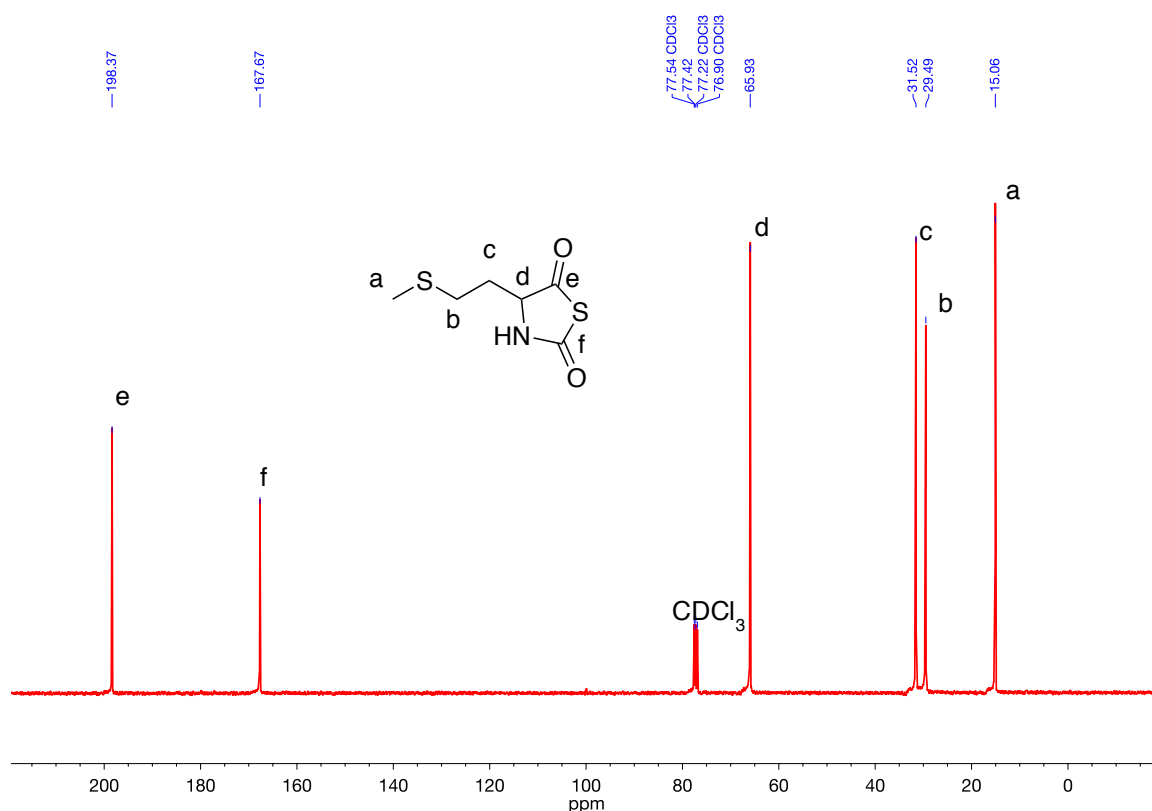


Figure 4.26.  $^{13}\text{C}^{23}$  NMR spectrum of DL-methionine NTA collected in  $\text{CDCl}_3$ .

conversion analysis via  $^1\text{H}$  NMR. Upon reaching quantitative conversion, the heterogeneous mixture was triturated with diethyl ether, filtered, and dried under vacuum to give poly(DL-methionine) as a white solid (57 mg, 54%)

#### 4.5.8 Methylation of poly(DL-methionine)

Poly(DL-methionine) was methylated using iodomethane according to a published procedure.<sup>132</sup> Briefly, poly(DL-methionine) (20 mg, 0.152 mmol) was suspended in DI water (3 mL) and iodomethane (28  $\mu\text{L}$ , 0.457 mmol, 3 equivalents per equivalent of polypeptide repeat unit) was subsequently added. The vial was covered with aluminum foil and stirred at ambient temperature for 48 h during which the suspension became homogeneous. The solution was further diluted with  $\text{H}_2\text{O}$  (5 mL) and dialyzed against  $\text{NaCl}$  (aq) (0.1 M) for 24 h and DI water for 48 h (MWCO=2 kDa). The contents of the bag were emptied and lyophilized to give the methylated product as a colorless solid. (11 mg, 49 %)

#### 4.5.9 Synthesis of $\gamma$ -benzyl-L-glutamate *N*-thiocarboxyanhydrosulfide (BLG NTA)

$\gamma$ -Benzyl-L-glutamate (10.30 g, 43.3 mmol) and XAA (7.82, 43.3 mmol) were suspended in saturated sodium bicarbonate solution (400 mL) and stirred for three days at ambient temperature during which the heterogeneous suspension became homogeneous. The solution was acidified with concentrated  $\text{HCl}$  and the aqueous solution was extracted with ethyl acetate ( $3 \times 100$  mL). The combined organic layers were dried over  $\text{MgSO}_4$  and concentrated to a viscous yellow liquid as the reaction intermediate. The reaction intermediate was dissolved in ethyl acetate (200 mL) and phosphorus trichloride (3.54 mL, 40.6 mmol) was added all at once. The reaction was stirred for 20 h before being washed with saturated sodium bicarbonate solution ( $2 \times 200$  mL), water (200 mL), and brine (100 mL). The organic layer was dried over  $\text{MgSO}_4$  and concentrated to yield the crude monomer as a white solid. Further purification was achieved via column



chromatography using an eluent of 3:2 hexanes:ethyl acetate. Crystals for X-ray crystallography analysis were grown from the slow evaporation of chloroform. (4.32 g, 42%)

#### 4.5.10 Solid state polymerization of BLG NTA

A typical solid state polymerization is as follows. BLG NTA (33 mg, 0.118 mmol) was weighed into a vial and suspended in hexanes (236  $\mu$ L). A known volume of a solution of hexylamine in hexanes (11  $\mu$ L, 133 mM) was subsequently added to the monomer suspension such that  $[M]_0=0.5$  M and  $[M]_0:[I]_0=80:1$ . The vial was sealed and stirred at 50  $^{\circ}$ C. Heterogenous aliquots were removed from the reaction vial, concentrated, and redissolved in  $CDCl_3$  for determining the percent conversion of monomer. PBLG as a white solid (16 mg, 62 %) was obtained by concentration of the heterogeneous reaction mixture under vacuum.

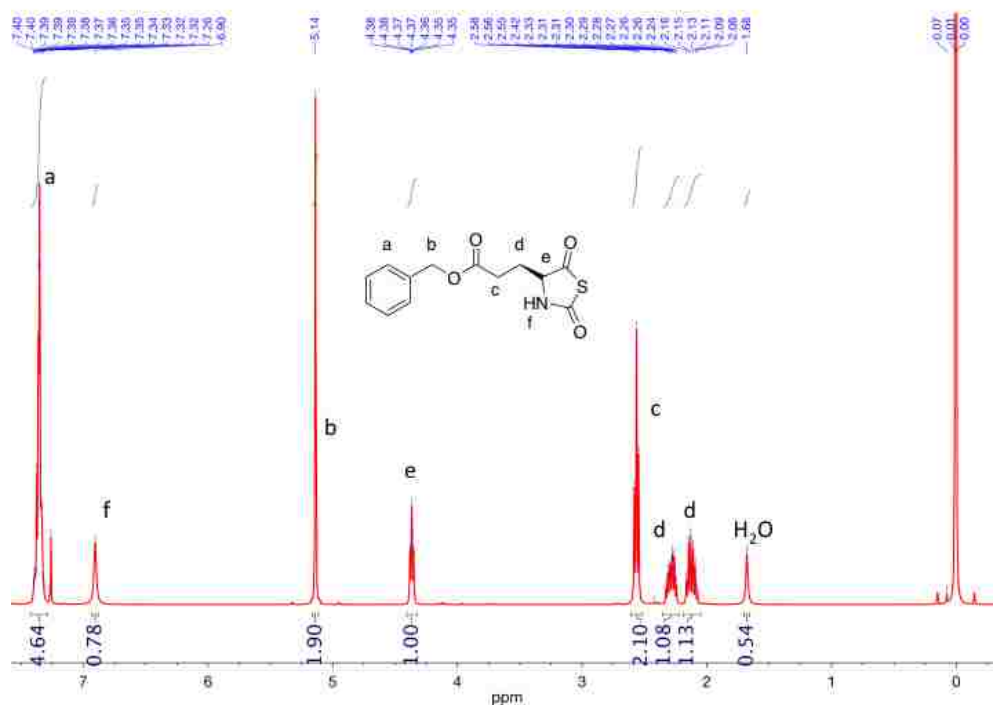


Figure 4.27.  $^1H$  NMR spectrum of BLG-NTA collected in  $CDCl_3$ .

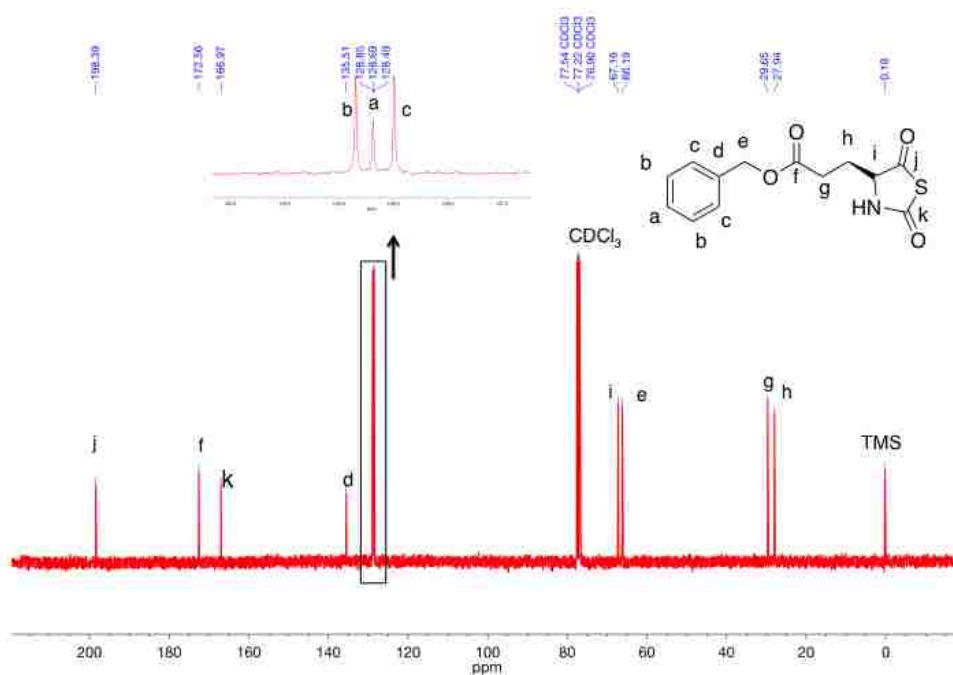


Figure 4.28.  $^{13}\text{C}\{^1\text{H}\}$  NMR spectrum of BLG NTA collected in  $\text{CDCl}_3$ .

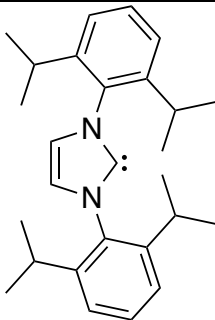
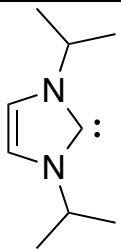
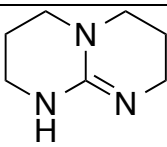
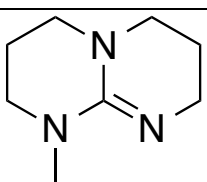
#### 4.6 Supplemental data for Chapter IV

Table C1. Molecular weight characterization data for HMDS initiated ROP of Me-NTA

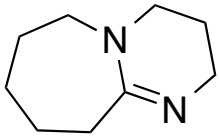
$[\text{M}]_0:[\text{BnNH}_2]_0$	$M_n$ (theo.) ( $\text{kg}\cdot\text{mol}^{-1}$ ) <sup>b</sup>	$M_n$ (GPC) ( $\text{kg}\cdot\text{mol}^{-1}$ ) <sup>c</sup>	PDI	$\text{DP}^d$
25	1.8	2.4	1.22	27
100	7.1	5.8	1.20	82
400	28.4	10.6	1.06	149

<sup>a</sup> All polymerizations were performed at  $[\text{M}]_0 = 1.0$  M in dichloromethane; <sup>b</sup> based on conversion calculated from FTIR analysis; <sup>c</sup> absolute molecular weights were calculated using previously determined  $\text{dn}/\text{dc} = 0.0987(17)$   $\text{mL}/\text{g}^{147}$ ; <sup>d</sup> based on  $M_n$  obtained from SEC-DRI-MALS and the repeat unit of PNMG =  $71$   $\text{g}\cdot\text{mol}^{-1}$ .

Table C2. Molecular weight characterization for a series of polymerizations of Me-NTA initiated by various organobases and organocatalysts

Initiator	$[M]_0:[I]_0$	$M_n$ (theo.) ( $\text{kg}\cdot\text{mol}^{-1}$ )	$M_n$ (SEC) ( $\text{kg}\cdot\text{mol}^{-1}$ )	PDI	DP
	25	1.8	2.4	1.30	34
	50	3.6	5.6	1.15	79
	100	7.1	9.3	1.05	131
	200	14.2	12.0	1.06	169
	400	28.4	16.2	1.03	228
	25	1.8	2.2	1.09	31
	50	3.6	3.9	1.12	55
	100	7.1	4.7	1.06	66
	200	14.2	6.4	1.04	90
	400	28.4	10.4	1.04	146
	25	1.8	4.8	1.16	68
	50	3.6	2.5	1.13	35
	100	7.1	3.6	1.05	50
	200	14.2	7.4	1.06	104
	400	28.4	16.8	1.07	236
	25	1.8	2.3	1.13	32
	50	3.6	3.8	1.20	54
	100	7.1	5.3	1.09	75
	200	14.2	8.1	1.04	114
	400	28.4	12.0	1.08	169

(Table C2 continued)

Initiator	$[M]_0:[I]_0$	$M_n$ (theo.) ( $\text{kg}\cdot\text{mol}^{-1}$ )	$M_n$ (SEC) ( $\text{kg}\cdot\text{mol}^{-1}$ )	PDI	DP
	25	1.8	2.3	1.17	32
	50	3.6	2.4	1.09	34
	100	7.1	13.5	1.07	190
	200	14.2	31.0	1.04	436
	400	28.4	37.4	1.01	526

<sup>a</sup> All polymerizations were performed at  $[M]_0 = 1.0$  M in dichloromethane; <sup>b</sup> based on conversion calculated from FTIR analysis; <sup>c</sup> absolute molecular weights were calculated using previously determined  $dn/dc = 0.0987$  mL/g; <sup>d</sup> based on  $M_n$  obtained from SEC-DRI-MALS and the repeat unit of PNMG= $71$   $\text{g}\cdot\text{mol}^{-1}$ .

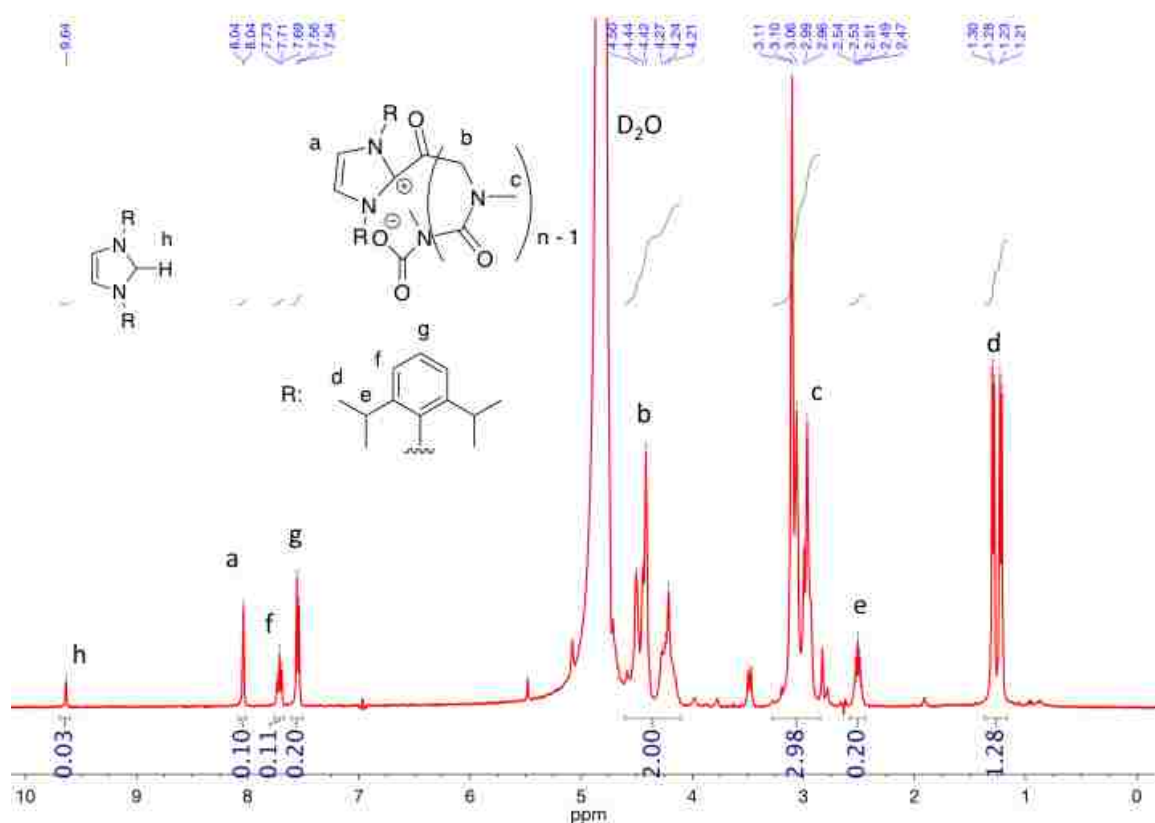


Figure C1. <sup>1</sup>H NMR spectrum of polysarcosine obtained from the ROP of Me-NTA with NHC initiator ( $[M]_0:[\text{NHC}]_0=25:1$ ,  $[M]_0=1.0$  M in  $\text{CH}_2\text{Cl}_2$ ). The spectrum was collected in  $\text{D}_2\text{O}$ .

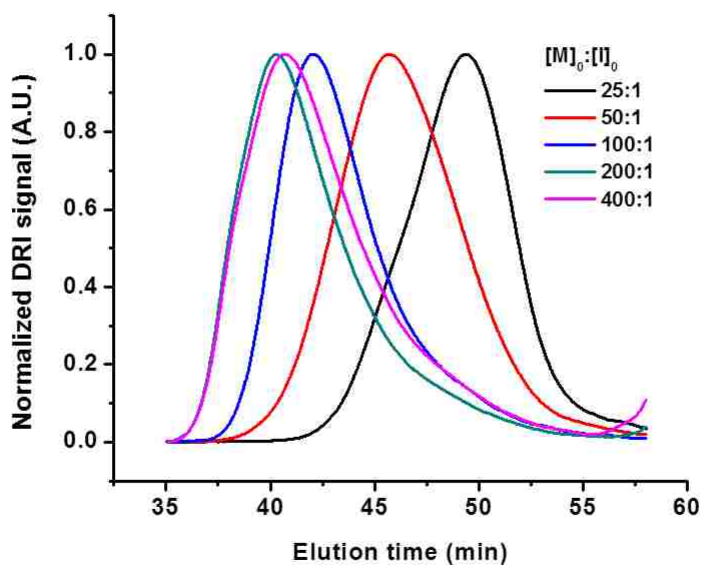


Figure C2. SEC-DRI-MALS chromatograms for a series of poly(Z-lysine)s obtained from the solid state ROP of Z-Lys NTA using hexylamine initiator ( $[M]_0=0.2$  M, 80 °C, 48 h in heptane).

## CHAPTER V. CONCLUSIONS AND FUTURE WORK

The findings covered in this work are only an iota of the ongoing research involved with polypeptides and polypeptoids. It is hoped that polypeptides and polypeptoids can serve as ideal biomaterials due to low exhibited cytotoxicity. This differs significantly from acrylic based polymers, which have been shown to illicit an immune response and are not degradable by proteolysis. There are numerous challenges to overcome such as the sensitivity of NCAs to moisture. However, research interest in polypeptides and polypeptoids is still growing and there are still many niches that can be further explored in the research and development of polypeptides and polypeptoids as ideal candidates for application as biomaterials.

A series of glycopolypeptides were synthesized and investigated to better understand carbohydrate-lectin interactions with ConA. It was found that polypeptide chain lengths had the most significant effect on the observed binding kinetics and binding stoichiometry as a high  $DP_n$  would provide the most binding sites to allow for fast binding with ConA and the most space to accommodate the large ConA tetramer. Backbone architecture was also found to affect binding kinetics as random coil glycopolypeptide analogs were found to bind to ConA slower than their helical counterparts. However, at higher  $DP_n$  it is proposed that the random coil structure is more extended, allowing for comparable binding kinetics to a helical analog of similar  $DP_n$ . Ultimately, even with ideal side chain presentation (helical conformation), sterics along the polypeptide backbone prevents many mannose binding sites from being accessed by ConA, lowering overall binding efficiency as suggested by the increasing mannose/ConA as measured by quantitative precipitation assay. The obtained results still pale in comparison to those of previously studied glycopolymers as they have been found to bind faster and more efficiently than the studied glycopolypeptides. Spacing the binding

epitopes apart using the non-binding galactose does not appear to be a sufficient remedy as the steric bulk along the polymer backbone is still the same and appeared to only further lower binding rate and efficiency. A possible solution may be to vary the distances between the polypeptide backbone and the mannose binding moieties in a mixed linker length glycopolyptide species. A series of mannose azides with varying carbon chain lengths (e.g. 2-azidooctyl, 2-azidodecyl mannose) could be synthesized using a parallel synthetic procedure used to obtain 2-azidoethyl mannose. Grafting mannose moieties with varying alkyl chain lengths will vary the side chain length in a particular glycopolyptide species. Used in conjunction with mannose moieties of shorter chain lengths, this could produce glycopolyptides with multiple “layers” on which binding events could occur. The variation side chain lengths would allow for some binding between ConA and mannose to occur farther away from the main chain and may relieve some steric overcrowding of the glycopolyptide chain although steric overcrowding appears to be inevitable. One potential setback of this synthetic strategy is that water solubility of the glycopolyptide may be affected through the introduction of long alkyl chains.

We have shown that the nucleophilicity of the hydroxyl group of alcohols can be activated in the presence of an organomediator and allow the alcohol to act as a nucleophile in the ROP of Bu-NCA to obtain well-defined high molecular weight polypeptoids. The biggest limiting factors were alcohol sterics and electronics. It was also noted that the organomediator of choice, TMG, was able to participate as an initiator in the reaction although its pathway was superseded by that of the alcohol. It would be interesting to investigate other species which may also activate the alcohol through hydrogen bonding interactions but not participate as an initiator. Additionally, although macroinitiation using a PEG-OH was demonstrated, other polymeric species could be

investigated as potential macroinitiators such as polyesters with terminal hydroxyl groups. Potential new interesting materials could be realized from the copolymerization of a polyester with a polypeptoid without the need for end chain functionalization.

*N*-thiocarboxyanhydrosulfides (NTA) are now being explored as potential candidates used in parallel to NCAs in the synthesis of polypeptides and polypeptoids. NTA monomers possess several advantages over NCAs that would present them as viable alternatives in the synthesis of polypeptoids. The first of these advantages is the simplicity of monomer synthesis. Because of the sensitivity of the oxygen anhydride to moisture, the synthesis of R-NCAs requires moisture-free conditions and the use of dry solvent for the cyclization reaction between the monomer precursor and the phosphorus trihalide cyclizing agent. R-NCAs are purified either by sublimation or column chromatography using dry solvent for the mobile phase and packing. In contrast, the synthesis of R-NTAs can be completed in open air and purification can be accomplished through vacuum distillation or column chromatography using regular solvents. NTA monomers have also been shown to remain stable under ambient conditions. The living nature of the ROP of Me-NTA using a variety of initiators to obtain high molecular weight polysarcosines was demonstrated under milder conditions than those previously reported. We believe that we can further expand the library of known R-NTAs using the synthetic techniques we have developed during the course of this study to demonstrate the feasibility of R-NTAs as alternative monomers to obtain well-defined polypeptoids. This would especially be helpful in the synthesis of poly(*N*-ethyl glycine) and poly(*N*-allyl glycine) whose respective R-NCA monomers have a propensity to self-initiate.

It is proposed that the same inherent advantages found in R-NTAs could be carried over to the synthesis of amino acid based NTAs. We have synthesized and characterized two polypeptide based NTA monomers based on poly( $\gamma$ -benzyl-L-



glutamate), one of the most widely studied polypeptides, and poly(DL-methionine), whose ability to undergo post-polymerization modification has been previously demonstrated. It was revealed that significant racemization occurs in the synthesis of BLG-NTA, affecting the optical purity of the product. Polymerization of racemic monomers can introduce disorder into the polypeptide system and affect the resulting secondary structure as demonstrated in Chapter II. Thus, prevention of racemization during NTA synthesis is important and must be addressed. Possible remedies to reduce or eliminate racemization to obtain optically pure NTAs that being explored are the reduction of reaction time and temperature, and the use of a less sterically hindered xanthate starting material, the latter of which has been demonstrated to reduce the rate of enolization of the azlactone cyclization reaction intermediate, which is susceptible to racemization.

The polymerization behavior of amino acid based NTAs is markedly different than that of R-NTAs; solution state polymerization activity appears to be poor. This is one area which will need to be further investigated as it has been shown that traditional polymerization techniques (e.g. primary amine mediation in solution state) either produce polypeptides whose molecular weights deviated significantly from theory or yielded no polymerization at all. Solid state polymerization of BLG NTA could be used to obtain well-controlled PBLGs but only up to approximately  $DP_n=140$ . Thus, additional work needs to be done to find an adequate initiating system to allow access to higher molecular weight polypeptides from the ROP of amino acid based NTAs. Advancement in polypeptide and polypeptoid synthesis from the ROP of NTAs could allow researchers without the advanced synthetic capability to handle NCAs access to well-defined polypeptides and polypeptoids.

## REFERENCES

1. Dalsin, J. L.; Hu, B.-H.; Lee, B. P.; Messersmith, P. B., Mussel Adhesive Protein Mimetic Polymers for the Preparation of Nonfouling Surfaces. *J. Am. Chem. Soc.* **2003**, *125* (14), 4253-4258.
2. Dalsin, J. L.; Lin, L.; Tosatti, S.; Vörös, J.; Textor, M.; Messersmith, P. B., Protein Resistance of Titanium Oxide Surfaces Modified by Biologically Inspired mPEG–DOPA. *Langmuir* **2005**, *21* (2), 640-646.
3. Statz, A. R.; Meagher, R. J.; Barron, A. E.; Messersmith, P. B., New Peptidomimetic Polymers for Antifouling Surfaces. *J. Am. Chem. Soc.* **2005**, *127* (22), 7972-7973.
4. Deming, T. J., Synthetic polypeptides for biomedical applications. *Prog. Polym. Sci.* **2007**, *32* (8–9), 858-875.
5. Statz, A. R.; Barron, A. E.; Messersmith, P. B., Protein, cell and bacterial fouling resistance of polypeptoid-modified surfaces: effect of side-chain chemistry. *Soft Matter* **2008**, *4* (1), 131-139.
6. Statz, A. R.; Park, J. P.; Chongsiriwatana, N. P.; Barron, A. E.; Messersmith, P. B., Surface-immobilized antimicrobial peptoids. *Biofouling* **2008**, *24* (6), 439-448.
7. Statz, A. R.; Kuang, J.; Ren, C.; Barron, A. E.; Szleifer, I.; Messersmith, P. B., Experimental and theoretical investigation of chain length and surface coverage on fouling of surface grafted polypeptoids. *Biointerphases* **2009**, *4* (2), FA22-FA32.
8. Brubaker, C. E.; Messersmith, P. B., The Present and Future of Biologically Inspired Adhesive Interfaces and Materials. *Langmuir* **2012**, *28* (4), 2200-2205.
9. Lau, K. H. A.; Ren, C.; Park, S. H.; Szleifer, I.; Messersmith, P. B., An Experimental–Theoretical Analysis of Protein Adsorption on Peptidomimetic Polymer Brushes. *Langmuir* **2012**, *28* (4), 2288-2298.
10. Lau, K. H. A.; Ren, C.; Sileika, T. S.; Park, S. H.; Szleifer, I.; Messersmith, P. B., Surface-Grafted Polysarcosine as a Peptoid Antifouling Polymer Brush. *Langmuir* **2012**, *28* (46), 16099-16107.
11. Lau, K. H. A., Peptoids for biomaterials science. *Biomater. Sci.* **2014**, *2* (5), 627-633.

12. Lau, K. H. A.; Sileika, T. S.; Park, S. H.; Sousa, A. M. L.; Burch, P.; Szleifer, I.; Messersmith, P. B., Molecular Design of Antifouling Polymer Brushes Using Sequence-Specific Peptoids. *Adv. Mater. Interf.* **2015**, *2* (1), 1400225.
13. Duncan, R., The dawning era of polymer therapeutics. *Nat. Rev. Drug Discov.* **2003**, *2* (5), 347-360.
14. Rickert, E. L.; Trebley, J. P.; Peterson, A. C.; Morrell, M. M.; Weatherman, R. V., Synthesis and Characterization of Bioactive Tamoxifen-Conjugated Polymers. *Biomacromolecules* **2007**, *8* (11), 3608-3612.
15. Colak, S.; Nelson, C. F.; Nüsslein, K.; Tew, G. N., Hydrophilic Modifications of an Amphiphilic Polynorbornene and the Effects on its Hemolytic and Antibacterial Activity. *Biomacromolecules* **2009**, *10* (2), 353-359.
16. Heller, P.; Birke, A.; Huesmann, D.; Weber, B.; Fischer, K.; Reske-Kunz, A.; Bros, M.; Barz, M., Introducing PeptoPlexes: Polylysine-block-Polysarcosine Based Polyplexes for Transfection of HEK 293T Cells. *Macromol. Biosci.* **2014**, *14* (10), 1380-1395.
17. Wang, H.; Tang, L.; Tu, C.; Song, Z.; Yin, Q.; Yin, L.; Zhang, Z.; Cheng, J., Redox-Responsive, Core-Cross-Linked Micelles Capable of On-Demand, Concurrent Drug Release and Structure Disassembly. *Biomacromolecules* **2013**, *14* (10), 3706-3712.
18. Birke, A.; Huesmann, D.; Kelsch, A.; Weilbacher, M.; Xie, J.; Bros, M.; Bopp, T.; Becker, C.; Landfester, K.; Barz, M., Polypeptoid-block-polypeptide Copolymers: Synthesis, Characterization, and Application of Amphiphilic Block Copolypept(o)ides in Drug Formulations and Miniemulsion Techniques. *Biomacromolecules* **2014**, *15* (2), 548-557.
19. Li, A.; Lu, L.; Li, X.; He, L.; Do, C.; Garno, J. C.; Zhang, D., Amidine-Mediated Zwitterionic Ring-Opening Polymerization of N-Alkyl N-Carboxyanhydride: Mechanism, Kinetics, and Architecture Elucidation. *Macromolecules* **2016**, *49* (4), 1163-1171.
20. Deming, T. J., Methodologies for preparation of synthetic block copolypeptides: materials with future promise in drug delivery. *Adv. Drug Deliv. Rev.* **2002**, *54* (8), 1145-1155.
21. Gibson, M. I.; Barker, C. A.; Spain, S. G.; Albertin, L.; Cameron, N. R., Inhibition of Ice Crystal Growth by Synthetic Glycopolymers: Implications for the Rational Design of Antifreeze Glycoprotein Mimics. *Biomacromolecules* **2009**, *10* (2), 328-333.

22. Reyes, F. T.; Guo, L.; Hedgepeth, J. W.; Zhang, D.; Kelland, M. A., First Investigation of the Kinetic Hydrate Inhibitor Performance of Poly(N-alkylglycine)s. *Energy & Fuels* **2014**, *28* (11), 6889-6896.
23. Cheng, Y.; He, C.; Xiao, C.; Ding, J.; Zhuang, X.; Chen, X., Versatile synthesis of temperature-sensitive polypeptides by click grafting of oligo(ethylene glycol). *Polym. Chem.* **2011**, *2* (11), 2627-2634.
24. Block, H., *Poly( $\gamma$ -benzyl-L-glutamate) and Other Glutamic Acid Containing Polymers*. Gordon and Breach: New York, 1983.
25. Whitesides, G. M.; Grzybowski, B., Self-Assembly at All Scales. *Science* **2002**, *295* (5564), 2418-2421.
26. Gkikas, M.; Iatrou, H.; Thomaidis, N. S.; Alexandridis, P.; Hadjichristidis, N., Well-Defined Homopolypeptides, Copolypeptides, and Hybrids of Poly(l-proline). *Biomacromolecules* **2011**, *12* (6), 2396-2406.
27. Guo, L.; Li, J.; Brown, Z.; Ghale, K.; Zhang, D., Synthesis and characterization of cyclic and linear helical poly( $\alpha$ -peptoid)s by N-heterocyclic carbene-mediated ring-opening polymerizations of N-substituted N-carboxyanhydrides. *Peptide Sci.* **2011**, *96* (5), 596-603.
28. Mannige, R. V.; Haxton, T. K.; Proulx, C.; Robertson, E. J.; Battigelli, A.; Butterfoss, G. L.; Zuckermann, R. N.; Whitlam, S., Peptoid nanosheets exhibit a new secondary-structure motif. *Nature* **2015**, *526* (7573), 415-420.
29. Barron, A. E.; Zuckerman, R. N., Bioinspired polymeric materials: in-between proteins and plastics. *Curr. Opin. Chem. Biol.* **1999**, *3* (6), 681-687.
30. Patch, J. A.; Barron, A. E., Mimicry of bioactive peptides via non-natural, sequence-specific peptidomimetic oligomers. *Curr. Opin. Chem. Biol.* **2002**, *6* (6), 872-877.
31. Webster, R.; Didier, E.; Harris, P.; Siegel, N.; Stadler, J.; Tilbury, L.; Smith, D., PEGylated Proteins: Evaluation of Their Safety in the Absence of Definitive Metabolism Studies. *Drug Metab. Dispos.* **2007**, *35* (1), 9-16.
32. Hamad, I.; Hunter, A. C.; Szebeni, J.; Moghimi, S. M., Poly(ethylene glycol)s generate complement activation products in human serum through increased alternative pathway turnover and a MASP-2-dependent process. *Mol. Immunol.* **2008**, *46* (2), 225-232.

33. Manning, M. C.; Patel, K.; Borchardt, R. T., Stability of Protein Pharmaceuticals. *Pharmaceut. Res.* **1989**, *6* (11), 903-918.
34. Moghimi, S. M.; Hunter, A. C.; Dadswell, C. M.; Savay, S.; Alving, C. R.; Szebeni, J., Causative factors behind poloxamer 188 (Pluronic F68, Flocor™)-induced complement activation in human sera: A protective role against poloxamer-mediated complement activation by elevated serum lipoprotein levels. *Biochim. Biophys. Acta* **2004**, *1689* (2), 103-113.
35. Shechter, Y.; Burstein, Y.; Patchornik, A., Selective oxidation of methionine residues in proteins. *Biochemistry* **1975**, *14* (20), 4497-4503.
36. Katchalski, E.; Grossfeld, I.; Frankel, M., Poly-condensation of  $\alpha$ -Amino Acid Derivatives. III. Poly-lysine. *J. Am. Chem. Soc.* **1948**, *70* (6), 2094-2101.
37. Lundbland, G.; Elander, M.; Manhem, L., Proteolysis of Some Synthetic Poly- $\alpha$ -amino Acids. *Acta Chem. Scand. B* **1975**, *29*, 937-947.
38. Martin, S. M.; Jönsson, A. G., An extracellular protease from *Aspergillus Fumigatus*. *Can. J. Biochem.* **1965**, *43* (10), 1745-1753.
39. Miller, W. G., Degradation of Poly- $\alpha$ ,L-glutamic Acid. I. Degradation of High Molecular Weight PGA by Papain. *J. Am. Chem. Soc.* **1961**, *83* (2), 259-265.
40. Waley, S. G.; Watson, J., The action of trypsin on polylysine. *Biochemical Journal* **1953**, *55* (2), 328-337.
41. Waley, S. G.; Watson, J., Trypsin-catalysed transpeptidations. *Biochemical Journal* **1954**, *57* (4), 529-538.
42. Cao, J.; Hu, P.; Lu, L.; Chan, B. A.; Luo, B.-H.; Zhang, D., Non-ionic water-soluble "clickable" [small  $\alpha$ ]-helical polypeptides: synthesis, characterization and side chain modification. *Polym. Chem.* **2015**.
43. Creel, H. S.; Fournier, M. J.; Mason, T. L.; Tirrell, D. A., Genetically directed syntheses of new polymeric materials: efficient expression of a monodisperse copolypeptide containing fourteen tandemly repeated -(AlaGly)<sub>4</sub>ProGluGly- elements. *Macromolecules* **1991**, *24* (5), 1213-1214.
44. McGrath, K. P.; Fournier, M. J.; Mason, T. L.; Tirrell, D. A., Genetically directed syntheses of new polymeric materials. Expression of artificial genes encoding proteins

with repeating -(AlaGly)<sub>3</sub>ProGluGly- elements. *J. Am. Chem. Soc.* **1992**, *114* (2), 727-733.

45. Merrifield, R. B., Solid Phase Peptide Synthesis. I. The Synthesis of a Tetrapeptide. *J. Am. Chem. Soc.* **1963**, *85* (14), 2149-2154.

46. Sun, H.; Zhang, J.; Liu, Q.; Yu, L.; Zhao, J., Metal-Catalyzed Copolymerization of Imines and CO: A Non-Amino Acid Route to Polypeptides. *Angew. Chem. Int. Ed.* **2007**, *46* (32), 6068-6072.

47. Leuchs, H., Ueber die Glycin-carbonsäure. *Ber. Dtsch. Chem. Ges.* **1906**, *39* (1), 857-861.

48. Kricheldorf, H. R., *α-Aminoacid-N-Carboxyanhydrides and Related Heterocycles*. Springer-Verlag: Germany, 1987.

49. Fuchs, F., Über N-Carbonsäure-anhydride. *Ber. Dtsch. Chem. Ges.* **1922**, *55* (9), 2943-2943.

50. Farthing, A. C., 627. Synthetic polypeptides. Part I. Synthesis of oxazolid-2 : 5-diones and a new reaction of glycine. *J. Chem. Soc.* **1950**, (0), 3213-3217.

51. Daly, W. H.; Poché, D., The preparation of N-carboxyanhydrides of  $\alpha$ -amino acids using bis(trichloromethyl)carbonate. *Tetrahedron Lett.* **1988**, *29* (46), 5859-5862.

52. Guillermain, C.; Gallot, B., Synthesis and liquid crystalline structures of poly(L-lysine) containing undecanamidobiphenyl units in the side chains. *Liq. Cryst.* **2002**, *29* (1), 141-153.

53. Poché, D. S.; Moore, M. J.; Bowles, J. L., An Unconventional Method for Purifying the N-carboxyanhydride Derivatives of  $\gamma$ -alkyl-L-glutamates. *Synth. Commun.* **1999**, *29* (5), 843-854.

54. Iwakura, Y.; Uno, K.; Kang, S., The Synthesis and Reactions of 2-Isocyanatoacyl Chlorides. *J. Org. Chem.* **1965**, *30* (4), 1158-1161.

55. Dorman, L. C.; Shiang, W. R.; Meyers, P. A., Purification of  $\gamma$ -Benzyl and  $\gamma$ -Methyl L-Glutamate N-Carboxyanhydrides by Rephosphonation. *Synth. Commun.* **1992**, *22* (22), 3257-3262.

56. Smeets, N. M. B.; van der Weide, P. L. J.; Meuldijk, J.; Vekemans, J. A. J. M.; Hulshof, L. A., A Scalable Synthesis of L-Leucine-N-carboxyanhydride. *Org. Process Res. Dev.* **2005**, *9* (6), 757-763.
57. Engler, A. C.; Lee, H.-i.; Hammond, P. T., Highly Efficient “Grafting onto” a Polypeptide Backbone Using Click Chemistry. *Angew. Chem. Int. Ed.* **2009**, *48* (49), 9334-9338.
58. Tang, H.; Zhang, D., General Route toward Side-Chain-Functionalized  $\alpha$ -Helical Polypeptides. *Biomacromolecules* **2010**, *11* (6), 1585-1592.
59. Hirschmann, R.; Schwam, H.; Strachan, R. G.; Schoenewaldt, E. F.; Barkemeyer, H.; Miller, S. M.; Conn, J. B.; Garsky, V.; Veber, D. F.; Denkewalter, R. G., Controlled synthesis of peptides in aqueous medium. VIII. Preparation and use of novel  $\alpha$ -amino acid N-carboxyanhydrides. *J. Am. Chem. Soc.* **1971**, *93* (11), 2746-2754.
60. Kramer, J. R.; Deming, T. J., General Method for Purification of  $\alpha$ -Amino acid-N-carboxyanhydrides Using Flash Chromatography. *Biomacromolecules* **2010**, *11* (12), 3668-3672.
61. Tang, H.; Yin, L.; Lu, H.; Cheng, J., Water-Soluble Poly(L-serine)s with Elongated and Charged Side-Chains: Synthesis, Conformations, and Cell-Penetrating Properties. *Biomacromolecules* **2012**, *13* (9), 2609-2615.
62. Poche, D. S. Ph.D. Dissertation, Louisiana State University, Baton Rouge, LA, 1990.
63. Waley, S. G.; Watson, J., The Kinetics of the Polymerization of Carbonic Anhydrides. *J. Am. Chem. Soc.* **1948**, *70* (6), 2299-2300.
64. Waley, S. G.; Watson, J., The Kinetics of the Polymerization of Sarcosine Carbonic Anhydride. *Proc. R. Soc. London, Ser. A* **1949**, *199* (1059), 499-517.
65. Deming, T. J., Polypeptide Materials: New synthetic methods and applications. *Adv. Mater.* **1997**, *9* (4), 299-311.
66. Dimitrov, I.; Schlaad, H., Synthesis of nearly monodisperse polystyrene-polypeptide block copolymers via polymerisation of N-carboxyanhydrides. *Chem. Commun.* **2003**, (23), 2944-2945.
67. Knobler, Y.; Bittner, S.; Frankel, M., 749. Reaction of N-carboxy-[small  $\alpha$ ]-amino-acid anhydrides with hydrochlorides of hydroxylamine, O-alkylhydroxylamines,

and amines; syntheses of amino-hydroxamic acids, amido-oxy-peptides, and [small alpha]-amino-acid amides. *J. Chem. Soc.* **1964**, 3941-3951.

68. Knobler, Y.; Bittner, S.; Virov, D.; Frankel, M., [small alpha]-Aminoacyl derivatives of aminobenzoic acid and of amino-oxy-acids by reaction of their hydrochlorides with amino-acid N-carboxyanhydrides. *J. Chem. Soc. (C)* **1969**, (14), 1821-1824.

69. Goodman, M.; Hutchison, J., Propagation Mechanism in Strong Base Initiated Polymerization of  $\alpha$ -Amino Acid N-Carboxyanhydrides. *J. Am. Chem. Soc.* **1965**, 87 (15), 3524-3525.

70. Rinaudo, M.; Domard, A., Kinetics of  $\gamma$ -benzyl-L-glutamate NCA's polymerizations and molecular-weight distributions on corresponding polymers. *Biopolymers* **1976**, 15 (11), 2185-2199.

71. Ballard, D. G. H.; Bamford, C. H.; Weymouth, F. J., Studies in Polymerization. VIII. Reactions of N-Carboxy- $\alpha$ -Amino Acid Anhydrides Initiated by Metal Cations. *Proc. R. Soc. London, Ser. A* **1955**, 227 (1169), 155-183.

72. Thunig, D.; Semen, J.; Elias, H.-G., Carbon dioxide influence on NCA polymerizations. *Makromol. Chem.* **1977**, 178 (2), 603-607.

73. Zou, J.; Fan, J.; He, X.; Zhang, S.; Wang, H.; Wooley, K. L., A Facile Glovebox-Free Strategy To Significantly Accelerate the Syntheses of Well-Defined Polypeptides by N-Carboxyanhydride (NCA) Ring-Opening Polymerizations. *Macromolecules* **2013**, 46 (10), 4223-4226.

74. Ling, J.; Huang, Y., Understanding the Ring-Opening Reaction of  $\alpha$ -Amino Acid N-Carboxyanhydride in an Amine-Mediated Living Polymerization: A DFT Study. *Macromol. Chem. Phys.* **2010**, 211 (15), 1708-1711.

75. Bamford, C. H.; Elliott, A.; Hanby, W. E., *Synthetic Polypeptides*. New York Academic Press: New York, 1956.

76. Sela, M.; Berger, A., The Mechanism of Polymerization of N-Carboxy- $\alpha$ -Amino Acid Anhydrides. *J. Am. Chem. Soc.* **1953**, 75 (24), 6350-6351.

77. Sela, M.; Berger, A., The Terminal Groups of Poly- $\alpha$ -amino Acids. *J. Am. Chem. Soc.* **1955**, 77 (7), 1893-1898.



78. Goodman, M.; Hutchison, J., The Mechanisms of Polymerization of N-Unsubstituted N-Carboxyanhydrides. *J. Am. Chem. Soc.* **1966**, *88* (15), 3627-3630.
79. Hadjichristidis, N.; Iatrou, H.; Pitsikalis, M.; Sakellariou, G., Synthesis of Well-Defined Polypeptide-Based Materials via the Ring-Opening Polymerization of  $\alpha$ -Amino Acid N-Carboxyanhydrides. *Chem. Rev.* **2009**, *109* (11), 5528-5578.
80. Katchalski, E.; Shalitin, Y.; Gehatia, M., Theoretical Analysis of the Polymerization Kinetics of N-Carboxy- $\alpha$ -amino Acid Anhydrides. *J. Am. Chem. Soc.* **1955**, *77* (7), 1925-1934.
81. Habraken, G. J. M.; Peeters, M.; Dietz, C. H. J. T.; Koning, C. E.; Heise, A., How controlled and versatile is N-carboxy anhydride (NCA) polymerization at 0 [degree]C? Effect of temperature on homo-, block- and graft (co)polymerization. *Polym. Chem.* **2010**, *1* (4), 514-524.
82. Habraken, G. J. M.; Wilsens, K. H. R. M.; Koning, C. E.; Heise, A., Optimization of N-carboxyanhydride (NCA) polymerization by variation of reaction temperature and pressure. *Polym. Chem.* **2011**, *2* (6), 1322-1330.
83. Kricheldorf, H. R.; v. Lossow, C.; Schwarz, G., Primary Amine and Solvent-Induced Polymerizations of L- or D,L-Phenylalanine N-Carboxyanhydride. *Macromol. Chem. Phys.* **2005**, *206* (2), 282-290.
84. Kricheldorf, H. R.; von Lossow, C.; Schwarz, G., Primary Amine-Initiated Polymerizations of Alanine-NCA and Sarcosine-NCA. *Macromol. Chem. Phys.* **2004**, *205* (7), 918-924.
85. Kricheldorf, H. R.; von Lossow, C.; Schwarz, G., Cyclic Polypeptides by Solvent-Induced Polymerizations of  $\alpha$ -Amino Acid N-Carboxyanhydrides. *Macromolecules* **2005**, *38* (13), 5513-5518.
86. Sigmund, F.; Wessely, F., Untersuchungen über  $\alpha$ -Amino-N-Carbonsäureanhydride. II. *Z. Physiol. Chem.* **1926**, *157*, 91-105.
87. Wessely, F.; Sigmund, F., Untersuchungen über  $\alpha$ -Amino-N-Carbonsäureanhydride. III. (Zur Kenntnis höhermolekularer Verbindungen.). *Z. Physiol. Chem.* **1926**, *159*, 102-119.
88. Wessely, F.; John, M., Untersuchungen über  $\alpha$ -Amino-N-carbonsäureanhydride. V. Nebenreaktionen der Pyridinzersetzung. *Z. Physiol. Chem.* **1927**, *170*, 38-43.

89. Bartlett, P. D.; Jones, R. H., A Kinetic Study of the Leuchs Anhydrides in Aqueous Solution. II. *J. Am. Chem. Soc.* **1957**, *79* (9), 2153-2159.
90. Bartlett, P. D.; Dittmer, D. C., A Kinetic Study of the Leuchs Anhydrides in Aqueous Solution. III. *J. Am. Chem. Soc.* **1957**, *79* (9), 2159-2160.
91. Miller, E.; Fankuchen, I.; Mark, H., Polymerization in the Solid State. *J. Appl. Phys.* **1949**, *20* (6), 531-533.
92. Ballard, D. G. H.; Bamford, C. H., 77. Reactions of N-carboxy-[small alpha]-amino-acid anhydrides catalysed by tertiary bases. *J. Chem. Soc.* **1956**, 381-387.
93. Bamford, C. H.; Block, H., 981. The initiation step in the polymerization of N-carboxy-[small alpha]-amino-acid anhydrides. Part I. Catalysis by tertiary bases. *J. Chem. Soc.* **1961**, 4989-4991.
94. Szwarc, M., The kinetics and mechanism of N-carboxy- $\alpha$ -amino-acid anhydride (NCA) polymerisation to poly-amino acids. In *Fortschritte der Hochpolymeren-Forschung*, Springer Berlin Heidelberg: 1965; Vol. 4/1, pp 1-65.
95. Harwood, H. J., Mechanism of N-Carboxy Anhydride Polymerization. In *Ring-Opening Polymerization*, American Chemical Society: 1985; Vol. 286, pp 67-85.
96. Terbojevich, M.; Pizziolo, G.; Peggion, E.; Cosani, A.; Scoffone, E., Mechanism of polymerization of N-carboxyanhydrides in dimethylformamide. Evidence of the presence of cyclic terminals in polymers obtained by strong-base initiation. *J. Am. Chem. Soc.* **1967**, *89* (11), 2733-2736.
97. Deming, T. J., Facile synthesis of block copolypeptides of defined architecture. *Nature* **1997**, *390* (6658), 386-389.
98. Deming, T. J., Amino Acid Derived Nickelacycles: Intermediates in Nickel-Mediated Polypeptide Synthesis. *J. Am. Chem. Soc.* **1998**, *120* (17), 4240-4241.
99. Cheng, J.; Deming, T. J., Synthesis of Polypeptides by Ring-Opening Polymerization of  $\alpha$ -Amino Acid N-Carboxyanhydrides. In *Peptide-Based Materials*, Deming, T., Ed. Springer Berlin Heidelberg: Berlin, Heidelberg, 2012; pp 1-26.
100. Deming, T. J., Cobalt and Iron Initiators for the Controlled Polymerization of  $\alpha$ -Amino Acid-N-Carboxyanhydrides. *Macromolecules* **1999**, *32* (13), 4500-4502.

101. Goodwin, A. A.; Bu, X.; Deming, T. J., Reactions of  $\alpha$ -amino acid-N-carboxyanhydrides (NCAs) with organometallic palladium(0) and platinum(0) compounds: structure of a metallated NCA product and its role in polypeptide synthesis. *J. Organomet. Chem.* **1999**, *589* (1), 111-114.
102. Lu, H.; Cheng, J., Hexamethyldisilazane-Mediated Controlled Polymerization of  $\alpha$ -Amino Acid N-Carboxyanhydrides. *J. Am. Chem. Soc.* **2007**, *129* (46), 14114-14115.
103. Lu, H.; Cheng, J., N-Trimethylsilyl Amines for Controlled Ring-Opening Polymerization of Amino Acid N-Carboxyanhydrides and Facile End Group Functionalization of Polypeptides. *J. Am. Chem. Soc.* **2008**, *130* (38), 12562-12563.
104. Lu, H.; Wang, J.; Song, Z.; Yin, L.; Zhang, Y.; Tang, H.; Tu, C.; Lin, Y.; Cheng, J., Recent advances in amino acid N-carboxyanhydrides and synthetic polypeptides: chemistry, self-assembly and biological applications. *Chem. Commun.* **2014**, *50* (2), 139-155.
105. Yuan, J.; Sun, Y.; Wang, J.; Lu, H., Phenyl Trimethylsilyl Sulfide-Mediated Controlled Ring-Opening Polymerization of  $\alpha$ -Amino Acid N-Carboxyanhydrides. *Biomacromolecules* **2016**, *17* (3), 891-896.
106. Sheiko, S. S.; Sumerlin, B. S.; Matyjaszewski, K., Cylindrical molecular brushes: Synthesis, characterization, and properties. *Prog. Polym. Sci.* **2008**, *33*, 759-785.
107. Compain, P., Olefin Metathesis of Amine-Containing Systems: Beyond the Current Consensus. *Adv. Synth. Catal.* **2007**, *349* (11-12), 1829-1846.
108. Lu, H.; Wang, J.; Lin, Y.; Cheng, J., One-Pot Synthesis of Brush-Like Polymers via Integrated Ring-Opening Metathesis Polymerization and Polymerization of Amino Acid N-Carboxyanhydrides. *J. Am. Chem. Soc.* **2009**, *131* (38), 13582-13583.
109. Bai, Y.; Lu, H.; Ponnusamy, E.; Cheng, J., Synthesis of hybrid block copolymers via integrated ring-opening metathesis polymerization and polymerization of NCA. *Chem. Commun.* **2011**, *47* (38), 10830-10832.
110. Wang, J.; Lu, H.; Kamat, R.; Pingali, S. V.; Urban, V. S.; Cheng, J.; Lin, Y., Supramolecular Polymerization from Polypeptide-Grafted Comb Polymers. *J. Am. Chem. Soc.* **2011**, *133* (33), 12906-12909.
111. Peng, H.; Ling, J.; Zhu, Y.; You, L.; Shen, Z., Polymerization of  $\alpha$ -amino acid N-carboxyanhydrides catalyzed by rare earth tris(borohydride) complexes: Mechanism and hydroxy-endcapped polypeptides. *J. Polym. Sci. Part A* **2012**, *50* (15), 3016-3029.

112. Shen, Y.; Shen, Z.; Zhang, Y.; Yao, K., Novel Rare Earth Catalysts for the Living Polymerization and Block Copolymerization of  $\epsilon$ -Caprolactone. *Macromolecules* **1996**, *29* (26), 8289-8295.
113. Ling, J.; Shen, Z.; Huang, Q., Novel Single Rare Earth Aryloxy Initiators for Ring-Opening Polymerization of 2,2-Dimethyltrimethylene Carbonate. *Macromolecules* **2001**, *34* (22), 7613-7616.
114. Guillaume, S. M.; Schappacher, M.; Soum, A., Polymerization of  $\epsilon$ -Caprolactone Initiated by  $\text{Nd}(\text{BH}_4)_3(\text{THF})_3$ : Synthesis of Hydroxytelechelic Poly( $\epsilon$ -caprolactone). *Macromolecules* **2003**, *36* (1), 54-60.
115. Palard, I.; Soum, A.; Guillaume, S. M., Rare Earth Metal Tris(borohydride) Complexes as Initiators for  $\epsilon$ -Caprolactone Polymerization: General Features and IR Investigations of the Process. *Macromolecules* **2005**, *38* (16), 6888-6894.
116. Palard, I.; Schappacher, M.; Belloncle, B.; Soum, A.; Guillaume, S. M., Unprecedented Polymerization of Trimethylene Carbonate Initiated by a Samarium Borohydride Complex: Mechanistic Insights and Copolymerization with  $\epsilon$ -Caprolactone. *Chem. Eur. J.* **2007**, *13* (5), 1511-1521.
117. Gao, W.; Cui, D.; Liu, X.; Zhang, Y.; Mu, Y., Rare-Earth Metal Bis(alkyl)s Supported by a Quinolinyl Anilido-Imine Ligand: Synthesis and Catalysis on Living Polymerization of  $\epsilon$ -Caprolactone. *Organometallics* **2008**, *27* (22), 5889-5893.
118. Zhao, W.; Cui, D.; Liu, X.; Chen, X., Facile Synthesis of Hydroxyl-Ended, Highly Stereoregular, Star-Shaped Poly(lactide) from Immortal ROP of rac-Lactide and Kinetics Study. *Macromolecules* **2010**, *43* (16), 6678-6684.
119. Zhao, W.; Gnanou, Y.; Hadjichristidis, N., From competition to cooperation: a highly efficient strategy towards well-defined (co)polypeptides. *Chem. Commun.* **2015**, *51* (17), 3663-3666.
120. Zhao, W.; Gnanou, Y.; Hadjichristidis, N., Fast and Living Ring-Opening Polymerization of  $\alpha$ -Amino Acid N-Carboxyanhydrides Triggered by an "Alliance" of Primary and Secondary Amines at Room Temperature. *Biomacromolecules* **2015**, *16* (4), 1352-1357.
121. Coleman, D., 505. Synthetic polypeptides. Part IV. Preparation and polymerisation of oxazolid-2 : 5-diones derived from [small alpha]-amino-dicarboxylic acids. *J. Chem. Soc.* **1951**, 2294-2295.

122. Yan, L.; Yang, L.; He, H.; Hu, X.; Xie, Z.; Huang, Y.; Jing, X., Photo-cross-linked mPEG-poly( $\gamma$ -cinnamyl-L-glutamate) micelles as stable drug carriers. *Polym. Chem.* **2012**, *3* (5), 1300-1307.
123. Xiao, C.; Zhao, C.; He, P.; Tang, Z.; Chen, X.; Jing, X., Facile Synthesis of Glycopolypeptides by Combination of Ring-Opening Polymerization of an Alkyne-Substituted N-carboxyanhydride and Click "Glycosylation". *Macromol. Rapid Commun.* **2010**, *31* (11), 991-7.
124. Poché, D. S.; Thibodeaux, S. J.; Rucker, V. C.; Warner, I. M.; Daly, W. H., Synthesis of Novel  $\gamma$ -Alkenyl L-Glutamate Derivatives Containing a Terminal C=C Double Bond To Produce Polypeptides with Pendent Unsaturation. *Macromolecules* **1997**, *30* (25), 8081-8084.
125. Tang, H.; Zhang, D., Multi-functionalization of helical block copoly([small alpha]-peptide)s by orthogonal chemistry. *Polym. Chem.* **2011**, *2* (7), 1542-1551.
126. Huang, J.; Bonduelle, C.; Thévenot, J.; Lecommandoux, S.; Heise, A., Biologically Active Polymersomes from Amphiphilic Glycopeptides. *J. Am. Chem. Soc.* **2012**, *134* (1), 119-122.
127. Huang, J.; Habraken, G.; Audouin, F.; Heise, A., Hydrolytically Stable Bioactive Synthetic Glycopeptide Homo- and Copolymers by Combination of NCA Polymerization and Click Reaction. *Macromolecules* **2010**, *43* (14), 6050-6057.
128. Bertozzi, C. R.; Kiessling, L., L., Chemical Glycobiology. *Science* **2001**, *291* (5512), 2357-2364.
129. Dwek, R. A., Glycobiology: Toward Understanding the Function of Sugars. *Chem. Rev.* **1996**, *96* (2), 683-720.
130. Van Heeswijk, W. A. R.; Eenink, M. J. D.; Feijen, J., An Improved Method for the Preparation of  $\gamma$ -Esters of Glutamic Acid and  $\beta$ -Esters of Aspartic Acid. *Synthesis* **1982**, *1982* (09), 744-747.
131. Lu, H.; Bai, Y.; Wang, J.; Gabrielson, N. P.; Wang, F.; Lin, Y.; Cheng, J., Ring-Opening Polymerization of  $\gamma$ -(4-Vinylbenzyl)-L-glutamate N-Carboxyanhydride for the Synthesis of Functional Polypeptides. *Macromolecules* **2011**, *44* (16), 6237-6240.
132. Kramer, J. R.; Deming, T. J., Preparation of Multifunctional and Multireactive Polypeptides via Methionine Alkylation. *Biomacromolecules* **2012**, *13* (6), 1719-1723.

133. Kramer, J. R.; Deming, T. J., Reversible chemoselective tagging and functionalization of methionine containing peptides. *Chem. Commun.* **2013**, 49 (45), 5144-5146.
134. Deming, T. J., Synthesis of Side-Chain Modified Polypeptides. *Chem. Rev.* **2016**, 116 (3), 786-808.
135. Sparks, B. J.; Ray, J. G.; Savin, D. A.; Stafford, C. M.; Patton, D. L., Synthesis of thiol-clickable and block copolypeptide brushes via nickel-mediated surface initiated polymerization of [small alpha]-amino acid N-carboxyanhydrides (NCAs). *Chem. Commun.* **2011**, 47 (22), 6245-6247.
136. Guinn, R. M.; Margot, A. O.; Taylor, J. R.; Schumacher, M.; Clark, D. S.; Blanch, H. W., Synthesis and characterization of polyamides containing unnatural amino acids. *Biopolymers* **1995**, 35 (5), 503-512.
137. Sun, J.; Schlaad, H., Thiol-Ene Clickable Polypeptides. *Macromolecules* **2010**, 43 (10), 4445-4448.
138. Fowler, S. A.; Blackwell, H. E., Structure-function relationships in peptoids: Recent advances toward deciphering the structural requirements for biological function. *Org. Biomol. Chem.* **2009**, 7 (8), 1508-1524.
139. Lee, J.; Udugamasooriya, D. G.; Lim, H.-S.; Kodadek, T., Potent and selective photo-inactivation of proteins with peptoid-ruthenium conjugates. *Nat. Chem. Biol.* **2010**, 6 (4), 258-260.
140. Seo, J.; Lee, B. C.; Zuckermann, R. N., 2.204 - Peptoids: Synthesis, Characterization, and Nanostructures A2 - Ducheyne, Paul. In *Comprehensive Biomaterials*, Elsevier: Oxford, 2011; pp 53-76.
141. Rosales, A. M.; Murnen, H. K.; Zuckermann, R. N.; Segalman, R. A., Control of Crystallization and Melting Behavior in Sequence Specific Polypeptoids. *Macromolecules* **2010**, 43 (13), 5627-5636.
142. Robinson, J. W.; Schlaad, H., A versatile polypeptoid platform based on N-allyl glycine. *Chem. Commun.* **2012**, 48 (63), 7835-7837.
143. Lahasky, S. H.; Serem, W. K.; Guo, L.; Garno, J. C.; Zhang, D., Synthesis and Characterization of Cyclic Brush-Like Polymers by N-Heterocyclic Carbene-Mediated Zwitterionic Polymerization of N-Propargyl N-Carboxyanhydride and the Grafting-to Approach. *Macromolecules* **2011**, 44 (23), 9063-9074.

144. Secker, C.; Robinson, J. W.; Schlaad, H., Alkyne-X modification of polypeptoids. *Eur. Polym. J.* **2015**, *62*, 394-399.
145. Simon, R. J.; Kania, R. S.; Zuckermann, R. N.; Huebner, V. D.; Jewell, D. A.; Banville, S.; Ng, S.; Wang, L.; Rosenberg, S.; Marlowe, C. K., Peptoids: a modular approach to drug discovery. *Proc. Natl. Acad. Sci.* **1992**, *89* (20), 9367-9371.
146. Zuckermann, R. N.; Kerr, J. M.; Kent, S. B. H.; Moos, W. H., Efficient method for the preparation of peptoids [oligo(N-substituted glycines)] by submonomer solid-phase synthesis. *J. Am. Chem. Soc.* **1992**, *114* (26), 10646-10647.
147. Guo, L.; Zhang, D., Cyclic Poly( $\alpha$ -peptoid)s and Their Block Copolymers from N-Heterocyclic Carbene-Mediated Ring-Opening Polymerizations of N-Substituted N-Carboxylanhydrides. *J. Am. Chem. Soc.* **2009**, *131* (50), 18072-18074.
148. Robinson, J. W.; Secker, C.; Weidner, S.; Schlaad, H., Thermoresponsive Poly(N-C3 glycine)s. *Macromolecules* **2013**, *46* (3), 580-587.
149. Yoon, U. C.; Jin, Y. X.; Oh, S. W.; Park, C. H.; Park, J. H.; Campana, C. F.; Cai, X.; Duesler, E. N.; Mariano, P. S., A Synthetic Strategy for the Preparation of Cyclic Peptide Mimetics Based on SET-Promoted Photocyclization Processes. *J. Am. Chem. Soc.* **2003**, *125* (35), 10664-10671.
150. Guo, L.; Lahasky, S. H.; Ghale, K.; Zhang, D., N-Heterocyclic Carbene-Mediated Zwitterionic Polymerization of N-Substituted N-Carboxyanhydrides toward Poly( $\alpha$ -peptoid)s: Kinetic, Mechanism, and Architectural Control. *J. Am. Chem. Soc.* **2012**, *134* (22), 9163-9171.
151. Katchalski, E.; Sela, M., Synthesis and Chemical Properties of Poly- $\alpha$ -Amino Acids. In *Advances in Protein Chemistry*, C.B. Anfinsen, M. L. A. K. B.; John, T. E., Eds. Academic Press: 1958; Vol. Volume 13, pp 243-492.
152. Secker, C.; Brosnan, S. M.; Luxenhofer, R.; Schlaad, H., Poly( $\alpha$ -Peptoid)s Revisited: Synthesis, Properties, and Use as Biomaterial. *Macromol. Biosci.* **2015**, 881-891.
153. Fetsch, C.; Grossmann, A.; Holz, L.; Nawroth, J. F.; Luxenhofer, R., Polypeptoids from N-Substituted Glycine N-Carboxyanhydrides: Hydrophilic, Hydrophobic, and Amphiphilic Polymers with Poisson Distribution. *Macromolecules* **2011**, *44* (17), 6746-6758.
154. Mavrogiorgis, D.; Bilalis, P.; Karatzas, A.; Skoulas, D.; Fotinogiannopoulou, G.; Iatrou, H., Controlled polymerization of histidine and synthesis of well-defined stimuli

responsive polymers. Elucidation of the structure-aggregation relationship of this highly multifunctional material. *Polym. Chem.* **2014**, *5* (21), 6256-6278.

155. Fetsch, C.; Luxenhofer, R., Highly Defined Multiblock Copolypeptoids: Pushing the Limits of Living Nucleophilic Ring-Opening Polymerization. *Macromol. Rapid Commun.* **2012**, *33* (19), 1708-1713.

156. Gangloff, N.; Fetsch, C.; Luxenhofer, R., Polypeptoids by Living Ring-Opening Polymerization of N-Substituted N-Carboxyanhydrides from Solid Supports. *Macromol. Rapid Commun.* **2013**, *34* (12), 997-1001.

157. Schneider, M.; Fetsch, C.; Amin, I.; Jordan, R.; Luxenhofer, R., Polypeptoid Brushes by Surface-Initiated Polymerization of N-Substituted Glycine N-Carboxyanhydrides. *Langmuir* **2013**, *29* (23), 6983-6988.

158. Lu, L.; Lahasky, S. H.; Zhang, D.; Garno, J. C., Directed Growth of Polymer Nanorods Using Surface-Initiated Ring-Opening Polymerization of N-Allyl N-Carboxyanhydride. *ACS Applied Materials & Interfaces* **2016**, *8* (6), 4014-4022.

159. Lee, C.-U.; Li, A.; Ghale, K.; Zhang, D., Crystallization and Melting Behaviors of Cyclic and Linear Polypeptoids with Alkyl Side Chains. *Macromolecules* **2013**, *46* (20), 8213-8223.

160. Lahasky, S. H.; Hu, X.; Zhang, D., Thermoresponsive Poly( $\alpha$ -peptoid)s: Tuning the Cloud Point Temperatures by Composition and Architecture. *ACS Macro Lett.* **2012**, *1* (5), 580-584.

161. Lahasky, S. H.; Lu, L.; Huberty, W. A.; Cao, J.; Guo, L.; Garno, J. C.; Zhang, D., Synthesis and characterization of thermo-responsive polypeptoid bottlebrushes. *Polym. Chem.* **2014**, *5* (4), 1418-1426.

162. Li, A.; Zhang, D., Synthesis and Characterization of Cleavable Core-Cross-Linked Micelles Based on Amphiphilic Block Copolypeptoids as Smart Drug Carriers. *Biomacromolecules* **2016**, *17* (3), 852-861.

163. Culkin, D. A.; Jeong, W.; Csihony, S.; Gomez, E. D.; Balsara, N. P.; Hedrick, J. L.; Waymouth, R. M., Zwitterionic Polymerization of Lactide to Cyclic Poly(Lactide) by Using N-Heterocyclic Carbene Organocatalysts. *Angew. Chem. Int. Ed.* **2007**, *46* (15), 2627-2630.

164. Jeong, W.; Hedrick, J. L.; Waymouth, R. M., Organic Spirocyclic Initiators for the Ring-Expansion Polymerization of  $\beta$ -Lactones. *J. Am. Chem. Soc.* **2007**, *129* (27), 8414-8415.



165. Jeong, W.; Shin, E. J.; Culkin, D. A.; Hedrick, J. L.; Waymouth, R. M., Zwitterionic Polymerization: A Kinetic Strategy for the Controlled Synthesis of Cyclic Polylactide. *J. Am. Chem. Soc.* **2009**, *131* (13), 4884-4891.
166. Dove, A. P.; Pratt, R. C.; Lohmeijer, B. G. G.; Culkin, D. A.; Hagberg, E. C.; Nyce, G. W.; Waymouth, R. M.; Hedrick, J. L., N-Heterocyclic carbenes: Effective organic catalysts for living polymerization. *Polymer* **2006**, *47* (11), 4018-4025.
167. Acharya, A. K.; Chang, Y. A.; Jones, G. O.; Rice, J. E.; Hedrick, J. L.; Horn, H. W.; Waymouth, R. M., Experimental and Computational Studies on the Mechanism of Zwitterionic Ring-Opening Polymerization of  $\delta$ -Valerolactone with N-Heterocyclic Carbenes. *J. Phys. Chem. B* **2014**, *118* (24), 6553-6560.
168. Jones, G. O.; Chang, Y. A.; Horn, H. W.; Acharya, A. K.; Rice, J. E.; Hedrick, J. L.; Waymouth, R. M., N-Heterocyclic Carbene-Catalyzed Ring Opening Polymerization of  $\epsilon$ -Caprolactone with and without Alcohol Initiators: Insights from Theory and Experiment. *J. Phys. Chem. B* **2015**, *119* (17), 5728-5737.
169. Raynaud, J.; Absalon, C.; Gnanou, Y.; Taton, D., N-Heterocyclic Carbene-Induced Zwitterionic Ring-Opening Polymerization of Ethylene Oxide and Direct Synthesis of  $\alpha,\omega$ -Difunctionalized Poly(ethylene oxide)s and Poly(ethylene oxide)-*b*-poly( $\epsilon$ -caprolactone) Block Copolymers. *J. Am. Chem. Soc.* **2009**, *131* (9), 3201-3209.
170. Brown, H. A.; Chang, Y. A.; Waymouth, R. M., Zwitterionic Polymerization to Generate High Molecular Weight Cyclic Poly(Carbosiloxane)s. *J. Am. Chem. Soc.* **2013**, *135* (50), 18738-18741.
171. Schmid, R., Re-interpretation of the solvent dielectric constant in coordination chemical terms. *J. Sol. Chem.* *12* (2), 135-152.
172. Lee, C.-U.; Smart, T. P.; Guo, L.; Epps, T. H.; Zhang, D., Synthesis and Characterization of Amphiphilic Cyclic Diblock Copolypeptoids from N-Heterocyclic Carbene-Mediated Zwitterionic Polymerization of N-Substituted N-Carboxyanhydride. *Macromolecules* **2011**, *44* (24), 9574-9585.
173. Brown, H. A.; De Crisci, A. G.; Hedrick, J. L.; Waymouth, R. M., Amidine-Mediated Zwitterionic Polymerization of Lactide. *ACS Macro Lett.* **2012**, *1* (9), 1113-1115.
174. Zhang, X.; Waymouth, R. M., Zwitterionic Ring Opening Polymerization with Isothioureas. *ACS Macro Lett.* **2014**, *3* (10), 1024-1028.

175. Hörtz, C.; Birke, A.; Kaps, L.; Decker, S.; Wächtersbach, E.; Fischer, K.; Schuppan, D.; Barz, M.; Schmidt, M., Cylindrical Brush Polymers with Polysarcosine Side Chains: A Novel Biocompatible Carrier for Biomedical Applications. *Macromolecules* **2015**, *48* (7), 2074-2086.
176. Nakamura, R.; Aoi, K.; Okada, M., Interactions of Enzymes and a Lectin with a Chitin-Based Graft Copolymer Having Polysarcosine Side Chains. *Macromol. Biosci.* **2004**, *4* (6), 610-615.
177. Nakamura, R.; Aoi, K.; Okada, M., Controlled Synthesis of a Chitosan-Based Graft Copolymer Having Polysarcosine Side Chains Using the NCA Method with a Carboxylic Acid Additive. *Macromol. Rapid Commun.* **2006**, *27* (20), 1725-1732.
178. Aoi, K.; Hatanaka, T.; Tsutsumiuchi, K.; Okada, M.; Imae, T., Synthesis of a novel star-shaped dendrimer by radial-growth polymerization of sarcosine N-carboxyanhydride initiated with poly(trimethyleneimine) dendrimer. *Macromol. Rapid Commun.* **1999**, *20* (7), 378-382.
179. Hara, E.; Ueda, M.; Makino, A.; Hara, I.; Ozeki, E.; Kimura, S., Factors Influencing in Vivo Disposition of Polymeric Micelles on Multiple Administrations. *ACS Med. Chem. Lett.* **2014**, *5* (8), 873-877.
180. Makino, A.; Yamahara, R.; Ozeki, E.; Kimura, S., Preparation of Novel Polymer Assemblies, "Lactosome", Composed of Poly(L-lactic acid) and Poly(sarcosine). *Chem. Lett.* **2007**, *36* (10), 1220-1221.
181. Tanaka, Y.; Arakawa, M.; Yamaguchi, Y.; Hori, C.; Ueno, M.; Tanaka, T.; Imahori, T.; Kondo, Y., NMR Spectroscopic Observation of a Metal-Free Acetylde Anion. *Chem. Asian J.* **2006**, *1* (4), 581-585.
182. Tao, X.; Deng, C.; Ling, J., PEG-Amine-Initiated Polymerization of Sarcosine N-Thiocarboxyanhydrides Toward Novel Double-Hydrophilic PEG-b-Polysarcosine Diblock Copolymers. *Macromol. Rapid Commun.* **2014**, *35* (9), 875-881.
183. Aubert, P.; Jeffreys, R. A.; Knott, E. B., 477. Thiazolid-2 : 5-dione. *J. Chem. Soc.* **1951**, (0), 2195-2197.
184. Bailey, J. L., 679. The synthesis of simple peptides from anhydro-N-carboxyamino-acids. *J. Chem. Soc.* **1950**, (0), 3461-3466.
185. Dewey, R. S.; Schoenewaldt, E. F.; Joshua, H.; Paleveda, W. J.; Schwam, H.; Barkemeyer, H.; Arison, B. H.; Veber, D. F.; Denkwalter, R. G.; Hirschmann, R., Synthesis of peptides in aqueous medium. V. Preparation and use of 2,5-

thiazolidinediones (NTA's). Use of the  $^{13}\text{C}$ -H nuclear magnetic resonance signal as internal standard for quantitative studies. *J. Am. Chem. Soc.* **1968**, *90* (12), 3254-3255.

186. Hirschmann, R.; Dewey, R. S.; Schoenewaldt, E. F.; Joshua, H.; Paleveda, W. J.; Schwam, H.; Barkemeyer, H.; Arison, B. H.; Veber, D. F., Synthesis of peptides in aqueous medium. VII. Preparation and use of 2,5-thiazolidinediones in peptide synthesis. *J. Org. Chem.* **1971**, *36* (1), 49-59.

187. Vinick, F. J.; Jung, S., Concerning the preparation of optically pure N-(thiocarboxy)-L-aspartic anhydride. *J. Org. Chem.* **1982**, *47* (11), 2199-2201.

188. Kato, H.; Higashimura, T.; Okamura, S., Condensation polymerization of N-dithiocarbonyl alkoxy-carbonyl amino acids. Part V. Studies on reaction mechanism. *Makromol. Chem.* **1967**, *109* (1), 9-21.

189. Bradbury, J. H.; Rogers, G. E., The Theory of Shrinkproofing of Wool: Part IV. Electron and Light Microscopy of Polyglycine on the Fibers. *Text. Res. J.* **1963**, *33* (6), 452-458.

190. Kricheldorf, H. R.; Sell, M.; Schwarz, G., Primary Amine-Initiated Polymerizations of  $\alpha$ -Amino Acid N-Thiocarbonyl Anhydrosulfide. *J. Macromol. Sci. Pure Appl. Chem.* **2008**, *45* (6), 425-430.

191. Tao, X.; Deng, Y.; Shen, Z.; Ling, J., Controlled Polymerization of N-Substituted Glycine N-Thiocarboxyanhydrides Initiated by Rare Earth Borohydrides toward Hydrophilic and Hydrophobic Polypeptides. *Macromolecules* **2014**, *47* (18), 6173-6180.

192. Tao, X.; Du, J.; Wang, Y.; Ling, J., Polypeptides with tunable cloud point temperatures synthesized from N-substituted glycine N-thiocarboxyanhydrides. *Polym. Chem.* **2015**, *6* (16), 3164-3174.

193. Yanagishita, M., Function of proteoglycans in the extracellular matrix. *Acta Pathol. Jpn.* **1993**, *43* (6), 283-293.

194. Melrose, J.; Ghosh, P.; Taylor, T. K. F., Proteoglycan heterogeneity in the normal adult ovine intervertebral disc. *Matrix Biol.* **1994**, *14* (1), 61-75.

195. Frick, C.; Dietz, A. C.; Merritt, K.; Umbreit, T. H.; Tomazic-Jezic, V. J., Effects of Prosthetic Materials on the Host Immune Response: Evaluation of Polymethylmethacrylate (PMMA), Polyethylene (PE), and Polystyrene (PS) Particles. **2006**, *16* (6), 423-433.

196. Brandley, B. K.; Schnaar, R. L., Cell-surface carbohydrates in cell recognition and response. *J. Leukoc. Biol.* **1986**, *40* (1), 97-111.
197. Chandrasekaran, S.; Dean, J. W.; Giniger, M. S.; Tanzer, M. L., Laminin carbohydrates are implicated in cell signaling. *J. Cell. Biochem.* **1991**, *46* (2), 115-124.
198. Perillo, N. L.; Pace, K. E.; Seilhamer, J. J.; Baum, L. G., Apoptosis of T cells mediated by galectin-1. *Nature* **1995**, *378* (6558), 736-739.
199. Pace, K. E.; Lee, C.; Stewart, P. L.; Baum, L. G., Restricted Receptor Segregation into Membrane Microdomains Occurs on Human T Cells During Apoptosis Induced by Galectin-1. *J. Immunol.* **1999**, *163* (7), 3801-3811.
200. Sacchettini, J. C.; Baum, L. G.; Brewer, C. F., Multivalent Protein–Carbohydrate Interactions. A New Paradigm for Supermolecular Assembly and Signal Transduction. *Biochemistry* **2001**, *40* (10), 3009-3015.
201. Zhang, R.-G.; Scott, D. L.; Westbrook, M. L.; Nance, S.; Spangler, B. D.; Shipley, G. G.; Westbrook, E. M., The Three-dimensional Crystal Structure of Cholera Toxin. *J. Mol. Biol.* **1995**, *251* (4), 563-573.
202. Yuriev, E.; Farrugia, W.; Scott, A. M.; Ramsland, P. A., Three-dimensional structures of carbohydrate determinants of Lewis system antigens: Implications for effective antibody targeting of cancer. *Immunol. Cell Biol.* **2005**, *83* (6), 709-717.
203. Grader-Beck, T.; Boin, F.; von Gunten, S.; Smith, D.; Rosen, A.; Bochner, B. S., Antibodies recognising sulfated carbohydrates are prevalent in systemic sclerosis and associated with pulmonary vascular disease. *Ann. Rheum. Dis.* **2011**.
204. Dingjan, T.; Spendlove, I.; Durrant, L. G.; Scott, A. M.; Yuriev, E.; Ramsland, P. A., Structural biology of antibody recognition of carbohydrate epitopes and potential uses for targeted cancer immunotherapies. *Mol. Immunol.* **2015**, *67* (2, Part A), 75-88.
205. Lundquist, J. J.; Toone, E. J., The Cluster Glycoside Effect. *Chem. Rev.* **2002**, *102* (2), 555-578.
206. Lee, Y. C.; Lee, R. T., Carbohydrate-Protein Interactions: Basis of Glycobiology. *Acc. Chem. Res.* **1995**, *28* (8), 321-327.
207. Palese, P.; Shaw, M. L., *Field's Virology*. 5th ed.; Williams & Wilkins: Lippincott, 2007; Vol. 2.

208. Dove, A., The bittersweet promise of glycobiology. *Nat. Biotech* **2001**, *19* (10), 913-917.
209. Becer, C. R.; Gibson, M. I.; Geng, J.; Ilyas, R.; Wallis, R.; Mitchell, D. A.; Haddleton, D. M., High-Affinity Glycopolymer Binding to Human DC-SIGN and Disruption of DC-SIGN Interactions with HIV Envelope Glycoprotein. *J. Am. Chem. Soc.* **2010**, *132* (43), 15130-15132.
210. Spain, S. G.; Cameron, N. R., A spoonful of sugar: the application of glycopolymers in therapeutics. *Polym. Chem.* **2011**, *2* (1), 60-68.
211. Geng, J.; Mantovani, G.; Tao, L.; Nicolas, J.; Chen, G.; Wallis, R.; Mitchell, D. A.; Johnson, B. R. G.; Evans, S. D.; Haddleton, D. M., Site-Directed Conjugation of “Clicked” Glycopolymers To Form Glycoprotein Mimics: Binding to Mammalian Lectin and Induction of Immunological Function. *J. Am. Chem. Soc.* **2007**, *129* (49), 15156-15163.
212. Ladmiral, V.; Mantovani, G.; Clarkson, G. J.; Cauet, S.; Irwin, J. L.; Haddleton, D. M., Synthesis of Neoglycopolymers by a Combination of “Click Chemistry” and Living Radical Polymerization. *J. Am. Chem. Soc.* **2006**, *128* (14), 4823-4830.
213. Geng, J.; Lindqvist, J.; Mantovani, G.; Chen, G.; Sayers, C. T.; Clarkson, G. J.; Haddleton, D. M., Well-Defined Poly(N-glycosyl 1,2,3-triazole) Multivalent Ligands: Design, Synthesis and Lectin Binding Studies. *QSAR Comb. Sci.* **2007**, *26* (11-12), 1220-1228.
214. Semsarilar, M.; Ladmiral, V.; Perrier, S., Highly Branched and Hyperbranched Glycopolymers via Reversible Addition–Fragmentation Chain Transfer Polymerization and Click Chemistry. *Macromolecules* **2010**, *43* (3), 1438-1443.
215. Becer, C. R.; Babiuch, K.; Pilz, D.; Hornig, S.; Heinze, T.; Gottschaldt, M.; Schubert, U. S., Clicking Pentafluorostyrene Copolymers: Synthesis, Nanoprecipitation, and Glycosylation. *Macromolecules* **2009**, *42* (7), 2387-2394.
216. Boyer, C.; Bousquet, A.; Rondolo, J.; Whittaker, M. R.; Stenzel, M. H.; Davis, T. P., Glycopolymer Decoration of Gold Nanoparticles Using a LbL Approach. *Macromolecules* **2010**, *43* (8), 3775-3784.
217. Matrosovich, M. N.; Mochalova, L. V.; Marinina, V. P.; Byramova, N. E.; Bovin, N. V., Synthetic polymeric sialoside inhibitors of influenza virus receptor-binding activity. *FEBS Lett.* **1990**, *272* (1), 209-212.

218. Slavin, S.; Burns, J.; Haddleton, D. M.; Becer, C. R., Synthesis of glycopolymers via click reactions. *Eur. Polym. J.* **2011**, *47* (4), 435-446.
219. Gress, A.; Völkel, A.; Schlaad, H., Thio-Click Modification of Poly[2-(3-butenyl)-2-oxazoline]. *Macromolecules* **2007**, *40* (22), 7928-7933.
220. Hu, Z.; Fan, X.; Zhang, G., Synthesis and characterization of glucose-grafted biodegradable amphiphilic glycopolymers P(AGE-glucose)-b-PLA. *Carbohydr. Polym.* **2010**, *79* (1), 119-124.
221. Mortell, K. H.; Gingras, M.; Kiessling, L. L., Synthesis of Cell Agglutination Inhibitors by Aqueous Ring-Opening Metathesis Polymerization. *J. Am. Chem. Soc.* **1994**, *116* (26), 12053-12054.
222. Sauter, N. K.; Bednarski, M. D.; Wurzburg, B. A.; Hanson, J. E.; Whitesides, G. M.; Skehel, J. J.; Wiley, D. C., Hemagglutinins from two influenza virus variants bind to sialic acid derivatives with millimolar dissociation constants: a 500-MHz proton nuclear magnetic resonance study. *Biochemistry* **1989**, *28* (21), 8388-8396.
223. Spaltenstein, A.; Whitesides, G. M., Polyacrylamides bearing pendant .alpha.-sialoside groups strongly inhibit agglutination of erythrocytes by influenza virus. *J. Am. Chem. Soc.* **1991**, *113* (2), 686-687.
224. Kingery-Wood, J. E.; Williams, K. W.; Sigal, G. B.; Whitesides, G. M., The agglutination of erythrocytes by influenza virus is strongly inhibited by liposomes incorporating an analog of sialyl gangliosides. *J. Am. Chem. Soc.* **1992**, *114* (18), 7303-7305.
225. Sparks, M. A.; Williams, K. W.; Whitesides, G. M., Neuraminidase-resistant hemagglutination inhibitors: acrylamide copolymers containing a C-glycoside of N-acetylneuraminic acid. *J. Med. Chem.* **1993**, *36* (6), 778-783.
226. Lees, W. J.; Spaltenstein, A.; Kingery-Wood, J. E.; Whitesides, G. M., Polyacrylamides Bearing Pendant .alpha.-Sialoside Groups Strongly Inhibit Agglutination of Erythrocytes by Influenza A Virus: Multivalency and Steric Stabilization of Particulate Biological Systems. *J. Med. Chem.* **1994**, *37* (20), 3419-3433.
227. Mammen, M.; Dahmann, G.; Whitesides, G. M., Effective Inhibitors of Hemagglutination by Influenza Virus Synthesized from Polymers Having Active Ester Groups. Insight into Mechanism of Inhibition. *J. Med. Chem.* **1995**, *38* (21), 4179-4190.
228. Sigal, G. B.; Mammen, M.; Dahmann, G.; Whitesides, G. M., Polyacrylamides Bearing Pendant  $\alpha$ -Sialoside Groups Strongly Inhibit Agglutination of Erythrocytes by

Influenza Virus: The Strong Inhibition Reflects Enhanced Binding through Cooperative Polyvalent Interactions. *J. Am. Chem. Soc.* **1996**, *118* (16), 3789-3800.

229. Choi, S.-K.; Mammen, M.; Whitesides, G. M., Generation and in Situ Evaluation of Libraries of Poly(acrylic acid) Presenting Sialosides as Side Chains as Polyvalent Inhibitors of Influenza-Mediated Hemagglutination. *J. Am. Chem. Soc.* **1997**, *119* (18), 4103-4111.

230. Mortell, K. H.; Weatherman, R. V.; Kiessling, L. L., Recognition Specificity of Neoglycopolymers Prepared by Ring-Opening Metathesis Polymerization. *J. Am. Chem. Soc.* **1996**, *118* (9), 2297-2298.

231. Gestwicki, J. E.; Strong, L. E.; Kiessling, L. L., Tuning chemotactic responses with synthetic multivalent ligands. *Chem. Biol.* **2000**, *7* (8), 583-591.

232. Gestwicki, J. E.; Strong, L. E.; Kiessling, L. L., Visualization of Single Multivalent Receptor-Ligand Complexes by Transmission Electron Microscopy. *Angew. Chem. Int. Ed.* **2000**, *39* (24), 4567-4570.

233. Gestwicki, J. E.; Cairo, C. W.; Strong, L. E.; Oetjen, K. A.; Kiessling, L. L., Influencing Receptor-Ligand Binding Mechanisms with Multivalent Ligand Architecture. *J. Am. Chem. Soc.* **2002**, *124* (50), 14922-14933.

234. Cairo, C. W.; Gestwicki, J. E.; Kanai, M.; Kiessling, L. L., Control of Multivalent Interactions by Binding Epitope Density. *J. Am. Chem. Soc.* **2002**, *124* (8), 1615-1619.

235. Weatherman, R. V.; Kiessling, L. L., Fluorescence Anisotropy Assays Reveal Affinities of C- and O-Glycosides for Concanavalin A1. *J. Org. Chem.* **1996**, *61* (2), 534-538.

236. Ringsdorf, H., Structure and properties of pharmacologically active polymers. *J. Polym. Sci.: Polymer Symposia* **1975**, *51* (1), 135-153.

237. Fleming, C.; Maldjian, A.; Da Costa, D.; Rullay, A. K.; Haddleton, D. M.; St John, J.; Penny, P.; Noble, R. C.; Cameron, N. R.; Davis, B. G., A carbohydrate-antioxidant hybrid polymer reduces oxidative damage in spermatozoa and enhances fertility. *Nat. Chem. Biol.* **2005**, *1* (5), 270-274.

238. Tallroth, K.; Eskola, A.; Santavirta, S.; Konttinen, Y.; Lindholm, T., Aggressive granulomatous lesions after hip arthroplasty. *Bone Joint J.* **1989**, *71-B* (4), 571-575.

239. Santavirta, S.; Konttinen, Y. T.; Bergroth, V.; Eskola, A.; Tallroth, K.; Lindholm, T. S., Aggressive granulomatous lesions associated with hip arthroplasty. Immunopathological studies. *J. Bone Joint Surg.* **1990**, *72* (2), 252-258.
240. Mitchell, S. A.; Pratt, M. R.; Hruby, V. J.; Polt, R., Solid-Phase Synthesis of O-Linked Glycopeptide Analogues of Enkephalin. *J. Org. Chem.* **2001**, *66* (7), 2327-2342.
241. Nakahara, Y.; Hojo, H., Solid-Phase Synthesis of Glycopeptides. In *Experimental Glycoscience: Glycochemistry*, Taniguchi, N.; Suzuki, A.; Ito, Y.; Narimatsu, H.; Kawasaki, T.; Hase, S., Eds. Springer Japan: Tokyo, 2008; pp 195-199.
242. Wang, Y.; Kiick, K. L., Monodisperse Protein-Based Glycopolymers via a Combined Biosynthetic and Chemical Approach. *J. Am. Chem. Soc.* **2005**, *127* (47), 16392-16393.
243. Liu, S.; Kiick, K. L., Architecture Effects on the Binding of Cholera Toxin by Helical Glycopolypeptides. *Macromolecules* **2008**, *41* (3), 764-772.
244. Kramer, J. R.; Deming, T. J., Recent advances in glycopolypeptide synthesis. *Polym. Chem.* **2014**, *5* (3), 671-682.
245. Råde, E.; Meyer-Delius, M., Synthesis of the N-carboxy- $\alpha$ -amino acid anhydrides of several O-acetylated serine glycosides. *Carbohydr. Res.* **1968**, *8* (2), 219-232.
246. Råde, E.; Westphal, O.; Hurwitz, E.; Fuchs, S.; Sela, M., Synthesis and antigenic properties of sugar-polypeptide conjugates. *Immunochemistry* **1966**, *3* (2), 137-151.
247. Gibson, M. I.; Hunt, G. J.; Cameron, N. R., Improved synthesis of O-linked, and first synthesis of S-linked, carbohydrate functionalised N-carboxyanhydrides (glycoNCAs). *Org. Biomol. Chem.* **2007**, *5* (17), 2756-2757.
248. Kramer, J. R.; Deming, T. J., Glycopolypeptides via Living Polymerization of Glycosylated-l-lysine N-Carboxyanhydrides. *J. Am. Chem. Soc.* **2010**, *132* (42), 15068-15071.
249. Kramer, J. R.; Deming, T. J., Glycopolypeptides with a Redox-Triggered Helix-to-Coil Transition. *J. Am. Chem. Soc.* **2012**, *134* (9), 4112-4115.
250. Pati, D.; Shaikh, A. Y.; Hotha, S.; Gupta, S. S., Synthesis of glycopolypeptides by the ring opening polymerization of O-glycosylated-[small  $\alpha$ ]-amino acid N-carboxyanhydride (NCA). *Polym. Chem.* **2011**, *2* (4), 805-811.



251. Pati, D.; Shaikh, A. Y.; Das, S.; Nareddy, P. K.; Swamy, M. J.; Hotha, S.; Gupta, S. S., Controlled Synthesis of O-Glycopolypeptide Polymers and Their Molecular Recognition by Lectins. *Biomacromolecules* **2012**, *13* (5), 1287-1295.
252. Tian, Z.; Wang, M.; Zhang, A.; Feng, Z., Study on synthesis of glycopeptide-based triblock copolymers and their aggregation behavior in water. *Front. Mater. Sci. China* **2007**, *1* (2), 162-167.
253. Tian, Z.; Wang, M.; Zhang, A.-Y.; Feng, Z.-G., Preparation and evaluation of novel amphiphilic glycopeptide block copolymers as carriers for controlled drug release. *Polymer* **2008**, *49* (2), 446-454.
254. Midoux, P.; Mendes, C.; Legrand, A.; Raimond, J.; Mayer, R.; Monsigny, M.; Roche, A. C., Specific gene transfer mediated by lactosylated poly-L-lysine into hepatoma cells. *Nucleic Acids Res.* **1993**, *21* (4), 871-878.
255. Wang, R.; Xu, N.; Du, F.-S.; Li, Z.-C., Facile control of the self-assembled structures of polylysines having pendent mannose groups via pH and surfactant. *Chem. Commun.* **2010**, *46* (22), 3902-3904.
256. Rostovtsev, V. V.; Green, L. G.; Fokin, V. V.; Sharpless, K. B., A Stepwise Huisgen Cycloaddition Process: Copper(I)-Catalyzed Regioselective "Ligation" of Azides and Terminal Alkynes. *Angew. Chem. Int. Ed.* **2002**, *41* (14), 2596-2599.
257. Tornøe, C. W.; Christensen, C.; Meldal, M., Peptidotriazoles on Solid Phase: [1,2,3]-Triazoles by Regiospecific Copper(I)-Catalyzed 1,3-Dipolar Cycloadditions of Terminal Alkynes to Azides. *J. Org. Chem.* **2002**, *67* (9), 3057-3064.
258. Dhaware, V.; Shaikh, A. Y.; Kar, M.; Hotha, S.; Sen Gupta, S., Synthesis and Self-assembly of Amphiphilic Homoglycopolypeptide. *Langmuir* **2013**, *29* (19), 5659-5667.
259. Shaikh, A. Y.; Das, S.; Pati, D.; Dhaware, V.; Sen Gupta, S.; Hotha, S., Cationic Charged Helical Glycopolypeptide Using Ring Opening Polymerization of 6-Deoxy-6-azido-glyco-N-carboxyanhydride. *Biomacromolecules* **2014**, *15* (10), 3679-3686.
260. Jeyachandran, R.; Potukuchi, H. K.; Ackermann, L., Copper-catalyzed CuAAC/intramolecular C-H arylation sequence: Synthesis of annulated 1,2,3-triazoles. *Beilstein J. Org. Chem.* **2012**, *8*, 1771-1777.
261. Kramer, J. R.; Schmidt, N. W.; Mayle, K. M.; Kamei, D. T.; Wong, G. C. L.; Deming, T. J., Reinventing Cell Penetrating Peptides Using Glycosylated Methionine Sulfonium Ion Sequences. *ACS Cent. Sci.* **2015**, *1* (2), 83-88.

262. Bonduelle, C.; Huang, J.; Ibarboure, E.; Heise, A.; Lecommandoux, S., Synthesis and self-assembly of "tree-like" amphiphilic glycopolypeptides. *Chem. Commun.* **2012**, 48 (67), 8353-8355.
263. Hasegawa, T.; Kondoh, S.; Matsuura, K.; Kobayashi, K., Rigid Helical Poly(glycosyl phenyl isocyanide)s: Synthesis, Conformational Analysis, and Recognition by Lectins. *Macromolecules* **1999**, 32 (20), 6595-6603.
264. Polizzotti, B. D.; Kiick, K. L., Effects of Polymer Structure on the Inhibition of Cholera Toxin by Linear Polypeptide-Based Glycopolymers. *Biomacromolecules* **2006**, 7 (2), 483-490.
265. Chen, C.; Wang, Z.; Li, Z., Thermoresponsive Polypeptides from Pegylated Poly-l-glutamates. *Biomacromolecules* **2011**, 12 (8), 2859-2863.
266. Hanson, J. A.; Li, Z.; Deming, T. J., Nonionic Block Copolypeptide Micelles Containing a Hydrophobic rac-Leucine Core. *Macromolecules* **2010**, 43 (15), 6268-6269.
267. Gou, Y.; Geng, J.; Richards, S.-J.; Burns, J.; Remzi Becer, C.; Haddleton, D. M., A detailed study on understanding glycopolymer library and Con A interactions. *J. Polym. Sci. Part A* **2013**, 51 (12), 2588-2597.
268. Urbani, C. N.; Bell, C. A.; Whittaker, M. R.; Monteiro, M. J., Convergent Synthesis of Second Generation AB-Type Miktoarm Dendrimers Using "Click" Chemistry Catalyzed by Copper Wire. *Macromolecules* **2008**, 41 (4), 1057-1060.
269. Morrow, J. A.; Segall, M. L.; Lund-Katz, S.; Phillips, M. C.; Knapp, M.; Rupp, B.; Weisgraber, K. H., Differences in Stability among the Human Apolipoprotein E Isoforms Determined by the Amino-Terminal Domain. *Biochemistry* **2000**, 39 (38), 11657-11666.
270. Naismith, J. H.; Emmerich, C.; Habash, J.; Harrop, S. J.; Helliwell, J. R.; Hunter, W. N.; Raftery, J.; Kalb, A. J.; Yariv, J., Refined structure of concanavalin A complexed with methyl  $\alpha$ -d-mannopyranoside at 2.0 Å resolution and comparison with the saccharide-free structure. *Acta Crystallogr. Sect. D: Biol. Crystallogr.* **1994**, 50 (6), 847-858.
271. Islam Khan, M.; Mandal, D. K.; Brewer, C. F., Interactions of concanavalin A with glycoproteins. A quantitative precipitation study of concanavalin A with the soybean agglutinin. *Carbohydr. Res.* **1991**, 213, 69-77.

272. Chan, B. A.; Xuan, S.; Horton, M.; Zhang, D., 1,1,3,3-Tetramethylguanidine-Promoted Ring-Opening Polymerization of N-Butyl N-Carboxyanhydride Using Alcohol Initiators. *Macromolecules* **2016**, *49* (6), 2002-2012.
273. Flory, P. J., A Comparison of Esterification and Ester Interchange Kinetics. *J. Am. Chem. Soc.* **1940**, *62* (9), 2261-2264.
274. Martello, M. T.; Burns, A.; Hillmyer, M., Bulk Ring-Opening Transesterification Polymerization of the Renewable  $\delta$ -Decalactone Using an Organocatalyst. *ACS Macro Lett.* **2011**, *1* (1), 131-135.
275. Lohmeijer, B. G. G.; Pratt, R. C.; Leibfarth, F.; Logan, J. W.; Long, D. A.; Dove, A. P.; Nederberg, F.; Choi, J.; Wade, C.; Waymouth, R. M.; Hedrick, J. L., Guanidine and Amidine Organocatalysts for Ring-Opening Polymerization of Cyclic Esters. *Macromolecules* **2006**, *39* (25), 8574-8583.
276. Chuma, A.; Horn, H. W.; Swope, W. C.; Pratt, R. C.; Zhang, L.; Lohmeijer, B. G. G.; Wade, C. G.; Waymouth, R. M.; Hedrick, J. L.; Rice, J. E., The Reaction Mechanism for the Organocatalytic Ring-Opening Polymerization of L-Lactide Using a Guanidine-Based Catalyst: Hydrogen-Bonded or Covalently Bound? *J. Am. Chem. Soc.* **2008**, *130* (21), 6749-6754.
277. Kiesewetter, M. K.; Scholten, M. D.; Kirn, N.; Weber, R. L.; Hedrick, J. L.; Waymouth, R. M., Cyclic Guanidine Organic Catalysts: What Is Magic About Triazabicyclodecene? *J. Org. Chem.* **2009**, *74* (24), 9490-9496.
278. Zhang, L.; Pratt, R. C.; Nederberg, F.; Horn, H. W.; Rice, J. E.; Waymouth, R. M.; Wade, C. G.; Hedrick, J. L., Acyclic Guanidines as Organic Catalysts for Living Polymerization of Lactide. *Macromolecules* **2010**, *43* (3), 1660-1664.
279. Pratt, R. C.; Lohmeijer, B. G. G.; Long, D. A.; Waymouth, R. M.; Hedrick, J. L., Triazabicyclodecene: A Simple Bifunctional Organocatalyst for Acyl Transfer and Ring-Opening Polymerization of Cyclic Esters. *J. Am. Chem. Soc.* **2006**, *128* (14), 4556-4557.
280. Zhang, L.; Nederberg, F.; Messman, J. M.; Pratt, R. C.; Hedrick, J. L.; Wade, C. G., Organocatalytic Stereoselective Ring-Opening Polymerization of Lactide with Dimeric Phosphazene Bases. *J. Am. Chem. Soc.* **2007**, *129* (42), 12610-12611.
281. Zhang, L.; Nederberg, F.; Pratt, R. C.; Waymouth, R. M.; Hedrick, J. L.; Wade, C. G., Phosphazene Bases: A New Category of Organocatalysts for the Living Ring-Opening Polymerization of Cyclic Esters. *Macromolecules* **2007**, *40* (12), 4154-4158.

282. Piedra-Arroni, E.; Ladavière, C.; Amgoune, A.; Bourissou, D., Ring-Opening Polymerization with Zn(C6F5)2-Based Lewis Pairs: Original and Efficient Approach to Cyclic Polyesters. *J. Am. Chem. Soc.* **2013**, *135* (36), 13306-13309.
283. Kricheldorf, H. R.; Lomadze, N.; Schwarz, G., Cyclic Poly(thioglycolide) and Poly(d,l-thiolactide) by Zwitterionic Polymerization of Dithiolane-2,4-diones. *Macromolecules* **2007**, *40* (14), 4859-4864.
284. Coulembier, O.; De Winter, J.; Josse, T.; Mespouille, L.; Gerbaux, P.; Dubois, P., One-step synthesis of polylactide macrocycles from sparteine-initiated ROP. *Polym. Chem.* **2014**, *5* (6), 2103-2108.
285. Kricheldorf, H. R.; Garaleh, M.; Schwarz, G., Tertiary Amine - Initiated Zwitterionic Polymerization of Pivalolactone—A Reinvestigation by Means of MALDI - TOF Mass Spectrometry. *J. Macromol. Sci., Pure Appl. Chem.* **2005**, *42* (2), 139-148.
286. Coulembier, O.; Josse, T.; Guillerm, B.; Gerbaux, P.; Dubois, P., An imidazole-based organocatalyst designed for bulk polymerization of lactide isomers: inspiration from Nature. *Chem. Commun.* **2012**, *48* (95), 11695-11697.
287. Kamber, N. E.; Jeong, W.; Gonzalez, S.; Hedrick, J. L.; Waymouth, R. M., N-Heterocyclic Carbenes for the Organocatalytic Ring-Opening Polymerization of  $\epsilon$ -Caprolactone. *Macromolecules* **2009**, *42* (5), 1634-1639.
288. Lai, C.-L.; Lee, H. M.; Hu, C.-H., Theoretical study on the mechanism of N-heterocyclic carbene catalyzed transesterification reactions. *Tetrahedron Lett.* **2005**, *46* (37), 6265-6270.
289. Wang, Y.; Zhang, L.; Guo, X.; Zhang, R.; Li, J., Characteristics and mechanism of L-lactide polymerization using N-heterocyclic carbene organocatalyst. *J. Polym. Res.* **2013**, *20* (3), 1-6.
290. Simón, L.; Goodman, J. M., The Mechanism of TBD-Catalyzed Ring-Opening Polymerization of Cyclic Esters. *J. Org. Chem.* **2007**, *72* (25), 9656-9662.
291. Nederberg, F.; Trang, V.; Pratt, R. C.; Mason, A. F.; Frank, C. W.; Waymouth, R. M.; Hedrick, J. L., New Ground for Organic Catalysis: A Ring-Opening Polymerization Approach to Hydrogels. *Biomacromolecules* **2007**, *8* (11), 3294-3297.
292. Miller, S. M.; Simon, R. J.; Ng, S.; Zuckermann, R. N.; Kerr, J. M.; Moos, W. H., Comparison of the proteolytic susceptibilities of homologous L-amino acid, D-amino

acid, and N-substituted glycine peptide and peptoid oligomers. *Drug Development Research* **1995**, *35* (1), 20-32.

293. Lee, C.-U.; Lu, L.; Chen, J.; Garno, J. C.; Zhang, D., Crystallization-Driven Thermoreversible Gelation of Coil-Crystalline Cyclic and Linear Diblock Copolypeptoids. *ACS Macro Lett.* **2013**, *2* (5), 436-440.

294. Chongsiriwatana, N. P.; Patch, J. A.; Czyzewski, A. M.; Dohm, M. T.; Ivankin, A.; Gidalevitz, D.; Zuckermann, R. N.; Barron, A. E., Peptoids that mimic the structure, function, and mechanism of helical antimicrobial peptides. *Proc. Natl. Acad. Sci.* **2008**, *105* (8), 2794-2799.

295. Barz, M.; Luxenhofer, R.; Zentel, R.; Vicent, M. J., Overcoming the PEG-addiction: well-defined alternatives to PEG, from structure-property relationships to better defined therapeutics. *Polym. Chem.* **2011**, *2* (9), 1900-1918.

296. Zhang, D.; Lahasky, S. H.; Guo, L.; Lee, C.-U.; Lavan, M., Polypeptoid Materials: Current Status and Future Perspectives. *Macromolecules* **2012**, *45* (15), 5833-5841.

297. Erlanger, B. F.; Brand, E., Optical Rotation of Peptides. I. Glycine and Alanine Dipeptides. *J. Am. Chem. Soc.* **1951**, *73* (7), 3508-3510.

298. Katchalski, E.; Spitnik, P., Ornithine Anhydride. *J. Am. Chem. Soc.* **1951**, *73* (6), 2946-2947.

299. Patchornik, A.; Sela, M.; Katchalski, E., Polytryptophan. *J. Am. Chem. Soc.* **1954**, *76* (1), 299-300.

300. Bergmann, M.; Zervas, L.; Ross, W. F., On proteolytic enzymes: VII. The synthesis of peptides of L-lysine and their behavior with papain. *J. Biol. Chem.* **1935**, *111* (1), 245-260.

301. Deng, Y.; Zou, T.; Tao, X.; Semetey, V.; Trepout, S.; Marco, S.; Ling, J.; Li, M.-H., Poly( $\epsilon$ -caprolactone)-block-polysarcosine by Ring-Opening Polymerization of Sarcosine N-Thiocarboxyanhydride: Synthesis and Thermoresponsive Self-Assembly. *Biomacromolecules* **2015**, *16* (10), 3265-3274.

302. Vazdar, K.; Kunetskiy, R.; Saame, J.; Kaupmees, K.; Leito, I.; Jahn, U., Very Strong Organosuperbases Formed by Combining Imidazole and Guanidine Bases: Synthesis, Structure, and Basicity. *Angew. Chem. Int. Ed.* **2014**, *53* (5), 1435-1438.

303. Kunetskiy, R. A.; Polyakova, S. M.; Vavřík, J.; Císařová, I.; Saame, J.; Nerut, E. R.; Koppel, I.; Koppel, I. A.; Kütt, A.; Leito, I.; Lyapkalo, I. M., A New Class of Organosuperbases, N-Alkyl- and N-Aryl-1,3-dialkyl-4,5-dimethylimidazol-2-ylidene Amines: Synthesis, Structure, pKBH<sup>+</sup> Measurements, and Properties. *Chem. Eur. J.* **2012**, *18* (12), 3621-3630.
304. Kaupmees, K.; Trummal, A.; Leito, I., Basicities of Strong Bases in Water: A Computational Study. *Croat. Chem. Acta* **2014**, *87* (4), 385-395.
305. Kaljurand, I.; Kütt, A.; Sooväli, L.; Rodima, T.; Mäemets, V.; Leito, I.; Koppel, I. A., Extension of the Self-Consistent Spectrophotometric Basicity Scale in Acetonitrile to a Full Span of 28 pK<sub>a</sub> Units: Unification of Different Basicity Scales. *J. Org. Chem.* **2005**, *70* (3), 1019-1028.
306. Pratt, R. C.; Nederberg, F.; Waymouth, R. M.; Hedrick, J. L., Tagging alcohols with cyclic carbonate: a versatile equivalent of (meth)acrylate for ring-opening polymerization. *Chem. Commun.* **2008**, (1), 114-116.
307. Leroux, F.; Montembault, V.; Pascual, S.; Guerin, W.; Guillaume, S. M.; Fontaine, L., Synthesis and polymerization of cyclobutenyl-functionalized polylactide and polycaprolactone: a consecutive ROP/ROMP route towards poly(1,4-butadiene)-g-polyesters. *Polym. Chem.* **2014**, *5* (10), 3476-3486.
308. Pascual, A.; Sardon, H.; Veloso, A.; Ruipérez, F.; Mecerreyes, D., Organocatalyzed Synthesis of Aliphatic Polyesters from Ethylene Brassylate: A Cheap and Renewable Macrolactone. *ACS Macro Lett.* **2014**, *3* (9), 849-853.
309. Todd, R.; Tempelaar, S.; Lo Re, G.; Spinella, S.; McCallum, S. A.; Gross, R. A.; Raquez, J.-M.; Dubois, P., Poly( $\omega$ -pentadecalactone)-b-poly(l-lactide) Block Copolymers via Organic-Catalyzed Ring Opening Polymerization and Potential Applications. *ACS Macro Lett.* **2015**, *4* (4), 408-411.
310. Olmstead, W. N.; Margolin, Z.; Bordwell, F. G., Acidities of water and simple alcohols in dimethyl sulfoxide solution. *J. Org. Chem.* **1980**, *45* (16), 3295-3299.
311. Ripin, D. H., Evans, D.A. [http://evans.rc.fas.harvard.edu/pdf/evans\\_pKa\\_table.pdf](http://evans.rc.fas.harvard.edu/pdf/evans_pKa_table.pdf) (accessed 11/17/2015).
312. Brown, W. H. F., C.S.; Iverson, B.L.; Anslyn, E., *Organic Chemistry, Enhanced Edition*. Brooks Cole: Boston, MA, 2010.

313. Dell'Amico, D. B.; Calderazzo, F.; Giurlani, U., Metal-assisted electrophilic reactions on carbon dioxide: synthesis of mixed carboxylato-carbamato anhydrides. *J. Chem. Soc. Chem. Commun.* **1986**, (13), 1000-1001.
314. Rawlinson, D. J.; Humke, B. M., Peroxyester reaction of dimethylformamide. *Tetrahedron Lett.* **1972**, 13 (43), 4395-4398.
315. Grainger, R. S.; Leadbeater, N. E.; Masdeu Pàmies, A., The tetramethylguanidine catalyzed Baylis–Hillman reaction: Effects of co-catalysts and alcohol solvents on reaction rate. *Catal. Commun.* **2002**, 3 (10), 449-452.
316. Bordwell, F. G.; Drucker, G. E.; Fried, H. E., Acidities of carbon and nitrogen acids: the aromaticity of the cyclopentadienyl anion. *J. Org. Chem.* **1981**, 46 (3), 632-635.
317. Yamada, S.; Koga, K.; Endo, T., Useful synthetic method of polypeptides with well-defined structure by polymerization of activated urethane derivatives of  $\alpha$ -amino acids. *J. Polym. Sci. Part A* **2012**, 50 (13), 2527-2532.
318. Doriti, A.; Brosnan, S. M.; Weidner, S. M.; Schlaad, H., Synthesis of polysarcosine from air and moisture stable N-phenoxy carbonyl-N-methylglycine assisted by tertiary amine base. *Polym. Chem.* **2016**, 7 (18), 3067-3070.
319. Kricheldorf, H. R., Über die Polymerisation von  $\alpha$ -Aminosäure-N-carboxyanhydriden (1,3-Oxazolidin-2,5-dionen) und  $\alpha$ -Aminosäure-N-thiocarboxyanhydriden (1,3-Thiazolidin-2,5-dionen). *Makromol. Chem.* **1974**, 175 (12), 3325-3342.
320. Kricheldorf, H. R.; Böisinger, K., Mechanismus der NCA-Polymerisation, 3. Über die Amin katalysierte Polymerisation von Sarkosin-NCA und -NTA. *Makromol. Chem.* **1976**, 177 (5), 1243-1258.
321. Kamber, N. E.; Jeong, W.; Waymouth, R. M.; Pratt, R. C.; Lohmeijer, B. G. G.; Hedrick, J. L., Organocatalytic Ring-Opening Polymerization. *Chem. Rev.* **2007**, 107 (12), 5813-5840.
322. Inomata, K.; Shimizu, H.; Nose, T., Phase equilibrium studies on rod/solvent and rod/coil/solvent systems containing poly( $\alpha$ , L-glutamate) having oligo(ethylene glycol) side chains. *J. Polym. Sci. Part B Polym. Phys.* **2000**, 38 (10), 1331-1340.
323. Tang, D.; Lin, J.; Lin, S.; Zhang, S.; Chen, T.; Tian, X., Self-Assembly of Poly( $\gamma$ -benzyl L-glutamate)-graft-Poly(ethylene glycol) and Its Mixtures with Poly( $\gamma$ -benzyl L-glutamate) Homopolymer. *Macromol. Rapid Commun.* **2004**, 25 (13), 1241-1246.

324. Watanabe, J.; Ono, H.; Uematsu, I.; Abe, A., Thermotropic polypeptides. 2. Molecular packing and thermotropic behavior of poly(L-glutamates) with long n-alkyl side chains. *Macromolecules* **1985**, *18* (11), 2141-2148.
325. Zhu, G.-Q., Structure and performance of poly( $\gamma$ -benzyl L-glutamate)-graft-poly(ethylene glycol) copolymer membrane. *Fibers and Polymers* **2009**, *10* (4), 425-429.
326. Kanazawa, H.; Kawai, T., Polymerization of N-carboxy-amino acid anhydrides in the solid state. I. Polymerizability of the various  $\alpha$ -amino acid NCAs in the solid state. *J. Polym. Sci. Part A* **1980**, *18* (2), 629-642.
327. Hernández, J. R.; Klok, H.-A., Synthesis and ring-opening (co)polymerization of L-lysine N-carboxyanhydrides containing labile side-chain protective groups. *J. Polym. Sci. Part A* **2003**, *41* (9), 1167-1187.



# APPENDIX – COPYRIGHT PERMISSIONS

Rightslink® by Copyright Clearance Center

10.05.16, 11:41



RightsLink®

Home

Account Info

Help



ACS Publications  
Most Trusted. Most Cited. Most Read.

**Title:** Amidine-Mediated Zwitterionic Ring-Opening Polymerization of N-Alkyl N-Carboxyanhydride: Mechanism, Kinetics, and Architecture Elucidation

Logged in as:  
Brandon Chan  
Account #:  
3000992882

LOGOUT

**Author:** Ang Li, Lu Lu, Xin Li, et al

**Publication:** Macromolecules

**Publisher:** American Chemical Society

**Date:** Feb 1, 2016

Copyright © 2016, American Chemical Society

## PERMISSION/LICENSE IS GRANTED FOR YOUR ORDER AT NO CHARGE

This type of permission/license, instead of the standard Terms & Conditions, is sent to you because no fee is being charged for your order. Please note the following:

- Permission is granted for your request in both print and electronic formats, and translations.
- If figures and/or tables were requested, they may be adapted or used in part.
- Please print this page for your records and send a copy of it to your publisher/graduate school.
- Appropriate credit for the requested material should be given as follows: "Reprinted (adapted) with permission from (COMPLETE REFERENCE CITATION). Copyright (YEAR) American Chemical Society." Insert appropriate information in place of the capitalized words.
- One-time permission is granted only for the use specified in your request. No additional uses are granted (such as derivative works or other editions). For any other uses, please submit a new request.

If credit is given to another source for the material you requested, permission must be obtained from that source.

BACK

CLOSE WINDOW

Copyright © 2016 Copyright Clearance Center, Inc. All Rights Reserved. [Privacy statement](#). [Terms and Conditions](#).  
Comments? We would like to hear from you. E-mail us at [customercare@copyright.com](mailto:customercare@copyright.com)



RightsLink®

Home

Account  
Info

Help

ACS Publications  
Most Trusted. Most Cited. Most Read.

**Title:** Fast and Living Ring-Opening  
Polymerization of  $\alpha$ -Amino Acid  
N-Carboxyanhydrides Triggered  
by an "Alliance" of Primary and  
Secondary Amines at Room  
Temperature

Logged in as:  
Brandon Chan  
Account #:  
3000992882

LOGOUT

**Author:** Wei Zhao, Yves Gnanou, Nikos  
Hadjichristidis

**Publication:** Biomacromolecules

**Publisher:** American Chemical Society

**Date:** Apr 1, 2015

Copyright © 2015, American Chemical Society

### PERMISSION/LICENSE IS GRANTED FOR YOUR ORDER AT NO CHARGE

This type of permission/license, instead of the standard Terms & Conditions, is sent to you because no fee is being charged for your order. Please note the following:

- Permission is granted for your request in both print and electronic formats, and translations.
- If figures and/or tables were requested, they may be adapted or used in part.
- Please print this page for your records and send a copy of it to your publisher/graduate school.
- Appropriate credit for the requested material should be given as follows: "Reprinted (adapted) with permission from (COMPLETE REFERENCE CITATION). Copyright (YEAR) American Chemical Society." Insert appropriate information in place of the capitalized words.
- One-time permission is granted only for the use specified in your request. No additional uses are granted (such as derivative works or other editions). For any other uses, please submit a new request.

If credit is given to another source for the material you requested, permission must be obtained from that source.

BACK

CLOSE WINDOW

Copyright © 2016 Copyright Clearance Center, Inc. All Rights Reserved. [Privacy statement](#). [Terms and Conditions](#).  
Comments? We would like to hear from you. E-mail us at [customercare@copyright.com](mailto:customercare@copyright.com)



RightsLink®

[Home](#)[Account Info](#)[Help](#)ACS Publications  
Most Trusted. Most Cited. Most Read.

**Title:** 1,1,3,3-Tetramethylguanidine-Promoted Ring-Opening Polymerization of N-Butyl N-Carboxyanhydride Using Alcohol Initiators

Logged in as:  
Brandon Chan  
Account #:  
3000992882

[LOGOUT](#)

**Author:** Brandon A. Chan, Sunting Xuan, Matthew Horton, et al

**Publication:** Macromolecules

**Publisher:** American Chemical Society

**Date:** Mar 1, 2016

Copyright © 2016, American Chemical Society

### PERMISSION/LICENSE IS GRANTED FOR YOUR ORDER AT NO CHARGE

This type of permission/license, instead of the standard Terms & Conditions, is sent to you because no fee is being charged for your order. Please note the following:

- Permission is granted for your request in both print and electronic formats, and translations.
- If figures and/or tables were requested, they may be adapted or used in part.
- Please print this page for your records and send a copy of it to your publisher/graduate school.
- Appropriate credit for the requested material should be given as follows: "Reprinted (adapted) with permission from (COMPLETE REFERENCE CITATION). Copyright (YEAR) American Chemical Society." Insert appropriate information in place of the capitalized words.
- One-time permission is granted only for the use specified in your request. No additional uses are granted (such as derivative works or other editions). For any other uses, please submit a new request.

[BACK](#)[CLOSE WINDOW](#)

Copyright © 2016 Copyright Clearance Center, Inc. All Rights Reserved. [Privacy statement](#). [Terms and Conditions](#).  
Comments? We would like to hear from you. E-mail us at [customercare@copyright.com](mailto:customercare@copyright.com)

**JOHN WILEY AND SONS LICENSE  
TERMS AND CONDITIONS**

May 10, 2016

---

This Agreement between Brandon A Chan ("You") and John Wiley and Sons ("John Wiley and Sons") consists of your license details and the terms and conditions provided by John Wiley and Sons and Copyright Clearance Center.

License Number	3865440082361
License date	May 10, 2016
Licensed Content Publisher	John Wiley and Sons
Licensed Content Publication	Journal of Polymer Science Part A: Polymer Chemistry
Licensed Content Title	Polymerization of $\alpha$ -amino acid N-carboxyanhydrides catalyzed by rare earth tris(borohydride) complexes: Mechanism and hydroxy-endcapped polypeptides
Licensed Content Author	Hui Peng, Jun Ling, Yinghong Zhu, Lixin You, Zhiquan Shen
Licensed Content Date	Apr 21, 2012
Pages	14
Type of use	Dissertation/Thesis
Requestor type	University/Academic
Format	Electronic
Portion	Figure/table
Number of figures/tables	1
Original Wiley figure/table number(s)	Scheme 2
Will you be translating?	No
Title of your thesis / dissertation	Peptidomimetic Polymers: Advances in Monomer Design and Polymerization Methods
Expected completion date	May 2016
Expected size (number of pages)	250
Requestor Location	Brandon A Chan 424 Chemistry and Materials Building Department of Chemistry Louisiana State University BATON ROUGE, LA 70803 United States Attn: Brandon A Chan
Billing Type	Invoice
Billing Address	Brandon A Chan 424 Chemistry and Materials Building Department of Chemistry Louisiana State University BATON ROUGE, LA 70803 United States

**JOHN WILEY AND SONS LICENSE  
TERMS AND CONDITIONS**

May 10, 2016

---

This Agreement between Brandon A Chan ("You") and John Wiley and Sons ("John Wiley and Sons") consists of your license details and the terms and conditions provided by John Wiley and Sons and Copyright Clearance Center.

License Number	3865440640674
License date	May 10, 2016
Licensed Content Publisher	John Wiley and Sons
Licensed Content Publication	Macromolecular Rapid Communications
Licensed Content Title	Highly Defined Multiblock Copolypeptoids: Pushing the Limits of Living Nucleophilic Ring-Opening Polymerization
Licensed Content Author	Corinna Fetsch, Robert Luxenhofer
Licensed Content Date	Jun 5, 2012
Pages	6
Type of use	Dissertation/Thesis
Requestor type	University/Academic
Format	Electronic
Portion	Figure/table
Number of figures/tables	1
Original Wiley figure/table number(s)	Figure 3
Will you be translating?	No
Title of your thesis / dissertation	Peptidomimetic Polymers: Advances in Monomer Design and Polymerization Methods
Expected completion date	May 2016
Expected size (number of pages)	250
Requestor Location	Brandon A Chan 424 Chemistry and Materials Building Department of Chemistry Louisiana State University BATON ROUGE, LA 70803 United States Attn: Brandon A Chan
Billing Type	Invoice
Billing Address	Brandon A Chan 424 Chemistry and Materials Building Department of Chemistry Louisiana State University BATON ROUGE, LA 70803 United States Attn: Brandon A Chan

Total 0.00 USD

Terms and Conditions

### TERMS AND CONDITIONS

This copyrighted material is owned by or exclusively licensed to John Wiley & Sons, Inc. or one of its group companies (each a "Wiley Company") or handled on behalf of a society with which a Wiley Company has exclusive publishing rights in relation to a particular work (collectively "WILEY"). By clicking "accept" in connection with completing this licensing transaction, you agree that the following terms and conditions apply to this transaction (along with the billing and payment terms and conditions established by the Copyright Clearance Center Inc., ("CCC's Billing and Payment terms and conditions"), at the time that you opened your RightsLink account (these are available at any time at <http://myaccount.copyright.com>).

#### Terms and Conditions

- The materials you have requested permission to reproduce or reuse (the "Wiley Materials") are protected by copyright.
- You are hereby granted a personal, non-exclusive, non-sub licensable (on a stand-alone basis), non-transferable, worldwide, limited license to reproduce the Wiley Materials for the purpose specified in the licensing process. This license, **and any CONTENT (PDF or image file) purchased as part of your order**, is for a one-time use only and limited to any maximum distribution number specified in the license. The first instance of republication or reuse granted by this license must be completed within two years of the date of the grant of this license (although copies prepared before the end date may be distributed thereafter). The Wiley Materials shall not be used in any other manner or for any other purpose, beyond what is granted in the license. Permission is granted subject to an appropriate acknowledgement given to the author, title of the material/book/journal and the publisher. You shall also duplicate the copyright notice that appears in the Wiley publication in your use of the Wiley Material. Permission is also granted on the understanding that nowhere in the text is a previously published source acknowledged for all or part of this Wiley Material. Any third party content is expressly excluded from this permission.
- With respect to the Wiley Materials, all rights are reserved. Except as expressly granted by the terms of the license, no part of the Wiley Materials may be copied, modified, adapted (except for minor reformatting required by the new Publication), translated, reproduced, transferred or distributed, in any form or by any means, and no derivative works may be made based on the Wiley Materials without the prior permission of the respective copyright owner. **For STM Signatory Publishers clearing permission under the terms of the STM Permissions Guidelines only, the terms of the license are extended to include subsequent editions and for editions in other languages, provided such editions are for the work as a whole in situ and does not involve the separate exploitation of the permitted figures or extracts**, You may not alter, remove or suppress in any manner any copyright, trademark or other notices displayed by the Wiley Materials. You may not license, rent, sell, loan, lease, pledge, offer as security, transfer or assign the Wiley Materials on a stand-alone basis, or any of the rights granted to you hereunder to any other person.

- The Wiley Materials and all of the intellectual property rights therein shall at all times remain the exclusive property of John Wiley & Sons Inc, the Wiley Companies, or their respective licensors, and your interest therein is only that of having possession of and the right to reproduce the Wiley Materials pursuant to Section 2 herein during the continuance of this Agreement. You agree that you own no right, title or interest in or to the Wiley Materials or any of the intellectual property rights therein. You shall have no rights hereunder other than the license as provided for above in Section 2. No right, license or interest to any trademark, trade name, service mark or other branding ("Marks") of WILEY or its licensors is granted hereunder, and you agree that you shall not assert any such right, license or interest with respect thereto
- NEITHER WILEY NOR ITS LICENSORS MAKES ANY WARRANTY OR REPRESENTATION OF ANY KIND TO YOU OR ANY THIRD PARTY, EXPRESS, IMPLIED OR STATUTORY, WITH RESPECT TO THE MATERIALS OR THE ACCURACY OF ANY INFORMATION CONTAINED IN THE MATERIALS, INCLUDING, WITHOUT LIMITATION, ANY IMPLIED WARRANTY OF MERCHANTABILITY, ACCURACY, SATISFACTORY QUALITY, FITNESS FOR A PARTICULAR PURPOSE, USABILITY, INTEGRATION OR NON-INFRINGEMENT AND ALL SUCH WARRANTIES ARE HEREBY EXCLUDED BY WILEY AND ITS LICENSORS AND WAIVED BY YOU.
- WILEY shall have the right to terminate this Agreement immediately upon breach of this Agreement by you.
- You shall indemnify, defend and hold harmless WILEY, its Licensors and their respective directors, officers, agents and employees, from and against any actual or threatened claims, demands, causes of action or proceedings arising from any breach of this Agreement by you.
- IN NO EVENT SHALL WILEY OR ITS LICENSORS BE LIABLE TO YOU OR ANY OTHER PARTY OR ANY OTHER PERSON OR ENTITY FOR ANY SPECIAL, CONSEQUENTIAL, INCIDENTAL, INDIRECT, EXEMPLARY OR PUNITIVE DAMAGES, HOWEVER CAUSED, ARISING OUT OF OR IN CONNECTION WITH THE DOWNLOADING, PROVISIONING, VIEWING OR USE OF THE MATERIALS REGARDLESS OF THE FORM OF ACTION, WHETHER FOR BREACH OF CONTRACT, BREACH OF WARRANTY, TORT, NEGLIGENCE, INFRINGEMENT OR OTHERWISE (INCLUDING, WITHOUT LIMITATION, DAMAGES BASED ON LOSS OF PROFITS, DATA, FILES, USE, BUSINESS OPPORTUNITY OR CLAIMS OF THIRD PARTIES), AND WHETHER OR NOT THE PARTY HAS BEEN ADVISED OF THE POSSIBILITY OF SUCH DAMAGES. THIS LIMITATION SHALL APPLY NOTWITHSTANDING ANY FAILURE OF ESSENTIAL PURPOSE OF ANY LIMITED REMEDY PROVIDED HEREIN.
- Should any provision of this Agreement be held by a court of competent jurisdiction to be illegal, invalid, or unenforceable, that provision shall be deemed amended to achieve as nearly as possible the same economic effect as the original provision, and the legality, validity and enforceability of the remaining provisions of this Agreement shall not be affected or impaired thereby.

- The failure of either party to enforce any term or condition of this Agreement shall not constitute a waiver of either party's right to enforce each and every term and condition of this Agreement. No breach under this agreement shall be deemed waived or excused by either party unless such waiver or consent is in writing signed by the party granting such waiver or consent. The waiver by or consent of a party to a breach of any provision of this Agreement shall not operate or be construed as a waiver of or consent to any other or subsequent breach by such other party.
- This Agreement may not be assigned (including by operation of law or otherwise) by you without WILEY's prior written consent.
- Any fee required for this permission shall be non-refundable after thirty (30) days from receipt by the CCC.
- These terms and conditions together with CCC's Billing and Payment terms and conditions (which are incorporated herein) form the entire agreement between you and WILEY concerning this licensing transaction and (in the absence of fraud) supersedes all prior agreements and representations of the parties, oral or written. This Agreement may not be amended except in writing signed by both parties. This Agreement shall be binding upon and inure to the benefit of the parties' successors, legal representatives, and authorized assigns.
- In the event of any conflict between your obligations established by these terms and conditions and those established by CCC's Billing and Payment terms and conditions, these terms and conditions shall prevail.
- WILEY expressly reserves all rights not specifically granted in the combination of (i) the license details provided by you and accepted in the course of this licensing transaction, (ii) these terms and conditions and (iii) CCC's Billing and Payment terms and conditions.
- This Agreement will be void if the Type of Use, Format, Circulation, or Requestor Type was misrepresented during the licensing process.
- This Agreement shall be governed by and construed in accordance with the laws of the State of New York, USA, without regards to such state's conflict of law rules. Any legal action, suit or proceeding arising out of or relating to these Terms and Conditions or the breach thereof shall be instituted in a court of competent jurisdiction in New York County in the State of New York in the United States of America and each party hereby consents and submits to the personal jurisdiction of such court, waives any objection to venue in such court and consents to service of process by registered or certified mail, return receipt requested, at the last known address of such party.

#### **WILEY OPEN ACCESS TERMS AND CONDITIONS**

Wiley Publishes Open Access Articles in fully Open Access Journals and in Subscription journals offering Online Open. Although most of the fully Open Access journals publish open access articles under the terms of the Creative Commons Attribution (CC BY) License only, the subscription journals and a few of the Open Access Journals offer a choice of Creative Commons Licenses. The license type is clearly identified on the article.



**The Creative Commons Attribution License**

The Creative Commons Attribution License (CC-BY) allows users to copy, distribute and transmit an article, adapt the article and make commercial use of the article. The CC-BY license permits commercial and non-

**Creative Commons Attribution Non-Commercial License**

The Creative Commons Attribution Non-Commercial (CC-BY-NC) License permits use, distribution and reproduction in any medium, provided the original work is properly cited and is not used for commercial purposes.(see below)

**Creative Commons Attribution-Non-Commercial-NoDerivs License**

The Creative Commons Attribution Non-Commercial-NoDerivs License (CC-BY-NC-ND) permits use, distribution and reproduction in any medium, provided the original work is properly cited, is not used for commercial purposes and no modifications or adaptations are made. (see below)

**Use by commercial "for-profit" organizations**

Use of Wiley Open Access articles for commercial, promotional, or marketing purposes requires further explicit permission from Wiley and will be subject to a fee.

Further details can be found on Wiley Online Library

<http://olabout.wiley.com/WileyCDA/Section/id-410895.html>

**Other Terms and Conditions:**

v1.10 Last updated September 2015

Questions? [customercare@copyright.com](mailto:customercare@copyright.com) or +1-855-239-3415 (toll free in the US) or +1-978-646-2777.

---

---

**ROYAL SOCIETY OF CHEMISTRY LICENSE  
TERMS AND CONDITIONS**

May 10, 2016

This Agreement between Brandon A Chan ("You") and Royal Society of Chemistry ("Royal Society of Chemistry") consists of your license details and the terms and conditions provided by Royal Society of Chemistry and Copyright Clearance Center.

License Number	3865431250785
License date	May 10, 2016
Licensed Content Publisher	Royal Society of Chemistry
Licensed Content Publication	Chemical Communications (Cambridge)
Licensed Content Title	Recent advances in amino acid N-carboxyanhydrides and synthetic polypeptides: chemistry, self-assembly and biological applications
Licensed Content Author	Hua Lu, Jing Wang, Ziyuan Song, Lichen Yin, Yanfeng Zhang, Haoyu Tang, Chunlai Tu, Yao Lin, Jianjun Cheng
Licensed Content Date	Oct 16, 2013
Licensed Content Volume Number	50
Licensed Content Issue Number	2
Type of Use	Thesis/Dissertation
Requestor type	academic/educational
Portion	figures/tables/images
Number of figures/tables/images	1
Format	electronic
Distribution quantity	4
Will you be translating?	no
Order reference number	None
Title of the thesis/dissertation	Peptidomimetic Polymers: Advances in Monomer Design and Polymerization Methods
Expected completion date	May 2016
Estimated size	250
Requestor Location	Brandon A Chan 424 Chemistry and Materials Building Department of Chemistry Louisiana State University BATON ROUGE, LA 70803 United States Attn: Brandon A Chan
Billing Type	Invoice
Billing Address	Brandon A Chan

424 Chemistry and Materials Building  
Department of Chemistry  
Louisiana State University  
BATON ROUGE, LA 70803  
United States  
Attn: Brandon A Chan

Total 0.00 USD

#### Terms and Conditions

This License Agreement is between {Requestor Name} ("You") and The Royal Society of Chemistry ("RSC") provided by the Copyright Clearance Center ("CCC"). The license consists of your order details, the terms and conditions provided by the Royal Society of Chemistry, and the payment terms and conditions.

#### RSC / TERMS AND CONDITIONS

##### INTRODUCTION

The publisher for this copyrighted material is The Royal Society of Chemistry. By clicking "accept" in connection with completing this licensing transaction, you agree that the following terms and conditions apply to this transaction (along with the Billing and Payment terms and conditions established by CCC, at the time that you opened your RightsLink account and that are available at any time at .

##### LICENSE GRANTED

The RSC hereby grants you a non-exclusive license to use the aforementioned material anywhere in the world subject to the terms and conditions indicated herein. Reproduction of the material is confined to the purpose and/or media for which permission is hereby given.

##### RESERVATION OF RIGHTS

The RSC reserves all rights not specifically granted in the combination of (i) the license details provided by your and accepted in the course of this licensing transaction; (ii) these terms and conditions; and (iii) CCC's Billing and Payment terms and conditions.

##### REVOCAION

The RSC reserves the right to revoke this license for any reason, including, but not limited to, advertising and promotional uses of RSC content, third party usage, and incorrect source figure attribution.

##### THIRD-PARTY MATERIAL DISCLAIMER

If part of the material to be used (for example, a figure) has appeared in the RSC publication with credit to another source, permission must also be sought from that source. If the other source is another RSC publication these details should be included in your RightsLink request. If the other source is a third party, permission must be obtained from the third party. The RSC disclaims any responsibility for the reproduction you make of items owned by a third party.

##### PAYMENT OF FEE

If the permission fee for the requested material is waived in this instance, please be advised that any future requests for the reproduction of RSC materials may attract a fee.

##### ACKNOWLEDGEMENT

The reproduction of the licensed material must be accompanied by the following acknowledgement:

Reproduced ("Adapted" or "in part") from {Reference Citation} (or Ref XX) with permission of The Royal Society of Chemistry.

If the licensed material is being reproduced from New Journal of Chemistry (NJC), Photochemical & Photobiological Sciences (PPS) or Physical Chemistry Chemical Physics (PCCP) you must include one of the following acknowledgements:

For figures originally published in NJC:

Reproduced ("Adapted" or "in part") from {Reference Citation} (or Ref XX) with

permission of The Royal Society of Chemistry (RSC) on behalf of the European Society for Photobiology, the European Photochemistry Association and the RSC.

For figures originally published in PPS:

Reproduced (“Adapted” or “in part”) from {Reference Citation} (or Ref XX) with permission of The Royal Society of Chemistry (RSC) on behalf of the Centre National de la Recherche Scientifique (CNRS) and the RSC.

For figures originally published in PCCP:

Reproduced (“Adapted” or “in part”) from {Reference Citation} (or Ref XX) with permission of the PCCP Owner Societies.

#### HYPERTEXT LINKS

With any material which is being reproduced in electronic form, you must include a hypertext link to the original RSC article on the RSC’s website. The recommended form for the hyperlink is <http://dx.doi.org/10.1039/DOI> suffix, for example in the link <http://dx.doi.org/10.1039/b110420a> the DOI suffix is ‘b110420a’. To find the relevant DOI suffix for the RSC article in question, go to the Journals section of the website and locate the article in the list of papers for the volume and issue of your specific journal. You will find the DOI suffix quoted there.

#### LICENSE CONTINGENT ON PAYMENT

While you may exercise the rights licensed immediately upon issuance of the license at the end of the licensing process for the transaction, provided that you have disclosed complete and accurate details of your proposed use, no license is finally effective unless and until full payment is received from you (by CCC) as provided in CCC’s Billing and Payment terms and conditions. If full payment is not received on a timely basis, then any license preliminarily granted shall be deemed automatically revoked and shall be void as if never granted. Further, in the event that you breach any of these terms and conditions or any of CCC’s Billing and Payment terms and conditions, the license is automatically revoked and shall be void as if never granted. Use of materials as described in a revoked license, as well as any use of the materials beyond the scope of an unrevoked license, may constitute copyright infringement and the RSC reserves the right to take any and all action to protect its copyright in the materials.

#### WARRANTIES

The RSC makes no representations or warranties with respect to the licensed material.

#### INDEMNITY

You hereby indemnify and agree to hold harmless the RSC and the CCC, and their respective officers, directors, trustees, employees and agents, from and against any and all claims arising out of your use of the licensed material other than as specifically authorized pursuant to this licence.

#### NO TRANSFER OF LICENSE

This license is personal to you or your publisher and may not be sublicensed, assigned, or transferred by you to any other person without the RSC’s written permission.

#### NO AMENDMENT EXCEPT IN WRITING

This license may not be amended except in a writing signed by both parties (or, in the case of “Other Conditions, v1.2”, by CCC on the RSC’s behalf).

#### OBJECTION TO CONTRARY TERMS

You hereby acknowledge and agree that these terms and conditions, together with CCC’s Billing and Payment terms and conditions (which are incorporated herein), comprise the entire agreement between you and the RSC (and CCC) concerning this licensing transaction, to the exclusion of all other terms and conditions, written or verbal, express or implied (including any terms contained in any purchase order, acknowledgment, check endorsement or other writing prepared by you). In the event of any conflict between your obligations

established by these terms and conditions and those established by CCC's Billing and Payment terms and conditions, these terms and conditions shall control.

#### JURISDICTION

This license transaction shall be governed by and construed in accordance with the laws of the District of Columbia. You hereby agree to submit to the jurisdiction of the courts located in the District of Columbia for purposes of resolving any disputes that may arise in connection with this licensing transaction.

#### LIMITED LICENSE

The following terms and conditions apply to specific license types:

##### Translation

This permission is granted for non-exclusive world English rights only unless your license was granted for translation rights. If you licensed translation rights you may only translate this content into the languages you requested. A professional translator must perform all translations and reproduce the content word for word preserving the integrity of the article.

##### Intranet

If the licensed material is being posted on an Intranet, the Intranet is to be password-protected and made available only to bona fide students or employees only. All content posted to the Intranet must maintain the copyright information line on the bottom of each image. You must also fully reference the material and include a hypertext link as specified above.

##### Copies of Whole Articles

All copies of whole articles must maintain, if available, the copyright information line on the bottom of each page.

##### Other Conditions

v1.2

Gratis licenses (referencing \$0 in the Total field) are free. Please retain this printable license for your reference. No payment is required.

If you would like to pay for this license now, please remit this license along with your payment made payable to "COPYRIGHT CLEARANCE CENTER" otherwise you will be invoiced within 48 hours of the license date. Payment should be in the form of a check or money order referencing your account number and this invoice number {Invoice Number}. Once you receive your invoice for this order, you may pay your invoice by credit card. Please follow instructions provided at that time.

##### Make Payment To:

Copyright Clearance Center  
Dept 001  
P.O. Box 843006  
Boston, MA 02284-3006

For suggestions or comments regarding this order, contact Rightslink Customer Support: [customercare@copyright.com](mailto:customercare@copyright.com) or +1-855-239-3415 (toll free in the US) or +1-978-646-2777.

**Questions? [customercare@copyright.com](mailto:customercare@copyright.com) or +1-855-239-3415 (toll free in the US) or +1-978-646-2777.**

## Synthesis of Side-Chain Modified Polypeptides

Timothy J. Deming<sup>\*</sup>

Department of Bioengineering, University of California, 5121 Engineering 5, Los Angeles, California 90095, United States  
Department of Chemistry and Biochemistry, University of California, 607 Charles E. Young Drive East, Los Angeles, California 90095, United States


*Chem. Rev.*, **2016**, *116* (3), pp 786–808

DOI: 10.1021/acs.chemrev.5b00292

Publication Date (Web): July 06, 2015

Copyright © 2015 American Chemical Society

\*E-mail: demingt@seas.ucla.edu. Phone: (310) 267-4450. Fax: (310) 794-5956.

 ACS AuthorChoice - This is an open access article published under an ACS AuthorChoice [License](#), which permits copying and redistribution of the article or any adaptations for non-commercial purposes.  
This article is part of the [Frontiers in Macromolecular and Supramolecular Science](#) special issue:

## **VITA**

Brandon Andrew Chan was born in Mineola, New York, and raised in Port Washington, New York, a suburb of New York City on Long Island. He received his Bachelor of Science in Chemistry from the University of Michigan – Ann Arbor in 2009. Brandon began his graduate studies at Louisiana State University in the fall semester of 2010, joining the group of Professor Donghui Zhang. He is married to Katherine Chan (née Russ) of Grosse Pointe Farms, Michigan. Brandon aspires to become a patent attorney and will be pursuing a Juris Doctor at Michigan State University College of Law following the completion of his Ph.D. studies.